The role of mitochondrial translocator protein 18kDa (TSPO) in regulating astrocyte metabolism

Submitted by

Wyn Firth

to the University of Exeter as a thesis for the degree of

Doctor of Philosophy in Medical Studies

in November 2023

I certify that all material in this thesis which is not my own work has been identified and that any material that has previously been submitted and approved for the award of a degree by this or any other University has been acknowledged.

Abstract

Astrocytes, a heterogeneous class of glial cells, play key roles in maintaining homeostasis in the central nervous system (CNS). This is achieved through multifaceted cellular responses; however, a growing body of evidence suggests that these are heavily associated with the capability of astrocytes to meet their energetic requirements. During CNS inflammation, a hallmark of many neuropathologies, astrocytes lose their homeostatic functions which correlates with significant alteration of their metabolic state. Related studies from the periphery indicate that modulating cellular metabolism may provide a tangible therapeutic target for inflammatory diseases, suggesting that this may represent a potential target for modulating astrocyte inflammatory responses to restore their homeostatic functions during CNS pathologies.

The 18-kilodalton translocator protein (TSPO) is a highly conserved outer mitochondrial membrane protein, expressed in glial cells such as astrocytes. Importantly, TSPO expression drastically increases during neuroinflammation in glial cells such as astrocytes. This has attracted much attention to the possibility of therapeutically modulating TSPO to treat CNS inflammation. However, to date this is hampered by the fact that the underlying function of TSPO remains unclear. An increasing body of evidence suggests that TSPO may regulate cellular metabolism, though this remains underexplored.

To test the overarching hypothesis that TSPO regulates cellular metabolism in astrocytes this study employed two distinct TSPO-deficient ($TSPO^{-/-}$) cell models: an astrocytoma cell line (U373 cells) and mouse primary astrocytes (MPAs). This thesis explored the metabolic ramifications of TSPO deficiency in these CNS cell models, characterised changes to the bioenergetic responses of $TSPO^{-/-}$ MPAs to lipopolysaccharide-induced inflammation, and then attempted to pharmacologically recapitulate these studies with TSPO ligands.

TSPO deficiency modulated MPA and U373 cell metabolism, albeit resulting in different bioenergetic profiles, suggestive of altered fuel preference. Fatty acid oxidation (FAO) was increased in $TSPO^{-/-}$ MPAs, and studies in U373 cells indicated that the mechanistic basis for this may be an interaction between TSPO and carnitine palmitoyltransferase-1a (CPT1a) the rate-limiting enzyme of FAO. In response to inflammatory stimulation, $TSPO^{-/-}$ MPAs showed no significant

differences in regulation of intracellular metabolic proteins, however secretion of the pro-inflammatory cytokine tumour necrosis factor from $TSPO^{-/-}$ MPAs was temporally modulated. Pharmacological recapitulation of these results was unsuccessful, however co-immunoprecipitation studies suggested that pharmacological inhibition of TSPO may modulate interactions between TSPO and other metabolic regulatory proteins. Taken together these studies have shown that TSPO acts as a regulator of cellular metabolism in astrocytes and may play a role in regulating cytokine release through a separate mechanism. These may represent two potential benefits following therapeutic modulation of TSPO that warrant further investigation.

Table of Contents

The role of mitochondrial translocator protein 18kDa (TSPO) in regulating astrocyte metabolism 1

Abstract 2

Table of Contents 4

List of Figures 11

List of Tables 14

List of Abbreviations 15

Publications arising from this thesis 19

Appendix 19

Author's declaration 20

Acknowledgements 21

Chapter 1: General introduction 23

1.1: Cellular metabolism 23

1.1.1: Glycolysis 24

1.1.2: Oxidative phosphorylation (OXPHOS) 26

1.1.3: Alternative substrates 28

1.1.3.1: Fatty acid oxidation (FAO) 28

1.1.3.2: Amino acid metabolism 30

1.2: Energy use in the brain 32

1.2.1: Glia 32

1.3: Astrocytes 33

1.3.1: Metabolism in astrocytes 36

1.3.1.1: Fatty acid oxidation (FAO) in astrocytes 38

1.3.2: Calcium ion (Ca^{2+}) signalling 39

1.3.3: Astrocyte reactivity 39

1.3.3.1: Astrogliosis and CNS pathologies 40

1.3.4: Metabolism in reactive astrocytes 41

1.4: Translocator protein 18kDa (TSPO) 45
1.4.1: Evolution of TSPO 45
1.4.2: Structure and function of TSPO 46
1.4.3: TSPO: a regulator of cellular metabolism? 51
1.4.4: Expression throughout the CNS 53
1.4.5: Expression and function in glia 53
1.4.5.1: TSPO in astrocytes 54
1.4.6: TSPO ligands 55
1.4.6.1: The rs6971 polymorphism 58
1.4.7: Beyond neuroimaging: TSPO as a therapeutic target in CNS disease 59
1.5: Summary, overarching hypothesis, and aims of this project 60
Chapter 2: Materials and Methods 62
2.1: Materials 62
2.2: Methods 67
2.2.1: Animal use and husbandry 67
2.2.2: Isolation of primary astrocytes 67
2.2.2.1: Immunocytochemistry 68
2.2.3: Genotyping 70
2.2.4: General cell culture 72
2.2.5: Generation of TSPO-deficient U373 cells 72
2.2.6: Bacterial transformations and plasmid extractions 73
2.2.7: Transient transfection of U373 cells 73
2.2.8: Cell treatments 74
2.2.9: Protein quantification 74
2.2.10: Co-immunoprecipitations 75
2.2.11: Immunoblotting 76
2.2.12: Extracellular flux analysis 79

2.2.12.1: Mitochondrial stress test (MST) 79

2.2.12.2: Glycolysis stress test 81

2.2.12.3: Fatty acid oxidation stress test 82

2.2.12.4: Substrate reintroduction tests 83

2.2.13: Quantification of extracellular lactate 85

2.2.14: FAO enzyme activity assay 85

2.2.15: Quantification of extracellular cytokine concentrations 86

2.2.16: Cell viability assay 86

2.2.17: Data handling and statistical analysis 87

Chapter 3: TSPO as a regulator of astrocyte metabolism 88

3.1: Introduction 88

3.2: Hypothesis 90

3.3: Methods 90

3.4: Results 91

3.4.1: TSPO deficiency reduced basal mouse primary astrocyte (MPA) metabolism 91

3.4.2: TSPO deficiency reduced mitochondrial respiration in MPAs .. 93

3.4.3: TSPO deficiency increased glycolysis in MPAs 95

3.4.4: TSPO deficiency reduced glycolytic rate, but increased glycolytic capacity, in U373 cells 97

3.4.5: TSPO$^{-/-}$ MPAs had a larger change in ECAR in response to 1000µM L-glutamine injection 99

3.4.6: TSPO$^{-/-}$ MPAs showed no difference in the change in OCR in response to L-glutamine injection 101

3.4.7: TSPO$^{-/-}$ MPAs had a reduced change to ECAR in response to reintroduction of 1mM, 5.5mM, and 7.5mM glucose 103

3.4.8: OCR of TSPO$^{-/-}$ MPAs did not significantly change in response to glucose injection 105

3.4.9: TSPO$^{-/-}$ MPAs maintained metabolic rates in the absence of glucose 107

3.4.10: The bioenergetic response of U373s to no glucose conditions was unchanged by genotype 109

3.4.11: L-lactate secretion was reduced in TSPO$^{-/-}$ MPAs and U373s 111

3.4.12: Basal and maximal fatty acid oxidation were increased in TSPO$^{-/-}$ MPAs 113

3.4.13: Fatty acid oxidation enzyme activity downstream of CPT1a was unchanged in TSPO$^{-/-}$ U373s 115

3.4.14: TSPO formed a complex with CPT1a in U373 astrocytoma cells 117

3.5: Discussion 119

3.5.1: TSPO deficiency modulates astrocyte metabolism 121

3.5.2: Regulation of FAO in astrocytes by TSPO 124

3.5.3: Limitations of this chapter 126

3.5.3.1: Bioenergetic phenotypes were different between cell types 128

3.6: Conclusion 129

Chapter 4: Regulation of astrocyte immunometabolism by TSPO 130

4.1: Introduction 130

4.2: Hypothesis 133

4.3: Methods 134

4.3.1: Use of C57BL/6J primary astrocytes 134

4.4: Results 134

4.4.1: Validation of the inflammatory model used 134

4.4.2: 3h LPS stimulation did not modulate TSPO expression 137

4.4.3: 3h LPS stimulation did not alter MPA bioenergetics 139

4.4.4: 24h LPS stimulation increased TSPO expression 141

4.4.5: 24h LPS stimulation increased MPA OCR and ECAR 143

4.4.6: 24h LPS stimulation did not reduce cell viability 145

4.4.7: TSPO deficiency altered the temporal release profile of TNF from MPAs 147

4.4.8: NFκB phosphorylation in $TSPO^{-/-}$ MPAs following 3h LPS stimulation was unchanged compared to $TSPO^{+/+}$ controls 150

4.4.9: GLUT1 and CPT1a expression were not modulated by 3h LPS stimulation in either genotype 153

4.4.10: NFκB phosphorylation in $TSPO^{-/-}$ MPAs following 24h LPS stimulation was unchanged compared to $TSPO^{+/+}$ controls 156

4.4.11: HK2 expression was altered by 24h LPS stimulation but not by TSPO genotype 158

4.4.12: Modulatory effects of 24h LPS stimulation on GLUT1 expression were not genotype-dependent 160

4.4.13: CPT1a expression was modulated by TSPO genotype but not 24h LPS stimulation 162

4.4.14: 24h LPS stimulation significantly increased IL-10 secretion from $TSPO^{-/-}$ MPAs but not $TSPO^{+/+}$ controls 164

4.4.15: The metabolic phenotype of $TSPO^{-/-}$ MPAs in response to 3h LPS stimulation was consistent with $TSPO^{+/+}$ controls 166

4.4.16: The metabolic response to 24h LPS stimulation was conserved in $TSPO^{-/-}$ MPAs 168

4.5: Discussion 170

4.5.1: TSPO expression during inflammation correlates with a metabolic shift in astrocytes 170

4.5.2: TSPO and astrocyte immunometabolism 172

4.5.3: Limitations and future directions 177

4.6: Conclusion 179

Chapter 5: Pharmacological inhibition of TSPO in astrocytes 180

5.1: Introduction 180

5.2: Hypothesis 184

5.3: Methods 184

5.3.1: Design of PCR primers specific for the rs6971 locus of the *Tspo* gene in mice and humans 184

5.3.2: Sequencing PCR products 187

5.4: Results 188

5.4.1: U373 astrocytoma cells have the rs6971 polymorphism 188

5.4.2: C57BL/6J MPA *Tspo* encodes 147Ala 190

5.4.3: TSPO$^{+/+}$ MPA *Tspo* encodes 147Ala 192

5.4.4: PK-11195 pre-treatment did not inhibit TSPO$^{+/+}$ MPA bioenergetics 194

5.4.5: PK-11195 pre-treatment did not inhibit TSPO$^{+/+}$ U373 bioenergetics 196

5.4.6: Transfection of U373 astrocytoma cells with a tagged TSPO construct did not modulate expression of key proteins and enzymes 198

5.4.7: Pharmacological inhibition of cellular metabolism and TSPO activity in U373 astrocytoma cells may alter TSPO protein complex stoichiometry 201

5.5: Discussion 203

5.5.1: Pharmacological modulation of TSPO and astrocyte bioenergetics 203

5.5.2: TSPO protein complex stoichiometry in response to metabolic state 206

5.5.3: The effect of rs6971 genotype on choice of TSPO ligand for these studies 208

5.6: Conclusion 209

Chapter 6: General discussion 210

6.1: Statement of key findings and contribution to knowledge 210

6.1.1: TSPO as a regulator of astrocyte metabolism 210

6.1.2: Altered temporal profile of LPS-induced cytokine release in TSPO$^{-/-}$ MPAs 216

6.2: General limitations 219

6.2.1: The models of TSPO deficiency used 219

6.2.2: Reliance on metabolic flux analyses 220

6.2.3: Limitations of *in vitro* methodology 221

6.3: Outstanding questions 222

6.3.1: How is TSPO regulated? 222

6.3.2: Does TSPO regulate calcium signalling in astrocytes? 225

6.3.3: What comes first *in situ*: the metabolic shift, or the inflammatory stimulus? 226

6.3.4: Are these outputs truly modulated by TSPO ligands? 227

6.4: Conclusions and future directions 229

Appendix 230

Appendix 1: Regulation of astrocyte metabolism by mitochondrial translocator protein. 230

References 231

List of Figures

Figure 1.1.1: An overview of glycolysis……..25
Figure 1.1.2: Oxidative phosphorylation……..……27
Figure 1.1.3.1: Fatty acid oxidation (FAO). 29
Figure 1.1.3.2: Amino acid metabolism. 31
Figure 1.3.4: Astrocyte inflammatory responses correlate with a metabolic shift……..……42
Figure 1.4.2.1: Structure of TSPO. 47
Figure 1.4.2.2: Putative TSPO interactions……..……50
Figure 2.2.2: Confirmation of astrocyte culture purity……69
Figure 2.2.3: Example gel showing PCR products from TSPO$^{-/-}$-line mice...71
Figure 3.4.1: TSPO deficiency reduced basal mouse primary astrocyte (MPA) metabolism. 92
Figure 3.4.2: TSPO deficiency reduced mitochondrial respiration in MPAs..... 94
Figure 3.4.3: TSPO deficiency increased glycolysis in MPAs. 96
Figure 3.4.4: TSPO deficiency reduced glycolytic rate, but increased glycolytic reserve, in U373 cells. 98
Figure 3.4.5: TSPO$^{-/-}$ MPAs had a larger change in ECAR in response to 1000μM L-glutamine injection. 100
Figure 3.4.6: TSPO$^{-/-}$ MPAs showed no difference in the change in OCR in response to L-glutamine injection. 102
Figure 3.4.7: TSPO$^{-/-}$ MPAs had an attenuated change in ECAR following reintroduction of 1mM, 5.5mM, and 7.5mM glucose. 104
Figure 3.4.8: OCR of TSPO$^{-/-}$ MPAs did not significantly change in response to glucose injection..... 106
Figure 3.4.9: TSPO$^{-/-}$ MPAs maintained the basal metabolic rate in the absence of glucose. 108
Figure 3.4.10: TSPO$^{-/-}$ U373s increased OCR in response to no glucose conditions. 110
Figure 3.4.11: L-lactate secretion was reduced in TSPO$^{-/-}$ MPAs and U373s. 112
Figure 3.4.12: Basal and maximal fatty acid oxidation were increased in TSPO$^{-/-}$ MPAs.....114

Figure 3.4.13: Fatty acid oxidation enzyme activity downstream of CPT1a was unchanged in TSPO$^{-/-}$ U373s.....116
Figure 3.4.14: TSPO formed a complex with CPT1a in U373 astrocytoma cells. 118
Figure 4.4.1: Validation of the inflammatory model used. 136
Figure 4.4.2: 3h LPS stimulation did not modulate TSPO expression..... 138
Figure 4.4.3: 3h LPS stimulation did not alter MPA bioenergetics..... 140
Figure 4.4.4: 24h LPS stimulation increased TSPO expression..... 142
Figure 4.4.5: 24h LPS stimulation increased MPA OCR and ECAR. 144
Figure 4.4.6: 24h LPS stimulation did not reduce cell viability. 146
Figure 4.4.7: TSPO deficiency altered the temporal release profile of TNF from MPAs..... 149
Figure 4.4.8: NFκB phosphorylation in TSPO$^{-/-}$ MPAs following 3h LPS stimulation was unchanged compared to TSPO$^{+/+}$ controls..... 152
Figure 4.4.9: GLUT1 and CPT1a expression were not modulated by 3h LPS stimulation in either genotype. 155
Figure 4.4.10: NFκB phosphorylation in TSPO$^{-/-}$ MPAs following 24h LPS stimulation was unchanged compared to TSPO$^{+/+}$ controls..... 157
Figure 4.4.11: HK2 expression was altered by 24h LPS stimulation but not by TSPO genotype. 159
Figure 4.4.12: 24h LPS stimulation but not TSPO genotype significantly reduced GLUT1 expression..... 161
Figure 4.4.13: CPT1a expression was not modulated by 24h LPS stimulation in either TSPO genotype..... 163
Figure 4.4.14: 24h LPS stimulation significantly increased IL-10 secretion from TSPO$^{-/-}$ MPAs but not TSPO$^{+/+}$ controls. 165
Figure 4.4.15: The metabolic phenotype of TSPO$^{-/-}$ MPAs in response to 3h LPS stimulation was consistent with TSPO$^{+/+}$ controls. 167
Figure 4.4.16: The metabolic response to 24h LPS stimulation was conserved in TSPO$^{-/-}$ MPAs..... 169
Figure 5.4.1: U373 astrocytoma cells have the rs6971 polymorphism. ... 189
Figure 5.4.2: C57BL/6J MPA *Tspo* encodes 147Ala..... 191
Figure 5.4.3: TSPO$^{+/+}$ MPA *Tspo* encodes 147Ala..... 193
Figure 5.4.4: PK-11195 pre-treatment did not inhibit TSPO$^{+/+}$ MPA bioenergetics..... 195

Figure 5.4.5: PK-11195 pre-treatment did not inhibit TSPO$^{+/+}$ U373 bioenergetics. 197
Figure 5.4.6: Transfection of U373 astrocytoma cells with a Myc-tagged TSPO construct did not modulate expression of key proteins and enzymes. 200
Figure 5.4.7: Pharmacological inhibition of cellular metabolism and TSPO activity in U373 astrocytoma cells may alter TSPO protein complex stoichiometry. 202
Figure 6.1.1: A proposed model for TSPO as a state-dependent regulator of astrocyte metabolism. 215
Figure 6.1.2: TSPO may regulate inflammatory responses by influencing Ca^{2+} flux..... 218
Figure 6.3.1: Theoretical mechanisms regulating TSPO activity and their potential effects on TSPO-containing complexes. 224

List of Tables

Table 2.1.1: List of consumables 62
Table 2.1.2: List of general equipment..... 65
Table 2.1.3: List of software and suppliers 66
Table 2.2.2.1: List of antibodies used for immunocytochemistry 68
Table 2.2.3: Primers used to genotype TSPO$^{-/-}$-line mice ……70
Table 2.2.9: Constitution of modified RIPA buffer ……75
Table 2.2.10: Co-immunoprecipitation buffer ……76
Table 2.2.11.1: Hand-cast polyacrylamide gels..... 77
Table 2.2.11.2: 4X SDS-PAGE sample buffer..... 77
Table 2.2.11.3: List of antibodies used for immunoblotting..... 78
Table 2.2.12.1: Calculations used for the mitochondrial stress test..... 80
Table 2.2.12.2: Calculations used for the glycolysis stress test 81
Table 2.2.12.3: Media compositions and calculations used for the FAO stress test 82
Table 2.2.12.4: Media composition and injection concentrations used during L-glutamine reintroduction test 84
Table 2.2.12.5: Media composition and concentrations injected during glucose reintroduction test 84
Table 2.2.16: Flow cytometry buffer ……..87
Table 3.5.1: Summary table outlining results from this chapter...... 120
Table 5.3.1.1: Primers used to genotype the human and mouse *Tspo* rs6971 locus ……186
Table 5.3.1.2: Settings used for human and mouse *Tspo* PCR ……186

List of Abbreviations

Abbreviation	Full term
2DG	2-deoxyglucose
2DG6P	2-deoxyglucose-6-phosphate
AA	Amino acid
ACBD3	Acyl-CoA binding domain containing 3
ACBP	Acyl-CoA binding protein (synonymous with: DBI)
ACC	Acetyl coenzyme A decarboxylase
ADP	Adenosine diphosphate
Ala	Alanine
ALDH1L1	Aldehyde dehydrogenase 1 family member L1
AMP	Adenosine monophosphate
AMPK	Adenosine monophosphate-activated protein kinase
ANOVA	Analysis of variance
ANT	Adenine nucleotide transporter
ApoE	Apolipoprotein E
ATAD3A	ATPase family AAA domain containing 3a
ATP	Adenosine triphosphate
BBB	Blood-brain barrier
BSA	Bovine serum albumin
C	Carbon
C16	Palmitate
CaMKKβ	Calcium/calmodulin-dependent protein kinase kinase 2
Ca^{2+}	Calcium ion
$[Ca^{2+}]_e$	Extracellular calcium ion concentration
$[Ca^{2+}]_i$	Intracellular calcium ion concentration
CD31	Cluster of differentiation 31
CD36	Cluster of differentiation 36
cDNA	Complementary DNA (see: DNA)
CMV	Cytomegalovirus
CNS	Central nervous system
CoA	Coenzyme A
Co-IP	Co-immunoprecipitation
CPT	Carnitine palmitoyltransferase
CPT1a	Carnitine palmitoyltransferase 1a
CRAC	Cholesterol recognition/interaction amino acid consensus motif
CRISPR-Cas9	Clustered regularly interspaced short palindromic repeats-CRISPR associated protein 9
CXC	Chemokine-axis-chemokine
CYP11A1	Cytochrome P450 family 11 subfamily A member 1
DAMP	Damage-associated molecular pattern
DBI	Diazepam binding inhibitor (synonymous with: ACBP)
ddH2O	Double distilled H_2O
DMEM	Dulbecco's Modified Eagle's Media

DMSO	Dimethyl sulfoxide
DNA	Deoxyribonucleic acid
DPA-713	*N,N*-diethyl-2-[2-(4-methoxyphenyl)-5,7-dimethylpyrazolo[1,5-α]pyrimidin-3-yl]acetamide
Drp1	Dynamin-related protein 1
EAAT	Extracellular amino acid transporter
ECAR	Extracellular acidification rate
EDTA	Ethylenediaminetetraacetic acid
EFA	Extracellular flux analysis
EGTA	Ethylene glycol-bis(2-aminoethylether)-*N,N,N′,N′*-tetraacetic acid
ELISA	Enzyme-linked immunosorbent assay
ER	Endoplasmic reticulum
Eto	Etomoxir
EV	Empty vector
FABP	Fatty acid binding protein
FAD	Flavin adenine dinucleotide
FADH	Reduced flavin adenine dinucleotide
FAF-BSA	Fatty acid free BSA
FAO	Fatty acid oxidation
FAOST	Fatty acid oxidation stress test
FCCP	Carbonyl cyanide p-trifluoro-methoxyphenyl hydrazone
FEPPA	*N*-(2-(2-fluoroethoxy)benzyl)-*N*-(4-phenoxypyridin-3-yl)acetamide
G6P	Glucose-6-phosphate
GABA	γ-aminobutyric acid
GAPDH	Glyceraldehyde-3-phosphate dehydrogenase
GFAP	Glial fibrillary acidic protein
Gluc	Glucose
GLUT	Glucose transporter
GLUT1	Glucose transporter 1
Glyco	Glycolysis
H^+	Proton
HFD	High-fat diet
HK	Hexokinase
HK2	Hexokinase 2
IL	Interleukin
IL-1β	Interleukin-1β
IL-10	Interleukin-10
JAK-STAT	Janus kinase-signal transducer and activator of transcription
K_{ATP}	Potassium-sensitive ATP channel
K_d	Dissociation constant
kDa	Kilodaltons
K_i	Inhibitory constant
K_m	Michaelis constant
LDH	Lactate dehydrogenase

LPS	Lipopolysaccharide
Malonyl-CoA	Malonyl-coenzyme A
Mito resp	Mitochondrial respiration
mL	Millilitre
mM	Millimolar
MPA(s)	Mouse primary astrocyte(s)
MPC	Mitochondrial pyruvate carrier
MPTP	Mitochondrial permeability transition pore
mRNA	Messenger RNA
Myc	Myelocytomatosis oncogene
NAD	Nicotinamide adenine dinucleotide
NADH	Reduced nicotinamide adenine dinucleotide
NFκB	Nuclear factor kappa B
nM	Nanomolar
nm	Nanometre
NOX	NAPDH oxidase
NRF2	Nuclear factor erythroid 2-related factor 2
NRLP3	Nod-like receptor family pyrin domain containing 3
OA	Oxaloacetate
OCR	Oxygen consumption rate
Oligo	Oligomycin
OMM	Outer mitochondrial membrane
OXPHOS	Oxidative phosphorylation
P2	Purinergic P2 receptor
P2X	Purinergic P2 X receptor
P2Y	Purinergic P2 Y receptor
PAMP	Pathogen-associated molecular pattern
PBR-28	*N*-Acetyl-*N*-(2-methoxybenzyl)-2-phenoxy-5-pyridinamine
PCR	Polymerase chain reaction
pCMV	Porcine cytomegalovirus
PDGFRβ	Platelet-derived growth factor receptor β
PDH	Pyruvate dehydrogenase
PFK1	Phosphofructinase-1
PGC-1α	Peroxisome-proliferator activated receptor gamma co-activator 1-alpha
PGI	Phosphoglucose isomerase
PGK	Phosphoglycerate kinase
PGM	Phosphoglycerate dismutase
Phys rel	Physiologically relevant
P_i	Inorganic phosphate
PIGA	*N,N*-dialkyl-2-phenylindol-3-ylglyoxylamide
PK	Pyruvate kinase
PK-11195	1-(2-chlorophenyl)-*N*-methyl-*N*-(1-methylpropyl)-3-isoquinoline carboxamide
R/AA	Rotenone/antimycin-A mix
Redox	Reduction/oxidation

RIPA	Radioimmunoprecipitation assay
RNA	Ribonucleic acid
Ro5-4864	4'-chlorodiazepam
ROS	Reactive oxygen species
S100β	S100 calcium-binding protein β
shRNA	Short hairpin RNA (see: RNA)
siRNA	Short interfering RNA (see: RNA)
SNP	Single nucleotide polymorphism
StAR	Steroidogenic acute regulatory protein
T_a	Annealing temperature
TCA	Tricarboxylic acid
TEMED	*N,N,N′,N′*-Tetramethylethylenediamine (TEMED)
Thr	Threonine
TLR	Toll-like receptor
T_m	Melting temperature
TMD	Transmembrane domain
TNF	Tumour necrosis factor
TNFR	TNF receptor
TOMM20	Translocase of the outer mitochondrial membrane complex 20
TSPO	Translocator protein 18kDa
VDAC	Voltage-dependent anion channel
vol/vol	Volume/volume
°C	Degrees Celsius
αKG	α-ketoglutarate
µL	Microlitre
$^{+/+}$	Wildtype; expressing
$^{-/-}$	Knockout; deficient
$^{+/-}$	Heterozygote

Publications arising from this thesis

Publications:

Chapter 3, 4:

Wyn Firth, Josephine L Robb, Daisy Stewart, Katherine R Pye, Rosemary Bamford, Asami Oguro-Ando, Craig Beall, Kate LJ Ellacott. *Regulation of astrocyte metabolism by mitochondrial translocator protein 18kDa*. BioRxiv preprint. doi: 10.1101/2023.09.29.560159.

Conference proceedings:

Wyn Firth, Josephine L Robb, Craig Beall, Kate LJ Ellacott. *Translocator protein 18kDa (TSPO) regulation of astrocyte metabolic flexibility.* Glia. 71:S1;E376. 06 July 2023.

Appendix

Appendix 230

Appendix 1: Regulation of astrocyte metabolism by mitochondrial translocator protein. 230

Author's declaration

All work presented in this thesis was carried out at the University of Exeter RILD laboratories or BRF by the author, Wyn Firth, with the exception of the following:

Chapter 3: Figure 3.4.4, 12. The data in these figures were generated by Dr Josephine L Robb and are included in this thesis for completeness.

Chapter 5: Human and mouse *Gapdh* and *Gfap* primers used as positive controls for polymerase chain reaction were designed by Asmaa Al-khalidi during her doctoral studies.

CRISPR-Cas9 mediated generation of TSPO-deficient U373 astrocytoma cells. This work was carried out by Daisy Stewart during her Professional Training Year under the supervision of Dr Josephine L Robb and Dr Rosemary Bamford.

Isolation (and genotyping via PCR) of primary astrocytes. On occasions where the author could not perform isolations or genotyping firsthand these were carried out by Katherine R Pye.

Acknowledgements

I would like to thank my brilliant supervisor, Dr Kate Ellacott, for her endless support, motivation, keen scientific insight, and reminders to “keep my eyes on the prize”. I will never forget the support you offered an inquisitive young scientist to start out on an MRes that transformed into a PhD. You have gone beyond anything I anticipated, and further still when you secured internal funding and supported my first grant application to the BSN. You have pushed me to grow in ways I didn’t think I would. Secondly, to my co-supervisor, Dr Craig Beall. I will miss our catchups outside your office door, and all the pensions/careers advice! You have offered endless insight into experiments and data interpretation, and encouraged me to “write with precision” and “remember the big picture” when I get caught up in the minutiae.

To the Beallacotts past, present, and the new blood: Paul, Ana, Katie, Josie, Katherine, Asmaa, Jiping, Ellie, and Natasha. In various ways you have offered me endless support with experiment planning, techniques, collecting primary cells, and pushing me to be a better mentor (the new blood!). You welcomed me in during 2020 and made me feel like part of the team. To the wider RILD staff – Afi, Helen, et al. Thanks for giving me such a great place to work for the last few years.

To all down at Central Dojo, who welcomed me in December 2022 and made me feel like part of the gang. In particular, thanks to Senseis Dave, Mike, Chris, Darren, and John, and my friends Paul and Max, for welcoming me in and whipping me into shape. Training on Tuesday and Thursday nights helped me stay sane when the PhD was driving me mad! I doubt they will read this, but thanks also to John Williams, Howard Shore, Koji Kondo, and Hans Zimmer. You have kept me company through many experiments and hard days.

To my family: Mum (Pauline), Dad (Ian), my sisters Miriam and Grace, my nephew Aidan and niece Kiera, and Ginny the dog. You have given me the greatest support possible and I could not have done this without you. I hope I have made you all proud. To my Godmother Helen and the Fletchers, for buying me all those science books when I was a tiddler.

To my wonderful partner Jess, who has put up with endless ramblings, awkward hours, and general cantankerousness. And using your cat as a prop for molecular biology. Love you.

Last but not least, thanks to God for giving me the strength, resilience, and insight to do this, particularly when I thought I could not. Isaiah 41:10. “Science is the exploration of God’s creation” – mum, and probably someone else.

Chapter 1: General introduction

1.1: Cellular metabolism

To many people, ‘metabolism’ is an abstract concept, possibly evoking latent memories of a series of complex biochemical pathways simply necessitated for maintaining life. However, cellular metabolism is increasingly being recognised as a crucially important regulatory player in a variety of cellular processes, beyond simply being required for the supply of energy to cells. Indeed, virtually any interaction a cell has with its environment – whether in ‘simple’, unicellular, prokaryotic life, or in ‘complex’, multicellular, eukaryotic life – incurs an energetic cost which must be met, thus allowing cells to sense and respond to stimuli.

The main ‘goal’ of energy metabolism is commonly regarded as the consumption of metabolic substrates (that is, ‘fuels’ – amino acids, carbohydrates, and lipids) to produce enough adenosine triphosphate (ATP) to meet the energetic demands of cellular activity[1,2]. These metabolic demands are constantly in flux, and change in response to the behaviour of the cell and wider organism[3,4]. The energetic requirements beyond basal metabolism that are imposed on cells are met in a variety of ways: energy-consuming processes can be slowed down or halted (insofar as is possible), and energy-producing processes can be promoted[5–9]. In a complex, multicellular organism, this may manifest as the promotion of feeding behaviours and cessation of vigorous, energy-intensive activities. ATP is derived from the breakdown of metabolic substrates in a complex series of biochemical pathways (**Chapter 1.1.1-1.1.3**). Substrates take the forms of carbohydrates, lipids, and amino acids. Importantly, the scope and impact of metabolism goes much further than maintaining ATP ratios and cellular energy levels: metabolic products and intermediates derived from these substrate groups are increasingly being recognised as crucial signalling molecules for intracellular communication[10–12] and intercellular signalling to communicate changes in whole-body energetic state[13–16] as well as cellular/tissue damage[17–21]. For example, cells can utilise or repurpose metabolic intermediates (such as the metabolite itaconate in the context of inflammatory responses[22]) to respond to their environments, as well as synthesise biomolecules such as glycerophosphoinositols[23] to activate various cellular signalling pathways in response to stimuli[23–26] (e.g, regulating cellular differentiation during development[24] or regulating inflammatory responses[25]). Thus, the important

contributions of cellular metabolism to facilitating myriad functions, in addition to the potential contributions of aberrant cellular metabolism to the development and resolution of pathogenic states[27–34], are increasingly being appreciated, expanding the scope of metabolism far beyond the traditional perspective of maintaining energy levels.

1.1.1: Glycolysis

Glucose, a simple hexose sugar, is commonly accepted as the universal fuel source for mammalian cells. Glucose is transported around the body via the circulatory system and is readily taken up into cells through the glucose transporter (GLUT) family of proteins by way of facilitated diffusion alongside sodium ions[35]. Once absorbed, glucose can either be stored as glycogen via glycogenesis (a process which typically occurs in hepatocytes, cardiac and skeletal muscle tissue[36], and astrocytes[37]), or is rapidly metabolised as part of a process termed glycolysis[35]. This involves the rapid phosphorylation of glucose via a family of enzymes known as hexokinases (HKs) which catalyse the conversion of glucose to glucose-6-phosphate (G6P)[38,39]. Following conversion between seven intermediate substrates, G6P is ultimately converted into two pyruvate molecules, with a net ATP gain of two molecules[38] (**Figure 1.1.1**). Pyruvate may then be converted to lactate in a reaction that is catalysed by lactate dehydrogenase, or converted into acetyl-coenzyme A (acetyl-CoA) by pyruvate dehydrogenase depending on the needs of the cell. Acetyl-CoA is used as a substrate to drive oxidative phosphorylation (**Chapter 1.1.2**), whereas lactate can be secreted to act as an intercellular signalling molecule during the pro-inflammatory phase of inflammatory responses[40–45]. Alongside this, lactate acts as an important signalling molecule in the central nervous system (CNS), influencing processes such as neuronal activity and memory formation[46–48], and has been implicated in neuropsychiatric conditions[49–51]. This highlights the importance of glycolysis for providing various substrates for downstream utilisation, and its influence on a variety of cellular processes.

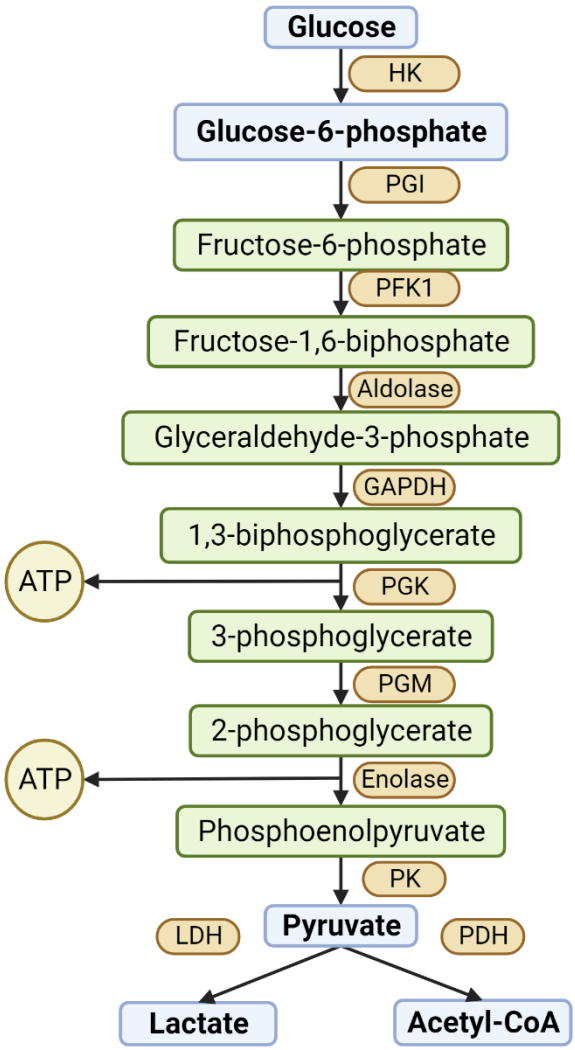

Figure 1.1.1: An overview of glycolysis.

An overview of the process of glycolysis. Substrates and products of interest are shown in blue rectangles with bold text. Intermediate substrates are shown in green normal text. ATP is shown in yellow circles. Enzymes are shown in yellow capsules. Glucose is phosphorylated by HK into glucose-6-phosphate (G6P). G6P undergoes further metabolism to produce pyruvate, which can be converted to lactate or acetyl-CoA. Acetyl-CoA serves as a substrate for the tricarboxylic acid cycle. Glycolysis is a rapid process that yields two molecules of ATP per molecule of glucose.

HK: hexokinase. PGI: phosphoglucose isomerase. PFK1: phosphofructinase-1. GAPDH: glyceraldehyde-3-phosphate dehydrogenase. PGK: phosphoglycerate kinase. PGM: phosphoglycerate mutase. PK: pyruvate kinase. LDH: lactate dehydrogenase. PDH: pyruvate dehydrogenase. Created with BioRender.com.

1.1.2: Oxidative phosphorylation (OXPHOS) and the tricarboxylic acid cycle

Following its generation, pyruvate is transported into the mitochondria via the mitochondrial pyruvate carrier (MPC)[38] and voltage-dependent anion channel (VDAC)[52] for conversion to acetyl-CoA and subsequent use as a substrate for the tricarboxylic acid cycle (TCA) cycle[38]. The TCA cycle describes a series of reactions which generate intermediates such as citrate, α-ketoglutarate, succinyl-CoA, and oxaloacetate[53]. Alongside this, CO_2 and reduced forms of the coenzymes nicotinamide adenine dinucleotide (NAD; reduced: NADH) and flavin adenine dinucleotide (FAD; reduced: $FADH_2$)[53] are produced. NADH and $FADH_2$ donate electrons to the electron transport chain, a series of protein complexes found on the inner mitochondrial membrane. Specifically, electrons from NADH are donated at mitochondrial complex 1, whereas electrons from FADH are donated at mitochondrial complex 2[53]. Alongside transporting electrons, the mitochondrial complexes 1, 3, and 4 serve as proton (H^+) pumps, shunting H^+ into the intermembrane space[53]. This increases the electrochemical gradient and readily facilitates the transport of H^+ back across the inner membrane via the F_O portion of the ATP synthase complex[53]. Here, energy derived from the electrochemical gradient (termed protonmotive force[53]) is used to fuel the synthesis of ATP from adenosine diphosphate (ADP) and inorganic phosphate via the F_1 portion of the ATP synthase complex[53], catalysed by a conformational change to one of the subunits of the F_1 portion[54]. This process, known as oxidative phosphorylation (OXPHOS), is much more efficient at producing ATP than glycolysis alone, generating a net gain of 30-36 ATP[55] (**Figure 1.1.2**). Thus, the approximate net ATP yield from both glycolysis and OXPHOS [i.e., the complete oxidation of glucose] is ~32-38 ATP. ATP is exported from the mitochondrion via the adenine nucleotide transporter (ANT)[56].

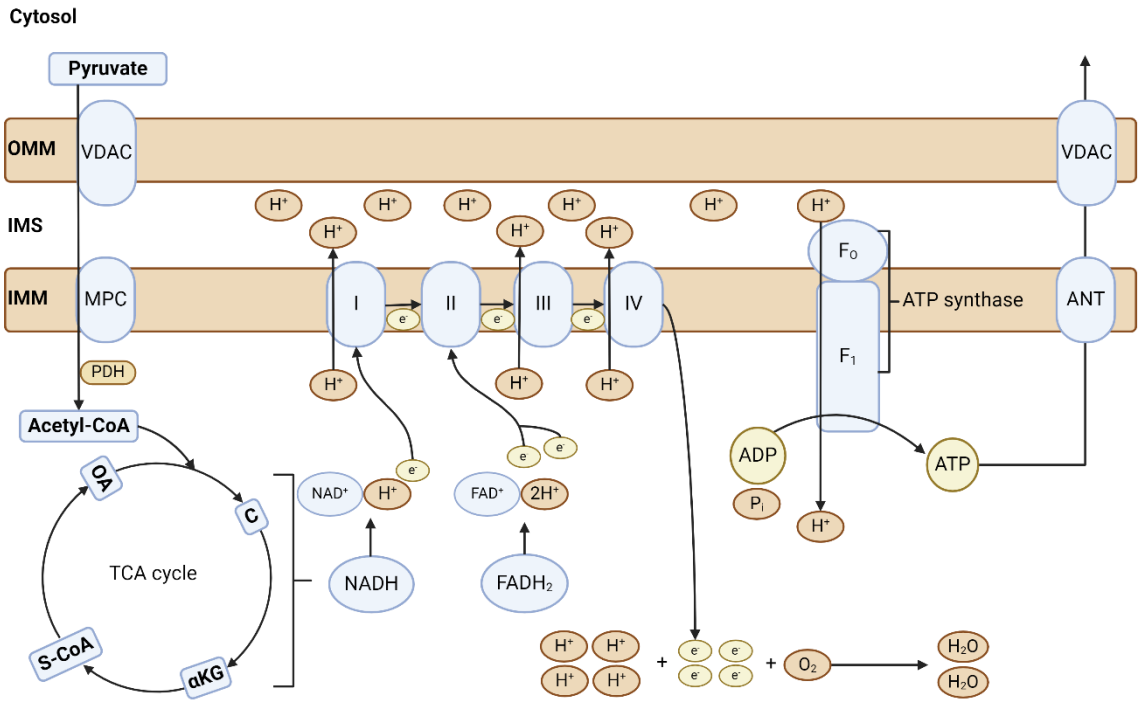

Figure 1.1.2: Oxidative phosphorylation.

Following glycolysis, pyruvate is transported into the mitochondria via VDAC and MPC prior to conversion into acetyl-CoA via PDH. Acetyl-CoA serves as a substrate for the TCA cycle, which generates NADH and $FADH_2$. H^+ from NADH and $FADH_2$ are pumped out of the proton pumps (complex I, III, IV) to the IMS. Complex II transports electrons from $FADH_2$ across to complex III and IV. H^+ from the IMS are transported back across the IMM via the ATP synthase, causing a conformational change in the F_1 subunit of the ATP synthase which catalyses the generation of ATP from ADP and P_i. Surplus H^+ and e^- react with O_2 to form H_2O. This efficient process generates 30-36 ATP molecules.

Acetyl-CoA: acetyl-coenzyme A. ADP: adenosine diphosphate. ATP: adenosine triphosphate. αKG: α-ketoglutarate. C: citrate. FAD: flavin adenine dinucleotide. FAD^+: oxidised FAD. $FADH_2$: reduced FAD. F_O: rotor subunit of ATP synthase. F_1: ATP synthesis subunit of ATP synthase. P_i: inorganic phosphate. MPC: mitochondrial pyruvate carrier. NAD: nicotinamide adenine dinucleotide. NAD^+: oxidised NAD. NADH: reduced NAD. OA: oxaloacetate. S-CoA: succinyl-CoA. VDAC: voltage-dependent anion channel. I: Complex 1. II: Complex 2. III: Complex 3. IV: Complex 4. H^+: proton. O/IMM: outer/inner mitochondrial membrane. IMS: intermembrane space. ANT: adenine nucleotide transporter. Created with BioRender.com.

1.1.3: Alternative substrates

In addition to glucose, lipids and amino acids may also be used by cells as metabolic substrates under certain conditions.

1.1.3.1: Fatty acid oxidation (FAO)

Following uptake, long chain fatty acids are converted to acyl-CoA[57]. Next, the acyl group is removed from CoA and added to carnitine[57], a reaction that is catalysed by the rate-limiting enzyme of fatty acid oxidation (FAO), carnitine palmitoyltransferase 1a (CPT1a)[57,58]. This process is essential for intramitochondrial transport of fatty acids[59,60] and generates acylcarnitines, which are shuttled into the mitochondria for downstream metabolism known as FAO or β-oxidation[57]. During this process (**Figure 1.1.3.1**, adapted from[57]), acylcarnitine is converted back into acyl-CoA, and carbons are successively removed from acyl-CoA until acetyl-CoA is ultimately generated[57]. This acetyl-CoA then serves as a substrate for the TCA cycle and OXPHOS, as outlined in **Figure 1.1.2**[57].

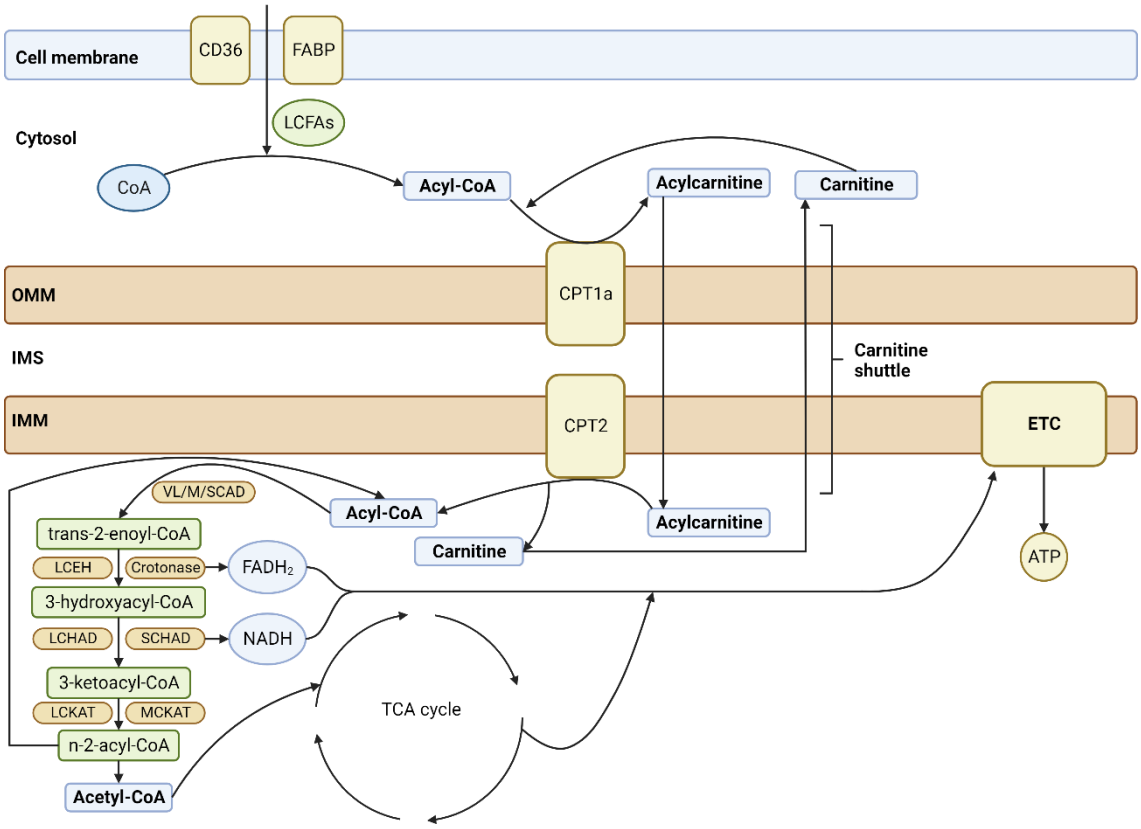

Figure 1.1.3.1: Fatty acid oxidation (FAO).

Simplified schematic outlining the process of FAO (adapted from[57]). Following uptake by CD36 and/or FABPs, LCFAs are combined with CoA to produce Acyl-CoA. CPT1a catalyses a reaction wherein the acyl group is removed from CoA and bound to carnitine, generating acylcarnitine. Acylcarnitine is transported into the mitochondria via the carnitine shuttle (where acylcarnitine is exchanged for carnitine). CPT2 catalyses the transfer of the acyl group back to CoA. Acyl-CoA is then degraded in a multi-step process resulting in the successive removal of two carbons from the acyl group. This process generates $FADH_2$ and NADH as substrates for the ETC, and continues until the generation of acetyl-CoA which serves as a substrate for the TCA cycle, fuelling ATP synthesis. Created with BioRender.com.

CD36: cluster of differentiation 36. FABP: fatty acid binding protein. LCFAs: long chain fatty acids. CoA: coenzyme A. CPT1a/2: carnitine palmitoyltransferase 1a/2. OMM: outer mitochondrial membrane. IMS: intermembrane space. IMM: inner mitochondrial membrane. VL/M/SCAD: very long/medium/short chain acyl-CoA dehydrogenase. LCEH: long chain enoyl-CoA hydrogenase. L/SCHAD: long/short chain (S)-3-hydroxyacyl-CoA dehydrogenase. L/MCKAT: long/medium chain 3-ketoacyl-CoA thiolase. NADH: reduced nicotinamide adenine dinucleotide. $FADH_2$: reduced flavin adenine dinucleotide. TCA: tricarboxylic acid cycle. ETC: electron transport chain. ATP: adenosine triphosphate.

Adapted from Figure 1 in[57].

1.1.3.2: Amino acid metabolism

Amino acid metabolism is a complex process, because there are 20 amino acids with varying chemical structures[61]. This thesis does not focus on amino acid metabolism extensively; therefore, the precise pathways required for metabolism of all 20 amino acids will not be explored here. However, because of its importance in the brain as a neurotransmitter precursor, of relevance to this thesis is the amino acid glutamine (**Chapter 1.3.1**) and an overview of glutamine metabolism is given below. Briefly, the first step of amino acid metabolism involves removing the amine group to generate ammonium ions (NH_4^+) and a carbon skeleton. This carbon skeleton can be used to generate intermediate metabolic products such as α-ketoglutarate (**Figure 1.1.3.2 A**), succinyl-CoA (**Figure 1.1.3.2 A**), pyruvate and acetyl-CoA (**Figure 1.1.3.2 A**)[61], which enter the TCA cycle at various points[61]. An overview of this process, with the entry points of glutamine and glutamate into this cycle, is given in **Figure 1.1.3.2 B**[61].

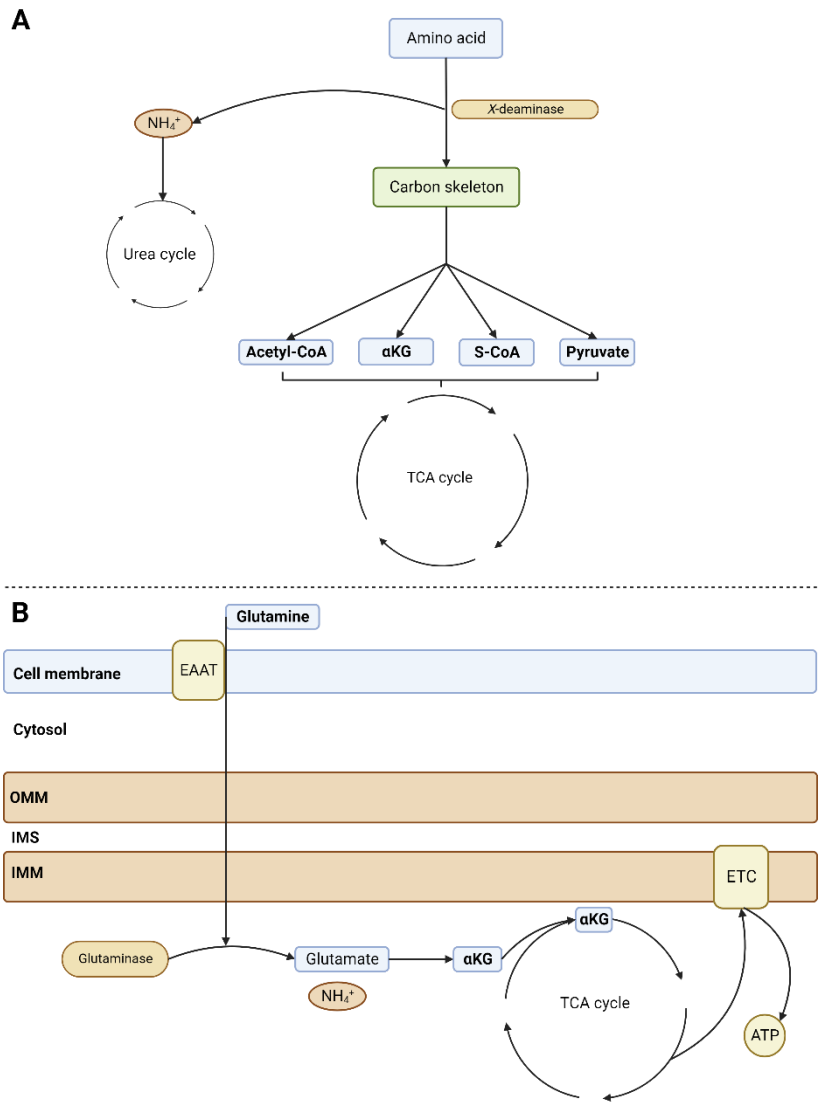

Figure 1.1.3.2: Amino acid metabolism.

A: a broad simplified overview of amino acid (AA) metabolism. AAs are taken up by cells and deaminated, producing a carbon structure and NH_4^+. NH_4^+ is detoxified via the urea cycle. The carbon structure can be modified into various intermediates which can serve as substrates for the TCA cycle, fuelling ATP synthesis. **B:** an overview of glutamine metabolism. Glutamine is taken up via EAATs and transported into the mitochondria. Glutaminase removes the amine group, producing glutamate and NH_4^+. Glutamate can be converted to αKG, fuelling the TCA cycle and ATP synthesis. Created with BioRender.com and adapted from[61].

AA: amino acid. CoA: coenzyme A. αKG: α-ketoglutarate. S-CoA: succinyl-CoA. EAAT: extracellular amino acid transporter. O/IMM: outer/inner mitochondrial membrane. IMS: intermembrane space. NH_4^+: ammonium ion. TCA: tricarboxylic acid. ETC: electron transport chain. ATP: adenosine triphosphate.

1.2: Energy use in the brain

The brain is the organ with the greatest weight-to-energy use ratio in the human body: ~20-25% of daily energy intake is devoted to fuelling this highly complex biological machine[62]. It is critical, therefore, to maintain and regulate energy availability and use in the brain. A major class of cells in the brain are neurons[63]. Neurons are well-characterised as facilitating intercellular communication by electrical impulses, typically manifesting in physiological responses such as memory formation[64], breathing[65], and feeding[66–68]. From a metabolic perspective, neurons are highly specialised cells with intense bioenergetic requirements[69–72], generating much of their energy from OXPHOS of pyruvate[69,71,73,74]. However, neurons are typically reliant on other cells to provide the metabolic support needed to meet the brain's energetic requirements[37,62,72,75–79]. This is facilitated by a second class of cells found in the nervous system, the glia.

1.2.1: Glia

Glia, from the Greek term roughly translating as 'glue' or 'putty'[80], relates to a heterogeneous group of non-neuronal cells in the CNS. The term 'glia' refers collectively to a multifaceted group of cells of various functions, that together play an indispensable role in supporting the nervous system. Unlike neurons, glia do not communicate intercellularly via electrical impulses and instead communicate through the release of 'gliotransmitters'[63,75], a varied group of substances that includes metabolic products such as ATP and lactate[80], L-[79]/D-serine and glutamate[63], as well as other molecules such as cytokines[80] and chemokines[80]. Gliotransmitters are classically considered to facilitate communication between neurons and glia, whereas glia-glia communication is classically considered to be facilitated by gap junctions and hemichannels[81–83]. Despite this, hemichannels and gap junctions are known to be involved with gliotransmitter release, and a role for interglial communication via gliotransmitters is emerging[81–83]. In addition to facilitating neuron-glia and glia-glia communication, gliotransmitters play key roles in CNS development[84–88], regulating neuronal function[89], and providing metabolic support to neurons[37,71,72,75,77,79,90]. Alongside this, glia influence feeding behaviour adaptations[91] to chronic stress[92], and in *Drosophila* glia have been shown to regulate sleep-wake cycles[93]. Moreover, glia help form the blood-brain-barrier (BBB) which facilitates the compartmentalisation of the CNS from the periphery[94–96]. Due to this intimate link with the BBB, glia can dynamically

influence CNS microvasculature to regulate blood flow to regions of the brain in response to changes in energetic or nutrient requirements[97,98] via the release of compounds such as 20-hydroxyeicosatetranoic acid[98] and prostaglandins[99].

There are four predominant classes of glial cells, with many sub-classifications still being elucidated. Broadly speaking, glia can be sub-divided into four classes of cells which help to fulfil the aforementioned functions. Microglia are considered to principally be responsible for controlling the inflammatory response of the CNS and repairing damage[100–104] – though this is influenced by other glial cells[105] – and play a key role in synaptic pruning during CNS development[106]. Another subtype of glial cell, the oligodendrocytes, play a key role in myelinating neurons[107–110] enabling rapid bidirectional neuronal communication throughout the brain, between the brain and the periphery, and influence complex behaviours such as fine motor skills[111]. Less is known of the third subtype, the ependymal cells (including tanycytes), though it is known that these cells help form the blood-brain barrier of the ventricular and subventricular areas of the brain[112,113] and may be involved with nutrient sensing[114–116]. While these various cell populations play indispensable roles in supporting the CNS parenchyma, they are not the focus of this thesis and so are not addressed in detail here.

1.3: Astrocytes

The remaining class of glial cell, astrocytes, are found throughout the brain and wider CNS tissue. These cells are typically defined by their largely stellate (‘star-like’) morphology and projections of fine processes which form close associations with synapses[80]. Unlike the other classes of glial cells, *in vivo* there is no single clear universal indicator of astrocytes, possibly due in part to the structural and functional heterogeneity of these cells. Astrocytes *in vivo* are typically identified by their expression of glial fibrillary acidic protein (GFAP, a component of the cytoskeleton), S100 calcium-binding protein B (S100β), aldehyde dehydrogenase 1 family member L1 (ALDH1L1), and/or vimentin[63,80,117–122]. Expression of these proteins in astrocytes varies depending on brain region – for example, in the hypothalamus, 80% of astrocytes are GFAP immunoreactive, a marked increase compared to other brain regions[80]. *In vitro*, however, astrocytes can be more readily characterised by their immunoreactivity: astrocytes *in vitro* are typically GFAP positive, though other markers such as ALDH1L1,

extracellular amino acid transporters 1 and 2 (EAAT1, EAAT2), and S100β can be used to demarcate astrocytes in culture[123,124].

The fine processes extended by astrocytes help form an intercellular macrostructure with neurons termed the tripartite synapse. Through this structure, and the expression of receptors for various neurotransmitters such as glutamate[123–129], γ-aminobutyric acid (GABA)[130], and potassium-sensitive ATP (K_{ATP}) channels[131–133], astrocytes are able to sense and respond to neurotransmission. Moreover, the tripartite synapse enables astrocytes to modulate neuronal activity through neurotransmitter release[134–137]. Alongside neurotransmitters, astrocytes secrete gliotransmitters, compounds which regulate the activity of neurons and other glial cells (**Chapter 1.2.1**). Among the gliotransmitters released by astrocytes, of increasing interest are products of cellular metabolism, notably, lactate and ATP.

Indeed, lactate is increasingly being recognised as an important signalling molecule in the CNS. Previously considered to be merely an end product of glycolysis, recent work has highlighted a diverse number of circumstances in which lactate signalling in the CNS is crucial to maintaining brain health and normal functioning[40–43,46–51]. Most lactate in the CNS is derived from astrocytes[30,46,80] and mature oligodendrocytes[138]. This is likely because these cells are more reliant on aerobic glycolysis (metabolism of glucose to produce lactate [a metabolite traditionally associated with anaerobic metabolism[139]] under normoxic conditions[139,140]) to meet their energetic requirements[79,141–143] than neurons[79,144,145] and microglia[146], which are more reliant on OXPHOS. To facilitate their lactate production, alongside readily metabolising glucose absorbed from the blood, astrocytes also hold large glycogen stores, which are used to supplement lactate production from astrocytes in response to increased neuronal activity or low glucose availability[147,148]. This has been shown to support cognitive functions such as learning and memory formation[148–151], highlighting the importance of astrocyte-derived lactate for maintaining CNS function. Meanwhile, astrocyte ATP secretion is facilitated by intracellular Ca^{2+}-dependent and -independent flux in response to stimuli such as neurotransmitter release, and is in turn associated with regulation of neuronal function[80,152–155]. This has been hypothesised to regulate whole organism behaviours such as food-seeking and resting in response changes to the energetic requirements of the brain[152,156,157].

Astrocytes also release ATP in response to CNS insults and trauma, where ATP acts as a damage-associated molecular pattern[19,20,152,154,158]. Astrocytes detect ATP signalling via purinergic (P2) P2X and P2Y receptors[152], thus ATP signalling has been suggested as a means by which astrocytes (or indeed glial cells more generally) can communicate intercellularly[159–161].

Astrocytes also provide structural and developmental support to the CNS. In conjunction with tanycytes and endothelial cells, astrocytes form the BBB[80,95–98,162–164]. Through projections termed endfeet, astrocytes absorb nutrients (i.e., glucose, lipids, cholesterol, H_2O, and inorganic ions) from the blood[165,166]. To facilitate this, astrocytes express various transporter proteins, such as glucose transporter 1[166,167] (GLUT1), cluster of differentiation 36 (CD36), fatty acid binding proteins (FABPs)[117,168,169], apolipoprotein E (ApoE)[170–172], aquaporin-4[165,166], and sodium/potassium ion transporters[173,174]. Nutrients can then subsequently be further distributed to other cells of the CNS to maintain homeostasis, or be metabolised by astrocytes. However, the relationship between astrocytes and the BBB extends beyond nutrient uptake: in response to fluctuations in neuronal activity or metabolic demand of the CNS tissue, astrocytes influence vasoconstriction and vasodilation of capillaries to modulate blood supply[16,97,98]. Astrocytes can promote vasoconstriction by modulating their secretion of 20-hydroxyeicosatetranoic acid, an eicosanoid and potent vasoconstrictor[98], whereas these cells may also promote vasodilation in response to hypoxia via the release of nitric oxide[175,176]. These effects have been touted as potential therapeutic targets for conditions where modulation of the fine control of the brain vasculature may prove beneficial. Furthermore, as constituents of the BBB, astrocytes are well positioned to sense and respond to circulating signalling molecules from the periphery, and CNS trauma or insult[102,104,177]. In response, astrocytes secrete a variety of pro- and anti-inflammatory compounds including cytokines, chemokines, and neurosteroids[102,104,167,178–180]. Moreover, astrocytes produce reactive oxygen species[181,182] and exhibit phagocytic potential[80,183–185], though this is not considered part of the typical astrocyte inflammatory response. In addition to this, astrocytes can participate in wound healing, migrating through tissue and undergoing profound morphological shifts thanks to their structural plasticity[80,186]. Many of these functions are reliant, at least in part, on the flexible and dynamic metabolic profile of astrocytes.

1.3.1: Metabolism in astrocytes

The importance of astrocyte metabolism for maintaining CNS homeostasis, and how this may go awry in pathogenic states, is increasingly being appreciated. As outlined in **Chapter 1.3**, astrocytes are a key source of lactate in the CNS and this molecule fulfils various functions. Alongside regulating cognitive functions and neurodevelopment, astrocyte-derived lactate (secreted through monocarboxylate transporters) is thought to provide neurons with critical trophic support as part of the astrocyte-neuron lactate shuttle[80,187]. This hypothesis posits that astrocytes help meet the energetic costs of neuronal activity by upregulating glycolysis and secreting the lactate produced into the extracellular milieu[187,188]. This lactate is thought to be taken up by neurons so to alleviate the metabolic burden on these cells by permitting the conversion of lactate to pyruvate and its subsequent incorporation into the TCA cycle (**Figure 1.1.2**)[187,188]. However, the astrocyte-neuron lactate shuttle hypothesis remains controversial[80] due to conflicting evidence – for example, alongside increases in astrocyte metabolism, a concomitant increase in neuronal glucose metabolism with increased neuronal activity has been reported[189], suggesting that neuronal activity may not be primarily fuelled by astrocyte-derived lactate. In contrast, astrocyte-derived lactate has been shown to regulate mRNA translation in neurons[150], suggesting that astrocyte-derived lactate is essential for at least some neuronal functions to take place following increased neuronal activity. Although the necessity of astrocyte-derived lactate for neuronal function remains an area of debate, the associations between astrocyte-derived lactate and cognitive functions (outlined in **Chapter 1.3**) nonetheless highlight the importance of astrocyte metabolism for proper CNS function[147–151,190–194].

Crucially, the function of astrocytic glycolysis extends beyond providing trophic support to neurons. Morphological plasticity is an energetically expensive process[195] yet is central to many key astrocyte functions, including the regulation of synaptic plasticity and the response to CNS injury (**Chapter 1.3**). Astrocytic morphological plasticity is also a key factor under physiological conditions astrocytes where these cells notably modulate their fine processes in response to neuronal activity[80,196]. Rapid morphological plasticity in the face of enhanced neuronal activity places an energetic burden on astrocytes, which may be readily countered by the high glycolytic capacity of astrocytes, providing both rapid ATP

and pyruvate as a substrate for further mitochondrial respiration[197]. The glycolytic profile of astrocytes is facilitated by abundant expression of enzymes associated with glycolysis, such as various hexokinases (HKs) and the enzyme 6-phosphofructo-2-kinase/fructose-2,6-biphosphatase 3[72,76]. In particular, HKs exhibit a strong affinity for glucose (Michaelis constant [K_m] = 0.3mM[198]), and catalyse one of the rate-limiting steps of glycolysis by phosphorylating glucose to form glucose-6-phosphate (**Figure 1.1.1**). Expression of 6-phosphofructo-2-kinase type 3 in astrocytes promotes glycolysis during metabolic stress[199]. The importance of glycolysis for facilitating astrocyte functionality is further underscored by its regulation as part of the astrocyte inflammatory response (covered in detail in **Chapter 1.3.3**). Briefly, during this process astrocytes undergo rapid morphological shifts such as hypertrophy and extension of processes toward sites of insults or injury, alongside migration through the brain parenchyma to aid wound healing[179,200–203]. This may be readily facilitated by the glycolytic profile of these cells enabling rapid ATP provision. Thus, a predominantly more glycolytic metabolic profile of astrocytes may facilitate the rapid responses to environmental fluctuations and perturbations required to maintain CNS homeostasis.

Although astrocytes are renowned for their glycolytic capacity, these cells are characterised by their metabolic flexibility. Indeed, astrocytes are readily able to metabolise a variety of substrates beyond glucose owing to their substantial expression of a variety of proteins involved with different metabolic pathways[204,205]. Notably, astrocytes express high levels of the rate-limiting enzyme of FAO, carnitine palmitoyltransferase 1a (CPT1a), relative to microglia[206,207]. FAO (discussed in detail in **Chapter 1.3.1.1**) is an important facet of astrocyte metabolism which helps fulfil various functions[89,208–210]. Astrocytic amino acid metabolism is also important: in the CNS, astrocytes are responsible for *de novo* synthesis of glutamate[211] (a process controlled by pyruvate decarboxylase[135]), which is then shuttled to neurons to fuel glutamatergic neurotransmission[212] a facet of astrocyte metabolism which further underscores key role of these cells in supporting the CNS. Excess glutamate can be taken up from the synaptic cleft by astrocytes and converted back into glutamine by glutamine synthetase[213] where it may then be used to fuel astrocytic

metabolism[214], be converted to glutamate[135], or used to fuel the inflammatory responses of astrocytes, as occurs in the peripheral immune system[215].

Crucially, loss of astrocyte metabolic flexibility has been implicated in a variety of conditions that associate with neuroinflammation or neurodegeneration[76,211,216–218] (**Chapter 1.3.3, 1.3.4**; **Figure 1.3.4**), highlighting the importance of this aspect of astrocyte biology to maintaining CNS functionality.

1.3.1.1: Fatty acid oxidation (FAO) in astrocytes

In addition to glycolysis, astrocyte FAO is important for maintaining CNS health and function. A byproduct of neuronal activity is the accumulation of intracellular lipid droplets containing a mixture of free fatty acids (including long chain fatty acids)[210,219], yet despite their predominant energetic reliance on OXPHOS neurons exhibit low levels of FAO activity[209]. This has speculatively been linked to the poorer ATP yield:oxygen ratio of FAO compared to a relatively more efficient process such as oxidative phosphorylation of glucose[220]. Astrocytes, however, are well-equipped to metabolise lipids. This is because astrocytes express the machinery required to take up and shuttle lipids intracellularly (ApoE[171,221,222], CD36[117], and FABPs[169,223]) and express CPT1a[206,207] in relative abundance compared to neurons[206] and microglia[206,207]. CPT1a catalyses the addition of the acyl group from acyl-coenzyme A (acyl-CoA) onto carnitine to facilitate mitochondrial import (the rate-limiting step of FAO; **Figure 1.1.3.1**)[9,224], thereby permitting ample FAO to take place within astrocytes.

Because lipids serve multiple roles within the cell such as the generation of eicosanoids[225], formation of organelle membranes or post-translational modifications[226], FAO activity in cells is usually maintained at a minimal level to conserve lipid levels. However, astrocyte FAO serves key functions in the CNS, thus this metabolic pathway exhibits relatively enhanced activity in these cells[89]. This is evidenced by the fact that as well as promoting neuronal survival through lipid shuttling, astrocyte FAO is crucial for maintaining cognitive faculties. Morant-Ferrando *et al*.[89] recently demonstrated that loss of FAO via selective CPT1a knockout in astrocytes induced increased abundance of long- and very-long chain fatty acids (such as palmitate [C16]). Moreover, this study found that astrocytes met approximately 35% of their metabolic requirements via FAO, and loss of astrocytic CPT1a worsened outcomes in behavioural assays of cognitive performance[89]. Separate bodies of evidence have demonstrated that, through an

as-yet unclear mechanism, prolonged exposure to these long- and very-long chain fatty acids is associated with cell death in the periphery[227–230]; thus astrocyte FAO capacity may also serve a neuroprotective function. Taken together, this combined body of evidence suggests that FAO is a tightly regulated and crucial process within astrocytes, and more widely demonstrates the importance of astrocyte metabolism for a variety of functions in the CNS beyond regulation of brain energy homeostasis. However, the mechanisms which regulate astrocyte metabolic flexibility, particularly regarding regulation of FAO, have yet to be fully elucidated.

1.3.2: Calcium ion (Ca^{2+}) signalling

Calcium ion (Ca^{2+}) signalling is an important ionic signalling mechanism in astrocytes which underlies many processes including cytoskeletal rearrangement and secretion of gliotransmitters[80,231–233]. For many years, due to the lack of overt electrical excitability observed in astrocytes, these and other glial cells were disregarded as unimportant for CNS functionality because of the prevailing view that electrical excitability governed the contribution of cells in the CNS to particular outcomes. In the 1990s, Ca^{2+} signalling in astrocytes was revealed to be an important ionic signalling mechanism by which astrocyte-astrocyte and astrocyte-glia communications were propagated and distributed[80,231]. Changes in astrocyte Ca^{2+} signalling may be facilitated by extracellular stimuli such as neurotransmitter binding[231,232]. Alongside this, astrocytes exhibit intracellular waves of Ca^{2+}, though the functions of these waves remain unclear[232]. Thus, alongside regulation of metabolism and substrate utilisation, Ca^{2+} signalling – perhaps related to interplay between the endoplasmic reticulum (ER) and mitochondria[234] – within these cells represents an important mechanism by which astrocytes maintain CNS homeostasis. As with many cells, this mechanism is closely linked to regulating cytoskeletal rearrangement[235,236], possibly as a key facilitator of astrocytic responses to stimuli.

1.3.3: Astrocyte reactivity

As mentioned above, as part of their role in maintaining CNS homeostasis, astrocytes detect and respond to a variety of stimuli. This includes inflammatory stimuli arising from trauma or insult to the CNS[20], CNS pathologies such as

Alzheimer's disease[218,237], or peripheral conditions associated with chronic low-grade inflammation such as obesity[14,238–241]. Therefore, these inflammatory signals may originate from peripheral immune cells[241,242], microglia[104,243], or other astrocytes[243,244]. These signals are detected by astrocytes via a variety of receptors, including toll-like receptors (TLRs)[245,246], various interleukin receptors[247–249], the tumour necrosis factor (TNF) receptor (TNFR)[250,251], and chemokine-axis-chemokine (CXC) receptors[252,253]. Activation of these receptors activates downstream signalling cascades, such as the Janus kinase-signal transducer and activator of transcription 3 (JAK-STAT3)[254] or the nuclear factor kappa light chain enhancer of activated B cells (NFκB) pathways[167,238,255]. In turn this leads to secretion of pro-inflammatory (e.g., TNF[167,243,245], IL-1β[248,249,254] , complement proteins[256,257]) and anti-inflammatory (e.g., IL-4[258], IL-10[167]) factors from astrocytes, alongside modulation of astrocyte metabolism[141,167,181,255] (**Chapter 1.3.3.1**) and reactive oxygen species production[119,182,259,260].

Astrocytes responding to inflammatory stimuli are colloquially said to become 'reactive'. This umbrella term reflects a spectrum of inflammatory responses in these highly complex cells, encompassing the potential for a wide variety of pro- and anti-inflammatory states[261]. These states are accompanied by the complex interplay of activation of inflammatory signalling pathways, morphological responses, Ca^{2+} signals, and metabolic changes (**Chapter 1.3.4**) which collectively preserve and restore CNS function[104,119,261–264]. Thus, this 'reactivity' is a key mechanism by which astrocytes support the CNS.

1.3.3.1: Astrogliosis and CNS pathologies

As outlined above, astrocyte 'reactivity' plays a key role in resolving CNS trauma and is essential for maintaining CNS physiology. However, during CNS pathologies, astrocytes may become chronically activated[119,261,265]. This chronic activation state is associated with various changes including marked upregulation of the cytoskeletal protein GFAP and hypertrophy (possibly linked to increased aquaporin-4 expression[266–268]), prolonged secretion of pro-inflammatory signalling molecules, and enhanced proliferation[261,262,264,265,269]. Termed 'astrogliosis'[270,271], this phenomenon forms a part of the larger and more widespread response of glial cells to chronic inflammation known as 'gliosis'[272,273]. Astrogliosis is associated with disorders including chronic traumatic encephalopathy[274], Alzheimer's disease[275], amyotrophic lateral sclerosis[276,277],

stroke[278–280] (ischaemic[279] and haemorrhagic[280]), and brain cancers[281]. Thus, astrogliosis has been employed as a port-mortem indicator of various CNS pathologies[270].

Curiously, astrogliosis has recently been touted as the result of a prolonged and initially protective phenotype *in vivo*[218]. In this paradigm, astrocytes initially adopt a more inflamed phenotype to facilitate neuroprotective and homeostatic responses to inflammatory stimuli and CNS insult[218,261]. With continuous exposure to inflammatory stimuli, it is thought that astrocytes lose their homeostatic function and become 'paralysed' in a reactive state, leading to continuous inflammatory responses from these cells and CNS degeneration[218,261]. Through complex interplay with other cells of the CNS, particularly microglia, this may manifest as one of several pathologies centring around a key theme of chronic neuroinflammation and neurodegeneration[218,261]. It is as yet unclear whether astrogliosis is a causative mechanism of CNS pathology, or a correlative one[270,282]. Regardless, it is known that (in common with astrocyte reactivity[141,167,181,255]) astrogliosis results in substantial modulation of astrocyte functionality which has been linked to a metabolic shift in the CNS[218,269,283].

1.3.4: Metabolism in reactive astrocytes

As indicated in **Chapters 1.3.3** and **1.3.3.1**, astrocyte reactivity is associated with modulation of astrocyte metabolism[141,167,181,255] (**Figure 1.3.4**). The plethora of changes associated with astrocyte reactivity incur intense metabolic costs, which likely underlie the observed shifts in astrocyte metabolism. This possibility is supported by observations in peripheral immune cells and microglia. During short-term (acute) inflammatory responses (up to ~6h), peripheral macrophages[41,284–286] and microglia[207,287,288] become more reliant on glycolysis. This is reflected by increased glucose uptake, hexokinase-2 (HK2) activity and lactate production. In contrast, during the chronic inflammatory response (≥~6h), these cells become more reliant on FAO and oxidative phosphorylation of pyruvate as sources of ATP[41,207,287,288]. These bodies of evidence have contributed to the proposition that inflammation and metabolism are intricately linked processes; this relationship has been termed 'immunometabolism'[40,289,290].

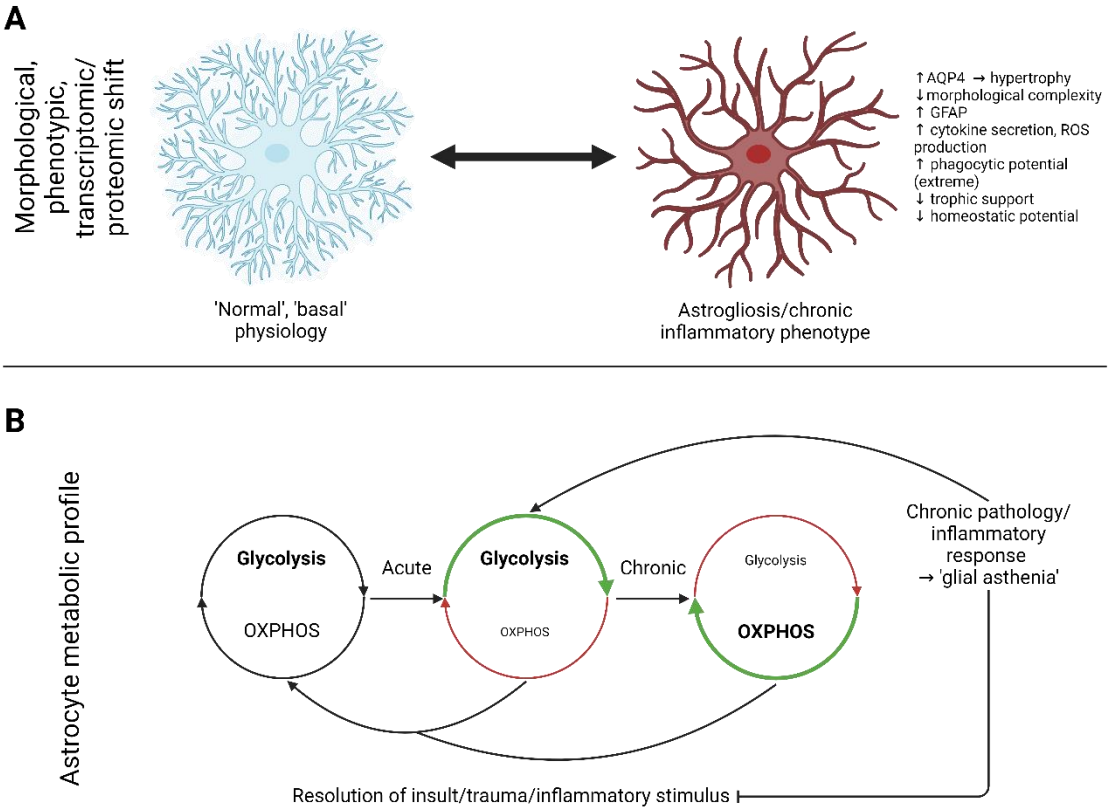

Figure 1.3.4: Astrocyte inflammatory responses correlate with a metabolic shift.

Upon inflammatory stimulation, astrocytes undergo a morphological shift (**A**). This includes morphological changes such as loss of fine processes and hypertrophy[241,273]. Increased GFAP expression, cytokine secretion and ROS production are also associated with the inflammatory responses of astrocytes[117,167,241,270,291–293]. Under extreme conditions, astrocytes may exhibit increased phagocytic potential[184]. These shifts are associated with a reduced ability of astrocytes to maintain homeostasis within the CNS parenchyma[294], and the capacity to provide trophic support to neurons may be reduced[261]. Upon resolution of the insult to the CNS parenchyma, 'astrogliotic'-like astrocytes (red) return to a 'normal' physiological state (blue) with the reversal of many of these phenotypes. Crucially, the inflammatory responses of astrocytes are accompanied by a shift in their metabolic profile (**B**)[167,255]. Normally reliant on glycolysis with some detectable OXPHOS activity[79,141–143], in the acute phase of inflammatory responses astrocytes become more reliant on glycolysis[167,255]. In chronic, long term inflammatory responses, astrocytes become more reliant on OXPHOS and less reliant on glycolysis to meet their bioenergetic requirements[167,255]. In chronic pathologies, 'glia asthenia' may occur as a result of prolonged astrogliosis[218,261]. Here, the astrocyte becomes paralysed in an inflamed state and cannot return to its 'basal' state. This may be due to continued pro-inflammatory stimulation, or an inhibited ability to resolve the inflammatory stimulus[218,261]. Alternatively, glial asthenia may prevent the resolution of the inflammatory stimulus. The mechanisms regulating the shifts in astrocyte metabolism during inflammatory responses remain unclear.

OXPHOS: oxidative phosphorylation. AQP4: aquaporin-4. GFAP: glial fibrillary acidic protein. CNS: central nervous system. ROS: reactive oxygen species.

Created with BioRender.com.

Similar trends been observed in astrocytes. Initial data in the early 2000s indicated that exposure to inflammatory stimuli modulates astrocyte metabolism[295] suggesting that the trends observed in the periphery might be conserved in the CNS. A recent study from our laboratory group demonstrated that 3h stimulation of mouse primary astrocytes *in vitro* with lipopolysaccharide (LPS; an outer membrane component of many Gram-negative bacteria[296] and potent inflammatory stimulus in mammalian cells[297]) was associated with increased glycolysis, whereas 24h stimulation of these cells with LPS reduced reliance on glycolysis and enhanced mitochondrial respiration in an NFκB-dependent manner[167]. Supporting this, using a model of multiple sclerosis, Chao *et al*.[255] demonstrated that reactive astrocytes exhibit reduced lactate secretion by inhibiting mitochondrial localisation of HK2 (required for its activity)[255]. Moreover, this study demonstrated that this contributed to reduced neuronal survival in an *in vitro* indirect co-culture system[255]. This trend has also been observed in astrocytes derived from rat neonates, suggesting functional conservation across species and indicating a role for modulation of astrocyte metabolism in astrocyte 'reactivity'[298]. These findings correlate with those from a murine model of neurodegeneration: using *ex vivo* primary astrocytes from the 5xFAD model of Alzheimer's disease, Gijsel-Bonnello *et al.*[299] highlighted significant reductions in the activity of the metabolic enzymes pyruvate kinase and glucose-6-phosphate dehydrogenase, as well as enhanced GFAP immunoreactivity and enhanced IL-1β secretion, suggesting these metabolic changes were linked to a 'reactive' phenotype. Furthermore, *in vivo* studies of neurodegenerative disorders have revealed an association between glucose uptake and astrocyte reactivity[218], supporting this link.

More generally, metabolic dysfunction in astrocytes also correlates with non-pathological cognitive ageing (i.e. normative cognitive ageing[300]), possibly due to gradual accumulation of systemic inflammation[301]. Jiang and Cadenas[302] demonstrated that astrocytes in aged Sprague-Dawley rats (18 months) were more reliant on mitochondrial respiration of pyruvate than younger (7 months) counterparts, suggesting a reduced ability to provide trophic support to neurons is associated with aged astrocytes. Crucially, increased age was associated with increased H_2O_2 production (13 months compared to 7 months), nuclear translocation of NFκB (signifying activation) (elevated at 13 and 18 months

relative to 7 months) and increased reliance on mitochondrial respiration in response to cytokine stimulation (13 months)[302]. Thus, the clinical potential of targeting mitochondrial function in astrocytes likely extends beyond applications to neurodegenerative conditions, and may represent a tangible therapeutic target to reverse the cognitive decline associated with healthy ageing by restoring mitochondrial functionality in astrocytes.

The chronic inflammation associated with systemic metabolic disorders such as obesity has also been associated with modulation of astrocyte metabolism and increased astrocyte 'reactivity'. Indeed, caloric excess associated with high-fat diet (HFD) consumption for three days is sufficient to incur a reactive phenotype in astrocytes of the mouse hippocampus, indicated by enhanced GFAP expression and morphological alterations[303]. Chronic HFD feeding in mice is associated with the induction of a similar phenotype (enhanced GFAP immunoreactivity and hypertrophied astrocytes) on a larger scale[14,241]. This demonstrates that perturbations to systemic energy availability have a profound effect on astrocytes. A separate study showed that the hypothalamic inflammation associated with HFD-induced obesity is reliant upon NFκB signalling in murine astrocytes, demonstrating the key role astrocytes play in regulating CNS inflammatory responses[238]. Crucially, these astrocytes exhibit a shift in metabolism toward FAO, supporting the notion that metabolic state may influence the inflammatory response of these cells. Despite our increasing understanding of how inflammation modulates astrocyte metabolism and how the metabolic state of the whole organism may influence astrocyte reactivity, the mechanisms which regulate astrocyte metabolic flexibility during reactivity remain to be fully elucidated.

Together, these data from both *in vivo* and *in vitro* studies indicate that cellular metabolism is a major determinant of astrocyte reactivity. Related studies from other immunocompetent cells indicate that modulation of astrocyte metabolism holds promise as a means of therapeutically alleviating astrocyte reactivity in a variety of pathological conditions and may have applications in preserving cognitive function during healthy ageing. However, the mechanisms which regulate astrocyte metabolic flexibility, and how these are affected during astrocyte reactivity, remain poorly understood.

1.4: Translocator protein 18kDa (TSPO)

The mitochondrial translocator protein 18kDa (TSPO) is a small pentameric transmembrane domain protein found on the outer mitochondrial membrane (OMM) of mammalian cells[304–306]. There are two isoforms of TSPO in humans, termed TSPO1 (herein referred to as 'TSPO') and TSPO2. TSPO2 is truncated, does not localise to the OMM, and is not the subject of this thesis. In humans, the *Tspo* gene is encoded on Chromosome 22 at the q13.2 locus. First discovered in 1977 as a binding site for benzodiazepines in the periphery[307], TSPO was later determined to be near-ubiquitous among mammalian cells and tissues[306,308–310]. Since its discovery, TSPO has been linked to a variety of cellular functions including steroidogenesis[308,311], inflammatory responses[312–314], and regulation of cellular metabolism, and has thus been posited as a therapeutic target; however, there is currently no consensus on the 'true' function of TSPO due to variability between studies focussing on different tissues and types of cells.

1.4.1: Evolution of TSPO

The evolution of organelles is somewhat difficult to establish using the traditional paleontological techniques that are employed to study macrostructures found within multicellular organisms, since organelles generally do not fossilise well. However, advances in phylogenetic techniques and genetic lineage tracing have meant TSPO is known to exhibit a very great degree of genetic conservation. The bacterial analogue *TspO* is widely expressed in bacteria, such that only a single bacterial species has reported to be naturally TSPO deficient (*Escherichia coli*)[315,316]. TSPO analogues are similarly expressed in the fungal kingdom with *Saccharomyces cerevisiae* being the only recorded exception[315,316]. In animals and plants, TSPO is near-ubiquitous[315,316] and at the time of writing there has been no report of complete endogenous TSPO deficiency in organisms of these kingdoms. In mammals, *Tspo* is expressed at some level in nearly every tissue[315–319], though according to one report the Syrian hamster does not express *Tspo* in its adrenal cortex[320].

The extent to which *Tspo* has been conserved perhaps indicates that TSPO plays a key role in cells. This notion is supported by evidence showing that the rat *Tspo* gene can functionally replace the *TspO* analogue in *Rhodobacter sphaeroides*, despite the gene sequences only being 35% homologous[321]. Further support for

this viewpoint stemmed from early observations that genetic ablation of TSPO in mice was lethal[322,323], thus fuelling speculation that TSPO may be a requisite component for organismal development, hence explaining the extent to which TSPO is conserved. Later developments in genome editing technologies refuted this hypothesis since these more refined techniques did not coincide with conditional lethality[324,325]. Indeed, several strains of TSPO-deficient mice have been independently developed, with no overt adverse basal phenotype observed during development or adulthood[324–328], suggesting that the presence of TSPO is not a prerequisite for life.

1.4.2: Structure and function of TSPO

The *Tspo* gene encodes 4 exons with an approximate amplicon length of 1075 base pairs, allowing once introns have been spliced out during the transcription process. These exons are ultimately translated into a 169 amino acid sequence with a molecular weight of ~18kDa, consisting of five transmembrane domains (TMDs)[329,330] (**Figure 1.4.2.1 A**). The TMDs are all α-helices[331] which assemble into the order 1-2-5-4-3, forming a hydrophobic macrostructure (**Figure 1.4.2.1 A**). Of notable interest is a region of TMD 5 encompassing amino acids 147 to 159[329,330], referred to as the cholesterol recognition/interaction amino acid consensus motif (CRAC motif, CRAC domain)[329,330,332] (**Figure 1.4.2.1 A, B**). These studies revealed that, alongside cholesterol, the TSPO CRAC domain is intimately involved with the binding of endogenous and synthetic TSPO ligands[329,330,332] (**Chapter 1.4.6**), and may have some involvement in the formation of protein complexes that include TSPO. Alongside cholesterol transport, TSPO has been linked to energetically expensive processes such as steroidogenesis. Combined findings from several reports demonstrate that TSPO and the steroidogenic acute regulatory protein (StAR) work in tandem to bind to cholesterol and facilitate its mitochondrial transfer as part of a wider complex involving the cytosolic proteins acyl-CoA binding domain containing 3 (ACBD3)[333], 14-3-3γ[315] and 14-3-3ε[315], and the intramitochondrial proteins cytochrome P450 family 11 subfamily A member 1 (CYP11A1) and ATPase family AAA domain containing 3a (ATAD3A)[315]. This may imply a role for TSPO as a regulator of inflammatory or metabolism: steroid biosynthesis is metabolically expensive[334,335], and steroids such as glucocorticoids[336–338] have immunomodulatory effects.

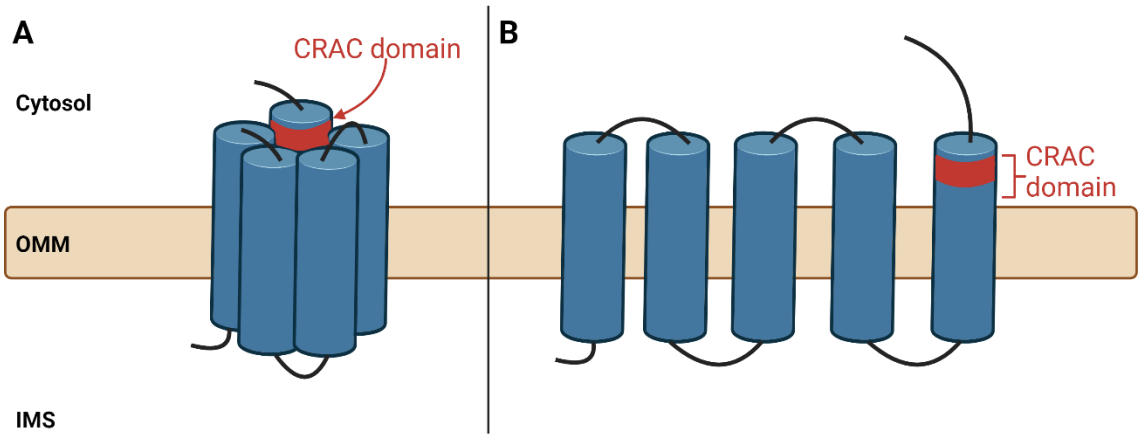

Figure 1.4.2.1: Structure of TSPO.

A: transverse view of the 3-dimensional structure of TSPO. α-helices assemble into a pore-like structure on the outer mitochondrial membrane. The CRAC domain is indicated by the red band. **B:** transverse view of TSPO in open linear conformation showing transmembrane domains, with the CRAC domain of TMD5 highlighted by the red bracket. The CRAC domain (red band) is thought to facilitate ligand binding to TSPO.

TSPO: translocator protein 18kDa. OMM: outer mitochondrial membrane. IMS: intermembrane space. CRAC: cholesterol recognition/interaction amino acid consensus. TMD: transmembrane domain.

Created with BioRender.com.

In addition to potentially modulating steroidogenesis, TSPO has been separately linked to the regulation of inflammatory responses, which is particularly apparent in the CNS where TSPO deficiency has been observed to affect the immune functions of microglia[339–341]. Inflammatory functions directly linked to TSPO by these bodies of evidence include phagocytosis[339,340] and cytokine release[339,341]. However, a putative link between TSPO and phagocytosis was first touted in neutrophils via an interaction with NAPDH oxidase 2 (NOX2)[342] and further substantiated by work in microglia using co-immunoprecipitation[343]. In the same year, an interaction between TSPO and another NOX isoform (NOX1) was reported[344]. NOX activity is largely responsible for the oxidative burst seen following phagocytosis, which may explain the findings from other studies showing that TSPO-deficient microglia show impaired phagocytic potential[339,340]. A link between TSPO and regulation of inflammatory responses was further supported by evidence from a study suggesting that TSPO radioligands activate the nuclear factor erythroid 2-related factor 2 (NRF2) pathway (which works to protect cells from oxidative stress during inflammatory responses) in retinal pigment epithelial cells, while attenuating IL-1β, IL-8, and IL-6 release from these cells in response to inflammatory stimulation[345]. A separate study showed that TSPO ligands could reduce activation of the nucleotide-binding oligomerization domain-like receptor family pyrin domain containing 3 (NLRP3) 'inflammasome' (a complex linked to secretion of IL-1β and IL-18), as did TSPO ablation via transient knockdown[346]. In common with steroidogenesis, inflammatory responses are energetically costly processes, hinting that TSPO may play a role in regulating processes requiring metabolic dynamism or flexibility.

TSPO is known to form a complex with the voltage-dependent anion channel (VDAC)[347,348], another constituent of the OMM (**Figure 1.4.2.2**). The function of this interaction remains unclear, but this may play a role in the formation of a multi-unit protein complex known as the mitochondrial permeability transition pore (MPTP)[349]. The MPTP is a channel which allows the influx of small molecules (~≤1.5kDa) and cations, notably Ca^{2+}, to the inner mitochondria[349]. Alongside VDAC, TSPO has been shown to form a complex with the adenine nucleotide transporter[350] (ANT; involved with cellular metabolism and thought to be linked to export of intramitochondrial ATP[56]), further substantiating associations between TSPO and cellular metabolism.

Interestingly, alongside its various direct interactions with cytosolic and mitochondrial proteins, TSPO has been reported to undergo homo-oligomerisation, forming polymers ranging from homodimers[329,351–354] to polymers[353,355] in a variety of model organisms from bacteria[354] to mice[332,353] and humans[304,355]. The true extent of TSPO oligomerisation and its effects on TSPO function have yet to be determined but remain an interesting potential avenue that may have therapeutic applications. As well as homo-oligomerisation, TSPO has also been proposed as a putative mediator of interactions between mitochondria and other organelles, notably the endoplasmic reticulum (ER). The ER is a major site of protein transport, and a role in cellular metabolism has also been touted, supporting the notion that TSPO also be involved with these processes (**Chapter 1.4.3**). The ER is also a major site of Ca^{2+} storage and has been linked to intramitochondrial transport of Ca^{2+} [356]. Curiously, a link between TSPO and regulation of Ca^{2+} dynamics has been suggested from data in mouse embryonic fibroblasts[357], neurons[357] and tanycytes *in vitro*[358], indicating that these mechanisms may also be present in other cell types. The body of work in tanycytes[358] also linked TSPO to regulation of cellular energy levels, further substantiating this link.

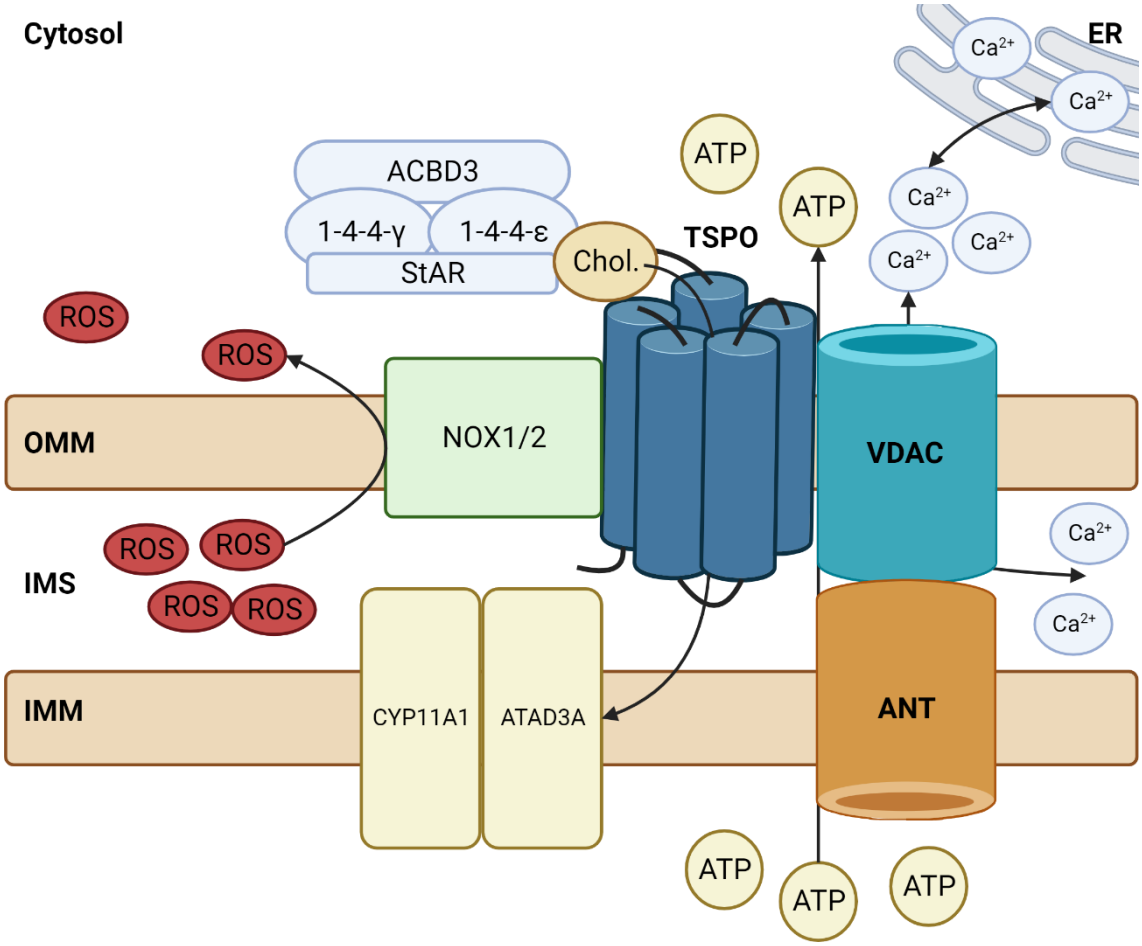

Figure 1.4.2.2: Putative TSPO interactions.

Schematic showing putative TSPO interactions. TSPO is thought to interact with ACBD3, 1-4-4γ, 1-4-4ε, and StAR to facilitate mitochondrial import of cholesterol[315,333]. TSPO interacts with VDAC and ANT, possibly to facilitate mitochondrial ATP export via ANT and Ca^{2+} flux via VDAC, potentially via an interaction with the ER[56,347–350,357,358]. TSPO interacts with NOX1 and 2, possibly to promote ROS production during inflammatory responses[342–344].

TSPO: translocator protein 18kDa. ACBD3: acetyl-coenzyme A binding domain containing 3. StAR: steroidogenic acute regulatory protein. CPY11A1: cytochrome P450 family 11 subfamily A member 1. ATAD3A: ATPase family AAA domain containing 3a. VDAC: voltage dependent anion channel. ANT: adenine nucleotide transporter. ROS: reactive oxygen species. NOX1/2: nicotinamide adenine dinucleotide phosphate oxidase 1, 2. ER: endoplasmic reticulum. ATP: adenosine triphosphate. Chol.: cholesterol. OMM: outer mitochondrial membrane. IMS: intermembrane space. IMM: inner mitochondrial membrane.

Created with BioRender.com.

1.4.3: TSPO: a regulator of cellular metabolism?

TSPO was first implicated in the regulation of cellular metabolism in the prokaryote *R. sphaeroides* in 1997 by Yeliseev *et al*., who demonstrated a role for TSPO as an oxygen sensor in this organism[321]. In 2000, the TSPO homologue in *Sinorhizobium meliloti* was shown to regulate gene expression in response to osmotic stress, as well as deprivation of oxygen, nitrogen and carbon, further suggesting a role in metabolic regulation in prokaryotes[359]. Later, in 2015, Busch and Montgomery demonstrated that deletion of a TSPO homologue in *Fremyella diplosiphon* reduced growth under salt stress, and induced sensitivity to oxidative stress induced by methyl viologen stimulation[360]. Moreover, TSPO expression was increased in response to green light exposure – likely correlating with enhanced energy production in *F. diplosiphon* as it is a cyanobacterium. In the same year, TSPO homologue expression in *Pseudomonas fluorescens* was shown to be regulated in response to osmotic stress[361]. Thus, given the extent to which TSPO is conserved (outlined in **Chapter 1.4.1**), this lends credence to the postulate that TSPO may be conserved across eukaryotes primarily as a regulator of cellular metabolism following the evolution of mitochondria.

This stance is further supported by evidence from plants, in which TSPO is also expressed. In *Arabidopsis thaliana*, expression of the *Tspo* gene homologue has been linked to salt stress[362,363], and TSPO knockdown in this organism represses genes involved with the synthesis of tetrapyrroles, which are important for detoxification of reactive oxygen species[362]. Conversely, overexpression of TSPO in *A. thaliana* reduces 'greening' of these plants in the presence of light, suggesting that TSPO overexpression is detrimental to these organisms[363]. In chronic neuroinflammation, TSPO is overexpressed within the CNS; thus, this body of evidence may further substantiate a link to stress responses and hint at resulting changes to energy production. Moreover, in *Physcomitrella patens*, TSPO is linked to redox homeostasis by binding to haem and porphyrins[364], and has been implicated in regulation of the oxidative burst in this organism[364,365].

In mammals, TSPO is linked to a wider range of apparently disparate functions, which are energetically expensive, suggesting that TSPO may be involved with regulating cellular energy homeostasis. The first direct evidence for TSPO in regulating cellular metabolism in mammals came in 2014 following the generation

of a complete TSPO knockout in mice[324]. This was closely followed by a study published in 2016 which showed that TSPO-deficient ($TSPO^{-/-}$) Leydig cells have lower metabolic rates than TSPO-expressing ($TSPO^{+/+}$) counterparts, are less reliant on aerobic glycolysis to meet their bioenergetic requirements, and derive much of their ATP generation from FAO[366]. $TSPO^{-/-}$ cells exhibited enhanced mRNA expression of the *Cpt1a* and *Cd36* genes, supporting the idea that TSPO regulates substrate utilisation and metabolic rates in these cells. The metabolic consequences of TSPO overexpression were also examined, and it was reported that this resulted in reduced expression of *Cpt1a*, suggesting that TSPO acts as a metabolic regulator. Following this report, the authors of this paper challenged the existing paradigm that TSPO was a requisite element of steroidogenesis (having observed that TSPO deficiency did not significantly reduce progesterone production[366]), and postulated that TSPO might in fact act as a regulator of cellular metabolism across all cells and tissues where it is expressed[367]. In 2017, the group who had generated the global $TSPO^{-/-}$ mice further published another study which supported the hypothesis that TSPO acts as a regulator of cellular metabolism in mammals[368]. They observed that insertion of the TSPO gene into Jurkat cells (a T-cell line which naturally expresses little-to-no TSPO) via stable transfection resulted in increased mitochondrial ATP production, cell migration (an energetically expensive process), proliferation, and reduced K^+ efflux[368]. Two years later, Milenkovic *et al*. published a report providing evidence that CRISPR-Cas9 induced $TSPO^{-/-}$ primary microglia exhibited no change in steroidogenic activity, less negative mitochondrial membrane potential and reduced basal and maximal mitochondrial respiration, measured via extracellular flux analysis (EFA), which was rescued by restoring TSPO expression[369].

In 2020, Yao *et al*. demonstrated that murine $TSPO^{-/-}$ microglia exhibited reduced glycolysis[339], while Fu *et al*. demonstrated that $TSPO^{-/-}$ GL261 (murine glioma) cells showed enhanced expression of GLUT1, HK2, lactate dehydrogenase, and the adenosine monophosphate activated protein kinase (AMPK) α subunit[370]. Meanwhile, Koganti and Selvaraj demonstrated enhancement of triglyceride metabolism in the adrenal cortex of the Syrian hamster, which exhibits low TSPO expression[320]. Thus, together, these studies highlight that TSPO acts as a key metabolic regulator in mammalian cells, though the precise effects of TSPO deficiency vary between the cell/tissue type in question. This suggests that TSPO

may play a key role in regulating the substrate preferences of cells where metabolic flexibility is crucial underlies many functions, such as in astrocytes.

1.4.4: Expression throughout the CNS

TSPO expression has been reported in the throughout the CNS, including the brain, spinal cord, and retina. Throughout these regions, TSPO expression has been reported in neurons[371], NG2 cells[331,372], astrocytes[373], and microglia[371,373]. In the brain, TSPO is largely expressed in glial cells. TSPO immunoreactivity has been observed under basal conditions in a variety of brain regions including the cortex, choroid plexus, hippocampus, brainstem and cerebellum, as reported by Betlazar *et al*.[374]. This study attributed much of the basal TSPO expression to astrocytes, endothelial cells, and pericytes[374]. Moreover, recent reports have clarified that TSPO is constitutively expressed in neurons[318,331], however neuronal TSPO expression is usually relatively low in comparison to glial cells. Despite this, it is known that neuronal TSPO expression positively correlates with enhanced neuronal activity[318,331], an energetically expensive process[219].

1.4.5: Expression and function in glia

Much knowledge of TSPO function in glial cells is derived from studies in microglia or glioma cells. This is due to the historical association of increased TSPO expression in microglia with chronic neuroinflammation and observations that TSPO expression increases in gliomas[375].

In 2019, Milenkovic *et al*. generated $TSPO^{-/-}$ microglia via CRISPR-Cas9-mediated knockout and lentiviral-mediated knockdown[369]. This study found that TSPO deficiency induced by TSPO knockdown had no overt effects on mitochondrial metabolism (measured via EFA), however TSPO knockout cells showed deficiencies in mitochondrial respiration and ATP-linked oxygen use, measured using the same paradigm[369]. Moreover, mitochondrial membrane potential and the intracellular concentration of calcium ions ($[Ca^{2+}]_i$) were significantly increased versus wildtype controls, results which also were not mimicked by the TSPO knockdown[369] suggesting this may be due to adaptations in the CRISPR model. Despite this, consistent metabolic shifts between the knockout and knockdown model suggest that TSPO plays a key role in regulating microglial cellular metabolism. The translational implications of this on

inflammatory function were assessed in 2020 by Yao *et al*., who used TSPO$^{-/-}$ primary murine microglia and BV-2 cells (a murine microglia line) and found that loss of TSPO reduced glycolysis, attenuated microglial phagocytosis, and diminished proinflammatory cytokine release in response to LPS stimulation[339]. Together, these studies suggest that TSPO may regulate cellular metabolism during energetically expensive processes such as inflammation.

To date, there have been few studies interrogating the function of TSPO specifically within glioma using a TSPO$^{-/-}$ model. However, in 2020, Fu *et al*. published findings suggesting that TSPO worsens outcomes in glioma[370]. This study demonstrated enhanced proliferation and apoptosis in TSPO$^{-/-}$ cells. Moreover, parameters associated with cellular metabolism were modulated in TSPO$^{-/-}$ glioma: mitochondrial fragmentation was enhanced, indicating enhanced reliance on glycolysis, which was supported by EFA[370]. Glucose uptake and lactate secretion were also increased. In line with this, mitochondrial respiration (also assessed by EFA) was reduced, as was mitochondrial membrane potential and ATP production. Similar results were observed in stem-like GBM1B cells[370]. In line with work in primary microglia, this suggests that TSPO plays a key role in regulating cellular metabolism. This work is supported by studies using TSPO ligands: pharmacological manipulation of TSPO is typically associated with modulation of ROS production (an indicator of mitochondrial energy production)[376–378]. Complementing this, pharmacological manipulation of TSPO has been shown to modulate mitochondrial membrane potential and may modulate mitochondrial respiration (measured by EFA) and cytokine release in BV-2 microglia[378,379]. Although some of these bodies of work may not have specifically focussed on the effects of TSPO on cellular metabolism in glia/glioma cell lines, many of the functions studied require effective adaptations in cellular energy utilisation, such as inflammatory function and steroidogenesis, implying that TSPO may play a key role as a metabolic regulator in glial cells. However, glioma cell lines typically represent mixed cell populations[380] that do not represent the physiology of non-cancerous glial cells[381], therefore it is important to confirm results in a more physiologically relevant *in vitro* model.

1.4.5.1: TSPO in astrocytes

Comparatively little is known about the role of TSPO in astrocytes. In 2005, Veiga *et al*. demonstrated that intracerebral LPS injection increased vimentin

expression (a marker of astrocyte reactivity) in cells of a stellate morphology, which was modulated by injection of TSPO ligands[312]. This provided evidence to suggest that TSPO expression in astrocytes correlated with astrocyte reactivity, and the Ellacott laboratory has previously published evidence demonstrating that inflamed astrocytes have altered metabolic profiles[167], supporting well-established linked between inflammation and metabolism from studies in the periphery[289,382–390]. Following this, an *in vivo* study in rats demonstrated that TSPO was upregulated in reactive astrocytes[391], and in 2016 *in vitro* astrocytoma cells were used to demonstrate a putative role for TSPO in modulating cell metabolism during a TSPO ligand synthesis study[377]. Further, a related study from the same group demonstrated a putative link between TSPO and metabolism in C6 glioma cells, a human astrocytoma cell line (U87MG), and human primary astrocytes[392]. In 2020, Tournier *et al*. demonstrated that TSPO expression increases in astrocytes prior to microglia in a rat model of Alzheimer's disease[393]. The same study found that this correlated with findings from samples of the temporal cortex of patients with Alzheimer's disease[393]. Importantly, the early stages of Alzheimer's disease correlate with a metabolic shift in the brain[269,394], suggesting that this may contribute to a reduced capability for astrocytes to provide trophic support to neurons, and highlights the importance of understanding TSPO function in astrocytes. Moreover, this suggests that therapeutically modulating astrocytic TSPO may present a viable therapeutic target for the treatment of neurodegenerative conditions. Together, these studies show that TSPO plays a role in regulating energetically expensive processes in astrocytes. However, the role of TSPO in regulating the cellular metabolism of astrocytes has not yet been fully elucidated, thus further study is needed.

1.4.6: TSPO ligands

As implied throughout the preceding sections, TSPO is upregulated in many pathologies affecting the CNS. Indeed, upregulated TSPO expression has been observed in ischaemic[395] and haemorrhagic stroke[396,397]; chronic traumatic encephalopathy[398]; traumatic brain injury[399,400] ; Alzheimer's disease[288,393,401]; Parkinson's disease[402]; frontotemporal dementia[403]; obesity[404]; diabetes[405]; amyotrophic lateral sclerosis[406]; CNS infections[407], and glioma[370,408]. Moreover, increased TSPO expression is employed in some clinics to monitor neuroinflammation[409,410], and the potential therapeutic modulation of TSPO for a

range of disorders is currently being explored in a number of clinical trials[406,411,412].

Initial observations of upregulated TSPO expression during chronic inflammation led to attempts to develop ligands targeting TSPO for neuroimaging purposes. These attempts were largely successful, and led to the generation of two distinct TSPO ligands: the isoquinoline carboxamide PK-11195 (1-[2-chlorophenyl]-*N*-methyl-*N*-[1-methylpropyl]-3-isoquinoline carboxamide) and the benzodiazepine derivative Ro5-4864 (4'-chlorodiazepam)[305]. These ligands were readily labelled for radioimaging, typically by the addition of tritium (^{3}H), ^{11}carbon (C) or ^{13}C. In particular, PK-11195 was found to have extremely good binding affinity for TSPO, reported as dissociation constant (K_d), of 0.41-2nM[413,414]. Unfortunately, Ro5-4864 did not share this property, and thus did not see widespread application[305]. Similarly, PK-11195 was not without its issues: despite its high affinity for TSPO, PK-11195 exhibited a great degree of non-specific binding due to its high lipophilicity[305]. This led to the development of second-generation TSPO ligands, such as *N*-acetyl-*N*-(2-methoxybenzyl)-2-phenoxy-5-pyridinamine (PBR-28) and *N,N*-diethyl-2-[2-(4-methoxyphenyl)-5,7-dimethylpyrazolo[1,5-α]pyrimidin-3-yl]acetamide (DPA-713), which show strong TSPO binding potential (reported as inhibitory constant, K_i; K_i [PBR] = 2.17-55nM[415,416], K_i [DPA-713] = 4.43nM[409]) and reduced non-specific binding in comparison to PK-11195 and Ro5-4864. Following the development of these compounds, TSPO ligands saw widespread preclinical use in attempts to determine TSPO functionality and the relationship between neurodegenerative disorders and TSPO expression. However, findings from these studies were mixed, and it later became apparent that this was because the binding of these 'second-generation' TSPO ligands was sensitive to a common genetic polymorphism (rs6971; discussed further below, **Chapter 1.4.6.1**) affecting the CRAC domain of TSPO[309,409,417].

Recent efforts by synthetic chemists has led to the development of third-generation TSPO ligands, such as *N,N*-dialkyl-2-phenylindol-3-ylglyoxylamide (PIGA)[377,392,418] ligands, which exhibit many of the benefits of second-generation TSPO ligands with less sensitivity to the rs6971 polymorphism[305,419–421]. Unfortunately, these developments are indeed so recent that the usage of these ligands is typically limited to laboratories with the facilities and knowledge to synthesise them, limiting the widespread application of these ligands at the

present time. This means that, despite the limitations of first-generation TSPO ligands, the widespread commercial availability of these drugs means they continue to be used in preclinical studies to evaluate the efficacy of TSPO as a therapeutic target. Moreover, with the exception of a few ligands[379], the specificity of many TSPO ligands from generations 1-3 have not been validated in TSPO deficient models[367].

Alongside synthetic ligands, the existence of endogenous ligands for TSPO has been evidenced. These include the protein diazepam binding inhibitor (DBI), also referred to as acyl-CoA binding protein (ACBP)[422–424]. This protein is implicated in the delivery of lipids to the mitochondria for FAO[422–424], and thus may help explain the results reported by Tu *et al*. showing that TSPO regulates FAO in Leydig cells[366]. Other examples of proposed endogenous ligands include: tetrapyrroles[425], including porphyrins[426,427] such as haem[308,343,428]; cholesterol[309,369,429], and phospholipase A2[425] (in *Naja naja*[425]).

Based on classic pharmacological terminology, for a long time TSPO ligands were separated into two main classes: ‘agonists’ or ‘antagonists’. While it was acknowledged that this nomenclature was imperfect because TSPO has no clearly defined downstream signalling cascade and does not act as a receptor (therefore cannot be agonised or antagonised in the traditional sense), these terms saw continued use because there was not an alternative which more accurately described their effects on TSPO function. More recently, the field has seen the adoption of new terms: ‘activator’ in place of ‘agonist’ (e.g. when discussing emapunil[430,431]), and ‘inhibitor’ in place of ‘antagonist’ (e.g. when discussing PK-11195[432]), as part of an effort to better describe the purported actions of TSPO ligands binding to their target. Unfortunately, this terminology remains imperfect, because TSPO (as yet) has no clearly defined downstream functions that may be ‘activated’ or ‘inhibited’. TSPO has been reported to be regulated by protein kinase A via a phosphorylation event[433], which has not subsequently been further elucidated. Regulation of TSPO via post-translational modifications in this manner is not well-studied and further developments here may yield outputs that enable better application of pharmacological nomenclature to the study of TSPO.

1.4.6.1: The rs6971 polymorphism

As mentioned briefly above, alongside poor understanding of the function of TSPO, attempts to therapeutically target TSPO in humans or human-derived tissues or cells have also been hindered by the presence of a common single nucleotide polymorphism (SNP) in the *Tspo* gene known as the rs6971 polymorphism[416]. This polymorphism has been reported in human and murine models[355,416]. A SNP is a form of genetic mutation, wherein a nucleotide in a given sequence is substituted for another nucleotide, changing the resulting DNA sequence. For example, 'guanine-adenine-cytosine' may mutate to 'thymine-adenine-cytosine'. SNPs can result in three different potential outcomes. The first possible outcome are 'silent' mutations, where although the encoded nucleotide has changed, the resulting amino acid is unchanged. Alternatively, 'missense' mutations may occur. Here, the altered nucleotide sequence encodes a different amino acid, which alters the structure of the resulting amino acid chain and protein product. The final possible outcome is a 'nonsense' mutation, wherein no amino acid is encoded, instead, a 'stop' or 'start' signal for gene transcription and translation may be inappropriately introduced, resulting in protein truncation or elongation and loss of function.

The rs6971 polymorphism is a missense mutation, resulting in Threonine (Thr) being substituted for Alanine (Ala) at amino acid (AA) 147 of the TSPO AA sequence (Ala147Thr)[416,434]. This stems from the substitution of 'adenine-cytosine-guanine' (encoding Thr) for 'guanine-cytosine-guanine' (encoding Ala) at the corresponding codon. As Ala is a nonpolar AA and Thr is a polar AA, this has downstream effects on the secondary and tertiary structure of TSPO. These manifest as changes to a region of TSPO known as the cholesterol recognition/interaction amino acid consensus sequence (CRAC domain)[416] (**Figure 1.4.2.1 B**). The CRAC domain is a region of the fifth TSPO transmembrane domain (**Figure 1.4.2.1 B**) and has been suggested as a likely binding site for endogenous and synthetic TSPO ligands and interacting partners[305,416]. Recent evidence has suggested that the rs6971 polymorphism affects the formation of complexes involving TSPO[347]. The rs6971 polymorphism exhibits a high degree of prevalence: estimations suggest that up to 30% of the general population carry this polymorphism (Thr147), though this varies depending on ethnicity[416,434]. The prevalence of the rs6971 polymorphism has

also hindered attempts to study it – as the polymorphism is, arguably, a minor allele variant, cause-and-effect relationships are harder to determine than with SNPs associated with severe phenotypes. Moreover, until recently, phenotypes associated with the rs6971 polymorphism beyond insensitivity to second-generation TSPO ligands had not been determined, however neoteric studies have suggested that rs6971 'status' (homozygous major allele variant [Ala/Ala147], heterozygote [Ala/Thr147], and homozygous minor allele variant [Thr/Thr147]) positively correlates with the incidence of neuropsychiatric conditions such as major depressive disorder[435,436], bipolar disorder[437] and schizophrenia[438,439]. Alongside this, presence of the rs6971 polymorphism was recently shown to be a predictor of survivability in human males with glioblastoma[440], suggesting that this polymorphism may promote subtle phenotypes in humans. Together these studies show that the rs6971 polymorphism may be clinically relevant, though full the extent to which the polymorphism determines clinical outcomes across a variety of neurological conditions remains unclear.

1.4.7: Beyond neuroimaging: TSPO as a therapeutic target in CNS disease

As outlined in **Chapter 1.4.6**, from a historical perspective TSPO ligands had primarily been developed and optimised to facilitate neuroimaging in a variety of disorders, largely due to the association of increased TSPO expression in the CNS during conditions with a neuroinflammatory element. Therefore, in the last two decades, there has been increasing attraction to employing TSPO as a therapeutic target, largely for neurological conditions. This has been partly fuelled by various reports of anti-inflammatory properties of TSPO ligands[377,441,442]. Following early reports that TSPO ligands may be beneficial in promoting neuroprotective or neuro-regenerative effects[443] or reducing ROS production and markers of apoptosis[443], this avenue gained mounting attention throughout the 2010s.

In 2013, Barron *et al*.[442] reported that the first-generation ligand, Ro5-4864, exerted anti-inflammatory effects in a mouse model of Alzheimer's disease when applied via intraperitoneal injection[442]. This was closely followed by Daugherty *et al*.[372] who demonstrated that the anxiolytic etifoxine was of benefit in a mouse model of multiple sclerosis; this study reported increased numbers of

oligodendrocyte precursor cells and reduced markers of microglial activation following intraperitoneal application of this compound[372]. These studies were followed by many others, demonstrating that TSPO ligands may offer therapeutic value to addressing neuronal damage and CNS inflammation in a variety of conditions including diabetes (currently in a Phase II clinical trial[412]), cancer[347,370], tauopathies[444], macular degeneration[344], amyotrophic lateral sclerosis[319,406], alongside psychiatric conditions such as major depressive disorder[435,436,445] and anxiety disorders[418,436], and peripheral disorders such as non-alcoholic fatty liver disease[446].

Despite these promising findings, studies regarding the therapeutic employment of TSPO are typically limited by at least two major factors. The first factor is that TSPO currently has no widely-accepted downstream functionality through which its activity can be measured[367]. Thus, the efficacy of TSPO ligands at activating or inhibiting TSPO in a clinically relevant manner are difficult to determine. Steroidogenesis is, arguably, the most well-researched function linked to TSPO, however this function remains a source of considerable controversy[320,328,367,433,447,448]. However, were a better-defined role for TSPO in regulating a cellular function to be determined, potential modulatory effects of these ligands could be interrogated using this output. A role for TSPO in steroidogenesis is not ideal for this, as not all cells generate steroids. A second factor is that many of these ligands have not yet been validated with TSPO-deficient models, thus the specificity of these effects cannot be reliably ascertained[367]. Moreover, the development of TSPO ligands for the purposes of bioimaging has hindered attempts to more widely employ these ligands due to a poor understanding of their function beyond their pharmacokinetic and pharmacodynamic properties[367].

1.5: Summary, overarching hypothesis, and aims of this project

To summarise, astrocytes play crucial roles as mediators of energy use within the CNS. Moreover, astrocyte metabolism is increasingly being appreciated as a mechanism that governs a variety of functions, including intercellular communication and inflammatory responses. Astrocytes undergo molecular and cellular changes during pathological states, and therefore represent tantalising therapeutic targets. The highly conserved 18kDa mitochondrial translocator protein, TSPO, is expressed at a low level in the CNS under physiological

conditions, while under pathological conditions levels of TSPO increase. Pathology-associated modulation of TSPO expression has historically been attributed to microglia, but mounting evidence suggests that this is conserved in astrocytes and may precede microglial increases in TSPO. TSPO has been implicated in a myriad of functions in mammals, all of which have changes in cellular metabolism as a common theme. The role TSPO plays in regulating astrocyte bioenergetics remains poorly understood, and enhancing our understanding of this may yield novel therapeutic applications of TSPO.

Therefore, this thesis tests the overarching hypothesis that TSPO acts as a key regulator of astrocyte metabolism and inflammatory responses, by influencing astrocyte immunometabolism.

This hypothesis was tested through the following aims:

1. To characterise the effects of TSPO deficiency on astrocyte cellular metabolism under basal conditions.
2. To evaluate the effect of TSPO deficiency on astrocyte bioenergetics following inflammatory stimulation, and assess any associated impact on the astrocyte inflammatory response.
3. Determine whether a TSPO ligand can modulate astrocyte metabolism and recapitulate the metabolic phenotype of TSPO deficiency.

Chapter 2: Materials and Methods

2.1: Materials

Table 2.1.1: List of consumables

Consumable	Supplier	Catalogue number
0.2µM filter	Sarstedt	83.1826.001
100mm dish	Sarstedt	83.9302
20mL syringe	Appleton Woods	GS577
2-deoxy-D-glucose	Merck Millipore	D8375-5G
4-(2-hydroxyethyl)-1-piperazineethanesulfonic acid (HEPES)	Merck	H0887-100ML
50mL syringe, Luer lock	Appleton Woods	GS586
60mm dish	Sarstedt	83.3901
6-well plate	Sarstedt	83.392
70µM sterile cell strainer	Fisher Scientific	11597522
96 well plate (flat bottom)	Starlab	E2996-1600
Acrylamide/Bisacrylamide 37.5:1, 30%	Fisher Scientific	15484099
Agarose	Fisher Scientific	10688973
Ammonium persulphate	Merck Millipore	A3678
Benzamidine	Merck Millipore	12072
Bio-Rad Protein Assay Dye Reagent Concentrate	Bio-Rad	5000006
BioTrace Nitrocellulose	VWR	732-3031
Bovine Serum Albumin (BSA), for biotechnology	VWR	0332-100G
Bovine Serum Albumin Fraction V, fatty acid free	Merck Millipore	10775835001
Bromophenol blue sodium salt	Merck Millipore	B5525
BstUI	Fisher Scientific	ER0921
$CaCl_2$ (calcium chloride)	Merck	C5670
Cryovials	Sarstedt	72.379
Culture tubes	VWR	211-0085
Cuvettes	Fisher Scientific	10412121

D-glucose	Merck Millipore	G7021
Dimethyl sulfoxide	Merck Millipore	D2650-5X5ML
DreamTaq Hot Start Green Master Mix	Fisher Scientific	15689374
Dulbecco's Modified Eagle's Medium (Glucose Free)	Fisher Scientific	11966-025
DuoSet ELISA Ancillary Reagent Kit	Bio-techne	DY0008B
Ethylene glycol-bis(2-aminoethylether)-*N,N,N′,N′*-tetraacetic acid (EGTA)	Merck Millipore	E0396-10G
Ethylenediaminetetraacetic acid (EDTA)	Merck Millipore	EDS-100G
Etomoxir	Merck Millipore	E1905-5MG
ExoSAP-IT	Fisher Scientific	78200.200.UL
Fatty acid free BSA (Fraction V)	Roche	10775835001
Fatty Acid Oxidation assay	AssayGenie	BR00001
Fluoroshield mounting medium with DAPI	Abcam	AB104139-20ML
Foetal Bovine Serum, South American Origin	Fisher Scientific	10270106
Gelatine	Merck Millipore	G-2500
GelRed® Nucleic Acid Gel Stain, 10,000XG	Cambridge Bioscience	88495
Glycerol	Merck Millipore	G5516-100ML
Glycine	Melford	G0709
Glycolysis stress test	Agilent	103020-100
Hank's Balanced Salt Solution	Fisher Scientific	11530476
HCl (hydrochloric acid)	Fisher Scientific	J/4320/15
High-Capacity RNA-to-cDNA Kit	Fisher Scientific	10704217
High glucose DMEM	Merck Millipore	D5671
Inoculating loops	Fisher Scientific	15792105
Intercept (TBS) Blocking Buffer	Merck Millipore	16341908
Kanamycin sulphate	Merck Millipore	K4000
KCl (potassium chloride)	Merck Millipore	P5405

LB Broth	Merck Millipore	L3022-250G
LB Broth with agar	Merck Millipore	L2897-250G
L-glutamine (200mM)	Fisher Scientific	11500626
Lipofectamine 3000	Fisher Scientific	15292465
Lipopolysaccharide	Merck Millipore	L8274-10MG
L-Lactate assay kit	Cayman Chemical	700510-96 wells
Methanol for HPLC, ≥99.9%	Merck Millipore	34860-2.5L-M
$MgCl_2 \bullet 6H_2O$ (Magnesium chloride hexahydrate)	Merck Millipore	M2393
$MgSO_4$ (magnesium sulphate)	Merck	M2643
Mitochondrial stress test	Agilent	103015-100
Mouse IL-1 beta/IL-1F2 DuoSet ELISA	Bio-techne	DY401-05
Mouse IL-10 DuoSet ELISA	Bio-techne	DY417-05
Mouse TNF-alpha DuoSet ELISA	Bio-techne	DY410-05
Myc-trap agarose beads	Proteintech	yta-20
$Na_4P_2O_7 \bullet 10H_2O$ (sodium pyrophosphate tetrabasic decahydrate)	Merck Millipore	S6422
NaCl (sodium chloride)	Merck Millipore	S7653
NaF (sodium fluoride)	Merck Millipore	S7920
NaH_2PO_4 (sodium dihydrogen phosphate)	Merck	RDD07
NaOH (sodium hydroxide)	Fisher Scientific	S/4920/53
$NaVO_4$ (sodium orthovanadate)	Merck Millipore	S6508
Nonidet P40 substitute	Merck Millipore	74385-1L
Palmitate	Merck Millipore	P0500
PBR (TSPO) Human Tagged ORF Clone	OriGene	RC220107
pCMV6-Entry Mammalian Expression Vector	OriGene	PS100001
Penicillin Streptomycin solution	Fisher Scientific	11528876
Phenylmethylsulfonyl fluoride	Merck Millipore	P7626
Phosphate buffered saline tablets	Fisher Scientific	10209252
PK11195	Merck Millipore	5059810001
Plasmid Midi Kit	Qiagen	12143
Plasmid Midi Kit (25)	Qiagen	12143

Poly-L-lysine hydrobromide	Merck Millipore	P1274-100MG
Ponceau S solution	Merck Millipore	P7120
Precision Plus Protein Dual Color Standards	Bio-Rad	1610374
Propidium iodide	Merck Millipore	P4864-10ML
Proteinase K (recombinant)	Fisher Scientific	10181030
RNase-free DNase set	Qiagen	79254
RNeasy Mini Kit	Qiagen	74104
RNeasy Plus Mini Kit	Qiagen	74134
Seahorse XF DMEM medium, pH 7.4	Agilent	103575-100
Seahorse XFe96 FluxPak	Agilent	102416-100
Sodium dodecyl sulphate (SDS)	Melford	B2008
Sodium pyruvate	Merck Millipore	P2256-100G
Stericup 38mm	Merck	SEPGU0538
Stericup 45mm	Merck	SEPGU0545
Sterile disposable scalpel	Fisher Scientific	11798343
Sucrose	Melford	S0809
T25 flask	Sarstedt	83.3910.002
T75 flask	Sarstedt	83.3911.002
N,N,N′,N′-Tetramethylethylenediamine (TEMED)	Merck Millipore	T7024
Tris base	Melford	B2005
Triton-X 100	VWR	M143
Trypsin 0.05% EDTA	Fisher Scientific	11590626
Trypsin from porcine pancreas (2.5% solution)	Merck Millipore	T4549
Tween-20	Merck Millipore	P2287
β-mercaptoethanol	Merck Millipore	M3148

Table 2.1.2: List of general equipment

Equipment	**Supplier**

BD Accuri C6 Plus Flow Cytometer	BD Biosciences
Biospectrophotometer	Eppendorf
DM4000 B LED Fluorescent microscope	Leica
Fibre optical illuminator	World Precision Instruments
GelMAX Imager	UVP
Mini-PROTEAN Tetra system	Bio-Rad
Nanodrop 2000	Fisher Scientific
Odyssey CLx	LI-COR Biosciences
PHERAstar FS microplate reader	BMG Labtech
Seahorse XFe96 Analyser	Agilent
SimpliAmp Thermocycler	Applied Biosystems
Sprout Mini Centrifuge	Fisher Scientific
TC20 Automated cell counter	Bio-Rad

Table 2.1.3: List of software and suppliers

Software	**Distributor/Supplier**
BD C6Plus Software	BD Biosciences
Benchling	Benchling
Ensembl	Ensembl
Excel	Microsoft
FIJI Is Just ImageJ (FIJI)	National Institutes for Health
ImageStudio (v5.2)	LI-COR Biosciences
Inkscape	Inkscape.org
Leica Acquisition Suite X	Leica
MARS	BMG Labtech
PowerPoint	Microsoft
Primer3Plus	Primer3
Prism (v10.0.2)	GraphPad
SnapGene Viewer (v5.2.3)	SnapGene (Dotmatics)
UCSC *in silico* PCR	University of California, Santa Cruz
Visionworks	Analytik Jena

Wave Analysis Software	Agilent

2.2: Methods

2.2.1: Animal use and husbandry

All animal studies were conducted in accordance with the UK Animals (Scientific Procedures) Act 1986 (ASPA) and study plans were approved by the institutional Animal Welfare and Ethical Review Body at the University of Exeter. Mice were group housed on a 12:12 light-dark cycle at 22 ± 2°C with *ad libitum* access to standard laboratory rodent diet (LabDiet [EU] Rodent diet 5LF2; LabDiet, London, UK) and water[449].

Mating pairs of TSPO heterozygote ($^{+/-}$) ($Tspo^{tm1b(EUCOMM)Wtsi}$) mice were used to produce the homozygote knockout ($TSPO^{-/-}$) and wildtype ($TSPO^{+/+}$) littermate mice used in these studies[326,449]. Mice were crossed >7 generations onto a C57BL/6J background[449].

Offspring of both sexes were used in this study.

2.2.2: Isolation of primary astrocytes

Mouse primary astrocytes (MPAs) were collected using a modified version of the method published by Schildge *et al*.[123,167]. Briefly, on postnatal days 1-5, pups were euthanised by rapid decapitation and brains were removed from skulls. Following removal of the meninges, the cerebellum and occipital lobes were removed, and the cortices extracted by blunt dissection using forceps. Homogenised cortices were placed into 1mL Hank's Balanced Salt Solution (Fisher Scientific) and manually disrupted using a scalpel. Dissected cortices were digested for 30 minutes in 0.5% (w/v; 0.5g/100mL) trypsin (Merck Millipore) and neutralised with an equal volume of 25mM glucose Dulbecco's Modified Eagle's Media (DMEM; Merck Millipore) supplemented with 10% (vol/vol) foetal bovine serum (FBS; Fisher Scientific), 8mM L-glutamine (Fisher Scientific) and 2% (vol/vol, ~86.2U/mL) penicillin-streptomycin (Fisher Scientific). Following this, cortices were further disrupted by manual pipetting prior to filtration with a 70µM filter (Fisher Scientific). Digested brains were placed onto poly-L-lysine (PLL; 4µg/mL; Merck Millipore) coated T25 flasks. The next day media was aspirated, and the cells washed with 0.01M phosphate buffered saline (PBS) before media was replaced. Thereafter the cells were washed with PBS and media replaced

every 2-3 days until confluent. To ensure sufficient cell numbers for assays, after genotyping, MPAs of the same TSPO genotype were pooled together into a T75 and grown until confluent. $TSPO^{+/+}$ and $TSPO^{-/-}$ MPAs, MPAs were frozen in 10% DMSO (vol/vol) in liquid nitrogen until use. Purity of astrocyte cultures was determined using immunocytochemistry for GFAP-immunoreactivity. The number of GFAP-immunoreactive astrocytes were determined by manual counting using the Cell Counter plugin for FIJI[450]. Primary antibody-free control coverslips were used to determine background fluorescence. Manual counting determined that astrocyte purity was ≥92% with a mean purity of 98.67 ± 1.61% across all coverslips counted (**Figure 2.2.2**).

2.2.2.1: Immunocytochemistry

Cells were seeded onto PLL-coated coverslips at $1x10^5$ cells per coverslip. Cells were fixed in 1mL ice-cold 100% methanol (Merck Millipore) for 90 seconds on ice. Methanol was removed and the cells washed three times with 0.01M PBS. Non-specific binding was minimised by blocking in 5% normal donkey serum (NDS; diluted in 0.01M PBS [0.3% Triton X-100] [PBS-T]) for 15 minutes at RTP. Anti-GFAP was diluted in 1% NDS-PBST and applied overnight at 4°C. Coverslips were washed three times with PBS and secondary antibodies (1% NDS-PBST) applied for 1h in darkness. Secondary antibodies (**Table 2.2.2.1**) were removed and coverslips washed three times with PBS before air drying in darkness. Coverslips were mounted onto slides using Fluoroshield Mounting Medium with DAPI (Abcam) and imaged within 7 days using a DM4000 B LED Fluorescent microscope (Leica). Slides were stored at 4°C.

Table 2.2.2.1: List of antibodies used for immunocytochemistry

Target	Host species	Dilution	Catalogue number	Supplier
GFAP	Mouse	1:1000, 1% NDS in PBST	mab360	Merck Millipore
Mouse (AlexaFluor-488)	Donkey	1:500, 1% NDS in PBST	A-21202	Invitrogen

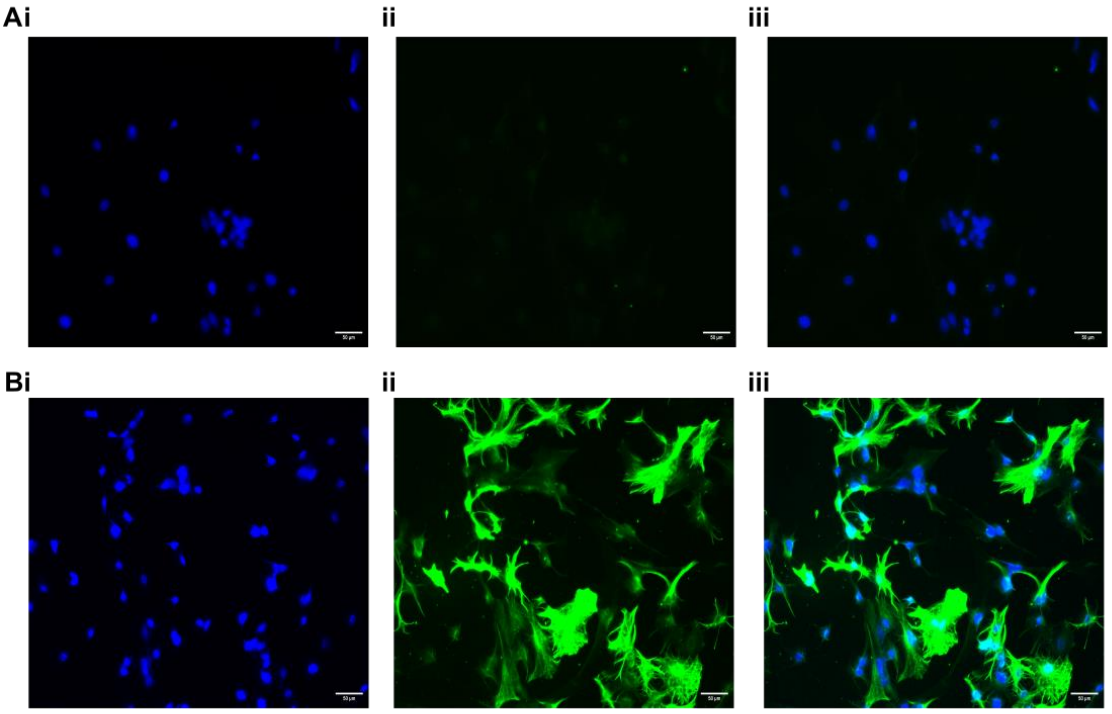

Figure 2.2.2: Confirmation of astrocyte purity.

MPAs were seeded onto coverslips, fixed, and purity determined via GFAP-immunoreactivity. GFAP-positive cells were accepted as astrocytes, and GFAP-negative cells were accepted as other brain cells. Mean astrocyte purity was determined to be 98.67% by manual counting.

A: Primary antibody-free negative control. B: GFAP staining. i: DAPI. ii: GFAP immunoreactivity. iii. Overlay.

n=10 coverslips, 2-5 images per coverslip over 3-4 individual collections (total cells counted = 3256).

2.2.3: Genotyping

Upon euthanasia of pups a small tissue sample was collected per pup. Tissue was digested in PBND buffer (50mM KCl, 10mM Tris-HCl pH 8.0, 2.5mM $MgCl_2$-$6H_2O$, 0.1mg/mL gelatine, 0.45% [vol/vol] Nonidet P40, 0.45% [vol/vol] Tween-20) and 1% (vol/vol) Proteinase K (Fisher) for 5h at 55°C before enzymes were denatured by heating at 95°C for 10 minutes. DNA samples were loaded into a PCR reaction containing primers (**Table 2.2.3**) for TSPO and a LAR3 construct (LAR3 construct present only in $TSPO^{-/-}$, $TSPO^{+/-}$ pups). PCR products were run on a 1.5% (w/vol) agarose gel and gels were scanned using a GelMax imager (UVP). TSPO genotype was determined by PCR product size. $TSPO^{+/+}$ mice were determined by the presence of a single band at 188bp, $TSPO^{-/-}$ by a band at 244bp, and $TSPO^{+/-}$ by both bands (**Figure 2.2.3**).

Table 2.2.3: Primers used to genotype $TSPO^{-/-}$-line mice

Primer name:	Sequence (5'-3'):
TSPO 5' arm	AGCAGAAGTAGGAAGAAGGTG
TSPO 3' arm	GTCAACCCATCACTGCCTTCA
LAR3	CAACGGGTTCTTCTGTTAGTCC

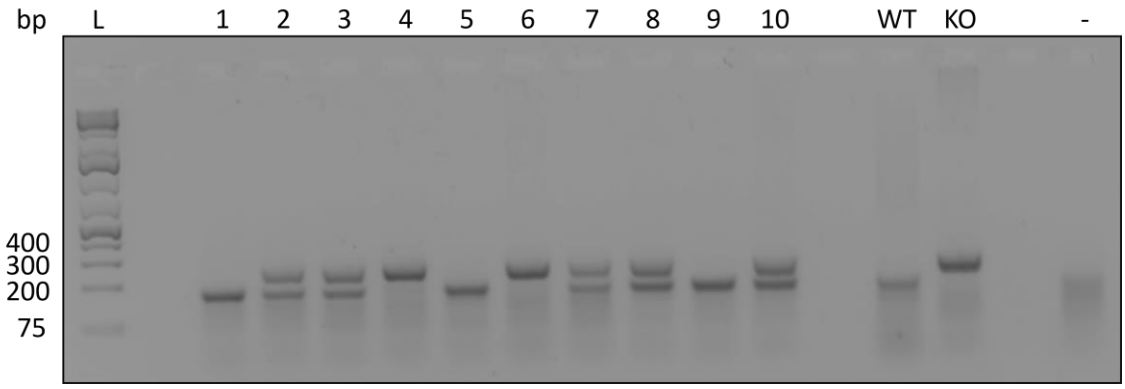

Figure 2.2.3: Example gel showing PCR products from TSPO$^{-/-}$-line mice.

PCR products from tissue samples of TSPO$^{-/-}$-line pups. bp: base pairs. L: ladder. 1-10: sample numbers. WT: positive control for TSPO-expressing pup. KO: positive control for TSPO-deficient pup. Presence of 2 bands in a single lane indicated TSPO heterozygosity. -: negative control, double distilled H_2O run in place of sample.

2.2.4: General cell culture

All cell cultures were maintained in 25mM glucose DMEM (Merck Millipore) with 10% (vol/vol) FBS (Fisher Scientific), 8mM L-glutamine (Fisher Scientific) and 2% (vol/vol; ~86.2U/mL) penicillin-streptomycin (Fisher Scientific). Cultures were maintained in humidified incubators at 37°C with 5% CO_2.

U373 astrocytoma cells were purchased from the European Collection of Authenticated Cell Cultures (U-373 MG [Uppsala] [ECACC 08061901])[451] (U373 cells). U373 cells that were not subject to previous genetic modification were maintained up to p30 for use in these studies. $TSPO^{-/-}$ and empty vector wildtype control U373 cells were p50-60. Though not ideal, this was unavoidable due to expanding single-cell colonies following genetic modification with the CRISPR-Cas9 system.

Cells were detached from surfaces for passaging (U373s, MPAs were not subcultured) or freezing (0.5% Trypsin-EDTA, Fisher Scientific) for 5 minutes at 37°C (5% CO_2). Trypsin was neutralised by the addition of 1 volume of serum-containing media. Cells were centrifuged at 161*xg* for 5 minutes, before resuspending in media and cell counting (if seeding for experiments; Bio-Rad).

The day before experiments, MPAs or U373 cells were trypsinised, counted, and seeded in DMEM (Fisher Scientific) with 7.5mM glucose (Merck Millipore), 10% (vol/vol) FBS, 8mM L-glutamine and 2% (vol/vol; ~86.2U/mL) penicillin-streptomycin. On the day of experiments involving treatments, cells were cultured in serum-free DMEM (11966) supplemented with 2.5mM glucose for 2h before treatments were applied in the same media. When performing metabolic flux analyses or measuring metabolite production, XF DMEM (pH 7.4) (Agilent) supplemented with appropriate concentrations of glucose, sodium pyruvate, and L-glutamine for the assay used.

2.2.5: Generation of TSPO-deficient U373 cells

These cells were generated and validated via PCR, immunoblotting, and immunocytochemistry by Daisy Stewart as part of her Professional Training Year. $TSPO^{+/+}$ U373 cells transfected with noncoding guide RNAs (‘empty vectors’, EV) were maintained as passage-equivalent controls. This work was carried out under the supervision of Dr Josephine Robb and Dr Rosemary Bamford. Full methods are presented in[449].

2.2.6: Bacterial transformations and plasmid extractions

Plasmids (Myelocytomatosis oncogene [Myc]-tagged TSPO ['TSPO-Myc'; OriGene]) or a porcine cytomegalovirus (pCMV) EV control (OriGene) were grown in chemically competent DH5α *E. coli* following transformation via heat shock. Briefly, DH5α *E. coli* were thawed on ice. 100ng of the relevant plasmid (1 plasmid per tube of bacteria) was added and mixed with gentle agitation. The bacteria-plasmid mix was placed on ice for 10 minutes prior to incubation at 42°C for 50 seconds. Bacteria were immediately returned to ice for 2 minutes, then placed into 900µL lysogeny broth (LB) in a culture tube (VWR). Bacteria were incubated for 1h at in a 37°C non-CO_2 incubator with gentle agitation (225rpm). Solution was centrifuged at 100*xg* and resuspended in 50µL LB broth. Resuspensions were inoculated via inoculating loop (Fisher Scientific) on hand-cast LB agar 100mm dishes (Sarstedt) containing 25µg/mL kanamycin (Merck Millipore) to select successful transformants. Plates were incubated overnight at in a 37°C non-CO_2 incubator. The next day, colonies were picked and added to 5mL LB broth (25µg/mL kanamycin) in culture tubes and incubated for 5-8h at 37°C in a non-CO_2 incubator with gentle agitation (225rpm). Optical density at 600nm (OD600) was monitored via cuvette and a biospectrophotometer (Eppendorf). When OD600 was between 0.3-1 arbitrary units (AU), a sample of this culture was diluted 1/500-1/1000 into 50-100mL LB broth (25µg/mL kanamycin) in a vented T75 flask and incubated at 37°C in a non-CO_2 incubator with gentle agitation (225rpm) for 16-20h overnight. When OD600 was between 2-3AU, cultures were transferred to 50mL tubes (Eppendorf) and centrifuged at 4600*xg* at room temperature and pressure. Plasmids were isolated using a Plasmid Midi Kit (Qiagen). All centrifugation steps were carried out at 4600*xg* RTP with appropriate modifications to spin duration (step 1: 15 minutes; step 10: 35 minutes; step 11: 15 minutes). Plasmids were allowed to air dry in a fume hood for 15 minutes before resuspension in 500µL Buffer TE (Qiagen). Plasmid concentration was quantified using a Nanodrop 2000 (Fisher Scientific).

2.2.7: Transient transfection of U373 cells

U373 cells were transiently transfected in 6-well plates with 2.5µg plasmid (TSPO-Myc or pCMV EV) per well using Lipofectamine 3000 (Fisher Scientific) according to the manufacturer's specifications with minor modifications:

transfection complexes were made up using serum-free 25mM DMEM (Merck Millipore) with 8mM L-glutamine and 2% (vol/vol; ~86.2U/mL) penicillin-streptomycin 10 minutes before use. Cells in DMEM (Fisher Scientific) with 7.5mM glucose, 10% (vol/vol) FBS, 8mM L-glutamine and 2% (vol/vol; ~86.2U/mL) penicillin-streptomycin were seeded directly into transfection complex mixes and left for 24h before cell lysates were harvested.

2.2.8: Cell treatments

Cells were seeded at a density of either $4x10^5$ cells per well in 60mm dishes (Sarstedt) or $2.1x10^5$ cells per well in 6 well plates (Sarstedt). Prior to treatment, cells were washed once with 0.01M PBS and incubated in serum-free 2.5mM glucose DMEM (Fisher Scientific) ('assay media') for 2h. Treatments were diluted to the appropriate concentrations in assay media immediately before application. 2-deoxyglucose (2DG; Merck Millipore; reconstituted in double distilled H_2O [ddH_2O]) was diluted to 10mM (final ddH_2O concentration was 2% [vol/vol]). Lipopolysaccharide from *Escherichia coli* (LPS; 026:B6; Merck Millipore; reconstituted in ddH_2O) was diluted to a working concentration of 100ng/mL (final ddH_2O concentration was 0.01% [vol/vol]). PK-11195 (Merck Millipore; reconstituted in 100% DMSO) was applied for 1h before use (final DMSO concentration was 0.01% [vol/vol]). Vehicle-treated control cells were incubated in an equal concentration of vehicle solution (0.01% or 2% ddH_2O, or 0.1% DMSO). Where DMSO and ddH_2O vehicles were used, vehicle groups were exposed to both an appropriate concentration of these compounds with inclusion of the alternative treatment in relevant groups (i.e., in **Chapter 5**, 2DG treatments were also exposed to 0.1% DMSO and PK-11195 treatments to 2% ddH_2O). Where vehicle solutions of ranging concentrations were used (**Chapter 4**, 0.01% and 2% ddH_2O), vehicle-treated groups were exposed to the greatest concentration of vehicle.

2.2.9: Protein quantification

Cell lysates were collected using modified radioimmunoprecipitation (RIPA) buffer (**Table 2.2.9**) and manual scraping. Collected lysates were frozen, thawed on ice, and centrifuged at 21,000xg for 20 minutes at 4°C. Protein content of supernatant was quantified via Bradford assay according to the manufacturer's instructions (Bio-Rad). Briefly, 1 part Bradford reagent concentrate was diluted in 4 parts ddH_2O to create a working stock. Working stocks were diluted immediately prior

to use. A standard curve was constructed using bovine serum albumin (BSA; 1mg/ml; Fisher Scientific) in triplicate on a 96-well plate. Standard curves ranged from 0-3mg/ml in integers. For immunoblotting, 1µL of sample was added to wells in triplicate. For extracellular flux analysis, 20µL sample was added to the wells in triplicate. An equal volume of lysis buffer (modified RIPA buffer [immunoblotting and co-immunoprecipitations] or 50mM NaOH [extracellular flux analysis]) to sample was added to the standard curve. 200µL of working concentration Bradford reagent was added per well. Plates were shaken at 300rpm for 300 seconds and absorbance was measured at 595nm using a Pherastar FS (BMG LABTECH).

Table 2.2.9: Constitution of modified RIPA buffer

Compound:	Concentration (mM):
Tris-HCl (pH 7.4)	25
NaF	50
NaCl	100
EDTA (pH 8)	1
EGTA (pH 8)	5
$Na_4P_2O_7 \bullet 10H_2O$	10
Triton-X 100	1%
Sucrose	269
β-mercaptoethanol	0.014
$NaVO_4$	1
Benzamidine	1
Phenylmethylsulfonyl fluoride	0.1

2.2.10: Co-immunoprecipitations

Co-immunoprecipitations (co-IPs) were performed using Myc-Trap agarose beads (Proteintech) according to the manufacturer's specifications with minor modifications. For semiquantitative co-IPs, 68µg protein was loaded per reaction; for confirmatory co-IPs (**Figure 3.4.14**), protein was not quantified.

Briefly, beads were equilibrated in 500µL co-immunoprecipitation buffer (**Table 2.2.10**) and centrifuged at 2500*xg* for 5 minutes at 4°C. This was repeated a total of 3 times. Cell lysate was diluted in 800µL co-IP buffer. 50µL diluted whole cell lysate was retained as the 'input fraction' for immunoblotting. The remainder was then incubated in 20µL equilibrated beads on a rotary mixer for 90 minutes at 4°C. Following centrifugation to isolate the beads (2500*xg* for 5 minutes at 4°C), 50µL supernatent was retained as the 'unbound fraction' for immunoblotting. Beads were washed three times in 500µL co-IP buffer and pelleted by centrifugation (2500*xg* for 5 minutes at 4°C). After the third centrifugation, supernatent was discarded and protein complexes eluted from the beads via the addition of 50µL 2X sodium dodecyl sulphate-polyacrylamide gel electrophoresis (SDS-PAGE) sample buffer (**Table 2.2.11.2**) and boiling at 95°C for 10 minutes. Beads were pelleted by centrifuging at 2500*xg* for 5 minutes at 4°C to isolate the 'bound fraction' for immunoblots.

Table 2.2.10: Co-immunoprecipitation buffer

Component:	Final concentration (mM)
Tris-HCl pH 7.5	10
EDTA	0.5
NaCl	150
$NaVO_4$	1
Benzamidine	1
Phenylmethylsulfonyl fluoride	0.1

2.2.11: Immunoblotting

Following sample quantification or co-immunoprecipitation, samples were run on hand-cast 15% (vol/vol) polyacrylamide gels. Resolving gel solutions were made up as described in **Table 2.2.11.1**, allowed to polymerise, and stacking gels were added to facilitate sample loading. In co-immunoprecipitation studies 20µL per fraction was loaded per well. For semi-quantifiable immunoblots, 10µg protein was loaded per well. 4X SDS-PAGE sample buffer (**Table 2.2.11.2**) was added to a final concentration of 1X to allow visualisation of samples and gel fronts. Gels

were run at 90V for 15 minutes, followed by 150V for 90 minutes. Gels were transferred onto nitrocellulose membranes via wet transfer at 100V for 70 minutes. Membranes were blocked using Odyssey blocking buffer (Tris-buffered saline [TBS]) (Licor, UK) for 1h. Primary antibodies (**Table 2.2.11.3**) were applied overnight at 4°C or RTP for 1h. Membranes were washed 3 times in TBS (20mM Tris-HCl [pH 7.4], 152mM NaCl) with 0.05% (vol/vol) Tween-20 (TBS-T) before application of secondary antibodies (**Table 2.2.11.3**). Membranes were scanned using an Odyssey CLx scanner (Licor, UK). Bands for proteins of interest were normalized to expression of GAPDH and data expressed as fold change over control.

Table 2.2.11.1: Hand-cast polyacrylamide gels

Reagent	15% resolving gel	4% stacking
ddH_2O	2.3mL	2.8mL
1.5M Tris-HCl (pH 8.8)	3.15mL	-
0.5M Tris-HCl (pH 6.8)	-	1.25mL
30% acrylamide	5.6mL	850µL
10% SDS	110µL	50µL
20% APS	55.4µL	50µL
TEMED	11µL	5.35µL

Table 2.2.11.2: 4X SDS-PAGE sample buffer

Component	Concentration
Tris-HCl (pH 6.8)	125mM
SDS	4%
Glycerol	20%
Bromophenol blue	>1%

Table 2.2.11.3: List of antibodies used for immunoblotting

Target	Host species	Dilution	Catalogue number	Supplier
TSPO	Rabbit	1:1000, 2.5% (vol/vol) BSA in TBS-T (0.05%)	ab109497	Abcam
CPT1a	Rabbit	1:1000, 2.5% (vol/vol) BSA in TBS-T (0.05%)	15184-1-AP	Proteintech
GLUT1	Rabbit	1:1000, 2.5% (vol/vol) BSA in TBS-T (0.05%)	07-1401	Merck Millipore
HK2	Rabbit	1:1000, 2.5% (vol/vol) BSA in TBS-T (0.05%)	2867S	Cell Signalling Technologies
pNFκB (p65) (Ser536)	Rabbit	1:1000, 2.5% (vol/vol) BSA in TBS-T (0.05%)	3033S	Cell Signalling Technologies
VDAC1	Rabbit	1:1000, 2.5% (vol/vol) BSA in TBS-T (0.05%)	ab15895	Abcam
GAPDH	Rabbit	1:1000, 2.5% (vol/vol) BSA in TBS-T (0.05%)	G9545	Merck Millipore
NFκB (p65)	Mouse	1:1000, 2.5% (vol/vol) BSA in TBS-T (0.05%)	6956S	Cell Signalling Technologies
Myc-tag	Mouse	1:1000, 5% milk (vol/vol) in TBS-T (0.05%)	66004-1-Ig	Proteintech
β-actin	Mouse	1:10,000, 5% milk (vol/vol) in TBS-T (0.05%)	NB600-501	Novus

Mouse (AlexaFluor 680)	Goat	1:10,000, 5% milk (vol/vol) in TBS-T (0.05%)	A21057	Abcam
Rabbit (DyLight 800 Conjugated)	Goat	1:10,000, 5% milk (vol/vol) in TBS-T (0.05%)	MX10	Rocklands

2.2.12: Extracellular flux analysis

Cells were seeded at a density of $4x10^4$ cells per well in 96 well plates 20-24h prior to experimentation. The exception is the FAO stress test (**Chapter 2.12.3**), where $4x10^4$ cells per well were seeded 48h prior to experimentation. XF DMEM was used for all metabolic flux assays. Media was supplemented as appropriate for the assay used: for basal measurements of cellular metabolism in the presence of glucose and the mitochondrial stress test (MST), XF DMEM was supplemented with 2.5mM glucose (Merck Millipore), 2.5mM sodium pyruvate (Merck Millipore), and 2mM L-glutamine (Fisher Scientific); for the glycolysis stress test, XF DMEM was supplemented with 2mM L-glutamine; for measurements of cellular metabolism in the absence of L-glutamine XF DMEM was supplemented with 2.5mM sodium pyruvate and 2.5mM glucose and for measurements of cellular metabolism in the absence of glucose XF DMEM was supplemented with 2.5mM sodium pyruvate and 2mM L-glutamine. Prior to the assay, cells were washed once with XF DMEM (containing supplements relevant to the test used), which was immediately aspirated and replaced with more fresh media XF DMEM of an appropriate composition for the assay used. Cells were placed into a humidified non-CO2 incubator at 37°C to 'degas' for 60 minutes immediately prior to the assays. This is to prevent acidification of media: because no CO_2 is supplied, a concentration gradient forms which causes CO_2 to diffuse out of the media. Following the degas period cells were placed into the XFe96 bioanalyzer (Agilent) and assays commenced. Readings were taken over 3-minute mix-measure cycles during the assay, with 3-4 measurements per cycle. A baseline read of 3-4 cycles was taken prior to any injections.

2.2.12.1: Mitochondrial stress test (MST)

The mitochondrial stress test was performed according to the manufacturer's instructions (Agilent). As part of this paradigm, cells are first incubated in media

that is serum free but otherwise ‘substrate-replete’, containing 2.5mM glucose, 2.5mM sodium pyruvate, and 2mM L-glutamine. The glucose concentration used in this thesis is physiologically relevant to the brain[76,124]. Following this incubation period, oxygen consumption rate (OCR) and extracellular acidification rate (ECAR) are measured to provide approximate rates of mitochondrial and glycolytic respiration in the cells. Oligomycin (0.5μM, Complex V inhibitor) is first injected. Inhibition of mitochondrial Complex V (ATP synthase unit, **Chapter 1**) allows the determination of oxygen use linked to ATP production. Injection of FCCP (1μM, OXPHOS uncoupler) removes the H^+ gradient between the mitochondrial matrix and intermembrane space, allowing maximum oxygen consumption to be measured. Finally, a mixture of rotenone and antimycin-A (0.5μM, Complex I and III) is injected. This inhibits the electron transport chain and therefore mitochondrial respiration, allowing one to make inferences regarding the contribution of other oxygen-consuming processes to the recorded OCR. Parameters of the MST were calculated as detailed in **Table 2.2.12.1.**

Table 2.2.12.1: Calculations used for the mitochondrial stress test

Parameter	Equation
Non-mitochondrial respiration	Minimum rate measurement after rotenone/antimycin A injection
Basal respiration	(Last rate measurement before first injection) – (Non-mitochondrial respiration rate)
Maximal respiration	(Maximum rate measurement after FCCP injection) – (Non-mitochondrial respiration)
H^+ (proton) leak	(Minimum rate measurement after oligomycin injection) – (Non-mitochondrial respiration)
Mitochondria-linked ATP production	(Last rate measurement before oligomycin injection) – (Minimum rate measurement after oligomycin injection)

Spare respiratory capacity	(Maximal respiration) – (Basal respiration)
Coupling efficiency	(ATP production rate) / (Basal respiration rate) × 100

2.2.12.2: Glycolysis stress test

The glycolysis stress test was used according to the manufacturer's specifications. In this experimental paradigm, cells are first incubated in glucose- and sodium pyruvate-free media in the presence of L-glutamine for 1h, during the degas period. This starves the cells of glucose in order to measure non-glycolytic acidification. 'Non-glycolytic acidification' describes a parameter which encompasses any pH changes that are attributed to other processes involving H^+ production, such as metabolism of fatty acids, or utilisation of intracellular glycogen stores. Following this, a supraphysiological glucose concentration (10mM) is injected to saturate the cells and promote glycolysis. Oligomycin (1µM) is then injected to inhibit ATP synthase and force the cells to rely mainly on aerobic glycolysis for fuel, before 2-deoxyglucose (50mM) is used to competitively inhibit hexokinase-2 (and other hexokinases), effectively stopping glycolysis. The post-2DG metabolism can then be used to confirm the accuracy of non-glycolytic acidification. Parameters of the glycolysis stress test were calculated as detailed in **Table 2.2.12.2.**

Table 2.2.12.2: Calculations used for the glycolysis stress test

Parameter	Equation
Glycolysis	(Maximum ECAR measurement pre-oligomycin injection) - (Lowest rate after 2DG)
Glycolytic capacity	(Maximum ECAR measurement post-oligomycin injection) - (Lowest rate after 2DG)
Glycolytic reserve	(Glycolytic capacity) - (Glycolysis)

Non-glycolytic acidification	Last ECAR measurement prior to glucose injection

2.2.12.3: Fatty acid oxidation stress test

This assay was performed on TSPO$^{-/-}$ MPAs by Dr Josephine Robb and is included in this thesis for completeness. A full account of the methods is given in[449,452]. Briefly, this assay is used to determine the contribution of FAO to meeting the metabolic demands of cells; i.e., how reliant cells are on fats as a metabolic substrate. This is achieved by 'priming' the cells for FAO by withdrawing glucose and supplying carnitine overnight in substrate-limited media (**Table 2.2.12.3**). 45 minutes before the assay, substrate-limited media was replaced with FAO media (**Table 2.2.12.3**). 15 minutes before the assay, half the cells were treated with 40μM etomoxir, an inhibitor of CPT1 function. This concentration was chosen to avoid off-target effects associated with higher concentrations of etomoxir[382]. By inhibiting FAO, one can calculate the proportion of OCR that can be attributed to this process. Immediately before running the assay, half of the etomoxir and control treated cells were treated with 200μM palmitate (Merck Millipore) (0.17mM bovine serum albumin [BSA] vehicle) or BSA vehicle (0.17mM, Roche). A MST was then performed to assess mitochondrial fatty acid oxidation. The calculations for basal and maximal FAO are shown in **Table 2.2.12.3**.

Table 2.2.12.3: Media compositions and calculations used for the FAO stress test

Component	Concentration
Substrate-limited media	
Glucose	0.5mM
Glutamate	1mM
Carnitine	0.5mM
FBS	1%
DMEM (Fisher Scientific)	-
FAO media	
NaCl	111mM
KCl	4.7mM

$CaCl_2$	1.25mM
$MgSO_4$	2mM
NaH_2PO_4	1.2mM
Glucose	2.5mM
Carnitine	0.5mM
HEPES	5mM
Parameter name	**Calculation**
Basal FAO	(Palmitate – etomoxir) – (palmitate + etomoxir) immediately before oligomycin injection
Maximal FAO	(Palmitate – etomoxir) – (palmitate + etomoxir) at highest OCR following FCCP injection

2.2.12.4: Substrate reintroduction tests

To interrogate the bioenergetic responses of $TSPO^{-/-}$ MPAs to the acute withdrawal and subsequent reintroduction of metabolic substrates, during the degas period cells were incubated in the absence of glucose or L-glutamine. The withdrawn metabolic substrate was reintroduced following a baseline read of 3-4 cycles. A range of concentrations of L-glutamine (**Table 2.2.12.4**) and glucose (**Table 2.2.12.5**) were injected. XF DMEM (Agilent) was used during these assays.

Table 2.2.12.4: Media composition and injection concentrations used during L-glutamine reintroduction test

Name of supplied substrates	Concentration for duration of assay (mM)	Injection of withdrawn substrate (concentration, µM)
Glucose	2.5	L-glutamine (0.1, 100, 250, 500, 1000, 2500) + glucose (2.5mM) and sodium pyruvate (2mM)
Sodium pyruvate	2.5	

Glucose and sodium pyruvate were included to avoid diluting these and confounding results.

Table 2.2.12.5: Media composition and concentrations injected during glucose reintroduction test

Name of supplied substrates	Concentration for duration of assay (mM)	Injection of withdrawn substrate (concentration, mM)
L-glutamine	2	Glucose (0.1, 0.5, 1, 2.5, 5.5, 7.5) + L-glutamine (2mM) and sodium pyruvate (2mM)
Sodium pyruvate	2.5	

L-glutamine and sodium pyruvate were included to avoid diluting these and confounding results.

2.2.13: Quantification of extracellular lactate

Cells were seeded at $2.1x10^5$ cells per well in 6-well dishes. The next day, cells were washed once with XF DMEM (2.5mM sodium pyruvate, 2mM L-glutamine) ± 2.5mM glucose and media immediately refreshed. Cells were incubated in a non-CO_2 incubator at 37°C for 60 minutes. Media samples were taken and deproteinated according to the manufacturer's instructions. Briefly, 1 volume of metaphosphoric acid (Cayman Chemical) was added to 1 volume of sample and incubated on ice for 5 minutes. Samples were centrifuged at 10,000*xg* for 5 minutes at 4°C. 50µL potassium carbonate (Cayman Chemical) was added to neutralise the acid and samples were centrifuged at 10,000*xg* for 5 minutes at 4°C to remove resulting salts. Supernatent was retained for L-lactate quantification using an L-lactate Assay Kit (Cayman Chemical), which included the metaphosphoric acid and potassium carbonate. The assay was performed according to the manufacturer's specifications. Briefly, samples were incubated for 20 minutes with lactate dehydrogenase, producing pyruvate and NADH. NADH reacts with substrates in the kit to allow fluorometric measurements. L-lactate standards were used to interpolate the lactate concentrations in samples. Samples and standards were run in duplicates to increase accuracy of results. Following incubation, fluorescence was measured at 535nm (excitation) and 590nm (emission).

2.2.14: FAO enzyme activity assay

Cells were seeded at $1x10^6$ cells per well in 100mm dishes. The next day, cells were washed once with XF DMEM (2.5mM sodium pyruvate, 2mM L-glutamine) ± 2.5mM glucose to remove serum and media was immediately refreshed. Cells were immediately incubated in a non-CO_2 incubator at 37°C for 60 minutes. Cell lysate was collected by manual scraping and centrifugation at 2000*xg* (5 minutes, 4°C). The resulting pellet was washed once with ice-cold 0.01M PBS and cells lysed with 50µL ice-cold 1X Cell Lysis Solution (AssayGenie) via gentle pipetting. Lysate was left on ice for 5 minutes with regular agitation (gentle flicking) and a further 50µL ice-cold 1X Cell Lysis Solution added. Lysate was centrifuged at 21,000*xg* for 5 minutes at 4°C to remove cellular debris. FAO enzyme activity was determined using the FAO Kit (AssayGenie) in a reaction where half the replicates are not supplied with FAO substrate (octanoyl-CoA). Because this reaction relies on lysed cells, mitochondrial import of fatty acids by CPT1a is bypassed and thus

FAO enzyme activity downstream of the rate-limiting step of FAO can be interpreted. The reaction was incubated for 360 minutes in a non-CO_2 incubator at 37°C. Absorbance values at 492nm were measured. FAO activity values were calculated by subtracting control wells (no FAO substrate) from reaction wells (supplied with FAO substrate) and enzyme activity per µg protein calculated according to the manufacturer's directions.

2.2.15: Quantification of extracellular cytokine concentrations

Following cell treatments, media samples were collected and centrifuged at 21,000xg for 5 mins (4°C). For TNF enzyme-linked immunosorbent assays (ELISAs), 1 volume of sample was diluted in 1 volume of assay media. Samples were stored at -70°C until use. Concentrations of extracellular cytokines (TNF, IL-10 [Bio-techne]) were quantified via DuoSet ELISAs (Bio-techne) according to the manufacturer's specifications. Samples for ELISAs were run in duplicate. Known concentrations of the relevant cytokine were used to interpolate the unknown concentrations in samples via a 4-parameter logistic curve. 4-parameter logistic curves were interpreted using an online Four Parameter Logistic Curve analysis tool[453].

2.2.16: Cell viability assay

Cells were seeded at $3.5x10^5$ cells per well in 6 well plates (Sarstedt). Following 24h treatments, a propidium iodide stain (Merck Millipore) was used to gauge cell viability using flow cytometry[167,449,454]. Propidium iodide accumulates in cells with disrupted membranes, providing an indication of cell death[454]. Briefly, at the end of treatment periods, media was collected into a centrifuge tube (Sarstedt). Cells were washed with PBS (also collected into a centrifuge tube) and detached via trypsinisation (**Chapter 2.2.4**). Trypsin was neutralised using flow cytometry buffer (**Table 2.2.16**) and cells pelleted via centrifugation (300*xg*, 5 minutes, 4°C). Supernatent was aspirated and cells were resuspended in flow cytometry buffer with propidium iodide (2µg/mL). Negative controls were not exposed to propidium iodide staining. Cells were incubated for 10 minutes on ice and cell viability quantified via flow cytometry (BD Accuri C6 Plus Flow Cytometer; BD Biosciences). Flow cytometry was run on the 'fast' setting, counting 10,000 events per sample. Gating was set using the aforementioned propidium iodide-free negative control, and a positive control for cell death was included by boiling cells at 55°C for 10 minutes.

Table 2.2.16: Flow cytometry buffer

Component	Final concentration	2mL stock:
0.01M PBS	-	1920µL
FBS (100%)	2% (vol/vol)	40µL
Propidium iodide stock solution (1mg/ml)	20µg/mL (2% vol/vol; i.e. 20µL/mL)	40µL

If making negative control stain, exclude propidium iodide.

2.2.17: Data handling and statistical analysis

Raw data were processed using Microsoft Excel and statistical analyses were performed using GraphPad Prism (v10.0.2). Extracellular flux analysis data were normalized to protein content per well using Wave Analysis Software (Agilent) and exported to Prism. For immunoblots, raw data (intensity per band) was normalized to a housekeeping control (β-actin or GAPDH) and expressed as the proportion of the protein of interest to housekeeping control (denoted as [protein of interest]/[housekeeping control]). When determining protein phosphorylation levels, the normalised intensity of the phosphorylated protein was expressed as a ratio of (normalised intensity of phosphorylated protein):(normalised intensity of total protein).

For all data sets, outliers were identified via the robust regression and outlier removal (ROUT) method (Q=1%). Outliers were removed from the dataset, and normality of data was then assessed using a D'Agostino & Pearson omnibus normality test (α=0.05). If data were determined to be non-parametric, a non-parametric statistical test (i.e., Mann-Whitney test or Kruskal Wallis test) were used as appropriate. Parametric datasets were analysed using parametric statistical tests (i.e., an unpaired two-tailed t-test or one-way analysis of variance [ANOVA]). Non-parametric and parametric data consisting of multiple groups with multiple interventions (e.g., TSPO$^{+/+}$, $^{-/-}$ MPAs ± LPS treatment) were analysed via a 2-way ANOVA. This is because at the time of analysis, Prism did not offer a mathematically reasonable non-parametric alternative to the 2-way ANOVA. For all statistical analyses, results were accepted as statistically significant if $p<0.05$.

Chapter 3: TSPO as a regulator of astrocyte metabolism

A modified version of this chapter is published as part of:

Regulation of astrocyte metabolism by mitochondrial translocator protein 18kDa.

Firth W, Robb JL, Stewart D, Pye KR, Bamford R, Oguro-Ando A, Beall C, Ellacott KLJ. ***BioRxiv preprint.*** *doi: 10.1101/2023.09.29.560159.*

3.1: Introduction

As outlined in **Chapter 1**, astrocytes are important for the sensing changes to the CNS microenvironment and maintaining CNS homeostasis[20,80,102]. By appropriately responding to environmental flux, astrocytes preserve the integrity and function of the CNS by altering blood flow[80,97,98], increasing nutrient uptake from the blood to provide trophic support to neurons[62,80], and managing inflammatory responses[20,80,102,258]. Changes to the ability of astrocytes to manage their bioenergetic state can, therefore, determine the timeliness, quality, and duration of the response to stimuli[72]. Prolonged exposure to harmful or noxious stimuli, such as chronic inflammation, can alter the metabolic phenotype of astrocytes[102,167,258]. For example, models of conditions such as diabetes – characterised by prolonged perturbations in the availability of metabolic substrates, i.e., glucose – have also been found to modulate astrocyte phenotypes[76,455]. This has been linked to altered mitochondrial substrate preferences in astrocytes[76], which may have bearing on the ability of these cells to fulfil their critical roles by impeding the trophic support to neurons, and modulating the inflammatory states of astrocytes[455]. Together, these studies highlight the importance of astrocytes in regulating CNS microenvironment and underscore the cruciality of regulation of cellular metabolism to ensuring astrocytes can meet this function.

TSPO, a protein known to regulate cellular metabolism in other cells[321,339,340,358,366,368–370] which is expressed in astrocytes under basal conditions[374,393,407,456], may play a role in regulating the cellular metabolism or bioenergetics of these cells. While changes to astrocytic TSPO expression correlating with a metabolic shift in the brain during Alzheimer's disease have been reported[393], the role TSPO plays in regulating the cellular metabolism of astrocytes remains unclear. Evidence for TSPO as a regulator of cellular

metabolism first emerged from prokaryotes in 1997[321,367], with this body of work proposing that TSPO functioned as an oxygen sensor in unicellular organisms. The first direct evidence for TSPO as a regulator of mammalian cellular metabolism followed in 2015 through studies of oxygen consumption rate [OCR] in murine primary microglia *in vitro*[324,367]. A role for TSPO in regulating fatty acid oxidation (FAO) was first touted in 2005, when TSPO was found to be upregulated in the 3T3-L1 cells, which serve as a model of adipocyte differentiation[457]. In keeping with these findings, previous evidence from the Ellacott laboratory has shown that TSPO expression in brown and white adipose tissue is reduced in HFD-induced obese mice[458]. Obese organisms exhibit reduced FAO, thus this study supports[459,460] the idea of a link between TSPO and fatty acid metabolism. In 2016, Tu *et al*.[366] provided evidence showing that loss of TSPO reduced mitochondrial respiration (a proxy of oxygen consumption) in Leydig cells, further demonstrating that this was concomitant with an increase in the use of fatty acid oxidation (FAO) to sustain bioenergetic rates in these cells. In this study, TSPO deficiency was associated with increased expression of the carnitine palmitoyltransferase 1a (*Cpt1a*) gene, which encodes the rate-limiting enzyme of FAO[366]. This led to speculation that TSPO may regulate FAO via a mechanism involving CPT1a, though this remains unconfirmed[367]. FAO in astrocytes is crucial for maintaining neural health[89,219] yet the mechanisms regulating this remain unclear; thus, a greater understanding of whether TSPO regulates FAO in these cells is required.

TSPO expression in the CNS increases during chronic neuroinflammation and has been associated with a variety of pathological states. Hence, the question of TSPO functionality in glial cells, and the possible therapeutic targeting of TSPO, have recently gained attention. In 2020, Fu *et al*.[370] demonstrated that a CRISPR-Cas9 mediated TSPO knockout in GL261 murine glioma cells reduced mitochondrial respiratory complex 1 expression and mitochondrial-linked ATP production, while increasing glycolysis and expression of the gene encoding lactate dehydrogenase (LDH). However, recapitulation of this model using a short hairpin RNA vector in GBM1B human stem-like cells and U87MG human glioma cells showed differential effects on metabolism: mitochondrial respiration and mitochondrial-linked ATP production were reduced in U87MG cells, but glycolytic rate and capacity were increased in the cells. The differences in results from this

study may have been due to the different species used or may be due to the fundamental differences between a genetic knockout and knockdown of the protein. Conversely, in the same year, Yao *et al*.[339] showed that TSPO$^{-/-}$ primary mouse microglia had reduced glycolysis and reduced mitochondrial function *in vitro*. In this model, phagocytosis and inflammatory responses – processes which, in the periphery, are well known to incur metabolic costs[289] – were impaired. Together, these data show that TSPO plays a role in regulating cellular bioenergetics, though the implications of this for primary cells remain unclear.

Thus, while links between increased TSPO expression in astrocytes and pathological state have been demonstrated[393], the role TSPO plays in regulating astrocyte bioenergetics has not yet been studied comprehensively. Furthermore, the role of TSPO in regulating astrocyte bioenergetics is poorly understood compared to other cell types. As tight control of cellular bioenergetics is crucial to enable astrocytes to maintain CNS homeostasis, an improved understanding of the role TSPO plays in regulating astrocyte metabolism may provide valuable information about astrocyte functionality and the potential therapeutic applications and ramifications of targeting TSPO for the treatment of neuroinflammatory conditions. In this chapter, I will explore the role of TSPO as a regulator of astrocyte mitochondrial and glycolytic respiration. The effect of TSPO deficiency on the responses of astrocytes to the absence and reintroduction of metabolic substrates will be explored and I will present evidence of a role for TSPO in regulating FAO in astrocytes.

3.2: Hypothesis

In this chapter, I tested the hypothesis that loss of TSPO will attenuate mitochondrial respiration and enhance glycolysis in astrocytes. I further tested the hypothesis that TSPO$^{-/-}$ astrocytes will have enhanced fatty acid oxidation, and that – when present – TSPO regulates FAO in astrocytes via an interaction with CPT1a.

3.3: Methods

All methods used in this chapter are described in full in **Chapter 2**.

3.4: Results

3.4.1: TSPO deficiency reduced basal mouse primary astrocyte (MPA) metabolism

As outlined in **Chapter 2**, a germline TSPO knockout mouse strain ($TSPO^{-/-}$) was employed to determine the role of TSPO in regulating primary astrocyte metabolism. I isolated astrocytes from the cortex of neonatal mice (p1-5) and used extracellular flux analysis to characterise the metabolic phenotype of these cells under basal conditions.

Initially I sought to recapitulate the metabolic phenotype of $TSPO^{-/-}$ mouse primary astrocytes (MPA) reported (reduced mitochondrial respiration) by a previous member of the Ellacott laboratory as part of their PhD thesis[452]. I found that basal oxygen consumption rate (OCR) – a proxy for mitochondrial respiration – was reduced by 31.1% in $TSPO^{-/-}$ MPAs compared to $TSPO^{+/+}$ MPA controls (**Figure 3.4.1 A, B**; $p<0.0001$). Similarly, mean basal extracellular acidification rate (ECAR) was reduced by 38.8% (**Figure 3.4.1 C, D**; $p<0.0001$). These data showed that the basal metabolic rates of $TSPO^{-/-}$ MPAs were reduced compared to $TSPO^{+/+}$ counterparts.

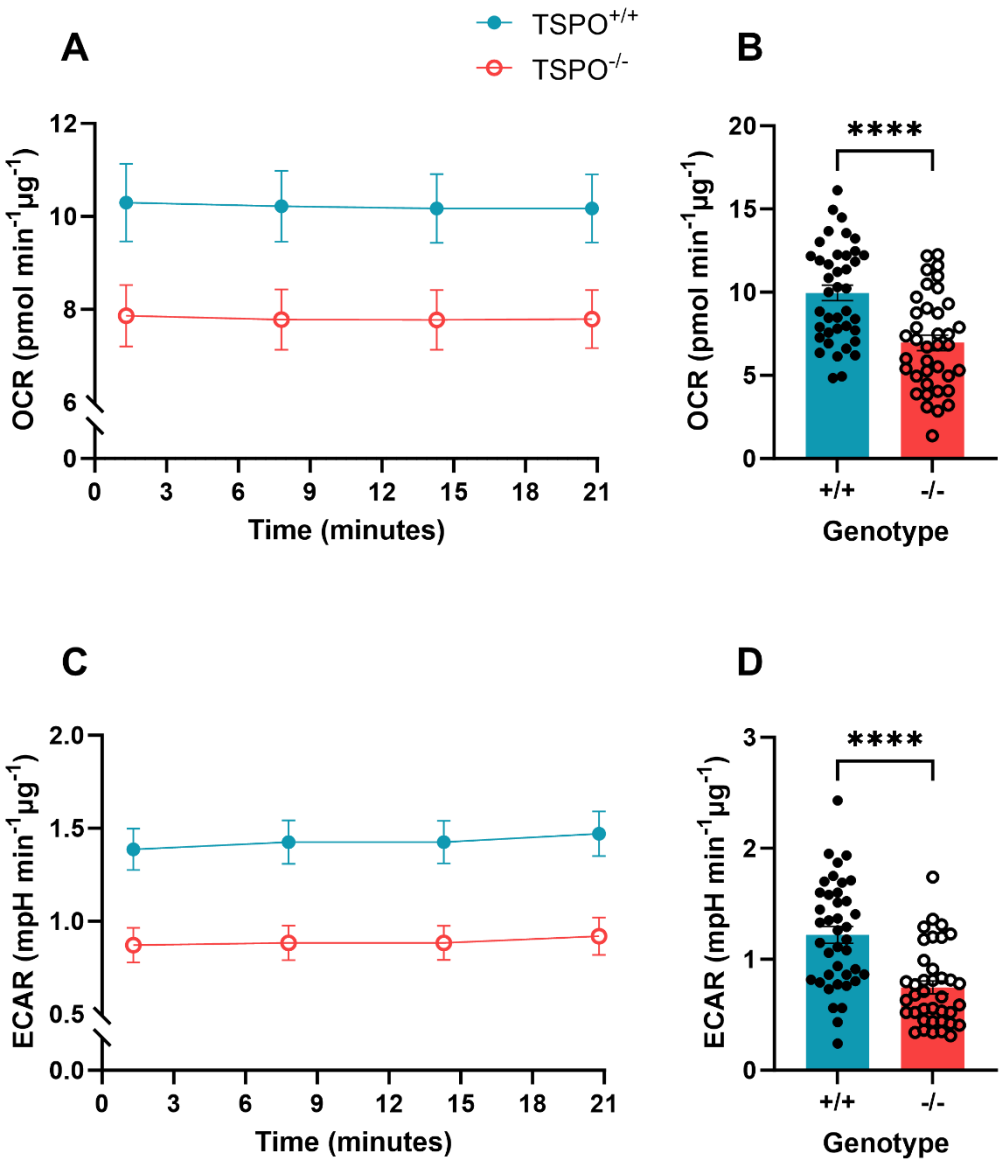

Figure 3.4.1: TSPO deficiency reduced basal mouse primary astrocyte (MPA) metabolism.

A: Oxygen consumption rate (OCR) of TSPO$^{-/-}$ MPAs and TSPO$^{+/+}$ controls measured over time. **B:** OCR was significantly reduced in TSPO$^{-/-}$ MPAs. n=30-32 wells, data are pooled from across 3 independent experiments. Unpaired t-test, p<0.0001. Datapoints were taken from time point 4 of **A**. **C:** Extracellular acidification rate (ECAR) of TSPO$^{-/-}$ and TSPO$^{+/+}$ MPAs measured over time. **D:** ECAR was significantly reduced in TSPO$^{-/-}$ MPAs. n=30-32 wells, data are pooled from across 3 independent experiments. Unpaired t-test, p<0.0001. Datapoints were taken from time point 4 of **C**.

****p<0.0001. Data are displayed as mean ± standard error of the mean.

3.4.2: TSPO deficiency reduced mitochondrial respiration in MPAs

Having established that TSPO deficiency reduced the basal bioenergetics of MPAs, I wanted to further interrogate any underlying changes to the mitochondrial function of $TSPO^{-/-}$ MPAs. During their doctoral studies, a previous student in our laboratory reported that $TSPO^{-/-}$ MPAs exhibited reduced mitochondrial respiration[452]. Thus, to confirm that I could recapitulate these results, and hypothesising that the reduction to basal bioenergetics I observed in **Figure 3.4.1** was due to the absence of TSPO impairing mitochondrial metabolism, I used the mitochondrial stress test (Agilent; **Chapter 2.2.12.1**; **Figure 3.4.2 A**) to further investigate changes to mitochondrial function, again via extracellular flux analysis. In line with my findings in **Figure 3.4.1**, basal mitochondrial respiration (OCR) was significantly reduced in $TSPO^{-/-}$ MPAs (**Figure 3.4.2 C**, $p<0.01$). Mitochondrial respiration linked to ATP production was similarly reduced in these cells (**Figure 3.4.2 E**, $p<0.05$). Although non-mitochondrial respiration (**Figure 3.4.2 B**), maximal mitochondrial respiration (**Figure 3.4.2 D**), proton leak, coupling efficiency, and spare respiratory capacity (**Figure 3.4.2 F-H**) trended towards a reduction, these values failed to reach statistical significance in my hands. Despite this, the trend shown in these data recapitulates that reported by the previous doctoral student in our research group[452].

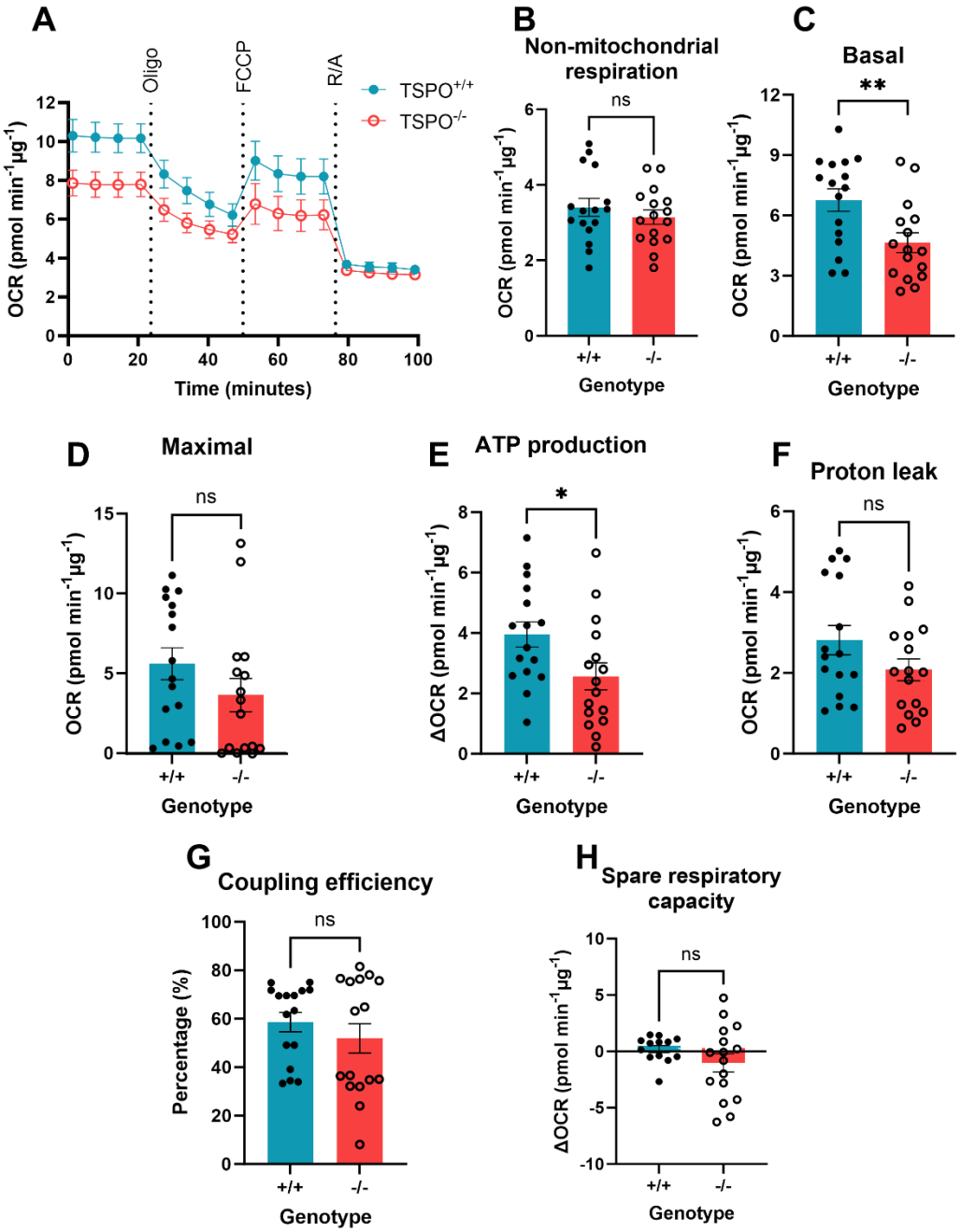

Figure 3.4.2: TSPO deficiency reduced mitochondrial respiration in MPAs. **A:** The mitochondrial stress test paradigm was used to investigate changes to mitochondrial function in TSPO$^{-/-}$ MPAs. **B:** non-mitochondrial respiration was unchanged in TSPO$^{-/-}$ MPAs. n=14-16 wells from 1 experiment. Unpaired t-test, p=0.4075. **C:** basal mitochondrial respiration was reduced in TSPO$^{-/-}$ MPAs. n=14-16 wells from 1 experiment. Unpaired t-test, p=0.0077. **D:** maximal mitochondrial respiration was unchanged in TSPO$^{-/-}$ MPAs. n=14-16 wells from 1 experiment. Mann-Whitney test, p=0.1100. **E:** mitochondrial respiration-linked ATP production was significantly reduced in TSPO$^{-/-}$ MPAs. n=14-16 wells from 1 experiment. Unpaired t-test, p=0.0310. **F:** proton leak was unchanged in TSPO$^{-/-}$ MPAs. n=14-16 wells from 1 experiment. Unpaired t-test, p=0.1134. **G:** coupling efficiency was unchanged in TSPO$^{-/-}$ MPAs. n=14-16 wells from 1 experiment. Unpaired t-test, p=0.3610. **H:** SRC was unchanged in TSPO$^{-/-}$ MPAs. n=14-16 wells from 1 experiment. Mann-Whitney test, p=0.3079.

ns: not significant, p>0.05. *p<0.05. **p<0.01. OCR: oxygen consumption rate. Oligo: oligomycin (0.5µM). FCCP: carbonyl cyanide-p-trifluoromethoxyphenylhydrazone (1µM). R/AA: rotenone/antimycin-A (0.5µM). TSPO: translocator protein 18kDa. $^{-/-}$: deficient/knockout. $^{+/+}$: expressing/wildtype.

3.4.3: TSPO deficiency increased glycolysis in MPAs

In vivo, astrocytes form the BBB alongside epithelial cells and tanycytes[80]. This enables astrocytes to control capillary vasodilation and vasoconstriction, and makes astrocytes well suited to nutrient uptake and distribution in order to provide trophic support for neurons[80,98]. As part of this trophic support, astrocytes break down glucose into lactate, which may be shuttled to neurons for oxidative phosphorylation, and can be secreted to act as a signalling molecule to other glial cells[62]. Resultantly, *in vivo* under non-pathological conditions astrocytes exhibit a predominantly glycolytic metabolic phenotype relative to neurons, being less reliant on oxidative phosphorylation. Evidence from glioma cells[370] and primary microglia[339,340] in culture has demonstrated that TSPO may play a role in regulating glycolysis; thus, I hypothesised that TSPO deficiency would impair the glycolytic metabolism of MPAs. I investigated this using the glycolysis stress test (see **Chapter 2.2.12.2**; **Figure 3.4.3 A**). I found that non-glycolytic acidification was significantly increased in $TSPO^{-/-}$ MPAs (**Figure 3.4.3 B**; $p<0.0001$). $TSPO^{-/-}$ MPAs exhibited increased glycolytic rate by a mean of 18.03% (**Figure 3.4.3 C**; $p<0.0001$). Further, glycolytic capacity was increased by a mean of 25.82% in $TSPO^{-/-}$ MPAs (**Figure 3.4.3 D**; $p<0.0001$), and mean glycolytic reserve was increased by 27.64% (**Figure 3.4.3 E**; $p<0.0001$).

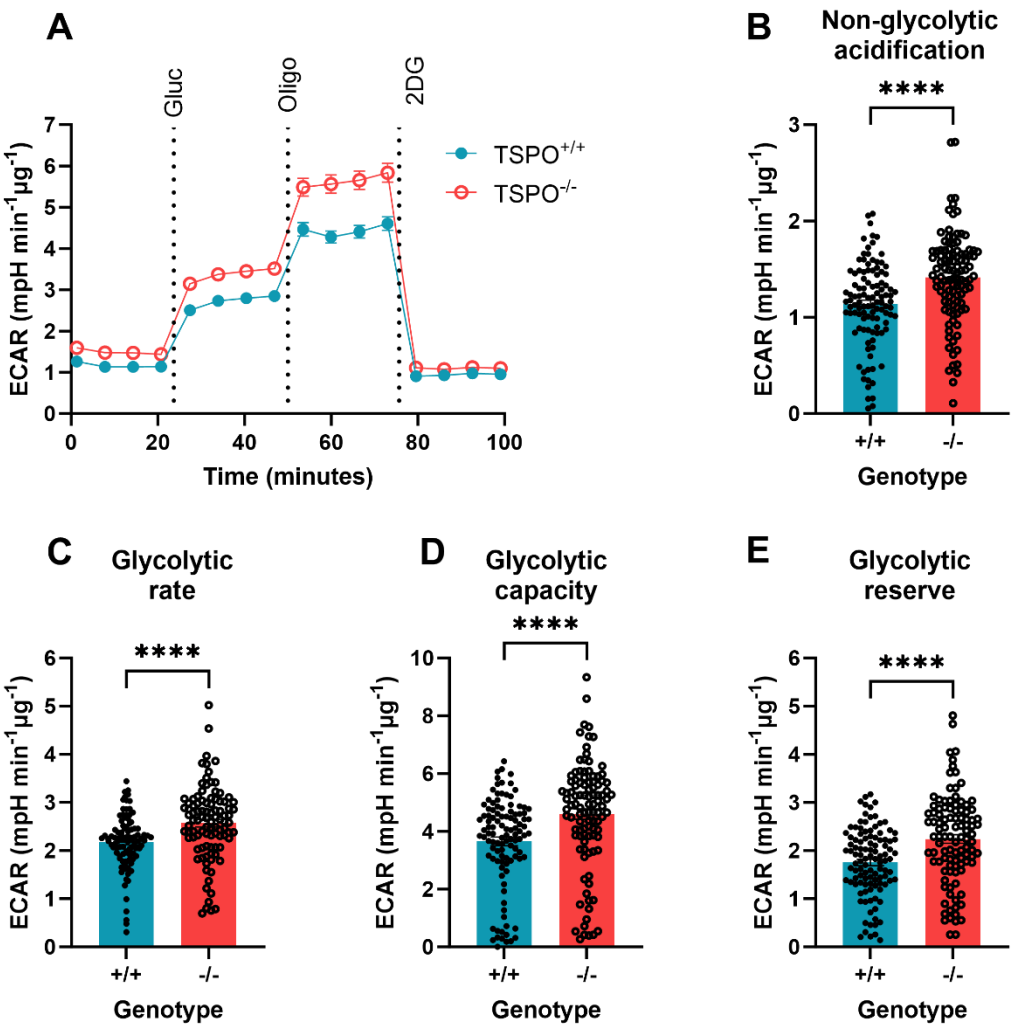

Figure 3.4.3: TSPO deficiency increased glycolysis in MPAs.

A: The glycolysis stress test paradigm was used to investigate changes to glycolytic metabolism in TSPO$^{-/-}$ MPAs. **B:** Non-glycolytic acidification was significantly increased in TSPO$^{-/-}$ MPAs. n=104-108 wells per genotype, data are pooled from across 3 independent experiments. Unpaired t-test, p<0.0001. **C:** Glycolytic rate was significantly increased in TSPO$^{-/-}$ MPAs. n=104-108 wells per genotype, data are pooled from across 3 independent experiments. Mann-Whitney test, p<0.0001. **D**: Glycolytic capacity was significantly increased in TSPO$^{-/-}$ MPAs. n=104-108 per genotype, data are pooled from across 3 independent experiments. Mann-Whitney test, p<0.0001. **E**: Glycolytic reserve was significantly increased in TSPO$^{-/-}$ MPAs. n=104-108 per genotype, data are pooled from across 3 independent experiments. Mann-Whitney test, p<0.0001.

****p<0.0001. Data are displayed as mean ± standard error of the mean. ECAR: extracellular acidification rate. Gluc: glucose (10mM). Oligo: oligomycin (1µM). 2DG: 2-deoxyglucose (50mM). TSPO: translocator protein 18kDa. $^{-/-}$: deficient/knockout. $^{+/+}$: expressing/wildtype.

3.4.4: TSPO deficiency reduced glycolytic rate, but increased glycolytic capacity, in U373 cells

To confirm my seemingly unexpected finding that TSPO$^{-/-}$ MPAs exhibited increased glycolysis, I sought to repeat this finding in an independent cell model. Hypothesising that the glycolytic phenotype we observed in TSPO$^{-/-}$ MPAs would be conserved in another model, we made use of a CRISPR-Cas9-generated TSPO$^{-/-}$ U373-MG astrocytoma cell line[451], generated by Daisy Stewart in our lab during her Professional Training Year in 2019. The data in this figure were generated by Dr Josephine L Robb, and are included in this thesis for completeness. The glycolysis stress test was again used here (**Figure 3.4.4 A**). In line with TSPO$^{-/-}$ MPAs, the non-glycolytic acidification from TSPO$^{-/-}$ U373 cells was significantly increased compared to TSPO$^{+/+}$ controls (**Figure 3.4.4 B**; $p<0.05$). However, the increased glycolytic phenotype we observed TSPO$^{-/-}$ MPAs in **Figure 3.4.3** was not conserved in TSPO$^{-/-}$ U373 cells. We found that U373 TSPO$^{-/-}$ cells exhibited a mean reduction in glycolytic rate of 26.46% (**Figure 3.4.4 C**, $p<0.0001$) and we observed no change in glycolytic capacity compared to U373 TSPO$^{+/+}$ EV controls [transfected with noncoding guide RNA; see **Chapter 2.2.5**] (**Figure 3.4.4 D**; $p=0.3776$). Supporting our finding from MPAs (**Figure 3.4.3 E**) mean glycolytic reserve was increased by 72.95% in TSPO$^{-/-}$ U373s (**Figure 3.4.4 E**; $p<0.0001$).

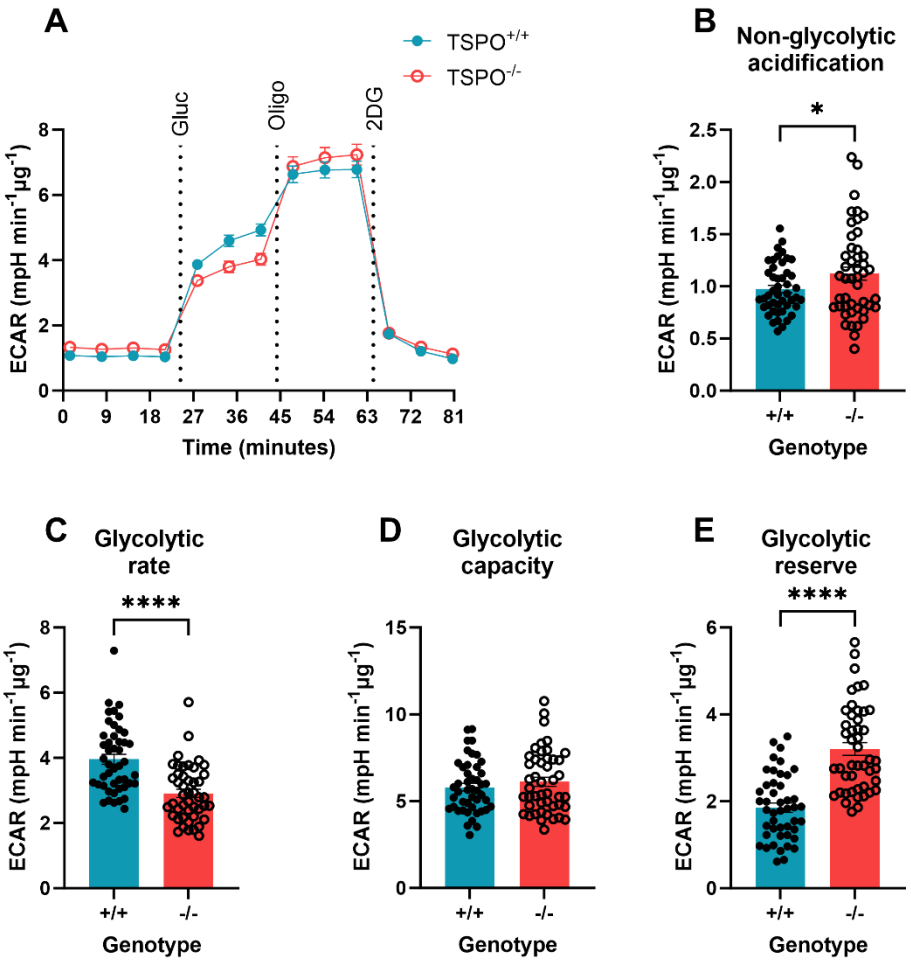

Figure 3.4.4: TSPO deficiency reduced glycolytic rate, but increased glycolytic reserve, in U373 cells.

A: The glycolysis stress test paradigm was used to investigate changes to glycolytic metabolism in TSPO$^{-/-}$ U373s. **B:** Non-glycolytic acidification was significantly increased in TSPO$^{-/-}$ U373s. n=46 wells per genotype, data are pooled from across 3 independent experiments. Unpaired t-test, p=0.042. **C:** glycolytic rate was reduced in TSPO$^{-/-}$ U373s. n=46 wells per genotype, data are pooled from across 3 independent experiments. Mann-Whitney test, p<0.0001. **D:** TSPO$^{-/-}$ U373s showed no significant difference in glycolytic capacity. n=46 wells per genotype, data are pooled from across 3 independent experiments. Unpaired t-test, p=0.3776. **E:** glycolytic reserve was significantly increased in TSPO$^{-/-}$ U373s. n=46 wells per genotype, data are pooled from across 3 independent experiments. This data was generated by Dr Josephine L Robb and is included in this thesis for completeness.

****p<0.0001. Data are displayed as mean ± standard error of the mean. ECAR: extracellular acidification rate. Gluc: glucose (10mM). Oligo: oligomycin (1µM). 2DG: 2-deoxyglucose (50mM). TSPO: translocator protein 18kDa. $^{-/-}$: deficient/knockout. $^{+/+}$: expressing/wildtype.

3.4.5: TSPO$^{-/-}$ MPAs had a larger change in ECAR in response to 1000μM L-glutamine injection

Following the unexpected increase in glycolytic activity of TSPO$^{-/-}$ MPAs I observed in **Figure 3.4.3**, I wanted to further investigate any underlying changes to the bioenergetic preferences of these cells. In bacteria and plants, TSPO has been linked to nutrient sensing[311,321,359–361,425], and in complex organisms, astrocytes play key roles in nutrient uptake and distribution (**Chapter 1.3**). Hence, I hypothesised that TSPO$^{-/-}$ MPAs may have altered nutrient sensing capabilities.

The mitochondrial (**Figure 3.4.2**) and glycolysis stress tests (**Figures 3.4.3, 3.4.4**) interrogate different aspects of cellular metabolism in part due to the differential provision of substrates to the cells via the media, to promote the use of particular metabolic pathways. For example, the glycolysis stress test begins with a glucose-free incubation during the degas period, to starve the cells of glucose and force the cells to utilise remaining glycogen stores, followed by the reintroduction of a high concentration of glucose to encourage glycolytic metabolism. To ensure cell survival in this low glucose period, cells are supplemented with L-glutamine, which undergoes oxidative phosphorylation to provide energy. In contrast, the mitochondrial stress test provides the cells with a physiologically relevant glucose concentration (2.5mM), as well as sodium pyruvate and L-glutamine. Because glucose must undergo glycolysis to form pyruvate, sodium pyruvate supplementation enables continuous use of oxidative phosphorylation to avoid cell stress. Given that L-glutamine is the nutrient consistently supplemented to the cells between these assays, I next tested the hypothesis that the TSPO$^{-/-}$ MPAs would show no difference in the metabolic response to the reintroduction of L-glutamine, following 1h L-glutamine starvation during the degas period.

For the majority of concentrations tested (**Figure 3.4.5 A-L**), I observed no significant difference in the metabolic response (ECAR, expressed here as change in ECAR [ΔECAR]) to the reintroduction of L-glutamine in TSPO$^{-/-}$ MPAs (**Figure 3.4.5 A-H, K, L)**. In response to the reintroduction of 1000μM L-glutamine, TSPO$^{-/-}$ MPAs showed a significantly increased metabolic response (ΔECAR) (**Figure 3.4.5 I, J**). However, this effect was not concentration-dependent so likely indicates a spurious finding.

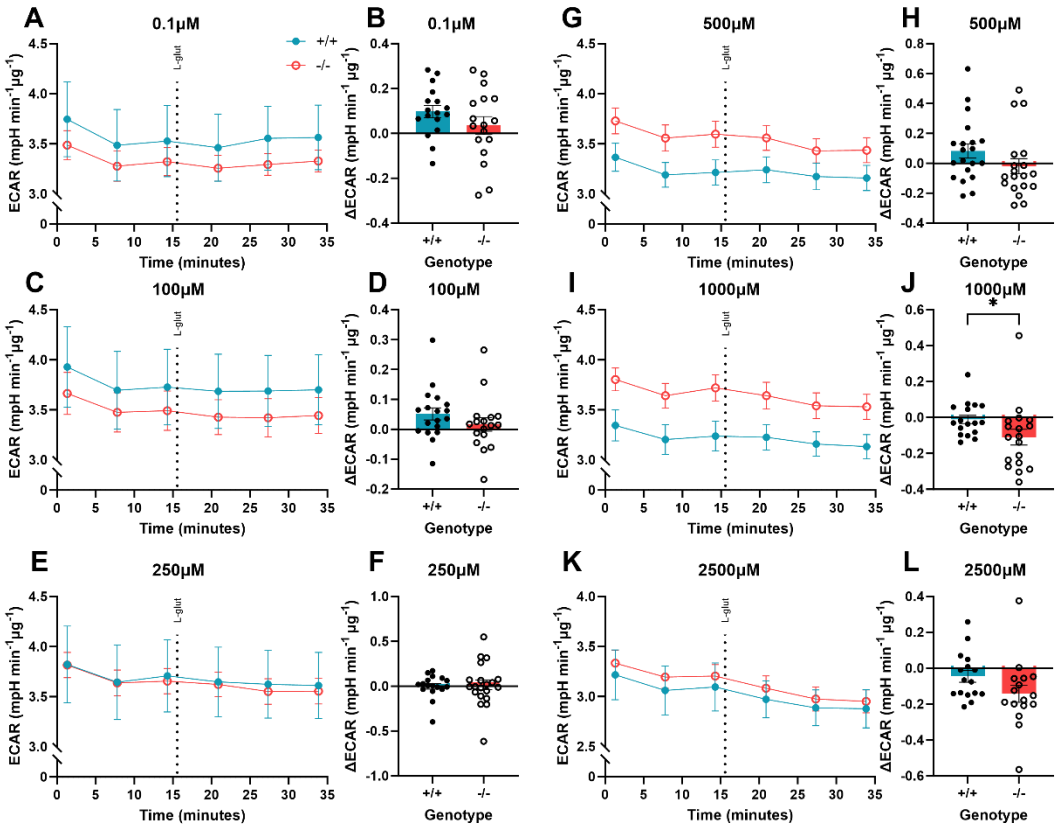

Figure 3.4.5: TSPO$^{-/-}$ MPAs had a larger change in ECAR in response to 1000µM L-glutamine injection.

Following starvation of L-glutamine during the degas period, L-glutamine was reintroduced to TSPO$^{+/+}$ and $^{-/-}$ MPAs following basal metabolism measurement, indicated by the dotted line in **A, C, E, G, I, K**. There was no significant difference in the change in ECAR observed following reintroduction of L-glutamine at 0.1 (**A, B**; unpaired t-test, p=0.2055), 100 (**C, D**; Mann-Whitney test, p=0.1178), 250 (**E, F**; Mann-Whitney test, p=0.8449), 500 (**G, H**; unpaired t-test, p=0.1502), or 2500µM L-glutamine (**K, L**; Mann-Whitney test, p=0.0562). TSPO$^{-/-}$ MPAs displayed an increased change in ECAR following 1000µM injection (**I, J**; Mann-Whitney test, p=0.0186). n=17-18 wells per genotype, data are pooled from across 4 independent experiments.

*p<0.05. Data are displayed as mean ± standard error of the mean. ECAR: extracellular acidification rate. L-glut: L-glutamine. TSPO: translocator protein 18kDa. $^{-/-}$: deficient/knockout. $^{+/+}$: expressing/wildtype. ΔECAR: change in ECAR.

3.4.6: TSPO$^{-/-}$ MPAs showed no difference in the change in OCR in response to L-glutamine injection

Because glutamine undergoes oxidative phosphorylation[61] (**Chapter 1.1.3.2**), and I had previously observed reduced mitochondrial metabolism in TSPO$^{-/-}$ MPAs (**Figure 3.4.2**), I hypothesised that TSPO$^{-/-}$ MPAs would show a reduced change in OCR (ΔOCR) following L-glutamine reintroduction. However, in contrast with my hypothesis, TSPO$^{-/-}$ MPAs did not show any significant difference in ΔOCR induced by L-glutamine reintroduction at any of the test concentrations (**Figure 3.4.6**).

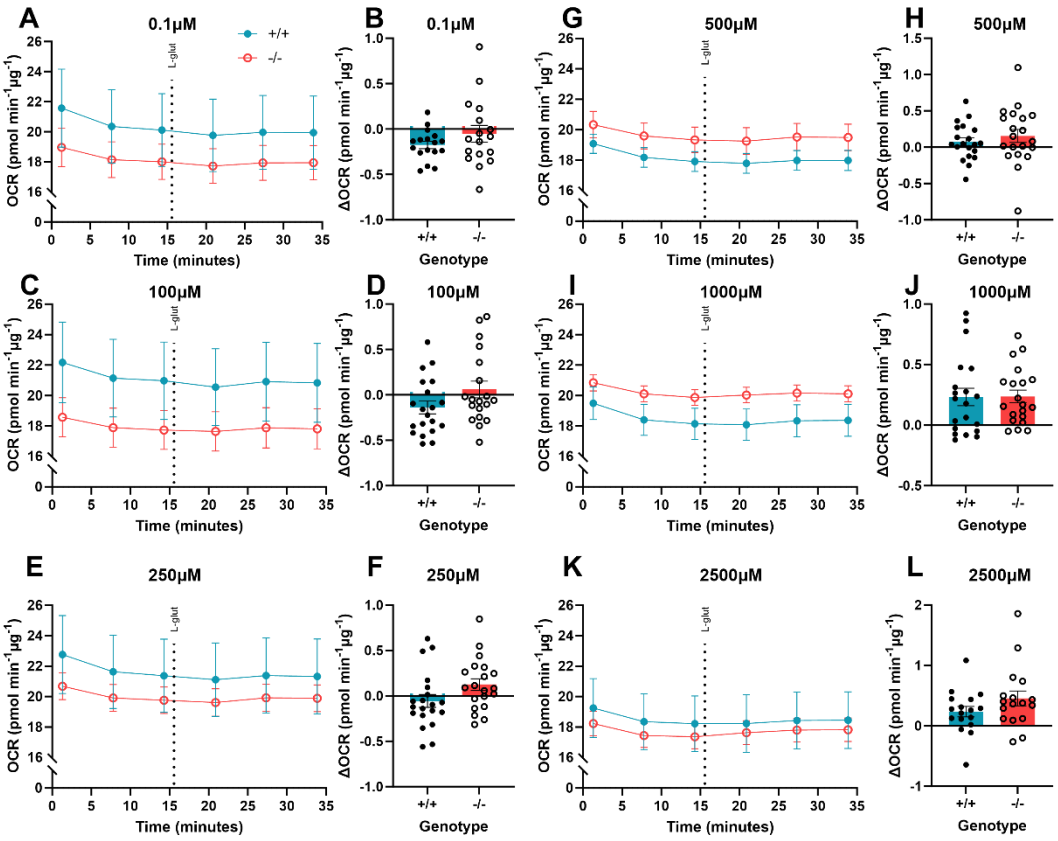

Figure 3.4.6: TSPO$^{-/-}$ MPAs showed no difference in the change in OCR in response to L-glutamine injection.

Following starvation of L-glutamine during the degas period, L-glutamine was reintroduced to TSPO$^{+/+}$ and $^{-/-}$ MPAs following basal metabolism measurements, indicated by the dotted line in **A, C, E, G, I, K**. There was no significant difference in ΔOCR observed following reintroduction of L-glutamine at 0.1 (**A, B**; unpaired t-test, p=0.2225), 100 (**C, D**; unpaired t-test, p=0.0906), 250 (**E, F**; unpaired t-test, p=0.0670), 500 (**G, H**; unpaired t-test, p=0.4359), 1000 (**I, J**; unpaired t-test, p=0.9622) or 2500µM L-glutamine (**K, L**; Mann-Whitney test, p=0.2313). n=17-18 wells per genotype, data are pooled from across 4 independent experiments.

Data are displayed as mean ± standard error of the mean. OCR: oxygen consumption rate. L-glut: L-glutamine. TSPO: translocator protein 18kDa. $^{-/-}$: deficient/knockout. $^{+/+}$: expressing/wildtype. ΔOCR: change in OCR.

3.4.7: TSPO$^{-/-}$ MPAs had a reduced change to ECAR in response to reintroduction of 1mM, 5.5mM, and 7.5mM glucose

Glucose is the main fuel source for nearly every mammalian cell. In the CNS, astrocytes are responsible for absorbing glucose from the blood (**Chapter 1**). Lactate can serve either as trophic support for neurons, which are less glycolytic than astrocytes, or can act as an intercellular signalling molecule within the CNS (**Chapter 1**). In my previous experiments examining the glycolytic metabolism of TSPO$^{-/-}$ MPAs (**Figure 3.4.3**), a supraphysiological concentration of glucose (10mM) was injected to saturate the cells and promote glycolytic metabolism. Based on these data, which showed that TSPO$^{-/-}$ MPAs showed a greater increase in ECAR following the reintroduction of glucose after a 1h starvation period (glucopenia) (**Figure 3.4.3 C**), I hypothesised that the TSPO$^{-/-}$ MPAs would display a greater sensitivity to glucose reintroduction, as reflected in a larger change in ECAR (ΔECAR) in response to the reintroduction of glucose concentrations <10mM compared to TSPO$^{+/+}$ MPAs. Glucose concentration used ranged from 0.1mM (physiologically relevant [to the CNS[76,124,461,462]] low glucose condition) to 7.5mM (physiologically relevant [to the CNS[461,462]] high glucose condition).

In contrast with my hypothesis, I observed no significant difference in ΔECAR induced by the reintroduction of glucose in TSPO$^{-/-}$ MPAs at 0.1 (**Figure 3.4.7 A, B**; p=0.1817), 0.5 (**Figure 3.4.7 C, D**; p=0.5385), or 2.5mM glucose (**Figure 3.4.7 G, H**; p=0.4875). However, compared to TSPO$^{+/+}$ cells, TSPO$^{-/-}$ MPAs showed an attenuated ECAR response following the reintroduction of 1mM ((**Figure 3.4.7 E, F**; p=0.0002), 5.5mM (**Figure 3.4.7 I, J**; p=0.0346), and 7.5mM glucose (**Figure 3.4.7 K, L**; p=0.0287).

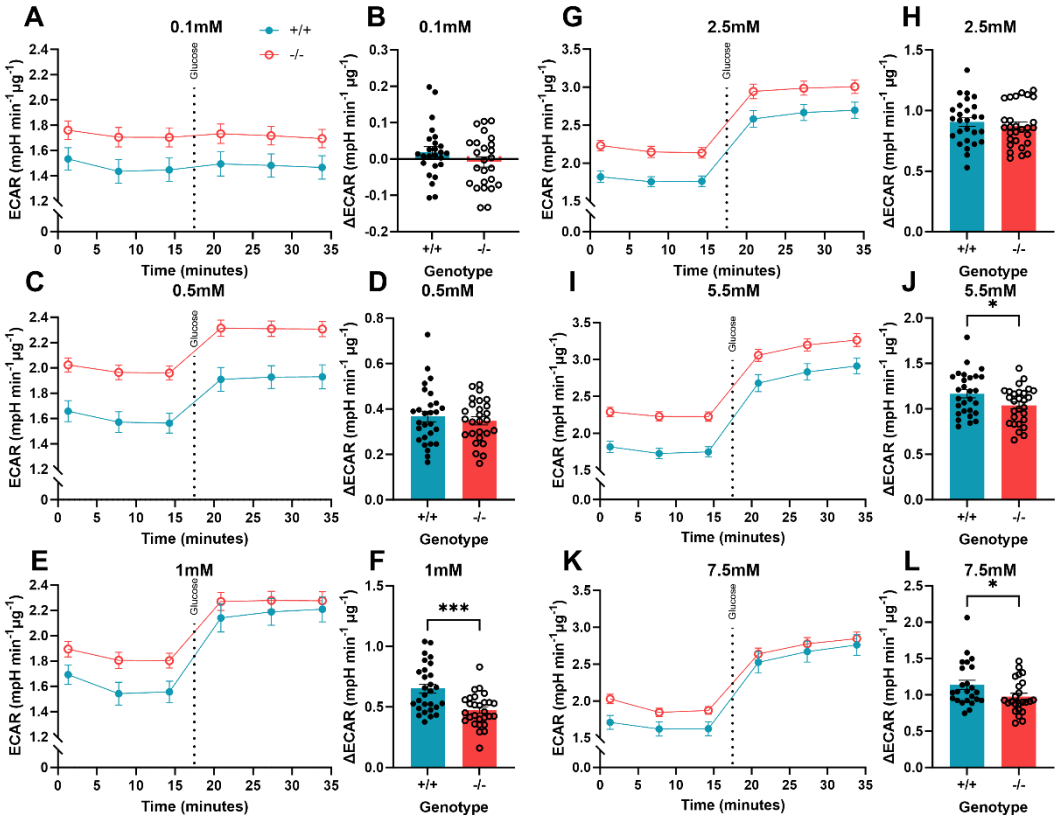

Figure 3.4.7: TSPO$^{-/-}$ MPAs had an attenuated change in ECAR following reintroduction of 1mM, 5.5mM, and 7.5mM glucose.

Following glucopenia during the degas period, glucose was reintroduced to TSPO$^{+/+}$ and $^{-/-}$ MPAs following basal metabolism measurements (indicated by the dotted line in **A, C, E, G, I, K**). There was no significant difference in ΔECAR following injection of 0.1 (**A, B**; unpaired t-test, p=0.1817), 0.5 (**C, D**; unpaired t-test, p=0.5385), or 2.5mM glucose (**G, H**; unpaired t-test, p=0.4875). Compared to TSPO$^{+/+}$ cells, TSPO$^{-/-}$ MPAs showed a significantly reduced ΔECAR following reintroduction of 1 (**E, F**; unpaired t-test, p=0.0002), 5.5 (**I, J**; unpaired t-test, p=0.0346), and 7.5mM glucose (**K, L**; Mann-Whitney test, p=0.0287).

n=24 wells per genotype, data are pooled from across 4 independent experiments.

*p<0.05, ***p<0.001. Data are displayed as mean ± standard error of the mean.

ECAR: extracellular acidification rate. TSPO: translocator protein 18kDa. $^{-/-}$: deficient/knockout. $^{+/+}$: expressing/wildtype. ΔECAR: change in ECAR.

3.4.8: OCR of TSPO$^{-/-}$ MPAs did not significantly change in response to glucose injection

I next tested the hypothesis that, concomitant with the predicted increase in ECAR in response to the reintroduction of glucose (**Figure 3.4.7**), TSPO$^{-/-}$ MPAs would show a further reduction in OCR (ΔOCR) following reintroduction of glucose.

Surprisingly, compared to TSPO$^{+/+}$ cells, TSPO$^{-/-}$ MPAs showed no significant difference in ΔOCR following the reintroduction of glucose at concentrations ranging from 0.1-7.5mM (**Figure 3.4.8**, $p>0.05$).

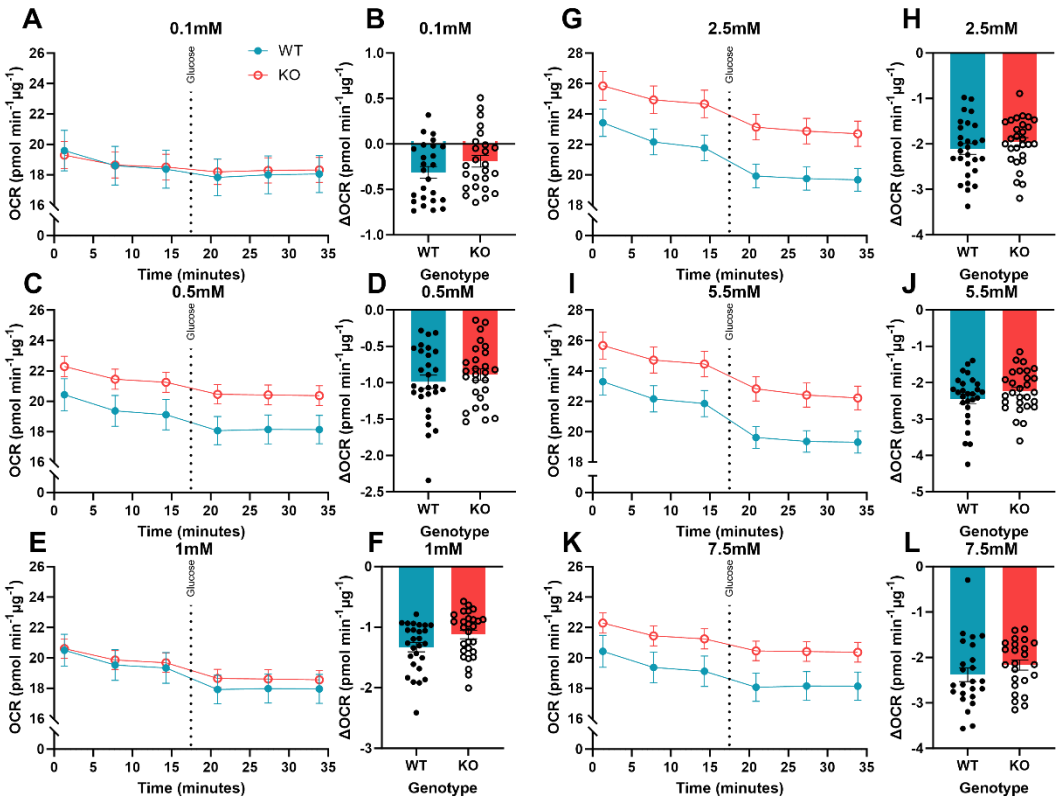

Figure 3.4.8: OCR of TSPO$^{-/-}$ MPAs did not significantly change in response to glucose injection.

Following glucopenia during the degas period, glucose was reintroduced to TSPO$^{+/+}$ and $^{-/-}$ MPAs following basal metabolism measurements. There was no significant difference in ΔOCR following injection of 0.1 (**A, B**; unpaired t-test, p=0.1828), 0.5 (**C, D**; unpaired t-test, p=0.4108), 1 (**E, F**; unpaired t-test, p=0.0502), 2.5 (**G, H**; unpaired t-test, p=0.3419), 5.5 (**I, J**; unpaired t-test, p=0.2125), or 7.5mM glucose (**K, L**; unpaired t-test, p=0.2640).

n=24 wells per genotype, data are pooled from across 4 independent experiments.

*p<0.05, ***p<0.001. Data are displayed as mean ± standard error of the mean.

OCR: oxygen consumption rate. ΔOCR: change in OCR. TSPO: translocator protein 18kDa. $^{-/-}$: deficient/knockout. $^{+/+}$: expressing/wildtype.

3.4.9: TSPO$^{-/-}$ MPAs maintained metabolic rates in the absence of glucose

Intrigued by the differences I observed in the responsiveness of TSPO$^{-/-}$ MPAs to the reintroduction of substrates following a 1h glucose-free period (**Figure 3.4.5-8**) and by the unexpected results of the glycolysis stress test (**Figure 3.4.3**), I wanted to further characterise the metabolic responses of TSPO$^{-/-}$ MPAs to nutrient stress.

My work examining the metabolic responses of TSPO$^{-/-}$ MPAs to the reintroduction of glucose (**Figure 3.4.7, 8**) led me to hypothesise that TSPO$^{-/-}$ MPAs utilised less glucose to maintain their bioenergetic rates. To investigate this hypothesis, I began by repeating the basal metabolism measurements under the initial conditions of the mitochondrial and glycolytic stress tests on the same Seahorse plate. This allowed me to generate data that was directly comparable. Using a 2-way ANOVA, I found no statistically significant effect of TSPO genotype on OCR (**Figure 3.4.9 A, C**; $p_{genotype}$=0.6373, $F_{(1,58)}$=0.2246). However, I found that glucose concentration had a statistically significant effect on OCR ($p_{glucose}$=0.0442, $F_{(1,58)}$=4.232). Moreover, there was a statistically significant interaction between TSPO genotype and glucose ($p_{interaction}$=0.0034, $F_{(1,58)}$=9.348). Similarly, I found no statistically significant effect of TSPO genotype on ECAR (**B, D**) ($p_{genotype}$=0.1640, $F_{(1,58)}$=1.987). I found that there was a statistically significant effect of glucose concentration on ECAR ($p_{glucose}$=0.0351, $F_{(1,58)}$=4.654), and that there was a statistically significant interaction of these variables ($p_{interaction}$=0.0191, $F_{(1,58)}$=5.186).

Using post-hoc analyses, I found that, unlike TSPO$^{+/+}$ MPAs – which reduced their basal metabolic rates in response to the absence of glucose and sodium pyruvate (glycolysis stress test basal media; **Figure 3.4.9**) – TSPO$^{-/-}$ MPAs showed no significant differences in their OCR (**Figure 3.4.9 A**; p=0.9823) or ECAR (**Figure 3.4.9 B**; p>0.9999) under these substrate-limited conditions.

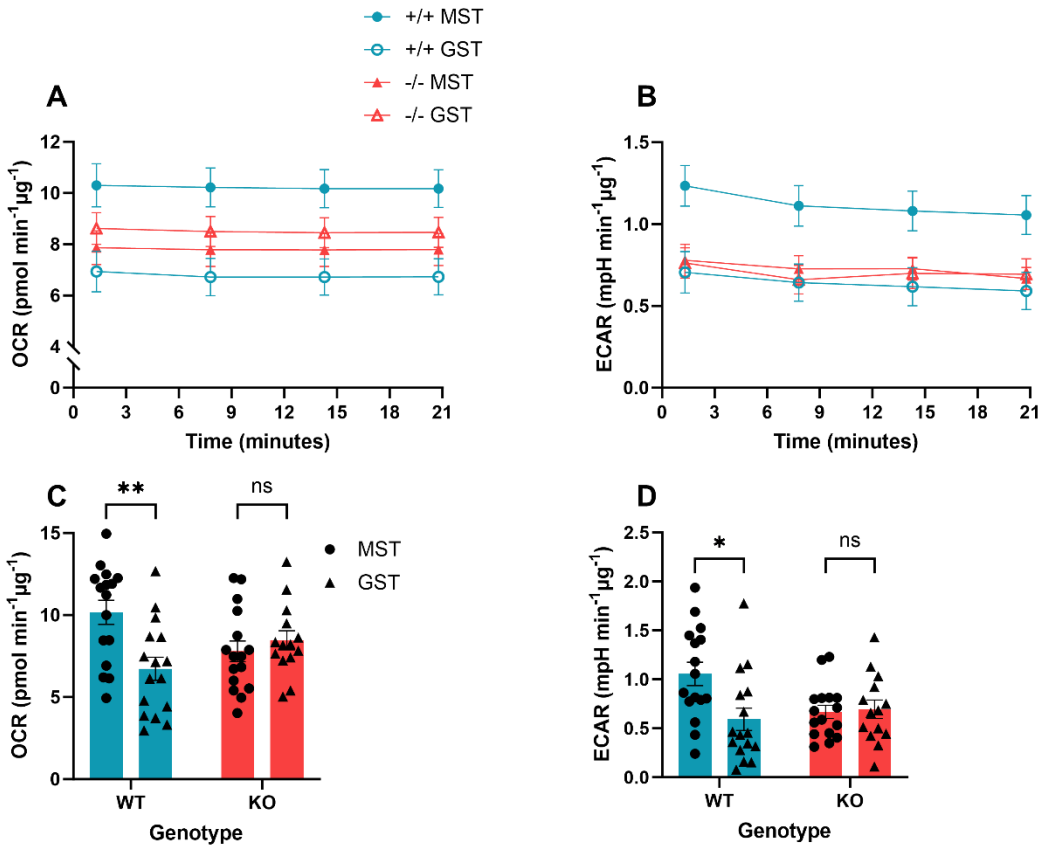

Figure 3.4.9: TSPO$^{-/-}$ MPAs maintained the basal metabolic rate in the absence of glucose.

To directly compare the differences in TSPO$^{-/-}$ MPA bioenergetics in the presence or absence of glucose and sodium pyruvate, both conditions were run on the same Seahorse plate.

No statistically significant effect of TSPO genotype on OCR (**A, C**) was observed ($p_{genotype}$=0.6373, $F_{(1,58)}$=0.2246). Glucose concentration significantly affected OCR ($p_{glucose}$=0.0442, $F_{(1,58)}$=4.232). There was a statistically significant interaction between these variables ($p_{interaction}$=0.0034, $F_{(1,58)}$=9.348). n=14-16 wells per genotype from 1 experiment. 2-way ANOVA with Šídák's multiple comparisons test.

There was no statistically significant effect of TSPO genotype on ECAR (**B, D**) ($p_{genotype}$=0.1640, $F_{(1,58)}$=1.987), however glucose concentration significantly affected ECAR ($p_{glucose}$=0.0351, $F_{(1,58)}$=4.654) and there was a statistically significant interaction of these variables ($p_{interaction}$=0.0191, $F_{(1,58)}$=5.186). n=14-16 wells per genotype from 1 experiment. 2-way ANOVA with Šídák's multiple comparisons test.

Post-hoc analyses demonstrated that TSPO$^{+/+}$ MPAs significantly reduced their OCR (**A**; p=0.0031) and ECAR (**B**; p=0.0103) in response to limited substrate availability, whereas TSPO$^{-/-}$ MPAs showed no significant difference in OCR (**A**; p=0.9823) or ECAR under substrate limited conditions (**B**; p>0.9999).

*p<0.05, **p<0.01, ns p>0.05. Data are displayed as mean ± standard error of the mean.

OCR: oxygen consumption rate. ECAR: extracellular acidification rate. TSPO: translocator protein 18kDa. $^{-/-}$: deficient/knockout. $^{+/+}$: expressing/wildtype. GST: glycolysis stress test. MST: mitochondrial stress test.

3.4.10: The bioenergetic response of U373s to no glucose conditions was unchanged by genotype

Next, I wanted to address the earlier apparent incongruity of results between $TSPO^{-/-}$ MPAs and U373s, where glycolytic rate was increased in $TSPO^{-/-}$ MPAs (**Figure 3.4.3**) but reduced in U373s (**Figure 3.4.4**). Therefore, I followed up on the results of **Figure 3.4.9** by repeating the experimental paradigm in $TSPO^{-/-}$ U373s. Here I tested the hypothesis that $TSPO^{-/-}$ U373s would reduce ECAR under no glucose conditions further than $TSPO^{+/+}$ controls. Analysis using a 2-way ANOVA showed a statistically significant effect of TSPO genotype on OCR (**A, C**) ($p_{genotype}$=0.0443, $F_{(1,86)}$=4.169). I found that glucose concentration did not statistically significantly affect OCR ($p_{glucose}$=0.0617, $F_{(1,86)}$=3.586) though this was fractionally above the threshold of statistical significance (p=0.05). Moreover, using this method of analyses I found no statistically significant interaction of these variables ($p_{interaction}$=0.5970, $F_{(1,86)}$=1.632). Unlike OCR, TSPO genotype had no statistically significant effect on ECAR (**B, D**) ($p_{genotype}$=0.1165, $F_{(1,86)}$=2.515). In contrast, glucose concentration had a statistically significantly effect on this parameter ($p_{glucose}$<0.0001, $F_{(1,86)}$=168.1) though I detected no statistically significant interaction between these effects ($p_{interaction}$=0.2049, $F_{(1,86)}$=1.632). Post-hoc testing confirmed that $TSPO^{+/+}$ and $^{-/-}$ U373s showed no significant difference in OCR in response to substrate limited conditions (**Figure 3.4.10 A**; p=0.4396 [$TSPO^{+/+}$], p=0.9135 [$TSPO^{-/-}$]). In contrast, the both $TSPO^{+/+}$ and $^{-/-}$ U373s exhibited significantly reduced ECAR in response to no glucose conditions (**Figure 3.4.10 B**; p<0.0001 [both genotypes]).

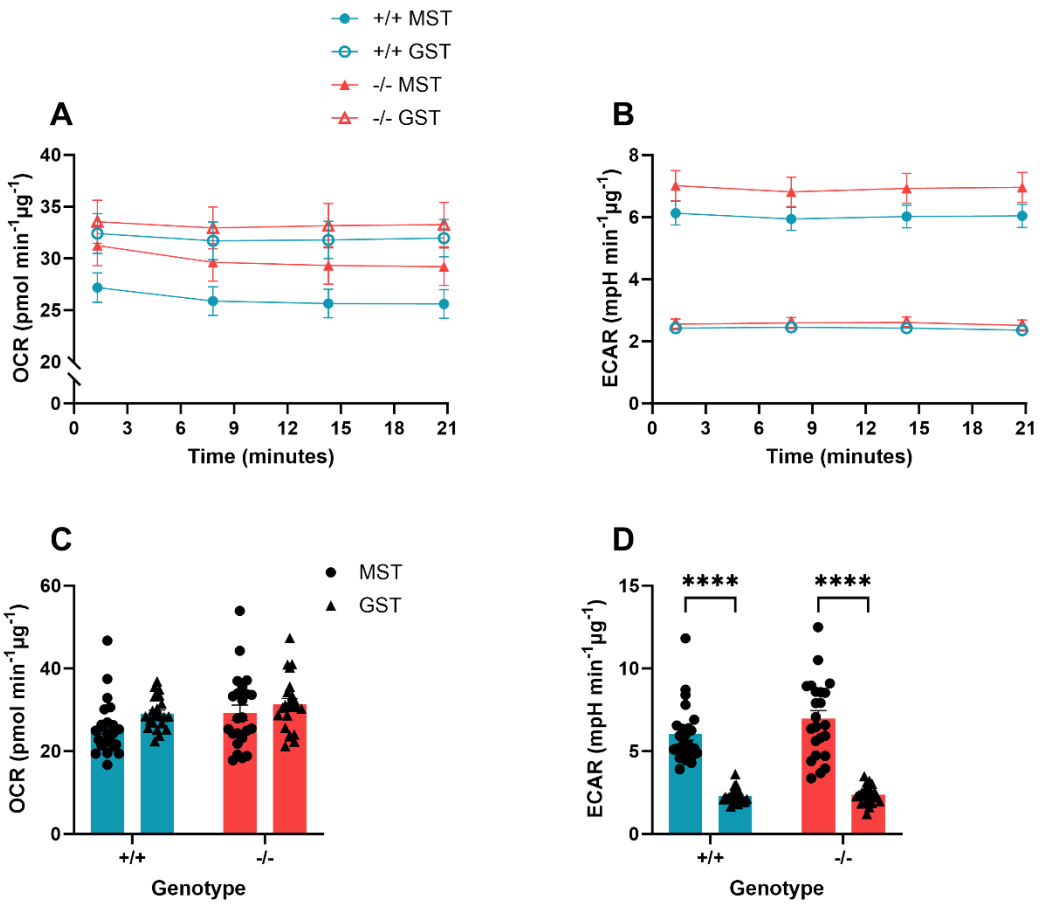

Figure 3.4.10: TSPO$^{-/-}$ U373s increased OCR in response to no glucose conditions.

To directly compare the differences in TSPO$^{-/-}$ U373 bioenergetics in the presence or absence of glucose and sodium pyruvate, both conditions were run on the same Seahorse plate.

TSPO genotype significantly affected OCR (**A, C**) ($p_{genotype}$=0.0443, $F_{(1,86)}$=4.169), however glucose concentration did not ($p_{glucose}$=0.0617, $F_{(1,86)}$=3.586). There was no statistically significant interaction of these effects ($p_{interaction}$=0.2049, $F_{(1,86)}$=1.632). n=23 wells per genotype from 1 experiment. 2-way ANOVA with Šídák's multiple comparisons test.

TSPO genotype did not significantly affect ECAR (**B, D**) ($p_{genotype}$=0.1165, $F_{(1,86)}$=2.515), however glucose concentration significantly affected this measure ($p_{glucose}$<0.0001, $F_{(1,86)}$=168.1). There was no statistically significant interaction between these effects ($p_{interaction}$=0.2049, $F_{(1,86)}$=1.632). n=23 wells per genotype from 1 experiment. 2-way ANOVA with Šídák's multiple comparisons test.

Post-hoc analysis revealed that both TSPO$^{+/+}$ U373s and TSPO$^{-/-}$ U373s showed no significant difference in OCR (**A**; p=0.4396 [TSPO$^{+/+}$], p=0.9135 [TSPO$^{-/-}$]) and reduced ECAR (**B**; p<0.0001 [both genotypes]) in response to limited substrate availability.

****p<0.0001. Data are displayed as mean ± standard error of the mean.

OCR: oxygen consumption rate. ECAR: extracellular acidification rate. TSPO: translocator protein 18kDa. $^{-/-}$: deficient/knockout. $^{+/+}$: expressing/wildtype. GST: glycolysis stress test. MST: mitochondrial stress test.

3.4.11: L-lactate secretion was reduced in TSPO$^{-/-}$ MPAs and U373s

As a secondary experimental measure of glycolysis in these cells, I quantified the secretion of L-lactate, a product of glycolysis. Being the conjugate base of lactic acid, when secreted from cells L-lactate would acidify media, contributing to the changes in ECAR observed in our metabolic flux assays.

I hypothesised that in line with the extracellular flux analysis data (**Figures 3.4.9** and **3.4.10**), compared to TSPO$^{+/+}$ MPAs, TSPO$^{-/-}$ MPAs would show reduced basal L-lactate secretion. I also tested the sub-hypothesis that L-lactate secretion from TSPO$^{-/-}$ MPAs would not be reduced further under no glucose conditions, and that TSPO$^{-/-}$ U373s would show no significant difference in L-lactate secretion compared to TSPO$^{+/+}$ U373 controls.

I found that the TSPO genotype of MPAs had a statistically significant effect on lactate secretion (**Figure 3.4.11 A**; $p_{genotype}$=0.0011, $F_{(1,20)}$=14.55), alongside glucose concentration ($p_{glucose}$<0.0001, $F_{(1,20)}$=25.04). Moreover, I found that there was a statistically significant interaction ($p_{interaction}$=0.0322, $F_{(1,20)}$=5.298) of these variables. Post-hoc analysis revealed that in the presence of glucose, TSPO$^{-/-}$ MPAs secreted a mean of 5.6% less L-lactate than TSPO$^{+/+}$ controls (**Figure 3.4.11 A**; p=0.0020). In the absence of glucose, whereas TSPO$^{+/+}$ MPAs reduced their L-lactate secretion by a mean of 6.7% (p=0.0003), L-lactate secretion was not altered in TSPO$^{-/-}$ MPAs (p=0.3549).

However, in U373 cells (**Figure 3.4.11 B**), I found that TSPO genotype had no statistically significant effect on lactate secretion ($p_{genotype}$=0.2011, $F_{(1,20)}$=1.748). In contrast, glucose concentration significantly affected lactate secretion from these cells ($p_{glucose}$=0.00145, $F_{(1,20)}$=7.159). Congruent with the MPAs, I found that there was a statistically significant interaction of these variables ($p_{interaction}$=0.0001, $F_{(1,20)}$=21.84). Post-hoc tests revealed that mean L-lactate secretion was reduced by 19.4% in TSPO$^{-/-}$ U373s compared to TSPO$^{+/+}$ EV controls (**Figure 3.4.11 B**; p=0.0024) under basal conditions. Further, unlike TSPO$^{+/+}$ EV controls, which altered their L-lactate secretion in response to no glucose exposure (p=0.0003), L-lactate secretion in response to no glucose exposure was unchanged in TSPO$^{-/-}$ U373s (p=0.6805).

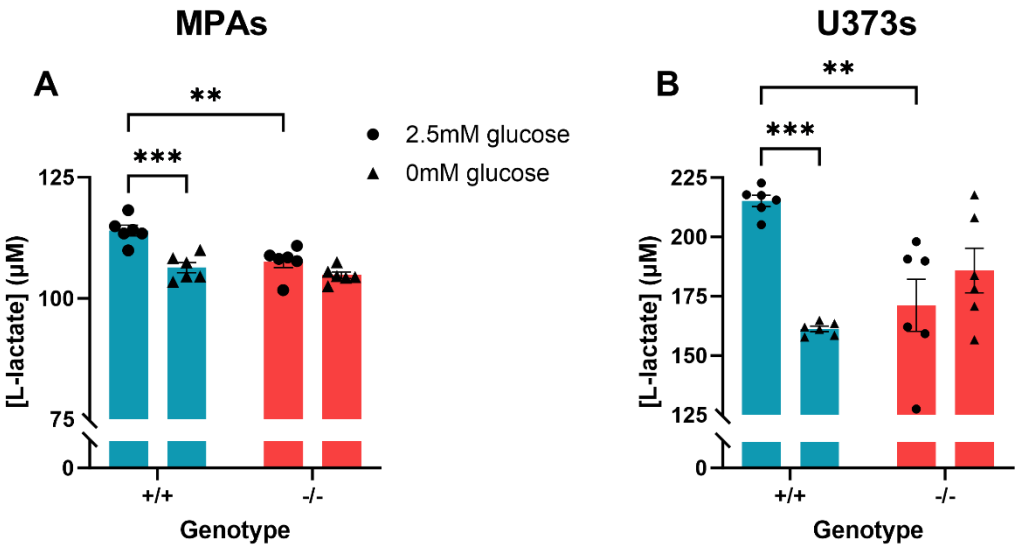

Figure 3.4.11: L-lactate secretion was reduced in TSPO$^{-/-}$ MPAs and U373s.

A: Lactate secretion from TSPO$^{-/-}$ MPAs. TSPO genotype significantly affected lactate secretion ($p_{genotype}$=0.0011, $F_{(1,20)}$=14.55), as did glucose concentration ($p_{glucose}$<0.0001, $F_{(1,20)}$=25.04), and there was a statistically significant interaction ($p_{interaction}$=0.0322, $F_{(1,20)}$=5.298) of these variables. n=6 wells from 1 experiment, 2-way ANOVA with Šídák's multiple comparisons test. Post-hoc analysis showed that TSPO$^{-/-}$ MPAs secreted significantly less L-lactate than $^{+/+}$ controls (p=0.0020). Whereas TSPO$^{+/+}$ MPAs reduced L-lactate secretion in response to no glucose conditions (p=0.0003), TSPO$^{-/-}$ MPAs showed no significant change in L-lactate secretion (p=0.3549).

B: Lactate secretion from TSPO$^{-/-}$ U373s. TSPO genotype had no statistically significant effect on lactate secretion ($p_{genotype}$=0.2011, $F_{(1,20)}$=1.748), however glucose concentration significantly affected this outcome ($p_{glucose}$=0.00145, $F_{(1,20)}$=7.159). There was a statistically significant interaction of these variables ($p_{interaction}$=0.0001, $F_{(1,20)}$=21.84). Post-hoc analysis showed that TSPO$^{-/-}$ U373ssecreted significantly less L-lactate than $^{+/+}$ controls (p=0.0024). Whereas TSPO$^{+/+}$ U373s reduced L-lactate secretion in response to no glucose conditions (p=0.0003), TSPO$^{-/-}$ U373s showed no significant change in L-lactate secretion (p=0.6805). n=6 wells from 1 experiment. 2-way ANOVA with Šídák's multiple comparisons test.

**p<0.01, ***p<0.001. Data are displayed as mean ± standard error of the mean. MPAs: mouse primary astrocytes. U373s: U373-MG astrocytoma cells. TSPO: translocator protein 18kDa. $^{-/-}$: deficient/knockout. $^{+/+}$: expressing/wildtype.

3.4.12: Basal and maximal fatty acid oxidation were increased in TSPO$^{-/-}$ MPAs

As I observed that TSPO$^{-/-}$ astrocytes were able to maintain their metabolic parameters (albeit at a lower basal metabolism) in the absence of glucose, I proposed that this may have been due to TSPO$^{-/-}$ astrocytes being more readily able to utilise other metabolic substrates than TSPO$^{+/+}$ controls. In other cell types also capable of fatty acid metabolism and steroidogenesis, loss of TSPO can increase FAO[366], and overexpression of TSPO is linked to reduced expression of genes involved with FAO[366]. Hence, I hypothesised that TSPO$^{-/-}$ astrocytes were meeting their bioenergetic requirements through enhanced fatty acid metabolism. The extracellular flux analysis data in this section was generated by Dr Josephine L Robb, and is included in this thesis for completeness.

The fatty acid oxidation stress test (FAOST; **Chapter 2.2.12.3**; **Figure 3.4.12 A**) showed that mean basal FAO was increased by 240.94% in TSPO$^{-/-}$ MPAs (**Figure 3.4.12 B**, p=0.0308) compared with TSPO$^{+/+}$ MPAs. This suggested that lipids constituted a greater proportion of the substrates used to maintain basal metabolic rates in TSPO$^{-/-}$ MPAs compared to TSPO$^{+/+}$ MPAs. By sequentially injecting the same compounds used in the MST paradigm, we were able to estimate maximal FAO, which provides an estimation of the contribution of FAO to the ability of cells to resolve metabolic stress and found that maximal FAO was enhanced in TSPO$^{-/-}$ MPAs (**Figure 3.4.12 C**, p=0.0004). Together these data suggest that loss of TSPO increased the contribution of fatty acids to the metabolism of MPAs, which may explain how the TSPO$^{-/-}$ astrocytes were better able to maintain their OCR and ECAR in the absence of glucose (**Figure 3.4.11**).

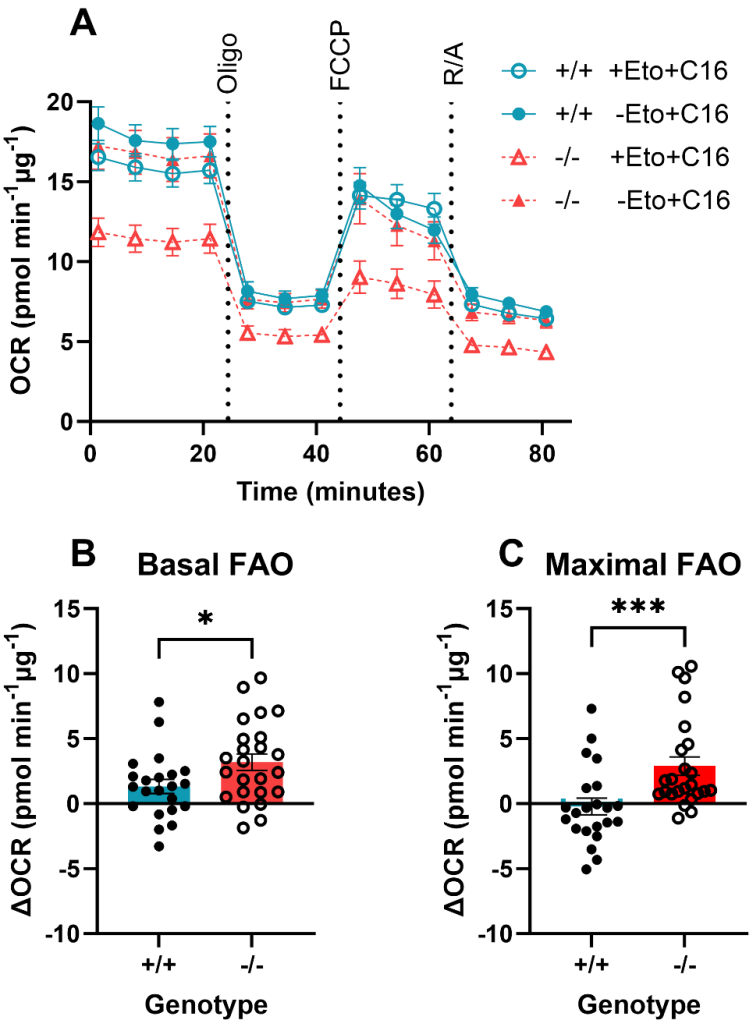

Figure 3.4.12: Basal and maximal fatty acid oxidation were increased in TSPO$^{-/-}$ MPAs.

A: The fatty acid oxidation stress test, which was used to measure FAO in TSPO$^{-/-}$ MPAs. **B:** Basal FAO was significantly increased in TSPO$^{-/-}$ MPAs. n=22-24 wells per genotype, data are pooled from across 2 independent experiments. Unpaired t-test, p=0.0308. **C:** Maximal FAO was significantly increased in TSPO$^{-/-}$ MPAs. n=22-24 wells per genotype, data are pooled from across 2 independent experiments. Mann-Whitney test, p=0.0004.

*p<0.05, ***p<0.001. Data are displayed as mean ± standard error of the mean.

OCR: oxygen consumption rate. FAO: fatty acid oxidation. Oligo: oligomycin (0.5µM). FCCP: carbonyl cyanide-p-trifluoromethoxyphenylhydrazone (1µM). R/AA: rotenone/antimycin-A (0.5µM). Eto: etomoxir (40µM). C16: palmitate (200µM). TSPO: translocator protein 18kDa. $^{-/-}$: deficient/knockout. $^{+/+}$: expressing/wildtype. This data was generated by Dr Josephine L Robb and is included for completeness.

3.4.13: Fatty acid oxidation enzyme activity downstream of CPT1a was unchanged in TSPO$^{-/-}$ U373s

In peripheral cells, TSPO deficiency has been reported to increase expression of enzymes involved with fatty acid metabolism[366]. However, the effect of TSPO deficiency on the activity of enzymes involved with FAO has not yet been explored. The data in **Figure 3.4.12** suggests that TSPO regulates FAO in astrocytes, hence, I next tested the hypothesis that TSPO was regulating the activity of enzymes involved with FAO within the mitochondria, and downstream of CPT1a, the rate-limiting enzyme of FAO. Unfortunately, due to poor protein yield from TSPO$^{-/-}$ MPAs, I could only utilise this methodology in TSPO$^{-/-}$ U373s.

This assay (AssayGenie, **Chapter 2.2.14**) utilises homogenised whole cell protein extracts to bypass the need for carnitylation and mitochondrial import of acyl-CoA (**Figure 1.1.3.1**). Octanoyl-CoA is added to cell lysate along with a tetrazolium salt. In the presence of NADH (produced by FAO; **Figure 1.1.3.1**), the salt is reduced to formazan, and absorption is read at 492nm (**Chapter 2.2.14**). This assay thus measures the activity of various enzymes involved with the intramitochondrial FAO pathway downstream of CPT1a (**Figure 1.1.3.1**). Although FAO enzyme activity trended towards an increase in TSPO$^{-/-}$ U373s, this data failed to reach statistical significance (**Figure 3.4.13**, p=0.5991). To better understand the activities of specific enzymes involved with FAO (**Figure 1.1.3.1**), I could have included inhibitors of FAO enzymes (such as CI 976, an inhibitor of acyl-CoA cholesterol acyltransferases[463]) to determine upregulation of activity of specific enzymes instead of the generic method applied here, though I did not proceed with this due to limited sample availability.

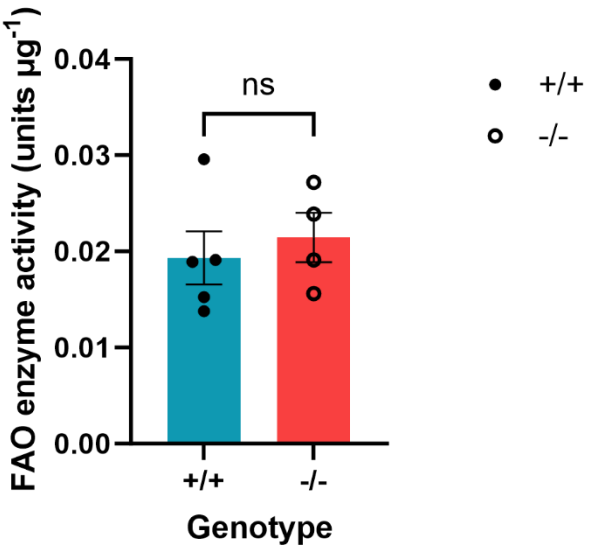

Figure 3.4.13: Fatty acid oxidation enzyme activity downstream of CPT1a was unchanged in TSPO$^{-/-}$ U373s.

Activity of enzymes involved with FAO, downstream of CPT1a, in TSPO$^{-/-}$ U373s compared to TSPO$^{+/+}$ controls. Data trended towards an increase, but failed to reach statistical significance.

n=4-5 from 3 independent experiments. Unpaired t-test, p=0.5991.

FAO: fatty acid oxidation. ns: not significant (p>0.05). TSPO: translocator protein 18kDa. $^{-/-}$: deficient/knockout. $^{+/+}$: expressing/wildtype. CPT1a: carnitine palmitoyltransferase 1a.

3.4.14: TSPO formed a complex with CPT1a in U373 astrocytoma cells

Having established that loss of TSPO increased FAO in astrocytes (**Figure 3.4.12**) I wanted to begin to explore the potential underlying mechanism. Carnitine palmitoyltransferase 1a (CPT1a) is a constituent of the outer mitochondrial membrane and is the rate-limiting enzyme of fatty acid metabolism (**Figure 1.1.3.1**)[58,206,464]. Previous work has established that CPT1a forms a complex with another constituent of the outer mitochondrial membrane, voltage-dependent anion channel (VDAC[465]). VDAC is known to form complexes with TSPO[315,347,428,466], but the existence of a complex between TSPO and CPT1a has not yet been experimentally confirmed. The data suggesting that TSPO deficiency increases FAO in astrocytes supports a potential role of TSPO in regulating FAO via a complex with CPT1a. To investigate the hypothesis that TSPO formed a complex with CPT1a, I transiently transfected U373 cells naïve to previous genetic modification with a Myc-DDK tagged TSPO construct (here termed TSPO-Myc). Co-immunoprecipitation (**Chapter 2.2.10**) was used to identify TSPO-containing complexes via a pulldown using anti-Myc bound agarose beads. Using this method, I established that TSPO forms a complex with the key FAO regulator CPT1a (**Figure 3.4.14**, n=4 independent immunoprecipitations). This represents a potential mechanism through which TSPO may regulate FAO in astrocytes.

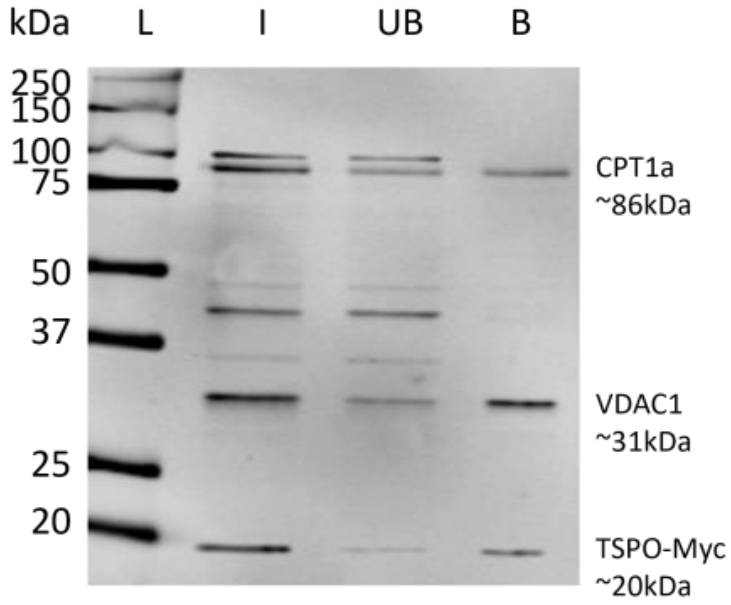

Figure 3.4.14: TSPO formed a complex with CPT1a in U373 astrocytoma cells.

Immunoblot of co-immunoprecipitation products confirming the existence of an interaction between TSPO and CPT1a in U373 astrocytoma cells. U373 cells naïve to previous genetic modification were transiently transfected with a Myc-tagged TSPO construct. TSPO-Myc containing complexes were isolated via Myc-tagged agarose beads. Immunoblots for Myc, CPT1a and VDAC1 were used to confirm existence of complexes.

n=4 independent immunoprecipitations.

kDa: kilodaltons. L: ladder. I: input fraction (cell lysate). UB: unbound fraction (supernatent). B: bound fraction (eluate). CPT1a: carnitine palmitoyltransferase 1a. VDAC1: voltage dependent anion channel 1. TSPO-Myc: Myc-tagged translocator protein (18kDa) construct.

3.5: Discussion

In this chapter, I have demonstrated that TSPO deficiency changes astrocyte metabolism. **Table 3.5** provides an outline of the key findings of this chapter. Loss of TSPO reduced basal metabolism in MPAs and reduced the contribution of glucose-based oxidative phosphorylation to maintaining astrocyte metabolism. $TSPO^{-/-}$ MPAs secreted less lactate than wildtype controls, and unlike wildtype controls lactate secretion was not affected by glucopenia. I propose that this may be due to an increased contribution of FAO to maintaining the bioenergetic rates of $TSPO^{-/-}$ MPAs. Using transiently transfected U373 astrocytoma cells, I have provided potential mechanistic evidence for this finding in the form of a protein complex between TSPO and the rate-limiting enzyme of fatty acid oxidation, CPT1a.

Cell:	Genotype:	Output:									
		Basal OCR	**Basal ECAR**	**Mito resp**	**Glyco (high gluc)**	**Glyco (phys rel gluc)**	**BR (± glucose)**	**Lactate**	**Lactate (± glucose)**	**Basal FAO**	**Maximal FAO**
MPA	+/+	-	-	-	-	-	Modulated OCR, ECAR	-	Modulated	-	-
	-/-	↓	↓	↓	↑	↓	Unresponsive	↓	Unchanged	↑	↑
U373	+/+	-	-	-	-	-	↓ECAR	-	Modulated	-	-
	-/-	-	-	-	↑	-	↓ECAR	↓	Unchanged	No change[452]	No change[452]

Table 3.5.1: Summary table outlining results from this chapter.

OCR: oxygen consumption rate. ECAR: extracellular acidification rate. Mito resp: mitochondrial respiration. Glyco: glycolysis. Gluc: glucose. Phys rel: physiologically relevant (to the brain). BR: bioenergetic rate. FAO: fatty acid oxidation. MPA: mouse primary astrocyte. U373: U373 astrocytoma cell line.

3.5.1: TSPO deficiency modulates astrocyte metabolism

The effect of TSPO deficiency on cellular metabolism has been well-characterised in the periphery, with a particular focus on the adrenals[320,327], androgen-secreting cells[366], and recent work in hepatocytes[446]. In mouse MA-10 Leydig cells, TSPO deficiency has been shown to increase rates of FAO and expression of the *Cpt1a* and *Hadha* genes, while overexpression of TSPO was shown to reduce expression of these genes[366]. This implies a role for TSPO in regulating FAO. However, with the exception of a reduction in mitochondrial spare capacity TSPO deficiency had no significant effect on rates of mitochondrial metabolism in these cells[366]. In the adrenal glands of Syrian hamsters, a correlation between low TSPO expression and high triglyceride metabolism was recently touted[320]. A separate body of work in hepatocytes demonstrated enhanced availability of free fatty acids in the liver of $TSPO^{-/-}$ animals[446], suggesting enhanced lipid metabolism, though this was accompanied by accumulation of lipid droplets and cholesterol. Together these data suggest that in the periphery TSPO plays a role in FAO. However, a similar role for TSPO in the CNS has not yet been reported. Tournier *et al*.[456] recently (August 2023) showed that overexpression of TSPO in the rat C6 glioma cell line increased mitochondrial density and ROS production, suggesting that TSPO is, at the very least, an important regulator of energy use in astrocyte-like cells. Though this work was published after my doctoral studies began in 2020, it supports the data I have presented in this chapter. In published literature concerning microglia, a role for TSPO in regulating FAO remains unclear, however, recent work in these cells has demonstrated that TSPO regulates glycolysis (measured using the glycolysis stress test)[339,340], and evidence from TSPO-deficient glioma cell lines suggests that TSPO regulates oxidative phosphorylation and glycolysis (measured using the glycolysis and mitochondrial stress tests)[370]. It should be noted that CPT1a expression (relative to astrocytes) is poor in microglia[206,207,287], which may explain why a link between TSPO and FAO remains unclear in these cells. Together, these data suggest that although TSPO is expressed in a variety of mammalian cells, the function of TSPO may be at least partially determined by the type of cell in question.

The data I have provided here, summarised in **Table 3.5.1**, are supportive of a role for TSPO in regulating cellular metabolism of astrocytes. Using primary astrocytes isolated from germline $TSPO^{-/-}$ mouse neonates, I have provided evidence that TSPO regulates astrocyte metabolism. Firstly, I have shown that loss of TSPO reduced the basal OCR (a proxy of mitochondrial respiration) and ECAR (a proxy of glycolysis) in these cells (**Figure 3.4.1**). This supported data from existing literature from other cell types[339,340,366,370] and independently recapitulated a finding first reported by another doctoral student in our research group[452]. This implies that TSPO plays an important role in regulating astrocyte bioenergetics, and shows that these prior results can be independently reproduced in my hands.

Whereas data from mouse primary microglia suggests that germline TSPO deficiency inhibits glycolytic metabolism[339], my experiments using the same paradigm show the opposite effect in $TSPO^{-/-}$ astrocytes (increased glycolysis [**Figure 3.4.3**], in line with Fairley *et al*. [February 2023, primary microglia][340]). However, in my hands this effect was constrained to a supraphysiological concentration of glucose (10mM). When I reintroduced glucose concentrations that were more physiologically relevant to the CNS, I found that $TSPO^{-/-}$ astrocytes were <u>less</u> responsive than $TSPO^{+/+}$ controls in response to 1mM, 5.5mM and 7.5mM glucose (**Figure 3.4.7**). This suggests that the glycolytic rate of $TSPO^{-/-}$ MPAs is reduced under normal conditions, and correlates with the data I present in **Figure 3.4.1** showing that TSPO deficiency reduces ECAR in the presence of glucose. I also investigated the metabolic responses of $TSPO^{-/-}$ MPAs to the reintroduction of L-glutamine, an amino acid. However, I did not observe any significant differences in the metabolic response of $TSPO^{-/-}$ MPAs any of the concentrations tested, bar one (1000μM) (**Figure 3.4.7**). Crucially, I observed no difference in the metabolic response of these cells to reintroduction of 2500μM (2.5mM) L-glutamine, i.e., the concentration used during the mitochondrial and glycolysis stress tests.

In support of this argument, I have also presented data herein on L-lactate secretion from $TSPO^{-/-}$ MPAs, showing that it is reduced under basal conditions and did not change significantly in response to glucopenic conditions (**Figure 3.4.11**). I investigated L-lactate production due to the observation that the ECAR and OCR values of $TSPO^{-/-}$ MPAs did not change significantly in response to

glucopenia (**Figure 3.4.9**). Glycolysis is generally accepted as being the main contributor to any change in ECAR, as assessed using EFA, due to the volume of H^+ produced by this process. However, I must acknowledge that other cellular processes (such as FAO[467]) also produce H^+ and may contribute to the acidification of media. Cells *in vitro* typically secrete lactate into the surrounding media, hence ECAR provides a proxy for glycolytic activity. Astrocytes – both *in vivo* and *in vitro* – secrete lactate for a variety of purposes ranging from providing trophic support to neurons to acting as a gliotransmitter[37,62,72,192,468,469], so assessment of L-lactate secretion from these cells has the potential to provide insights into a range of processes. For example, reduced L-lactate secretion from $TSPO^{-/-}$ MPAs may provide an indication of changes in the ability of these astrocytes to fulfil their vital functions *in vivo*; such as a reduced ability to provide trophic support to neurons. In the intact animal, this may manifest as altered outcomes in paradigms designed to interrogate behaviour or cognition, which to my knowledge have not yet been examined in $TSPO^{-/-}$ mice. This is pertinent, because astrocyte-specific CPT1a-deficient mice were recently shown to have cognitive deficits[89], suggesting that fine regulation of astrocytic FAO during neurodevelopment is crucial for healthy CNS functionality in adulthood.

In isolation, the data I present in **Figure 3.4.11** cannot be used to draw inferences about the metabolic profiles of the $TSPO^{-/-}$ MPAs. This is because I examined only secretion of L-lactate, which was achieved by quantifying the L-lactate concentration in cell culture media. The possibility remains that $TSPO^{-/-}$ MPAs may simply be <u>secreting</u> less lactate than their wildtype counterparts, but their overall lactate production is unaltered; my work did not examine intracellular L-lactate stores and therefore I cannot address this possibility based on **Figure 3.4.11** alone. Additionally, the L-lactate data I present here are in contrast with the recently published findings from Fairley *et al*. (February 2023)[340], who demonstrated that TSPO deficiency enhances glycolysis and lactate secretion from microglia[340]. However, it is important to note that microglia exhibit a different developmental lineage[470] and gene expression profile from astrocytes: notably, microglia express little-to-no CPT1a[206]. While FAO occurs in microglia, this occurs at a lower rate than astrocytes[471] and is possibly reflective of the relative reduction in CPT1a expression. This may partially explain the similarity of mouse primary microglia and astrocytes to the reintroduction of glucose following

glucopenia (**Figure 3.4.3**, Fairley *et al*.[340] [February 2023]) and yet the difference in lactate secretion between these cell types (**Figure 3.4.11**, Fairley *et al*.[340]), as enhanced FAO at the expense of glucose metabolism in astrocytes would reduce lactate secretion and overall lactate production. Furthermore, Fairley *et al*. do not explicitly state the glucose concentration at which their lactate measurements were made. If these took place at high glucose concentrations (relative to brain, ~5mM), this may also explain the divergence in observations regarding lactate secretion from these cells.

Complementing my L-lactate data, in **Figure 3.4.9** I present evidence that albeit maintained at a lower level (**Figure 3.4.1**), the OCR of TSPO$^{-/-}$ MPAs does not significantly change in the absence of glucose. Crucially, OCR of TSPO$^{+/+}$ MPAs under glucopenia is reduced, suggesting that there is reduced availability of metabolic substrates to undergo mitochondrial respiration. This is important as lactate can be converted to pyruvate, which is then imported to the mitochondria and used as a substrate for the tricarboxylic acid (TCA) cycle (**Figure 1.1.1, 1.1.2**). The TCA cycle consumes oxygen to fuel ATP production (**Figure 1.1.2**). This consumption of oxygen translates as increased OCR. One could anticipate, therefore, that were TSPO$^{-/-}$ MPAs meeting their bioenergetic requirements through this mechanism, withdrawal of glucose would be met by a concomitant increase in OCR, which I did not observe. Given that glucose is unavailable as a metabolic substrate, lactate cannot be generated in this paradigm and no concomitant increase in OCR was observed in TSPO$^{-/-}$ MPAs (**Figure 3.4.9**). Thus, taken together, these data support the notion that TSPO$^{-/-}$ MPAs meet their bioenergetic requirements through preferential metabolism of alternative substrates.

3.5.2: Regulation of FAO in astrocytes by TSPO

As outlined in **Chapter 3.5.1**, there is evidence from the existing literature demonstrating that TSPO deficiency enhances FAO in Leydig cells[366]. Moreover, enhanced triglyceride metabolism has been demonstrated in the adrenal glands of the Syrian hamster, which naturally express low levels of TSPO[320]. In hepatocytes, TSPO deficiency is associated with increased free fatty acid availability (indicating enhanced FAO)[446]. Based on this I hypothesised that a similar mechanism was at play in TSPO$^{-/-}$ astrocytes. I then confirmed that FAO

provided a greater contribution towards the bioenergetic requirements of TSPO$^{-/-}$ MPAs compared to wildtype controls under basal conditions (**Figure 3.4.12**). Furthermore, when an energy stress was simulated via FCCP injection, these cells were more reliant on FAO to meet the increased energetic demand (**Figure 3.4.12**). When I interrogated the activity of enzymes associated with FAO downstream of CPT1a (using lysed cell extracts, enabling one to bypass the need for mitochondrial import of FAO substrates), I found there was no statistically significant change in FAO-associated enzyme activity (**Figure 3.4.13**). This supports a role for TSPO in regulating FAO via CPT1a. Due to technical difficulties involving the efficacy of the lysis buffer used and thus low protein yield, this finding was limited by a small and inconsistent sample size (n=4-5) and would benefit from further optimisation and repetition to confirm these results. In a variety of cells, TSPO ligands have been demonstrated to modulate cellular bioenergetics and inflammatory responses[472]. Despite the issues associated with these ligands (**Chapter 1.4.6**), this may suggest that TSPO ligands modulate cellular metabolism to promote an anti-inflammatory phenotype[346,377,378] or a phenotype biased towards the resolution of inflammatory stimuli. In the periphery, such a phenotype has been associated with FAO (though FAO is also associated with pro-inflammatory phenotypes, and is associated with pro- and anti-inflammatory phenotypes in astrocytes)[41,207,287,288], perhaps suggesting that TSPO ligands promote FAO by modulating its interaction with CPT1a (**Figure 3.4.13**). Indeed, *in vivo*, administration of the TSPO ligand Ro5-4864 via intraperitoneal injection in a mouse model of tauopathy has been associated with reduced microglial activation[444], which may have been mediated, at least in part, by promoting a resolutory phenotype in astrocytes potentially ameliorating activation of the complement pathway in microglia (a hypothesis which remains to be explored in this context)[257,473,474].

In support of the hypothesis that TSPO influences astrocytic FAO via CPT1a, by transiently transfecting U373 cells naïve to previous genetic modification with a Myc-tagged TSPO plasmid (TSPO-Myc), I was able to demonstrate that TSPO forms a protein complex with CPT1a, the rate-limiting enzyme of fatty acid oxidation (**Figure 3.4.14**). The TSPO-Myc construct interacted with the endogenous CPT1a, supporting an earlier finding of a TSPO-CPT1a protein complex established using endogenous protein by another member of the

Ellacott lab[452]. Usually, in energy-replete conditions, CPT1a activity is suppressed by malonyl-coenzyme A (malonyl-CoA), preventing the mitochondrial import of FAO substrates in the form of acyl-CoA via CPT1a and thus inhibiting FAO. Besides this mechanism, regulation of CPT1a activity remains unclear. This provides an exciting avenue for further studies, as these data suggest that TSPO may regulate CPT1a activity. This could be explored using more sensitive techniques such as immunoprecipitation-mass spectrometry to further validate the TSPO-CPT1a interaction, and any effect of a TSPO-CPT1a complex on the structure of these two proteins could be established via X-ray crystallography. If structural alterations as a result of this complex are not found, phosphorylation arrays and arrays for other post-translational modifications could be employed to elucidate the mechanism by which the TSPO-CPT1a interaction regulates FAO. These studies could then interrogate the effect of modulating the TSPO-CPT1a interaction under a variety of stimuli ranging from nutrient stresses (deficits and excesses) to cellular responses to inflammation in disease states to further elucidate the function of this interaction. The results of these investigations may hold sway over the proposed therapeutic employment of TSPO during chronic inflammatory conditions: CPT1a modulation is an attractive therapeutic target for a variety of disorders[58,89,382,460,464,475,476]. Furthermore, should TSPO truly act as a modulator of CPT1a activity, chronic pharmacological inhibition or activation of TSPO to treat one condition (and its downstream effects on cellular metabolism, substrate preferences, and CPT1a activity) may place patients at risk of developing unforeseen complications or comorbidities. Particularly crucial here would be the use of TSPO inhibition to treat chronic inflammatory conditions given the recently-established critical role of CPT1a in regulating cognition[89].

3.5.3: Limitations of this chapter

The data I have presented in this chapter support the argument that TSPO$^{-/-}$ astrocytes are less reliant on glucose metabolism and more reliant on FAO. Moreover, I demonstrate that the bioenergetic rates of and metabolic intermediates produced by TSPO$^{-/-}$ MPAs are not modulated by glucopenia (**Figures 3.4.9, 11**), suggesting impaired glucose sensing or reliance in these cells. However, my work did not examine changes in the activity or expression of proteins or enzymes involved with regulation of cellular energy production associated with TSPO deficiency. Therefore, I cannot comment on a mechanism

by which the 'glucose-sensing' ability of these astrocytes may have become impaired. However, I would postulate that this may be due to deficits in energy-sensing mechanisms. Indeed, a role for adenosine monophosphate-activated protein kinase (AMPK, a key cellular energy sensor[9]) in regulating TSPO expression has been postulated[358,477], and this may well present a mechanism by which TSPO facilitates cellular responses to variations in nutrient availability. Furthermore, in this chapter, I did not examine the expression of transporter proteins associated with metabolite uptake such as glucose transporter 1 (GLUT1), extracellular amino acid transporters and sodium-coupled neutral amino acid transporters. Thus, in this chapter, I cannot account for any variation in the expression of these membrane transporter proteins in TSPO$^{-/-}$ MPAs. Reduced expression of these key transporter proteins would result in a reduced ability to take up metabolic substrates. This may explain the reduced metabolic rates of TSPO$^{-/-}$ MPAs, as well as the lack of a metabolic response to the no glucose conditions (though this is well accounted for by the data presented in **Figures 3.4.11, 12**). Future studies could investigate this possibility by employing immunocytochemistry for these transport proteins, which could be quantified to determine changes in expression level and localisation. Like extracellular receptors, transport proteins on the cell surface membrane may be endocytosed and stored in vesicles. Enhanced receptor internalisation in this manner may mean that there is no net change in membrane transporter expression, but a reduction in the availability of these transporters to take up metabolic substrates.

Additionally, this chapter did not pursue any potential mechanism by which TSPO may influence the availability of lipids for mitochondrial import and thus FAO. In hepatocytes, TSPO deficiency has been associated with enhanced lipid droplet and FFA accumulation, together implying greater lipid metabolism in these cells[446]. One can therefore form the hypothesis that TSPO may regulate FAO via both formation of a complex with CPT1a (**Figure 3.4.14**), and by regulating lipid droplet-mitochondria interactions. Lipid droplets 'dock' on the OMM to facilitate the import of fatty acids for FAO, through mechanisms that remain unclear. This may occur via the formation of an interaction between acyl-CoA binding protein (ACBP), TSPO, and CPT1a. ACBP is regarded as a TSPO ligand[313,423,430,478,479], but the function of the TSPO-ACBP interaction remains unclear. Crucially, ACBP is implicated in regulating FAO[423,480,481]. Therefore, it is plausible that TSPO

exerts its regulatory effects on FAO in astrocytes not only via an interaction with CPT1a, but also by modulating lipid droplet-mitochondria interactions.

3.5.3.1: Bioenergetic phenotypes were different between cell types

The extracellular flux analysis data generated using the CRISPR-Cas9 $TSPO^{-/-}$ and $TSPO^{+/+}$ EV control U373 cells were not always congruent with the data I generated using MPAs. It is worth nothing that the data in **Figure 3.4.4** was not generated by myself, and was included in this body of work for completeness. Therefore, the possibility of slight technical differences between experimenters exists, which may have contributed to the slightly different results obtained. However, because a similar incongruity can be observed in **Figure 3.4.10**, I argue that it is more likely that these differences are more likely to be due to fundamental differences in the bioenergetics between U373 astrocytoma cells and MPAs. U373 cells were isolated from a donor with an aggressive glioblastoma (astrocytoma) and are therefore cancerous in nature. This has inherent implications for the bioenergetics of these cells, as cancer cells have long been known to have different bioenergetic requirements from non-cancerous cells, typically exemplified by an increased reliance on glycolysis and reduced utilisation of oxidative phosphorylation for energy production[482–484]. This may well explain the enhanced glycolytic reserve I observed in $TSPO^{-/-}$ U373s (**Figure 3.4.4**).

In primary microglia, TSPO was recently demonstrated to regulate mitochondrial hexokinase 2 (HK2) localisation[340]. Mitochondrial HK2 localisation is associated with enhanced glycolysis, and this was diminished in $TSPO^{-/-}$ microglia[340]; therefore, $TSPO^{+/+}$ U373s may have been better able to metabolise glucose due to this reason, potentially explaining the reduced glycolytic rate I observed in $TSPO^{-/-}$ U373s. This is reinforced by the enhanced glycolytic reserve of these cells as glycolytic reserve is an indicator of how capably cells can use glycolysis to meet ATP demands during energy stress[485]. Thus, the enhanced glycolytic reserve I reported in $TSPO^{-/-}$ U373 cells may similarly be explained as being a product of the lower initial rate of glycolysis in these cells, and is potentially linked to the enhanced maximal FAO in $TSPO^{-/-}$ MPAs reported later in this chapter (**Figure 3.4.12**).

The phenotype of enhanced glycolytic reserve in U373 astrocytoma cells may also explain the finding that basal FAO was significantly increased in $TSPO^{-/-}$

MPAs but not U373 cells[452]. This notion is supported by the congruence of L-lactate secretion by TSPO$^{-/-}$ U373 cells and MPAs (**Figure 3.4.11 C, D**): despite differences in the bioenergetic profiles of these cell types, when measuring metabolite secretion I found that TSPO deficiency in both U373 cells and MPAs significantly reduced L-lactate secretion, and that this was not further modulated by withdrawal of glucose in TSPO$^{-/-}$ U373 cells and MPAs. However, the difference in the bioenergetic responses of these cells to glucopenia must be acknowledged: TSPO$^{-/-}$ MPAs do not modulate their OCR or ECAR in response to glucopenia, whereas the response of TSPO$^{-/-}$ U373s did not differ from their TSPO$^{+/+}$ controls (**Figure 3.4.9, 10**). I argue that this difference could be attributed to inherent differences between the bioenergetics of U373 cells and MPAs, and is likely not indicative of a difference in TSPO functionality between models.

Despite these limitations, I have reinforced my extracellular flux analyses using metabolite assays and enzyme activity assays. Furthermore, I have independently recapitulated data demonstrating a potential mechanistic basis for the role of TSPO in regulating the bioenergetics of astrocytes, which may explain the reduced bioenergetic rate and increased contribution of FAO to meeting the bioenergetic requirements of TSPO$^{-/-}$ astrocytes.

3.6: Conclusion

In conclusion, here I have demonstrated that TSPO plays a key role in regulating astrocyte bioenergetics. I have shown that loss of TSPO changes sensitivity to glucose, a key metabolic substrate and the progenitor of lactate, which is an important signalling molecule in the CNS. Moreover, I have shown that TSPO$^{-/-}$ MPAs are more reliant on FAO to meet their bioenergetic requirements, and propose that, when expressed, TSPO may regulate FAO via an interaction with CPT1a. This may have important bearing on the ability of TSPO$^{-/-}$ astrocytes to respond to inflammatory stimuli, or to regulate their metabolism in the presence of additional stresses, such as inflammatory stimuli.

Chapter 4: Regulation of astrocyte immunometabolism by TSPO

A modified version of this chapter is published as part of:

Regulation of astrocyte metabolism by mitochondrial translocator protein 18kDa.

Firth W, Robb JL, Stewart D, Pye KR, Bamford R, Oguro-Ando A, Beall C, Ellacott KLJ. ***BioRxiv preprint.*** *doi: 10.1101/2023.09.29.560159.*

4.1: Introduction

Astrocytes play critical roles in maintaining CNS homeostasis. While this includes providing metabolic support to the brain parenchyma, astrocytes are also important players during the CNS inflammatory response[80,104,105,261]. Due to their intimate relationship with the BBB, astrocytes are among the first glial cells to sense peripheral inflammation, secreting cytokines to initiate a wider inflammatory response in the CNS (**Chapter 1.3.3**). During traumatic brain injuries, such as stroke, astrocytes migrate to the wound site alongside microglia and participate in the formation of the glial scars to 'wall off' the damaged area and prevent the spread of damaging stimuli[20,80,102,186,258,486]. At the same time, astrocytes are important for phagocytosing debris, dead or irreparably damaged neurons[80,105,186,486], as well as facilitating the growth of new neurites and neo-synaptogenesis to overcome neuronal loss incurred by CNS damage[20,186,486]. Furthermore, astrocytes play key roles in regulating neuronal activity via the secretion of gliotransmitters such as ATP, D-serine, and glutamate[20,80,97,98,102], which, as outlined in **Chapter 1.3**, serve to modulate neuronal activity and facilitate intercellular communication; these molecules can promote or inhibit important various processes including myelination, a process critical for appropriate CNS communication and development, and wound healing[63,80,102,107,186,258,486]. Thus, astrocyte reactivity plays a key role in various facets of the CNS inflammatory response.

During chronic inflammation, glial cells (particularly microglia and astrocytes) are known to undergo a process called 'gliosis', in the case of astrocytes, astrogliosis (**Chapter 1.3.3.1**)[20,80,163,261,313]. Broadly speaking, gliosis is a state of chronic glial cell activation, which may or may not be irreversible[80,261]. Studies in peripheral

immune cells have highlighted that inflammation is a metabolically expensive process[289,382–385]. Thus, the ability of cells to meet the metabolic demands of inflammation – and therefore keep fuelling it to prolong and resolve their responses as necessary – is being increasingly appreciated for a wider array of cell types[289,382–384]. The term 'immunometabolism' describes the metabolic changes that accompany an inflammatory response in a variety of cells[289,290]. While the importance of immunometabolism to the CNS inflammatory response is a developing area of understanding, changes to the metabolic state of the brain are known to accompany many CNS pathologies[167,207,255,287,382,487]. *In vitro* studies demonstrate that inflammatory stimulation modulates the metabolic phenotype of microglia and astrocytes[339,340,488–491]. Indeed, the Ellacott laboratory have previously shown that astrocytes have distinct metabolic phenotypes following exposure to acute or chronic inflammatory stimulation[167]. Importantly, studies in macrophages have revealed that exposure to chronic inflammatory stimuli results in metabolic adaptations in these cells[43,390,492–497], and similar mechanisms are thought to be at play in glial cells[290].

Alongside widespread gliosis, chronic neuroinflammation (i.e., neuroinflammation present for weeks, months, or years) is typically accompanied by an increase in TSPO expression[314,316,319,498,499], such that radiolabelled TSPO ligands are employed in some clinics as an imaging biomarkers to monitor the progression of neuroinflammatory and neurodegenerative conditions[410,415,472,500,501] (**Chapter 1.4.6**). However, it is worth noting that some bodies of evidence from *in vivo* studies have also reported an increase in TSPO levels following an acute proinflammatory stimulus (i.e., neuroinflammation present for approximately 1 day)[501]; a notable example is a recent study examining Zika virus infection in a murine model[502] (published in 2023). In this study the median reported survival time post-infection was only 8 days[502], which may suggest that the *severity* of the inflammatory stimulus influences the extent of TSPO upregulation within a given timeframe. The study attributed the increases in CNS TSPO expression to microglia and infiltrating peripheral immune cells, a phenomenon which occurs following significant disruption of the BBB (which may be considered a correlate of severe CNS conditions[503])[502]. One may thus posit that more extreme proinflammatory stimuli that exhibit greater cytotoxicity accompanied by significant upregulation of TSPO within a

comparatively short timeframe (e.g., a few hours) *in vitro*. Furthermore, increased TSPO expression is widely reported in gliomas, a form of brain cancer[311,375,498,504].

Due to microglia traditionally being regarded as the principle immune cells of the CNS, elevated TSPO expression observed in various pathologies was initially attributed to these cells, with little regard for other TSPO-expressing glia such as tanycytes[358] and astrocytes[373,374]. The function of TSPO in microglia is thus currently better understood than in other glial cell types. Indeed, recent studies have characterised the role of TSPO in microglia via germline genetic ablation[339,340] or pharmacological inhibition of TSPO[378,379,397,505–508], but the role played by TSPO during the inflammatory responses of astrocytes remains less clear. To date, few studies have directly examined this in astrocytes *in vitro*. One recent example (published in August 2023, following the initiation of my doctoral work in 2020) was focused on examining the pathways which lead to enhanced TSPO expression during inflammation and the potential contribution made by enhanced TSPO expression in regulating astrocyte reactivity using astrocytoma cells[456]. Despite being informative, studies in cell lines do not always recapitulate physiologically relevant healthy astrocytes[381], therefore it would be important to investigate whether similar mechanisms are at play in primary astrocyte cultures. Furthermore, as astrocytes, like microglia, can undergo an inflammatory response[167], it is likely that TSPO plays a role in regulating the inflammatory responses of both microglia and astrocytes.

As I have shown that TSPO acts as a metabolic regulator in mouse primary astrocytes (MPAs) (**Chapter 3**), I postulated that TSPO plays a role in regulating energy use during the MPA response to inflammation. Data from our group has previously shown that acute and chronic exposure to an inflammatory stimulus differentially alters the metabolic phenotype of astrocytes: following acute inflammatory stimulation with lipopolysaccharide (LPS), astrocytes are more glycolytic, and following chronic inflammatory stimulation with LPS the cells become more reliant on oxidative phosphorylation to meet their bioenergetic needs[167]. Crucially, this study showed that pharmacological inhibition of the nuclear factor kappa B (NFκB) pathway attenuated the metabolic response of astrocytes to LPS stimulation[167]. Often predominantly regarded as a master regulator of cellular inflammatory responses, NFκB plays important roles regulating other processes including metabolism and cancer[509–511]. Moreover,

evidence suggests that the NFκB and TSPO may bidirectionally regulate each other[512,513]. A study of TSPO deficiency in MA-10 Leydig cells increases *Nfκb1* gene expression and reduces *Rel* (an NFκB subunit) gene expression[512], and a separate body of work in the C20 microglial cell line showed that the *Tspo* gene contains a promoter binding sequence for NFκB[513]. This suggests that NFκB may actively upregulate TSPO during the inflammatory response, and that this may represent a mechanism through which cells meet the metabolic costs of inflammatory responses. However, the consequences of TSPO deficiency to NFκB signalling in astrocytes remains poorly understood.

Therefore, in this chapter, I postulated that alongside its impact on metabolic flexibility, TSPO deficiency will impair activation of NFκB, a key regulator of the inflammatory response, and alter cytokine release from MPAs. Towards testing this possibility, I characterised expression of proteins and enzymes involved with metabolism in TSPO$^{-/-}$ MPAs, as well as the bioenergetics of TSPO$^{-/-}$ MPAs, in the presence and absence of the inflammatory stimulus LPS. I used LPS as a pro-inflammatory stimulus due to its well-known potent activation of an inflammatory response in various mammalian cells[167,514,515], thus enabling me to rapidly induce an inflammatory response *in vitro*. Despite this, I must acknowledge that LPS is a bacterial endotoxin and thus best recapitulates the inflammatory response of astrocytes to CNS infection. Whilst this does provoke an inflammatory response from these cells, this may differ in subtleties from the inflammatory response associated with chronic low-grade inflammation seen in various neurodegenerative conditions[104]. Such a model could have been achieved with a tumour necrosis factor, complement component 1 subcomponent q, and interleukin 1α cocktail[104] as an alternative means of investigating this hypothesis. However, I chose to use LPS as this was a model previously validated in our laboratory[167] and due to the advantages of its utilisation explored above.

4.2: Hypothesis

In this chapter, I test the overarching hypothesis that loss of TSPO will attenuate NFκB phosphorylation and cytokine release from MPAs in response to LPS treatment, and that TSPO$^{-/-}$ MPAs will have a reduced bioenergetic response to LPS treatment.

4.3: Methods

Any variations in methods from the general methodology listed in **Chapter 2** are outlined here.

4.3.1: Use of C57BL/6J primary astrocytes

C57BL/6J primary astrocytes were isolated and cultured as described in **Chapter 2.2.2**. Mating pairs of wildtype C57BL/6J mice were used to generate the pups. Animals were housed under ASPA as described in **Chapter 2.2.1**. Offspring of both sexes were used in these studies. Data from these mice are presented in **Figures 4.4.1-6**.

4.4: Results

4.4.1: Validation of the inflammatory model used

The Ellacott lab has previously shown that LPS stimulation of MPA cultures induces a shift in MPA metabolism[167]. Acute (3h) LPS stimulation was shown to enhance glycolysis, whereas chronic (24h) LPS stimulation was shown to increase OXPHOS and reduce expression of glucose transporter 1[167]. This study was performed using fraction V fatty acid- and endotoxin-free bovine serum albumin as an LPS carrier[167]. In attempting to recapitulate the results and methodology the Ellacott lab previously published in 2020[167] using a new stock of fatty-acid free bovine serum albumin (FAF-BSA) as a vehicle for LPS treatments, I found that the MPA metabolic phenotype of the FAF-BSA vehicle-treated cells was not as anticipated. The same catalogue number had been ordered, but due to animal-derived products being finite in nature the same lot number we had previously used was unavailable. After weeks of unexpected results, I postulated that the FAF-BSA might be the cause of this, and that it might be possible to remove this from the treatment paradigm. Studies using LPS as an inflammatory stimulus in peripheral immune cells (and as it later transpired, astrocytoma cells[456]) typically do not conjugate LPS to a carrier compound such as BSA[516–520]. In these protocols, LPS is reconstituted in water or media and diluted in media to a working concentration, and the effects compared to 'control' cells incubated in media (± vehicle) alone. Thus, I postulated that the same treatment paradigm might be appropriate for MPAs. Therefore, I stimulated cells with either LPS (100ng/mL) or 0.1-10% FAF-BSA (both diluted in treatment media) for 24h and measured secretion of tumour necrosis factor (TNF) in response to these treatments via ELISA (**Chapter 2.2.15**). The previous studies

from our group used 0.017mM BSA vehicle as a carrier for LPS[167], and 0.01% BSA is approximately equal to 0.017mM (actual molarity: 0.015mM). TNF is a pro-inflammatory cytokine[521], and therefore in this context served as an indicator of whether these treatments induced an inflammatory response from MPAs. To maintain as much consistency as possible with the protocol previously published by our lab[167], MPAs used to assess this were isolated from wildtype C57BL/6J mice, not the $TSPO^{-/-}$ strain.

Using ELISAs (**Chapter 2.2.15**), I found that both FAF-BSA and LPS induced TNF secretion from MPAs (**Figure 4.4.1 A**; p=0.0364 [LPS v control], p=0.0113 [0.01% FAF-BSA v control], p=0.0130 [1% FAF-BSA v control], p=0.0245 [10% FAF-BSA v control]). From this I concluded that this FAF-BSA was unsuitable as a vehicle for my experiments using LPS. Because each BSA lot is isolated from a different animal, the quality of the BSA likely depends on the health of the animal at the time of isolation. Therefore in the animal of origin, low-level infections that may not yet have reached a symptomatic stage, or chronic inflammation through an undetected health condition, may impact the quality of the BSA. Another possible cause of the issues with the BSA vehicle may also have been manufacturing issues or deviations from standard protocols, as BSA variability is a well known yet poorly reported issue in life sciences[522,523]. Thus, I next investigated the possibility of using LPS (100ng/mL, diluted in treatment media) alone as an inflammatory treatment protocol for MPAs. I had already ascertained that 24h LPS treatment in the absence of BSA vehicle is sufficient to induce secretion of TNF from MPAs (**Figure 4.4.1 A**), therefore I quantified activation of NFκB (p65 subunit) via phosphorylation at amino acid residue Ser536 as a secondary measurement of an inflammatory response to LPS treatment in the absence of BSA vehicle (**Figure 4.4.1 B-D**) using immunoblotting (**Chapter 2.2.11**). I found that 24h treatment with LPS was sufficient to induce NFκB phosphorylation in MPAs (**Figure 4.4.1 D**; p=0.0075), supporting the TNF ELISA results.

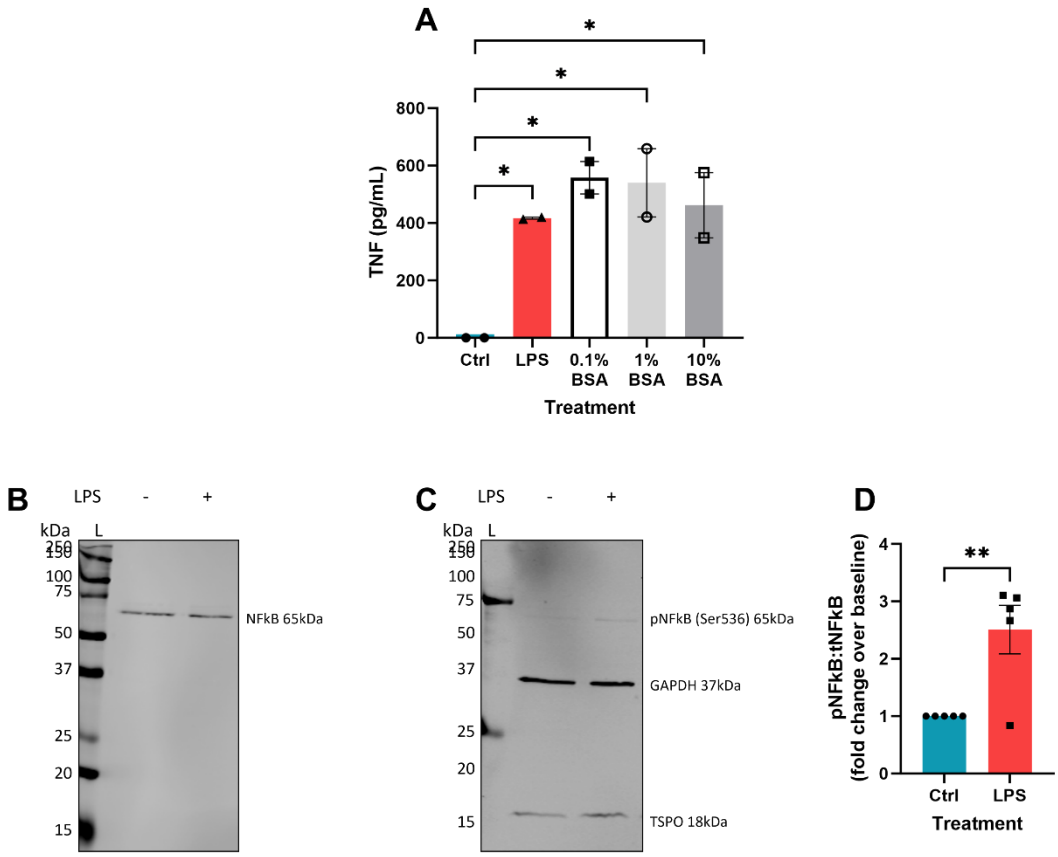

Figure 4.4.1: Validation of the inflammatory model used.

MPAs isolated from C57BL/6J neonates were stimulated with either lipopolysaccharide (LPS; 100ng/mL) or 0.1-10% fatty acid-free bovine serum albumin (BSA) for 24h. **A:** both LPS ($p=0.0364$) and BSA (0.1%: $p=0.0113$; 1%: $p=0.0130$; 10%: $p=0.0245$) elicited TNF secretion from C57BL/6J MPAs, as measured by ELISA. n=2 wells from 1 experiment, one-way ANOVA with Dunnett's multiple comparisons test. **B, C:** representative immunoblots showing induction of NFκB signalling by 24h LPS stimulated in C57BL/6J MPAs. **D:** quantification of NFκB phosphorylation expressed as the ratio of phosphorylated NFκB:total NFκB levels. 24h LPS stimulation induced NFκB phosphorylation ($p=0.0075$). n=5 plates from 2 independent experiments, unpaired t-test.

*$p<0.05$, **$p<0.01$. Data are displayed as mean ± standard error of the mean.

TNF: tumour necrosis factor. kDa: kilodaltons. L: ladder. LPS: lipopolysaccharide. BSA: fatty-acid free bovine serum albumin. ELISA: enzyme-linked immunosorbent assay. NFκB: nuclear factor kappa B. GAPDH: glyceraldehyde-3-phosphate dehydrogenase. TSPO: translocator protein 18kDa. Ctrl: vehicle-treated control group (0.01% vol/vol ddH_2O).

4.4.2: 3h LPS stimulation did not modulate TSPO expression

Increased expression of TSPO in response to inflammatory stimuli has been reported in both primary microglia[339,340,371] and glioma cell lines[371,456]. Indeed, a recent study (August 2023) by Tournier *et al*. using rat C6 glioma cells (an astrocyte cell model) showed that LPS stimulation led to increased binding of the TSPO ligand [^{125}I]CLINDE, which was attenuated by inhibition of the STAT/extracellular signal-related kinases (ERK) pathways[456]. These data suggest that TSPO plays a role in cellular responses to chronic inflammatory stimuli.

While TSPO expression has predominantly been examined in the context of chronic inflammation[313,458,524], it has been linked to acute inflammation in some studies[501,502]; therefore, I wanted to confirm in my hands whether 3h LPS treatment would be sufficient to increase TSPO expression. Our lab has previously demonstrated that inflammatory stimulation of MPAs induces a metabolic shift[167]. Therefore, as a control for metabolic flux that may be associated with a change in TSPO expression, I included 2-deoxyglucose (2DG; 10mM) treatments and immunoblots for glucose transporter 1 (GLUT1) expression to investigate a potential shift in glucose uptake in response to metabolic stress. I found that, following 3h LPS stimulation, NFκB phosphorylation was significantly increased in LPS-stimulated MPAs (**Figure 4.4.2 A-C**; $p<0.0001$), suggesting that the MPAs were responding to the inflammatory stimulus. NFκB phosphorylation was unchanged in response to 3h 2DG treatment (**Figure 4.4.2 A-C**; $p=0.3910$). TSPO expression was unchanged in C57BL/6J MPAs in response to 3h LPS (**Figure 4.4.2 B, D**; $p=0.9984$) or 2DG treatment (**Figure 4.4.2 B, D**; $p=0.4655$). I confirmed that glucose transporter 1 (GLUT1) expression was unchanged by LPS (**Figure 4.4.2 B, E**; $p=0.6030$) or 2DG treatment (**Figure 4.4.2 B, E**; $p=0.0764$) suggesting that this paradigm induces a similar inflammatory phenotype to the previously published protocol from our research team[167].

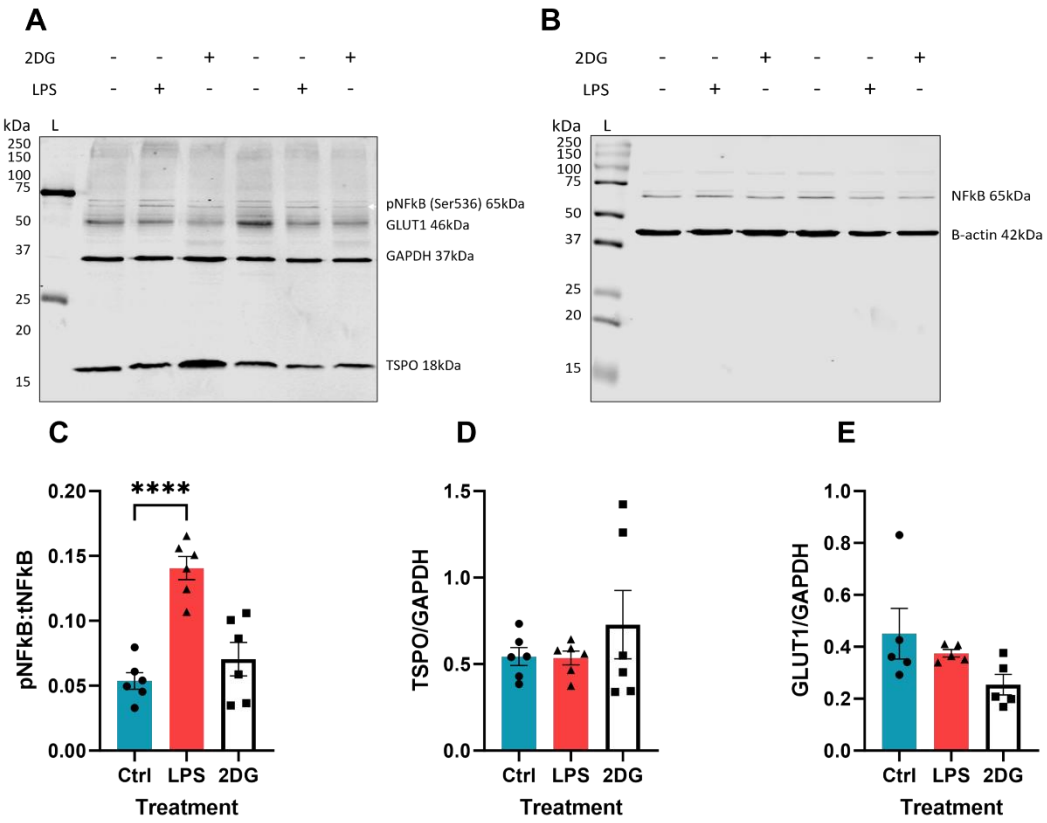

Figure 4.4.2: 3h LPS stimulation did not modulate TSPO expression.

A, B: representative immunoblots following 3h lipopolysaccharide (LPS; 100ng/mL) or 2-deoxyglucose (2-DG; 10mM) stimulation of MPAs. **C:** NFκB phosphorylation (lower band quantified as indicated by white arrow in **A**) was significantly increased by 3h LPS treatment ($p<0.0001$) but not 2DG treatment ($p=0.3910$). n=6 dishes from 2 independent experiments, one-way ANOVA with Dunnett's multiple comparisons test. **D:** Neither 3h LPS stimulation ($p=0.9984$) nor 2DG stimulation ($p=0.4655$) altered TSPO expression. n=6 dishes from 2 independent experiments, one-way ANOVA with Dunnett's multiple comparisons test. **E:** GLUT1 expression was unchanged by 3h LPS treatment ($p=0.6030$) or 2DG ($p=0.0764$). n=5 dishes from 2 independent experiments, one-way ANOVA with Dunnett's multiple comparisons test.

****$p<0.0001$. Data are displayed as mean ± standard error of the mean.

kDa: kilodaltons. L: ladder. LPS: lipopolysaccharide. 2DG: 2-deoxyglucose. NFκB: nuclear factor kappa B. GAPDH: glyceraldehyde-3-phosphate dehydrogenase. TSPO: translocator protein 18kDa. Ctrl: control group exposed to highest concentration of vehicle (2% vol/vol ddH_2O).

4.4.3: 3h LPS stimulation did not alter MPA bioenergetics

Having shown that 3h LPS stimulation had not induced a change in TSPO or GLUT1 expression, I wanted to confirm the corresponding metabolic phenotype of MPAs in response to this treatment paradigm. Hence, based on prior data from our research group, I tested the hypothesis that 3h LPS stimulation would increase extracellular acidification rate (ECAR) in MPAs without altering oxygen consumption rate (OCR). 2DG treatments (10mM) were included as a positive control for a metabolic shift in MPAs. 2DG is phosphorylated by hexokinase 2 (HK2) to form 2-deoxyglucose-6-phosphate (2DG6P), which cannot undergo further metabolism and thus inhibits glycolysis[525,526]. As glycolysis is regarded as the main contributor to ECAR[527], 2DG treatment should thus reduce ECAR and provide a positive control for a shift in the bioenergetic state of the cells.

3h LPS treatment did not significantly reduce the OCR of MPAs (**Figure 4.4.3 A, C**; p=0.9996), and unexpectedly in contrast to my hypothesis I did not see a concomitant increase in the ECAR of MPAs (**Figure 4.4.3 B, D**; p=0.5914). 3h 2DG treatment significantly reduced MPA OCR (**Figure 4.4.3 A, C**; p<0.0001) and ECAR (**Figure 4.4.3 B, D**; p<0.0001), confirming a metabolic shift in MPAs.

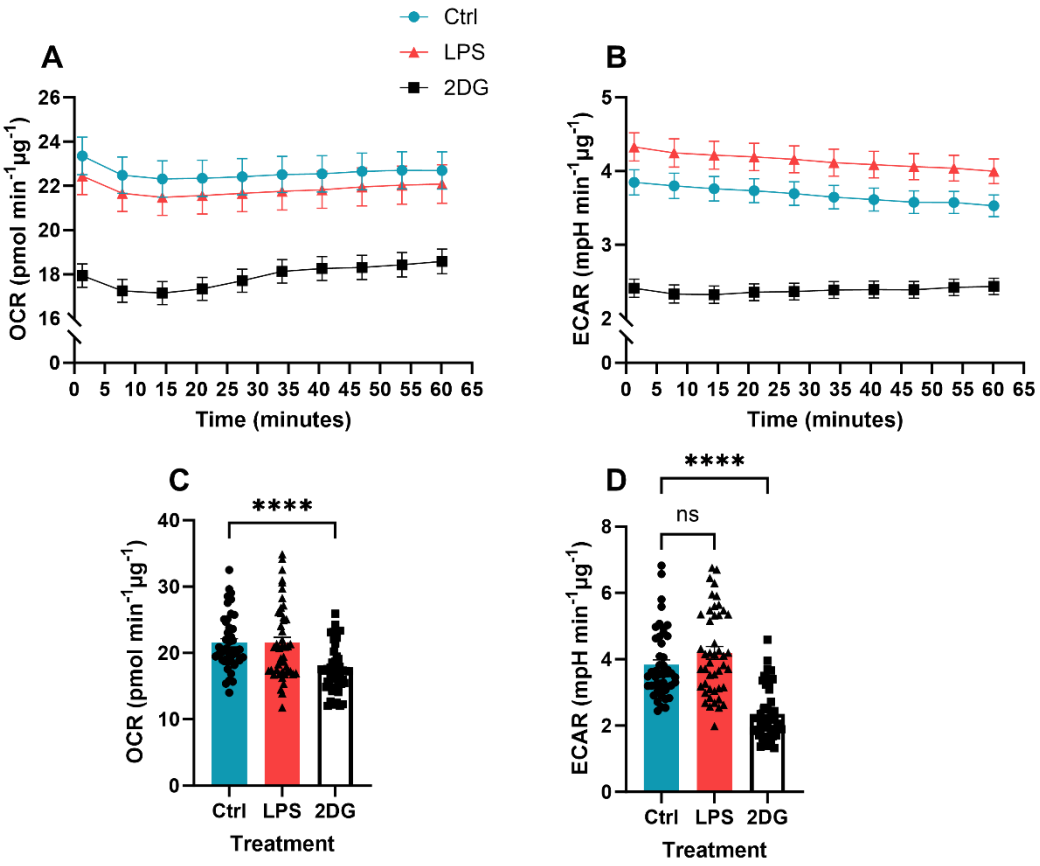

Figure 4.4.3: 3h LPS stimulation did not alter MPA bioenergetics.

OCR (**A**) and ECAR (**B**) traces following 3h lipopolysaccharide (LPS; 100ng/mL) or 2-deoxyglucose (2DG; 10mM) treatment. **C:** quantification of **A**. 3h LPS stimulation had no effect on OCR of MPAs ($p=0.9996$). 3h 2DG treatment significantly reduced MPA OCR ($p<0.0001$). n=46 wells per treatment, data are pooled from across 3 independent experiments. One-way ANOVA with Dunnett's multiple comparisons test. **D:** quantification of **B**. 3h LPS treatment had no effect on ECAR of MPAs ($p=0.5914$). 3h 2DG treatment significantly reduced MPA ECAR ($p<0.0001$). n=46 wells per treatment, data are pooled from across 3 independent experiments. Kruskal-Wallis test with Dunn's multiple comparisons test.

ns $p>0.05$, ****$p<0.0001$. Data are displayed as mean ± standard error of the mean.

OCR: oxygen consumption rate. ECAR: extracellular acidification rate. Ctrl: control group exposed to highest concentration of vehicle (2% vol/vol ddH_2O).

4.4.4: 24h LPS stimulation increased TSPO expression

CNS TSPO expression is upregulated in many disorders with an element of chronic neuroinflammation, such that TSPO is used some in clinics to track neuroinflammation levels via positron emission tomography[410]. Studies in glioma cell lines[370,371,456] and primary glial cell cultures[339,340,371,444] have demonstrated that this effect is conserved *in vitro*. As TSPO has been linked to inflammatory responses, I wanted to determine if chronic inflammatory stimulation of MPAs with LPS would recapitulate this upregulation of TSPO, with a view to using this treatment paradigm to investigate the immunometabolic phenotype of $TSPO^{-/-}$ MPAs. Thus, the aim of this section was to evaluate the effects of 24h LPS treatment on TSPO expression in astrocytes.

I began by determining the effect of chronic LPS stimulation on the expression of the glycolytic enzyme glyceraldehye-3-phosphate dehydrogenase (GAPDH), which I used as the loading control for my immunoblotting experiments. Concerned that alterations in the metabolic phenotype of the cells may in turn modulate GAPDH expression, I first validated the use of GAPDH as a loading control for experiments involving chronic inflammatory stimulation by using β-actin as a secondary control. I found that GAPDH expression did not change in response to 24h LPS (**Figure 4.4.4 A-C**; p=0.5618) nor 24h 2DG treatment (**Figure 4.4.4 A-C**; p=0.8650), therefore I proceeded to use GAPDH to normalise these data. I then quantified NFκB phosphorylation to reinforce the findings presented in **Figure 4.4.1** and found that NFκB phosphorylation was significantly upregulated in MPAs after 24h LPS treatment (**Figure 4.4.4 A, B, D**; p<0.0001) but not 2DG treatment (**Figure 4.4.4 A, B, D**; p=0.7103). Finally, I tested the hypothesis that 24h LPS stimulation would increase TSPO expression in MPAs and found that TSPO expression was increased by 24h LPS stimulation (**Figure 4.4.4 A, E**; p=0.0477) but not 2DG treatment (**Figure 4.4.4 A, E**; p=0.9839).

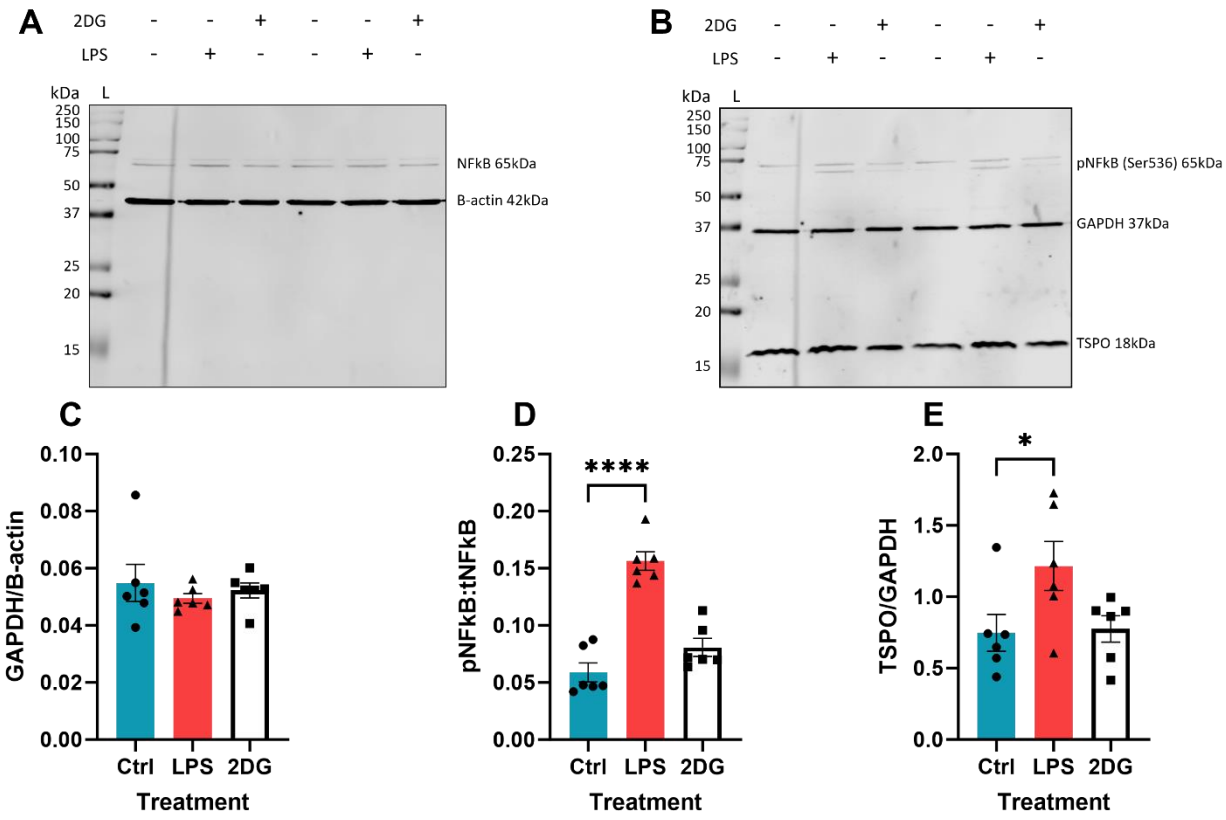

Figure 4.4.4: 24h LPS stimulation increased TSPO expression.

A, B: representative immunoblots showing the effect of 24h lipopolysaccharide (LPS; 100ng/mL) or 2-deoxyglucose (2DG; 10mM) treatment on expression of proteins of interest in MPAs. **C:** 24h stimulation with LPS or 2DG had no effect on GAPDH expression ($p=0.5618$ [LPS], $p=0.8650$ [2DG]). n=6 dishes from 2 independent experiments. One-way ANOVA with Dunnett's multiple comparisons test. **D:** 24h LPS treatment significantly increased NFκB phosphorylation in MPAs ($p<0.0001$) but 2DG treatment did not ($p=0.7103$). n=6 dishes from 2 independent experiments. One-way ANOVA with Dunnett's multiple comparisons test. **E:** 24h LPS treatment significantly increased TSPO expression in MPAs ($p=0.0477$), whereas 2DG treatment did not ($p=0.9839$). n=6 dishes from 2 independent experiments. One-way ANOVA with Dunnett's multiple comparisons test.

*p<0.05, ****p<0.0001. Data are displayed as mean ± standard error of the mean.

kDa: kilodaltons. L: ladder. LPS: lipopolysaccharide. 2DG: 2-deoxyglucose. NFκB: nuclear factor kappa B. GAPDH: glyceraldehyde-3-phosphate dehydrogenase. TSPO: translocator protein 18kDa. Ctrl: control group exposed to highest concentration of vehicle (2% vol/vol ddH_2O).

4.4.5: 24h LPS stimulation increased MPA OCR and ECAR

Having confirmed that TSPO expression increased in MPAs in response to 24h LPS treatment, I next wanted to ascertain that the metabolic shift in astrocytes following chronic exposure to proinflammatory stimulation previously reported by the Ellacott lab was conserved in my treatment paradigm[167]. 2DG was again included as a positive control for a shift in the bioenergetic state of the cells.

I found that 24h LPS stimulation using my treatment paradigm increased the OCR of MPAs (**Figure 4.4.5 A, C**; $p<0.0001$). However, in contrast to previously published data[167], I also found that 24h LPS stimulation increased MPA ECAR (**Figure 4.4.5 B, D**; $p=0.0141$).

The positive control, 24h 2DG treatment significantly reduced OCR (**Figure 4.4.5 A, C**; $p=0.0479$) and ECAR (**Figure 4.4.5 B, D**; $p<0.0001$), confirming the ability of these cells to undergo a metabolic shift.

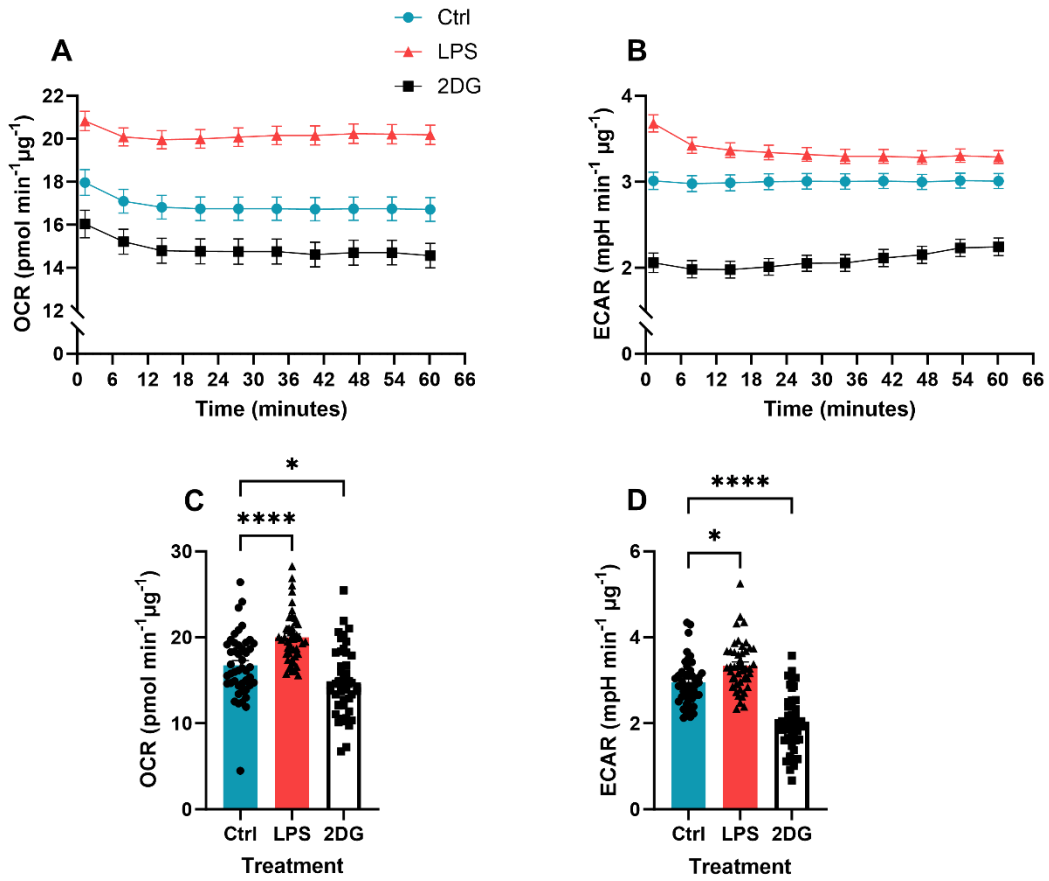

Figure 4.4.5: 24h LPS stimulation increased MPA OCR and ECAR.

OCR (**A**) and ECAR (**B**) of MPAs stimulated for 24h with lipopolysaccharide (LPS; 100ng/mL) or 2-deoxyglucose (2DG; 10mM). **C:** quantification of **A**. 24h stimulation with LPS increased OCR in MPAs ($p<0.0001$), while 2DG reduced OCR ($p=0.0479$). n=46 wells, data are pooled from across 3 experiments. One-way ANOVA with Dunnett's multiple comparisons test. **D:** quantification of **B**. 24h LPS treatment significantly increased ECAR in MPAs ($p=0.0141$), while 2DG treatment reduced ECAR ($p<0.0001$). n=46 wells, data are pooled from across 3 experiments. One-way ANOVA with Dunnett's multiple comparisons test.

*$p<0.05$, ****$p<0.0001$. Data are displayed as mean ± standard error of the mean.

OCR: oxygen consumption rate. ECAR: extracellular acidification rate. LPS: lipopolysaccharide. 2DG: 2-deoxyglucose. Ctrl: control group exposed to highest concentration of vehicle (2% vol/vol ddH_2O).

4.4.6: 24h LPS stimulation did not reduce cell viability

To confirm that the metabolic phenotypes I observed in **Figures 4.4.4-5** were not solely due to cell death following chronic LPS or 2DG stimulation, I measured cell viability via propidium iodide uptake (**Chapter 2.2.16**). Propidium iodide accumulates in cells with disrupted membranes, allowing one to differentiate between alive and dead/dying cells[454].

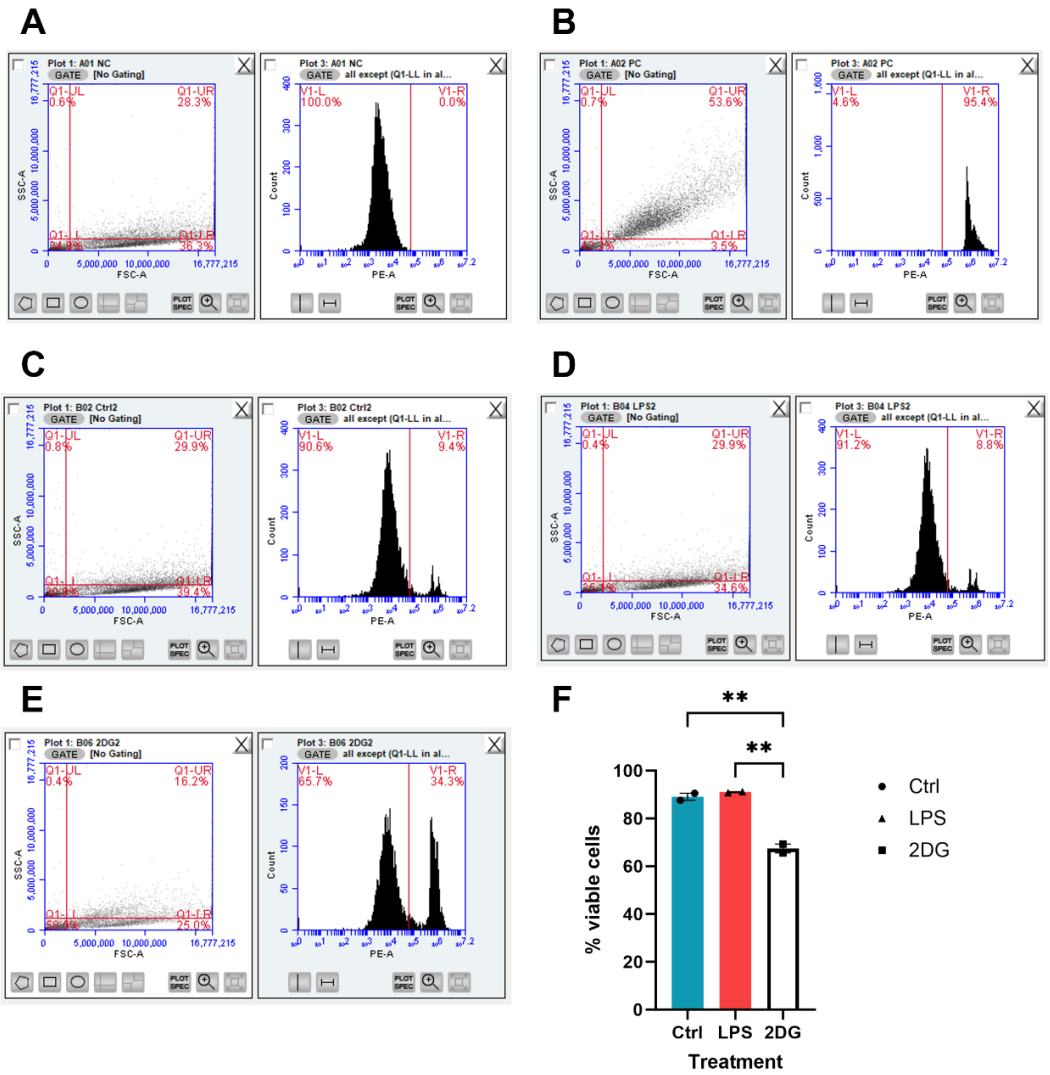

Figure 4.4.6: 24h LPS stimulation did not reduce cell viability.

Cells were stimulated with lipopolysaccharide (LPS; 100ng/mL) or 2-deoxyglucose (2DG; 10mM) for 24h and viability measured via propidium iodide (2µg/mL) uptake and flow cytometry. Settings used for gating flow cytometry for cell viability assay, measured by propidium iodide uptake, and example data. **A:** Negative control data used to gate experiment. Counts from Q1LL were deemed to be debris and excluded from counts. **B:** Example positive control data (MPAs boiled at 55°C for 10 minutes) to confirm validity of gating. **C:** Example data from control treated MPAs. **D:** Example data from 24h LPS stimulated MPAs. **E:** Example data from 24h 2DG stimulated MPAs. **F:** Cell viability data showing that 24h LPS stimulation did not significantly change MPA viability (p=0.6306 v control). 24h 2DG stimulation significantly reduced MPA viability (p=0.0030 v control).

n=2 dishes from 1 experiment, one-way ANOVA with Tukey's multiple comparison's test. **p<0.01. Ctrl: control group exposed to highest concentration of vehicle (2% vol/vol ddH_2O).

4.4.7: TSPO deficiency altered the temporal release profile of TNF from MPAs

Early in this chapter (**Chapter 4.4.2-5**), I provide evidence that TSPO expression in astrocytes correlates with the metabolic and inflammatory state of cells *in vitro*. Given the intense metabolic cost of fuelling an inflammatory response, which I have shown to be conserved in MPAs, changes to cells' ability to utilise metabolic substrates may impact their inflammatory response. In **Chapter 3** I provided evidence that TSPO acts as a regulator of cellular metabolism, and that loss of TSPO alters fuel preference in MPAs, wherein the MPAs become more reliant on fats to meet their bioenergetic requirements.

Studies in the peripheral immune system have demonstrated that chronic inflammation leads to a similar metabolic shift to the data I have reported in MPAs: an increased reliance on mitochondrially-mediated OXPHOS and FAO. In macrophages and other peripheral immune cells, this has been linked to an "M2-like" phenotype, wherein the cell is hypothesised to be fulfilling a reparative or protective role in the resolution of inflammation[289,386–390]. Similarly to macrophages, different phenotypes associated with inflammation have been reported in brain immune competent cells, including astrocytes, where under certain conditions they adopt a more proinflammatory and neurotoxic[20,80,104,105,163,261,455], or anti-inflammatory and phagocytic/neuroprotective phenotypes[80,179,237,258,261,528,529]. Therefore, I postulated that the increased reliance on FAO I observed in TSPO$^{-/-}$ MPAs (**Figure 3.4.12**) might result in an altered inflammatory phenotype of the cells by reducing the pro-inflammatory response. To test this hypothesis, I stimulated TSPO$^{-/-}$ MPAs with LPS for 3 or 24h and measured TNF secretion.

Analysis via a 2-way ANOVA (variables: TSPO genotype and LPS stimulation) revealed that TSPO genotype ($p_{genotype}$<0.0001, $F_{(1,16)}$=141.2) and 3h LPS stimulation (p_{LPS}=0.0007, $F_{(1,16)}$=17.41) had statistically significant effects on TNF secretion and there was a statistically significant interaction between these variables ($p_{interaction}$=0.0007, $F_{(1,16)}$=17.41). The statistically significant effects of TSPO genotype ($p_{genotype}$=0.0102, $F_{(1,20)}$=8.038) and LPS stimulation (p_{LPS}<0.0001, $F_{(1,20)}$=91.97) were maintained after 24h treatment, as was the statistically significant interaction ($p_{interaction}$=0.0102, $F_{(1,20)}$=8.038). Using post-hoc analyses I found that, following 3h LPS stimulation, TSPO$^{-/-}$ MPAs released

significantly less TNF than $TSPO^{+/+}$ controls (**Figure 4.4.7 A**, p=0.0001), whereas following 24h LPS stimulation TNF release was significantly enhanced in $TSPO^{-/-}$ MPAs (**Figure 4.4.7 B**, p=0.0035).

Hypothesising that I would see reduced secretion of interleukin-1β, an early-phase inflammatory cytokine released by astrocytes[164,254], I attempted to measure IL-1β secretion from the same samples, but could not detect it using an ELISA following either 3h or 24h LPS stimulation (data not shown).

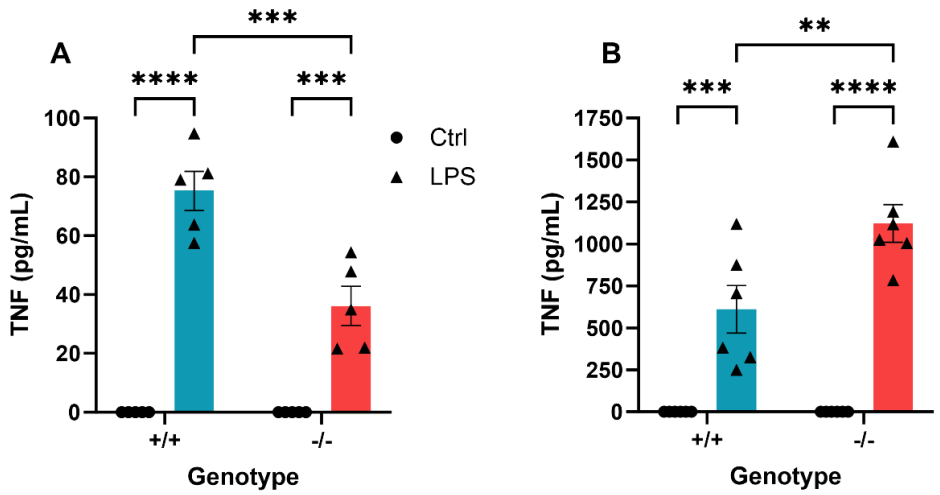

Figure 4.4.7: TSPO deficiency altered the temporal release profile of TNF from MPAs.

TSPO$^{-/-}$ MPAs and wildtype controls were stimulated with lipopolysaccharide (LPS; 100ng/mL) for 3h or 24h and TNF secretion quantified. **A:** TNF release from TSPO$^{-/-}$ MPAs following 3h LPS stimulation. n=5 dishes from 2 independent experiments, 2-way ANOVA with Šídák's multiple comparisons test. Both TSPO genotype ($p_{genotype}$<0.0001, $F_{(1,16)}$=141.2) and LPS stimulation (p_{LPS}=0.0007, $F_{(1,16)}$=17.41) had statistically significant effects on TNF secretion. There was a statistically significant interaction of these variables ($p_{interaction}$=0.0007, $F_{(1,16)}$=17.41). Post-hoc analysis revealed that TNF secretion from TSPO$^{-/-}$ MPAs was significantly reduced compared to TSPO$^{+/+}$ controls in response to 3h LPS stimulation (p=0.0001). **B:** TNF release from TSPO$^{-/-}$ MPAs was significantly increased compared to TSPO$^{+/+}$ controls in response to 24h LPS stimulation (p=0.0035). n=5 dishes from 2 independent experiments, 2-way ANOVA with Šídák's multiple comparisons test. Both TSPO genotype ($p_{genotype}$=0.0102, $F_{(1,20)}$=8.038) and LPS stimulation (p_{LPS}<0.0001, $F_{(1,20)}$=91.97) had statistically significant effects on TNF secretion, and there was a statistically significant interaction ($p_{interaction}$=0.0102, $F_{(1,20)}$=8.038). The statistically significant effects of TSPO genotype ($p_{genotype}$=0.0102, $F_{(1,20)}$=8.038) and LPS stimulation (p_{LPS}<0.0001, $F_{(1,20)}$=91.97) were maintained at 24h, as was the statistically significant interaction ($p_{interaction}$=0.0102, $F_{(1,20)}$=8.038).

**p<0.01. ***p<0.001. ****p<0.0001. Data are displayed as mean ± standard error of the mean.

TNF: tumour necrosis factor. Ctrl: vehicle-treated control (0.01% ddH_2O).

4.4.8: NFκB phosphorylation in TSPO$^{-/-}$ MPAs following 3h LPS stimulation was unchanged compared to TSPO$^{+/+}$ controls

Having observed that TNF secretion from TSPO$^{-/-}$ MPAs was reduced following 3h LPS inflammation (**Figure 4.4.7 A**), I postulated that this finding may be due to altered activity of inflammatory signalling pathways in astrocytes.

Pharmacological evidence using TSPO ligands suggests that modulation of TSPO activity impacts NFκB signalling[530]. Along with the STAT family of proteins[531], the NFκB signalling pathway is a key regulator of cellular inflammatory responses, as well as cellular metabolism and growth[509,511]. Moreover, the Ellacott lab have previously shown that altering NFκB signalling is sufficient to regulate the immunometabolic responses of MPAs[167]. Alongside this, the NFκB and STAT pathways have been linked to regulation of TSPO expression in separate studies[441,530,532]. In the case of NFκB, this regulation occurs via a promoter domain in *Tspo*[513]. Furthermore, TSPO deficiency has been shown to affect *NFκB* and *Stat1* gene expression via retrograde signalling during a study where TSPO was knocked out of Leydig cells[512]. This suggests a potentially bidirectional relationship, possibly a feedback or feed-forward loop between these proteins. However, the mechanism underlying this remains unclear. Given the importance of the NFκB response to astrocyte immunometabolism[167], and my results suggesting that loss of TSPO modulates cytokine release from MPAs (**Figure 4.4.7**), I hypothesised that loss of TSPO was associated with reduced LPS-induced NFκB phosphorylation.

As I had previously shown that loss of TSPO alters the bioenergetic parameters of MPAs (**Chapter 3**), to ensure accurate quantification of immunoblots, I wanted to ascertain that if GAPDH expression were modulated by TSPO deficiency, and whether this was impacted by a potentially altered inflammatory response. Using a 2-way ANOVA, I found that neither TSPO genotype ($p_{genotype}$=0.8707, $F_{(1,19)}$=0.02722) nor LPS stimulation had a statistically significant effect on GAPDH expression (p_{LPS}=0.6334, $F_{(1,19)}$=0.2350). Moreover, I did not observe a statistically significant interaction between these variables ($p_{interaction}$=0.1721, $F_{(1,19)}$=2.014). Post-hoc analysis confirmed that TSPO deficiency did not have an effect on GAPDH expression in MPAs (**Figure 4.4.8 A-C**, p=0.8691). Hence, I continued to use GAPDH as a loading control.

Next, I wanted to confirm whether TSPO deficiency affected NFκB protein expression (**Figure 4.4.8 A, D**). Neither TSPO genotype ($p_{genotype}$=0.1949) nor LPS stimulation (p_{LPS}=0.4697) had a statistically significant effect on NFκB expression. No statistically significant interaction between these variables was observed ($p_{interaction}$=0.2374). Post hoc analysis confirmed that total NFκB expression was unchanged between control-treated $TSPO^{-/-}$ and $TSPO^{+/+}$ MPAs (p=0.9998) or in LPS-stimulated MPAs (p=0.9861).

I next tested the hypothesis that the observed attenuated TNF release from $TSPO^{-/-}$ MPAs following 3h LPS treatment was due to reduced NFκB phosphorylation. While there was no statistically significant effect of TSPO genotype on NFκB phosphorylation ($p_{genotype}$=0.3408, $F_{(1,19)}$=0.9547), 3h LPS stimulation significantly affected this parameter (p_{LPS}<0.0001, $F_{(1,19)}$=41.25). However, there was no statistically significant interaction between these variables ($p_{interaction}$=0.1829, $F_{(1,19)}$=1.911). Using post-hoc analyses, I found that, while 3h LPS stimulation increased NFκB phosphorylation in both $TSPO^{+/+}$ (**Figure 4.4.8 A, B, E**; p=0.0002) and $TSPO^{-/-}$ MPAs (**Figure 4.4.8 A, B, E**; p=0.0093), there was no significant difference in NFκB phosphorylation between $TSPO^{+/+}$ and $TSPO^{-/-}$ MPAs (**Figure 4.4.8 A, B, E**; p=0.4812). In line with my findings from C57BL/6J MPAs, TSPO expression in $TSPO^{+/+}$ MPAs was not affected by 3h LPS stimulation (**Figure 4.4.8 B, F**; p=0.7137).

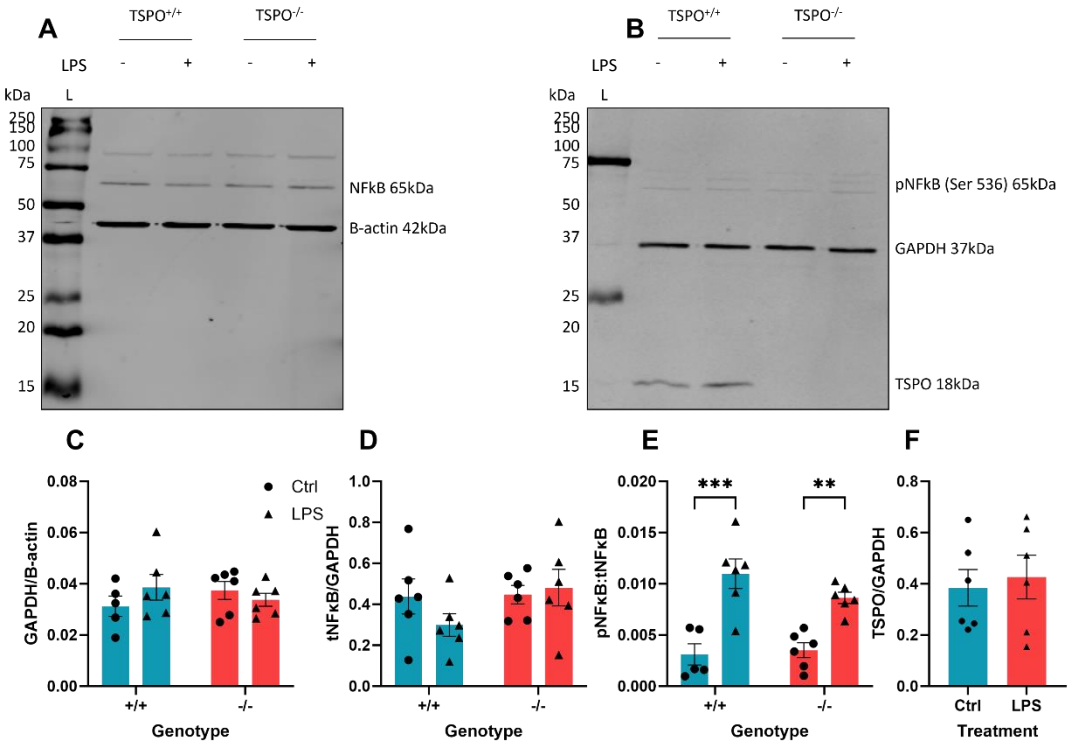

Figure 4.4.8: NFκB phosphorylation in TSPO$^{-/-}$ MPAs following 3h LPS stimulation was unchanged compared to TSPO$^{+/+}$ controls.

TSPO$^{+/+}$ and TSPO$^{-/-}$ MPAs were stimulated with lipopolysaccharide (LPS; 100ng/mL) for 3h and NFκB phosphorylation quantified. **A:** representative immunoblot showing B-actin and total NFκB p65 expression. **B:** representative immunoblot showing GAPDH, TSPO, and phospho-NFκB p65 (Ser536) expression. TSPO$^{-/-}$ MPAs did not express TSPO. **C:** quantification of **B**. n=5-6 dishes from 3 independent experiments, 2-way ANOVA with Šídák's multiple comparisons test. TSPO genotype had no statistically significant effect on GAPDH expression ($p_{genotype}$=0.8707, $F_{(1,19)}$=0.02722). LPS stimulation did not have a statistically significant effect on GAPDH expression (p_{LPS}=0.6334, $F_{(1,19)}$=0.2350). I did not observe a statistically significant interaction of these variables ($p_{interaction}$=0.1721, $F_{(1,19)}$=2.014). Post-hoc analysis confirmed that GAPDH expression was unchanged between control-treated TSPO$^{-/-}$ and wildtype control MPAs (p=0.8691) or in LPS-stimulated MPAs (p=0.9403). **D:** quantification of total NFκB expression. n=6 dishes from 3 independent experiments, 2-way ANOVA with Šídák's multiple comparisons test. No statistically significant effect of TSPO genotype ($p_{genotype}$=0.1949) or LPS stimulation (p_{LPS}=0.4697) was observed. No statistically significant interaction of these variables was observed ($p_{interaction}$=0.2374). Post hoc analysis confirmed that total NFκB expression was unchanged between control-treated TSPO$^{-/-}$ and TSPO$^{+/+}$ MPAs (p=0.9998) or in LPS-stimulated MPAs (p=0.9861). **E:** quantification of NFκB phosphorylation. n=5-6 dishes from 3 independent experiments, 2-way ANOVA with Šídák's multiple comparisons test. No statistically significant effect of TSPO genotype on NFκB phosphorylation ($p_{genotype}$=0.3408, $F_{(1,19)}$=0.9547) was observed. 3h LPS stimulation significantly affected this parameter (p_{LPS}<0.0001, $F_{(1,19)}$=41.25). There was no statistically significant interaction between these variables ($p_{interaction}$=0.1829, $F_{(1,19)}$=1.911). Post-hoc analysis revealed that 3h LPS treatment increased NFκB phosphorylation in both genotypes (p=0.0002 [TSPO$^{+/+}$], p=0.0093 [TSPO$^{-/-}$]). NFκB activation was unchanged in TSPO$^{-/-}$ MPAs stimulated with 3h LPS compared to TSPO$^{+/+}$ controls (p=0.4812). **F:** 3h LPS treatment did not affect TSPO expression in wildtype controls (p=0.7137). n=6 dishes from 3 independent experiments, unpaired t-test.

**p<0.01, ***p<0.001. Data are presented as mean ± standard error of the mean. kDa: kilodaltons. L: ladder. Ctrl: vehicle-treated control (0.01% ddH_2O). NFκB: nuclear factor kappa B. GAPDH: glyceraldehyde-3-phosphate dehydrogenase. TSPO: translocator protein 18kDa.

4.4.9: GLUT1 and CPT1a expression were not modulated by 3h LPS stimulation in either genotype

Glucose transporter 1 (GLUT1) is a transporter protein found on the cell membrane, which facilitates the uptake of glucose from the bloodstream to fuel downstream metabolism or to be stored as glycogen. In **Chapter 3**, I showed that $TSPO^{-/-}$ MPAs were less responsive to the reintroduction of 1mM and 5.5mM glucose: physiologically relevant low-euglycaemic and hyperglycaemic glucose conditions relative to the brain. Furthermore, as the metabolic response of astrocytes to acute inflammatory stimulation relies heavily on glycolysis[167], I tested the hypothesis that the reduced secretion of TNF from $TSPO^{-/-}$ MPAs observed was due to altered expression of GLUT1 in these cells, either under basal conditions or in response to 3h LPS stimulation.

In contrast to my expectations, I observed no statistically significant effect of TSPO genotype (**Figure 4.4.9 A, B**; $p_{genotype}$=0.8707, $F_{(1,19)}$=0.02722) nor of 3h LPS stimulation on GLUT1 expression in MPAs (**Figure 4.4.9 A, B**; p_{LPS}=0.6334, $F_{(1,19)}$=0.2350). No statistically significant interaction of these variables was observed (**Figure 4.4.9 A, B**; $p_{interaction}$=0.1721, $F_{(1,19)}$=2.014). Post-hoc analysis confirmed that GLUT1 expression was unchanged by in $TSPO^{-/-}$ MPAs compared to $TSPO^{+/+}$ controls (**Figure 4.4.9 A, B**; control-treated $TSPO^{+/+}$ v control-treated $TSPO^{-/-}$, p=0.9571). Moreover, GLUT1 expression in both $TSPO^{+/+}$ and $TSPO^{-/-}$ MPAs did not change in response to 3h LPS stimulation (**Figure 4.4.9 A, B**; p>0.9999 [$TSPO^{+/+}$], p=0.7871 [$TSPO^{-/-}$]).

In **Chapter 3** I observed that $TSPO^{-/-}$ MPAs were more reliant on FAO to meet their basal bioenergetic requirements (**Figure 3.4.12**). Carnitine palmitoyltransferase 1a (CPT1a) is the rate-limiting enzyme of FAO, and in 2016 Tu *et al*. demonstrated that TSPO deficiency increases *Cpt1a* gene expression in Leydig cells[366]. I wanted to determine whether this translated to increased CPT1a expression in $TSPO^{-/-}$ MPAs under basal conditions. Following my observation that $TSPO^{-/-}$ MPAs secreted less TNF in response to 3h LPS stimulation, I hypothesised that this may be explained by either a change to basal CPT1a expression, or further enhanced CPT1a expression following 3h LPS stimulation – thereby facilitating further FAO, and delaying the proinflammatory response of $TSPO^{-/-}$ MPAs.

I observed no statistically significant effect of TSPO genotype (**Figure 4.4.9 A, C**; $p_{genotype}$=0.6950, $F_{(1,20)}$=0.1582) nor of 3h LPS stimulation on CPT1a expression in MPAs (**Figure 4.4.9 A, C**; p_{LPS}=0.5721, $F_{(1,20)}$=0.33). No statistically significant interaction of these variables was observed (**Figure 4.4.9 A, C**; $p_{interaction}$=0.8628, $F_{(1,20)}$=0.003066). Post-hoc analysis confirmed that CPT1a expression was unchanged between TSPO genotypes (**Figure 4.4.9 A, C**; control-treated $TSPO^{+/+}$ v control-treated $TSPO^{-/-}$, p=0.9986), and that CPT1a expression in $TSPO^{-/-}$ MPAs did not change in response to 3h LPS stimulation (**Figure 4.4.9 A, C**; p=0.9919 [$TSPO^{+/+}$ control v LPS], p=0.9508 [$TSPO^{-/-}$ control v LPS]).

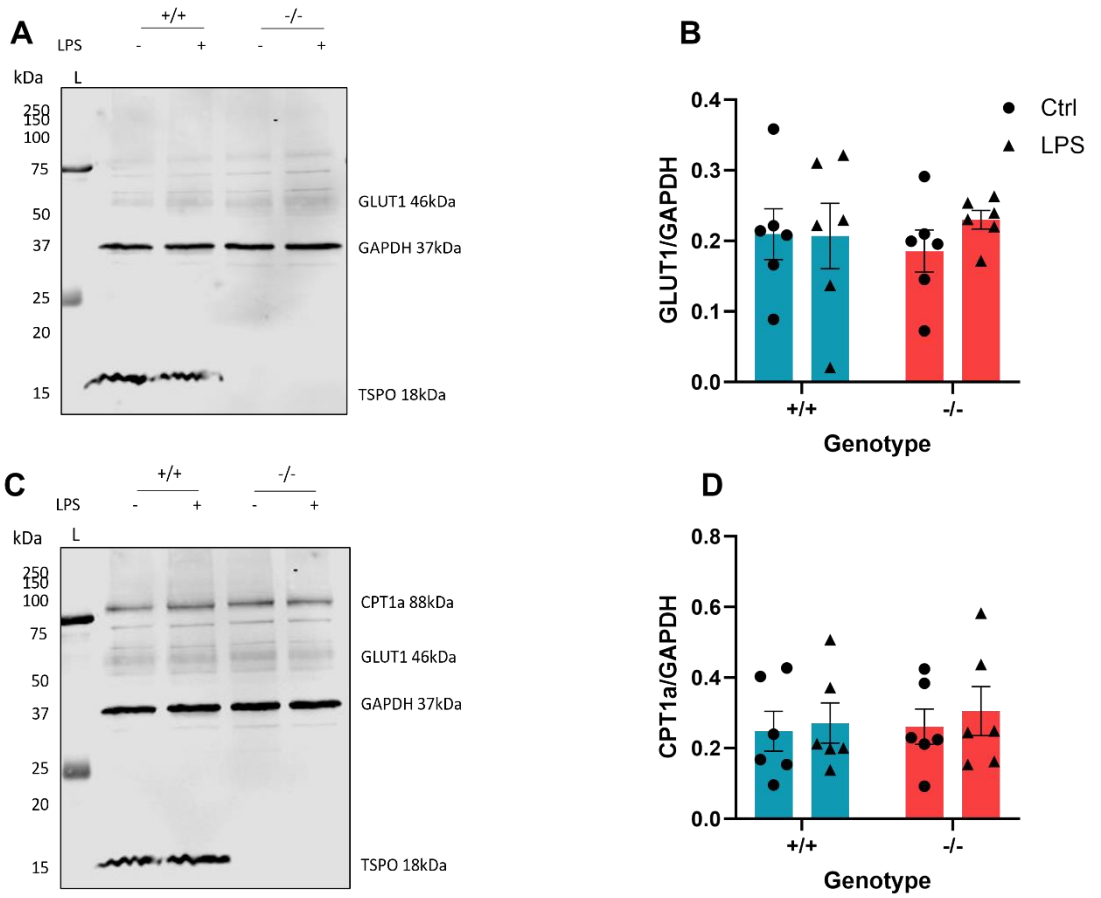

Figure 4.4.9: GLUT1 and CPT1a expression were not modulated by 3h LPS stimulation in either genotype.

$TSPO^{+/+}$ and $TSPO^{-/-}$ MPAs were stimulated with lipopolysaccharide (LPS; 100ng/mL) for 3h, and expression of GLUT1 and CPT1a quantified via immunoblotting. **A:** representative immunoblot showing GLUT1, GAPDH, and TSPO expression. $TSPO^{-/-}$ MPAs did not express TSPO. **B:** GLUT1 expression was not affected by genotype ($p_{genotype}$=0.8707, $F_{(1,19)}$=0.02722) or LPS stimulation (p_{LPS}=0.6334, $F_{(1,19)}$=0.2350). No interaction of these variables was observed ($p_{interaction}$=0.1721, $F_{(1,19)}$=2.014). n=6 dishes from 3 independent experiments. 2-way ANOVA with Tukey's multiple comparisons test. Post-hoc analysis confirmed that GLUT expression was unchanged in control-treated $TSPO^{-/-}$ MPAs compared to $TSPO^{+/+}$ controls (p=0.9571) and was not affected by 3h LPS stimulation (p>0.9999 [$TSPO^{+/+}$], p=0.7871 [$TSPO^{-/-}$]. **C:** representative immunoblot showing CPT1a expression. **D:** CPT1a expression was not affected by genotype ($p_{genotype}$=0.6950, $F_{(1,20)}$=0.1582) or LPS stimulation (p_{LPS}=0.5721, $F_{(1,20)}$=0.33). No statistically significant interaction between these variables was observed ($p_{interaction}$=0.8628, $F_{(1,20)}$=0.003066). n=6 dishes from 3 independent experiments, 2-way ANOVA with Tukey's multiple comparisons test. Post-hoc analysis confirmed that CPT1a expression was unchanged in control-treated $TSPO^{-/-}$ MPAs compared to $TSPO^{+/+}$ controls (p=0.9986) and was not affected by 3h LPS stimulation (p=0.9919 [$TSPO^{+/+}$ - LPS v $TSPO^{+/+}$ + LPS], p=0.9508 [$TSPO^{-/-}$ - LPS v $TSPO^{-/-}$ + LPS]).

Data are presented as mean ± standard error of the mean.

kDa: kilodaltons. L: ladder. Ctrl: control. LPS: lipopolysaccharide. GLUT1: glucose transporter 1. CPT1a: carnitine palmitoyltransferase 1a. GAPDH: glyceraldehyde-3-phosphate dehydrogenase. TSPO: translocator protein 18kDa.

4.4.10: NFκB phosphorylation in TSPO$^{-/-}$ MPAs following 24h LPS stimulation was unchanged compared to TSPO$^{+/+}$ controls

Existing evidence in the literature suggests that TSPO and NFκB may bidirectionally regulate each other[512,513], and in **Chapter 3** I provided evidence to suggest that TSPO deficiency alters the metabolic state of astrocytes, increasing FAO and inducing metabolic insensitivity to glucopenia (**Figure 3.4.9, 11, 12**). In peripheral macrophages, enhanced FAO is associated with an anti-inflammatory phenotype[289,384,385,389,493]. Thus, I postulated that enhanced FAO in TSPO$^{-/-}$ MPAs may underlie the altered temporal release profile of TNF I reported in **Figure 4.4.7**. I hypothesised that this may be due to a compensatory mechanism in TSPO$^{-/-}$ MPAs, such as enhanced NFκB phosphorylation following 24h LPS stimulation.

First, I confirmed that, in TSPO$^{+/+}$ MPAs, 24h LPS stimulation increased TSPO expression as expected (**Figure 4.4.10 B, D**; p=0.0493) and observed previously (**Figure 4.4.4**). Next I confirmed that neither genotype nor 24h LPS stimulation affected NFκB expression (**Figure 4.4.10 A, E**; $p_{genotype}$=0.3660, p_{LPS}=0.6043) and that these variables did not show a statistically significant interaction ($p_{interaction}$=0.7637). This was further supported by post-hoc analysis (p=0.9711 [TSPO$^{+/+}$ - LPS v TSPO$^{-/-}$ - LPS]; p=0.8204 [TSPO$^{+/+}$ + LPS v TSPO$^{-/-}$ + LPS]). I then tested the hypothesis that NFκB phosphorylation would be enhanced in TSPO$^{-/-}$ MPAs following 24h LPS stimulation. Via a 2-way ANOVA, I observed no statistically significant effect of genotype on NFκB phosphorylation (**Figure 4.4.10 A, B, F**; $p_{genotype}$=0.9731, $F_{(1,19)}$=0.001168). In contrast, 24h LPS stimulation had a statistically significant effect on NFκB phosphorylation (p_{LPS} p<0.0001, $F_{(1,19)}$=25.52). However, there was no evidence of a statistically significant interaction between these variables ($p_{interaction}$=0.5738, $F_{(1,19)}$=0.3276). Post-hoc analysis indicated that NFκB phosphorylation in TSPO$^{-/-}$ MPAs was not reduced following 24h LPS treatment compared to equivalently treated TSPO$^{+/+}$ controls (p=0.9986).

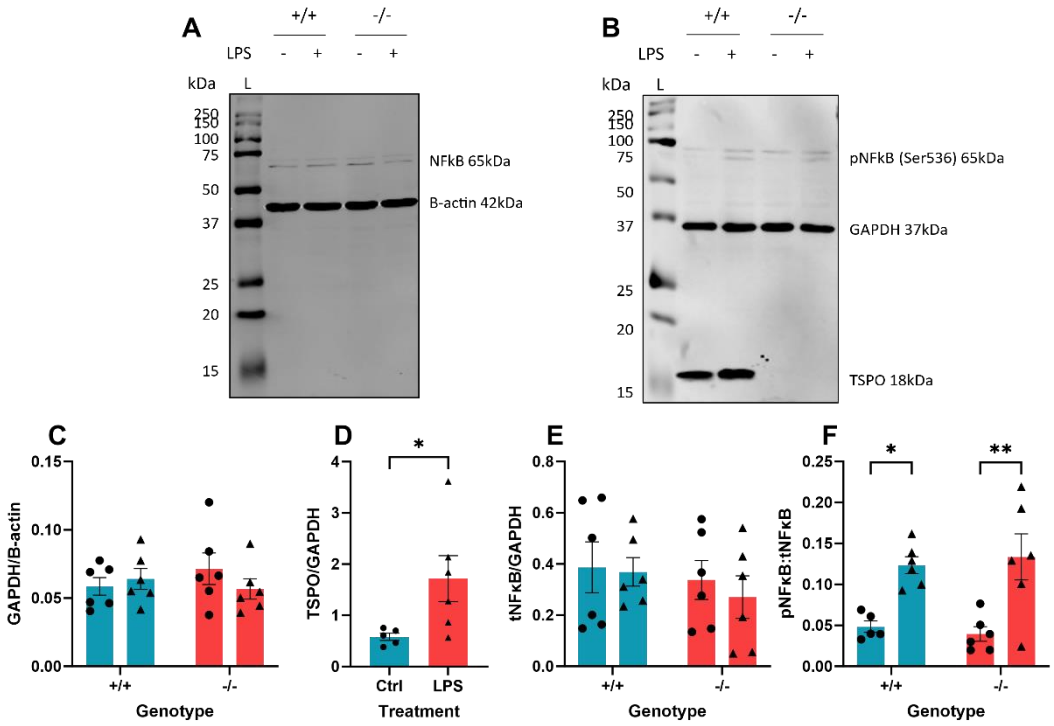

Figure 4.4.10: NFκB phosphorylation in TSPO$^{-/-}$ MPAs following 24h LPS stimulation was unchanged compared to TSPO$^{+/+}$ controls.

A, B: representative immunoblots showing expression of proteins of interest in TSPO$^{-/-}$ and $^{+/+}$ MPAs ± 24h stimulation with lipopolysaccharide (LPS; 100ng/mL). **C:** There was no statistically significant effect of TSPO genotype (**A-C**; $p_{genotype}$=0.7502, $F_{(1,20)}$=0.1042) or of 24h LPS stimulation (**A-C**; p_{LPS}=0.5908, $F_{(1,20)}$=0.2986) on GAPDH expression. There was no statistically significant interaction between these variables (**A-C**; $p_{interaction}$=0.2439, $F_{(1,20)}$=1.442). n=6 dishes from 3 independent experiments, 2-way ANOVA with Šídák's multiple comparisons test. Post-hoc analysis confirmed that GAPDH expression was not altered by TSPO deletion or 24h LPS stimulation (p=0.7069 [TSPO$^{+/+}$, $^{-/-}$ - LPS]; p=0.9663 [TSPO$^{+/+}$ + LPS], p=0.6125 [TSPO$^{-/-}$ + LPS]). **D:** TSPO expression in TSPO$^{+/+}$ MPAs was increased by 24h LPS stimulation (p=0.0493). n=6 dishes from 3 independent experiments, unpaired t-test. **E:** There was no statistically significant effect of TSPO genotype ($p_{genotype}$=0.3660) or 24h LPS stimulation (p_{LPS}=0.6043) on NFκB expression. There was no statistically significant interaction of these variables ($p_{interaction}$=0.7637). Post-hoc analysis reinforced this (p=0.9711 TSPO$^{+/+}$ - LPS v TSPO$^{-/-}$ - LPS; p=0.8204 TSPO$^{+/+}$ + LPS v TSPO$^{-/-}$ + LPS). **F:** NFκB phosphorylation was not significantly affected by TSPO genotype (**A, B, F**; $p_{genotype}$=0.9731, $F_{(1,19)}$=0.001168). 24h LPS stimulation had a statistically significant effect on NFκB phosphorylation (**A, B, F**; p_{LPS} p<0.0001, $F_{(1,19)}$=25.52). There was no evidence of a statistically significant interaction between these variables ($p_{interaction}$=0.5738, $F_{(1,19)}$=0.3276). Post-hoc analysis found that NFκB phosphorylation in TSPO$^{-/-}$ MPAs was not reduced compared to TSPO$^{+/+}$ controls by 24h LPS stimulation (p=0.9986). n=5-6 dishes from 3 independent experiments, 2-way ANOVA with Šídák's multiple comparisons test.

*p<0.05, **p<0.01. Data are displayed as mean ± standard error of the mean.

kDa: kilodaltons. L: ladder. LPS: lipopolysaccharide. NFκB: nuclear factor kappa B. GAPDH: glyceraldehyde-3-phosphate dehydrogenase. TSPO: translocator protein 18kDa.Ctrl: vehicle-treated control (0.01% ddH_2O).

4.4.11: HK2 expression was altered by 24h LPS stimulation but not by TSPO genotype

Studies in glioma cell lines and primary microglia have linked TSPO to expression and function of hexokinase 2 (HK2), a key glycolytic enzyme[340,370]. HK2 catalyses one of the rate-limiting steps of glucose metabolism[38,526,533] and is therefore an enzyme important for regulating cellular bioenergetics. Because the initiation of a proinflammatory response in astrocytes is linked to increased glycolysis[167], I postulated that the increased basal FAO I had observed in TSPO$^{-/-}$ MPAs might impede the switch to glycolysis required to respond rapidly to proinflammatory stimulation.

As I had showed TSPO$^{-/-}$ MPAs to be more reliant on FAO (**Chapter 3**), I hypothesised that TSPO$^{-/-}$ MPAs would display reduced HK2 expression compared to TSPO$^{+/+}$ control cells. I also hypothesised that, because chronic inflammatory stimulation promotes mitochondrial respiration over glycolysis, HK2 expression in TSPO$^{-/-}$ cells would not be modulated by 24h LPS stimulation. I investigated this via immunoblotting, to allow semi-quantification of protein levels, though I could not investigate the functionality or activity of HK2 with this method.

There was no statistically significant effect of TSPO genotype on HK2 expression (**Figure 4.4.11 A-C**; $p_{genotype}$=0.7600, $F_{(1,20)}$=0.09589), however, 24h LPS stimulation significantly increased HK2 levels (**Figure 4.4.11 A-C**; p_{LPS}=0.0025, $F_{(1,20)}$=11.90). There was no statistically significant interaction between TSPO genotype and LPS stimulation on HK2 levels (**Figure 4.4.11 A-C**; $p_{interaction}$=0.6544, $F_{(1,20)}$=0.2065). Post-hoc analyses confirmed that there was no significant difference in basal HK2 expression in TSPO$^{-/-}$ MPAs compared to TSPO$^{+/+}$ controls (**Figure 4.4.11 A-C**; p>0.9999). I also found that there was no significant difference in HK2 expression between TSPO$^{+/+}$ and $^{-/-}$ MPAs following 24h LPS stimulation (**Figure 4.4.11 B, C**; p=0.9956, TSPO$^{+/+}$ + LPS v TSPO$^{-/-}$ + LPS). However, contrary to my hypothesis I observed modest trends towards an increase in HK2 expression following 24h LPS stimulation (**Figure 4.4.11 B, C**; p=0.0702 [TSPO$^{+/+}$ - LPS v TSPO$^{+/+}$ + LPS], p=0.2503 [TSPO$^{-/-}$ - LPS v TSPO$^{-/-}$ + LPS]), although this did not reach statistical significance in either genotype.

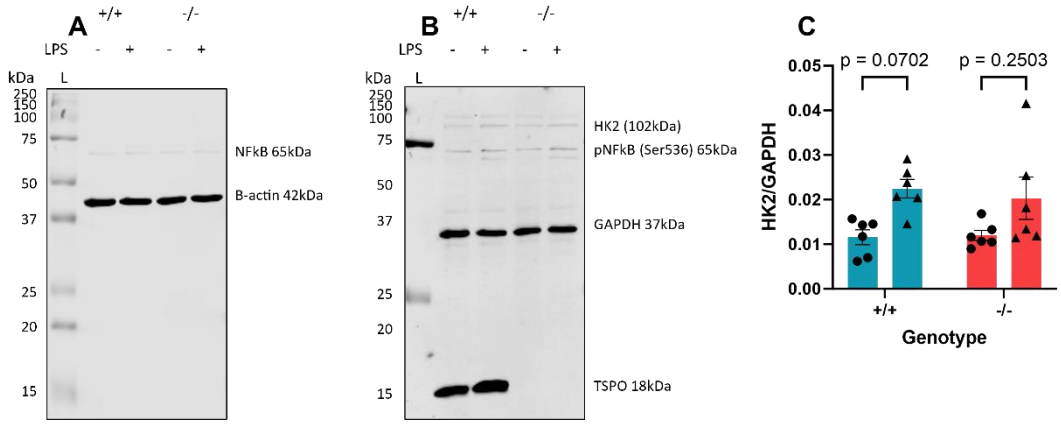

Figure 4.4.11: HK2 expression was altered by 24h LPS stimulation but not by TSPO genotype.

A, B: representative immunoblots showing expression of proteins of interest in TSPO$^{-/-}$ and $^{+/+}$ MPAs ± 24h stimulation with lipopolysaccharide (LPS; 100ng/mL). **C:** basal HK2 expression was not statistically significantly affected by TSPO genotype ($p_{genotype}$=0.7600, $F_{(1,20)}$=0.09589). 24h LPS stimulation significantly modulated HK2 expression (p_{LPS}=0.0025, $F_{(1,20)}$=11.90), however there was no statistically significant interaction of these variables ($p_{interaction}$=0.6544, $F_{(1,20)}$=0.2065). n=6 dishes from 3 independent experiments. 2-way ANOVA with Šídák's multiple comparisons test. Post-hoc analysis confirmed that HK2 expression was not statistically significantly altered by TSPO deletion (p>0.9999, TSPO$^{+/+}$ v TSPO$^{-/-}$). 24h LPS stimulation did not lead to a statistically significant increase in HK2 expression in TSPO$^{+/+}$ (p=0.0702, TSPO$^{+/+}$ - LPS v TSPO$^{+/+}$ + LPS) or TSPO$^{-/-}$ MPAs (p=0.2503 TSPO$^{-/-}$ - LPS v TSPO$^{-/-}$ + LPS).

Data are displayed as mean ± standard error of the mean.

kDa: kilodaltons. L: ladder. LPS: lipopolysaccharide. HK2: hexokinase 2. TSPO: translocator protein 18kDa. Ctrl: vehicle-treated control (0.01% ddH_2O).

4.4.12: Modulatory effects of 24h LPS stimulation on GLUT1 expression were not genotype-dependent

Reduced GLUT1 expression in astrocytes has been demonstrated during chronic inflammation[167], whereas increased GLUT1 expression has been reported in $TSPO^{-/-}$ murine glioma cells[370]. I wanted to investigate whether GLUT1 expression was increased in $TSPO^{-/-}$ MPAs under basal conditions, and how this was impacted by exposure to chronic inflammatory stimulation. Therefore, I hypothesised that basal GLUT1 would be increased in $TSPO^{-/-}$ MPAs, and that GLUT1 expression would not be reduced in these cells in response to 24h LPS stimulation (thus prolonging the proinflammatory phenotype associated with enhanced glycolysis), postulating that this may explain the shift in TNF release in response to LPS treatment I had observed (**Figure 4.4.7**).

GLUT1 expression (**Figure 4.4.12 A**) was not statistically significantly altered by TSPO genotype (**Figure 4.4.12 B**; $p_{genotype}=0.5249$, $F_{(1,20)}=0.4188$), however 24h LPS stimulation significantly reduced GLUT1 expression (**Figure 4.4.12 B**; $p_{LPS}<0.0001$, $F_{(1,20)}=89.35$). I did not observe a statistically significant interaction between these variables (**Figure 4.4.12 B**; $p_{interaction}=0.3435$, $F_{(1,20)}=0.9143$). Post-hoc analyses confirmed that GLUT1 expression was not significantly reduced in control-treated $TSPO^{-/-}$ MPAs in comparison to control-treated $TSPO^{+/+}$ MPAs (**Figure 4.4.12 B**; p=0.8440). Post hoc analyses indicated a statistically significant reduction in GLUT1 expression induced by 24h LPS stimulation in both genotypes (**Figure 4.4.12 B**; p<0.0001 [$TSPO^{+/+}$ - LPS v $TSPO^{+/+}$ + LPS], [$TSPO^{-/-}$ - LPS v $TSPO^{-/-}$ + LPS]), and confirmed that there was no significant difference in GLUT1 expression in $TSPO^{-/-}$ MPAs compared to $TSPO^{+/+}$ controls following 24h LPS stimulation (**Figure 4.4.12 B**; p>0.9999; $TSPO^{+/+}$ + LPS v $TSPO^{-/-}$ + LPS).

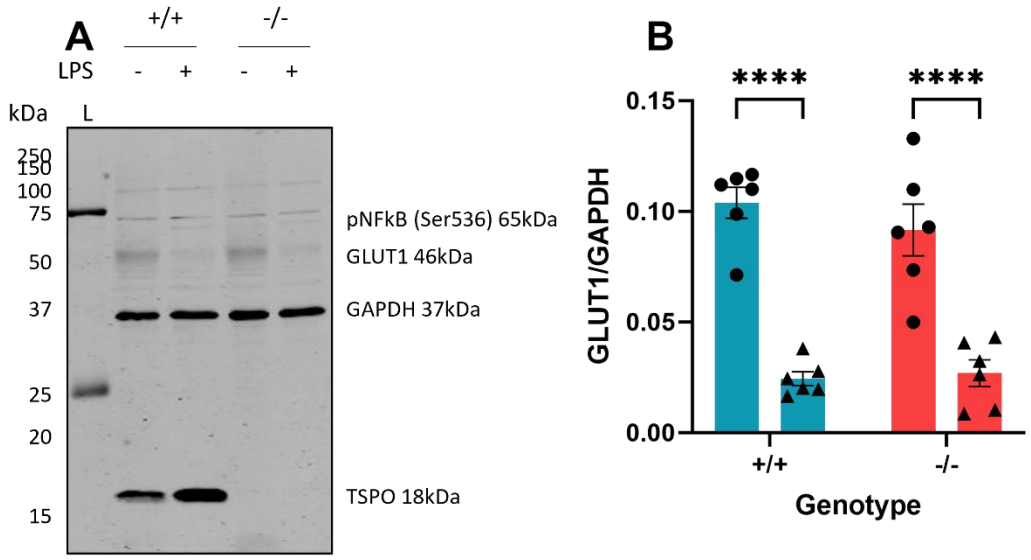

Figure 4.4.12: 24h LPS stimulation but not TSPO genotype significantly reduced GLUT1 expression.

A: representative immunoblots showing expression of proteins of interest in TSPO$^{-/-}$ and $^{+/+}$ MPAs ± 24h stimulation with lipopolysaccharide (LPS; 100ng/mL). **B:** GLUT1 expression was not statistically significantly altered by TSPO genotype ($p_{genotype}$=0.5249, $F_{(1,20)}$=0.4188). 24h LPS stimulation significantly altered GLUT1 expression (p_{LPS}<0.0001, $F_{(1,20)}$=89.35). I did not observe a statistically significant interaction of these variables ($p_{interaction}$=0.3435, $F_{(1,20)}$=0.9143). n=6 dishes from 3 independent experiments. 2-way ANOVA with Šídák's multiple comparisons test. Post-hoc testing confirmed that basal GLUT1 expression was not altered by TSPO deletion (p=0.8440, TSPO$^{+/+}$ v TSPO$^{-/-}$ [both control]). 24h LPS stimulation reduced GLUT1 expression in TSPO$^{-/-}$ and TSPO$^{+/+}$ MPAs (p<0.0001 [both; TSPO$^{+/+}$ - LPS v TSPO$^{+/+}$ + LPS; TSPO$^{-/-}$ - LPS v TSPO$^{-/-}$ + LPS]). TSPO deficiency did not affect GLUT1 ablation in response to 24 LPS stimulation (p>0.9999; TSPO$^{+/+}$ + LPS v TSPO$^{-/-}$ + LPS).

****p<0.0001. Data are displayed as mean ± standard error of the mean.

kDa: kilodaltons. L: ladder. LPS: lipopolysaccharide. GLUT1: glucose transporter 1. TSPO: translocator protein 18kDa. Ctrl: vehicle-treated control (0.01% ddH_2O).

4.4.13: CPT1a expression was modulated by TSPO genotype but not 24h LPS stimulation

Although I had shown that CPT1a expression was not modulated in $TSPO^{-/-}$ MPAs under basal conditions or following 3h LPS stimulation, I wanted to examine if there were changes to CPT1a expression following 24h LPS stimulation. In **Figure 4.4.7**, I showed that TNF secretion from $TSPO^{-/-}$ MPAs is significantly enhanced following 24h LPS stimulation. This is suggestive of an enhanced proinflammatory response, which is associated with enhanced glycolysis in astrocytes[167]. Therefore, I hypothesised that following 24h LPS stimulation, CPT1a expression would be significantly reduced in $TSPO^{-/-}$ MPAs. Using a 2-way ANOVA, I found that CPT1a expression was significantly affected by genotype (**Figure 4.4.13 A, B**; $p_{genotype}=0.0165$, $F_{(1,20)}=6.848$), but not 24h LPS treatment ($p_{LPS}=0.2485$, $F_{(1,20)}=1.413$). Moreover, there was no statistically significant interaction of these variables ($p_{interaction}=0.8470$, $F_{(1,20)}=0.03820$). Post-hoc analyses indicated that that there was no significant difference in CPT1a expression in vehicle treated $TSPO^{-/-}$ MPAs compared to equivalently treated $TSPO^{+/+}$ controls (p=0.3437). CPT1a expression was reduced in 24h LPS-stimulated MPAs of both genotypes, although this did not reach statistical significance (p=0.8950 [$TSPO^{+/+}$ - LPS v $TSPO^{+/+}$ + LPS], p=0.7630 [$TSPO^{-/-}$ - LPS v $TSPO^{-/-}$ + LPS]). Furthermore, I found that there was no significant difference in CPT1a expression between 24h LPS stimulated $TSPO^{+/+}$ and $^{-/-}$ MPAs (p=0.2253 [$TSPO^{+/+}$ + LPS v $TSPO^{-/-}$+ LPS]).

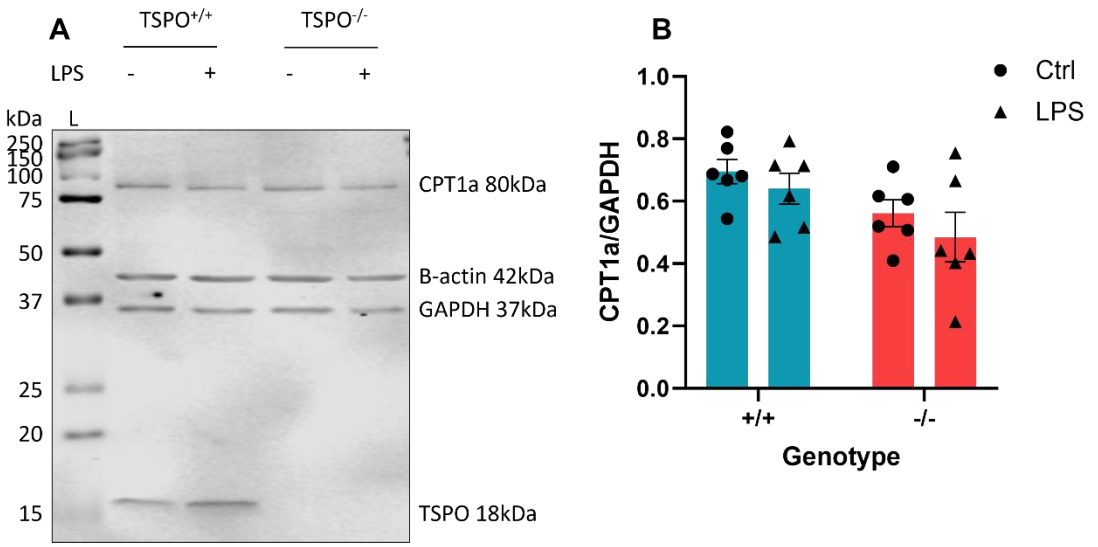

Figure 4.4.13: CPT1a expression was not modulated by 24h LPS stimulation in either TSPO genotype.

A: Representative immunoblot showing CPT1a, B-actin, GAPDH, and TSPO expression ± 24h stimulation with lipopolysaccharide (LPS; 100ng/mL). **B:** quantification of immunoblot in **A**. TSPO genotype significantly affected CPT1a expression ($p_{genotype}$=0.0165, $F_{(1,20)}$=6.848). 24h LPS stimulation had no statistically significant effect on CPT1a expression (p_{LPS}=0.2485, $F_{(1,20)}$=1.413). No significant interaction was observed between these variables ($p_{interaction}$=0.8470, $F_{(1,20)}$=0.03820). n=6 dishes from 3 independent experiments. 2-way ANOVA with Tukey's multiple comparisons test. Post-hoc testing revealed that CPT1a expression was unchanged when comparing $TSPO^{-/-}$ MPAs to $TSPO^{+/+}$ controls (p=0.3437). CPT1a expression did not change in response to 24h LPS treatment in either $TSPO^{+/+}$ and $TSPO^{-/-}$ MPAs (p=0.8950 [$TSPO^{+/+}$ - LPS v $TSPO^{+/+}$ + LPS], p=0.7630 [$TSPO^{-/-}$ - LPS v $TSPO^{-/-}$ + LPS]. Relative to 24h LPS-stimulated $TSPO^{+/+}$ MPAs, CPT1a expression in $TSPO^{-/-}$ was unchanged by 24h LPS stimulation (p=0.2253 [$TSPO^{+/+}$ + LPS v $TSPO^{-/-}$ + LPS]).

Data are displayed as mean ± standard error of the mean.

kDa: kilodaltons. L: ladder. Ctrl: control. LPS: lipopolysaccharide. CPT1a: carnitine palmitoyltransferase 1a. TSPO: translocator protein 18kDa. Ctrl: vehicle-treated control (0.01% ddH_2O).

4.4.14: 24h LPS stimulation significantly increased IL-10 secretion from TSPO$^{-/-}$ MPAs but not TSPO$^{+/+}$ controls

As I had observed no significant differences in NFκB phosphorylation or expression of proteins associated with metabolism following LPS stimulation of TSPO$^{-/-}$ MPAs compared with TSPO$^{+/+}$ MPAs, I postulated that the altered temporal profile of TNF release from TSPO$^{-/-}$ MPAs following LPS stimulation (**Figure 4.4.7**) might be explained by enhanced secretion of anti-inflammatory cytokines. FAO is associated with a reparative phenotype, including secretion of anti-inflammatory cytokines such as interleukin-10 (IL-10) which is released during wound healing in the periphery and the CNS[534–536]. Therefore, to test this hypothesis, I measured IL-10 secretion from the same samples used to produce **Figure 4.4.7**.

Using a 2-way ANOVA, I found that there was no statistically significant effect of TSPO genotype on IL-10 secretion (**Figure 4.4.14**; $p_{genotype}$=0.1733, $F_{(1,19)}$=2.002) while 24h LPS stimulation significantly increased IL-10 secretion (p_{LPS}<0.0001, $F_{(1,19)}$=27.66). There was a significant interaction of these two variables ($p_{interaction}$=0.0452, $F_{(1,19)}$=4.594). Post-hoc comparisons showed that there was no significant difference in basal IL-10 secretion between TSPO$^{+/+}$ and TSPO$^{-/-}$ MPAs (p=0.9970 [TSPO$^{+/+}$ - LPS v TSPO$^{-/-}$ - LPS]). Following 24h LPS stimulation, IL-10 secretion from TSPO$^{+/+}$ MPAs increased but failed to reach statistical significance (p=0.2385 [TSPO$^{+/+}$ - LPS v TSPO$^{+/+}$ + LPS]). In contrast, IL-10 secretion was significantly increased following 24h LPS stimulation of TSPO$^{-/-}$ MPAs (p=0.0002 [TSPO$^{-/-}$ - LPS v TSPO$^{-/-}$ + LPS]). However, there was no significant difference in 24h LPS-induced IL-10 secretion between genotypes (p=0.1056 [TSPO$^{+/+}$+ LPS v TSPO$^{-/-}$ + LPS]).

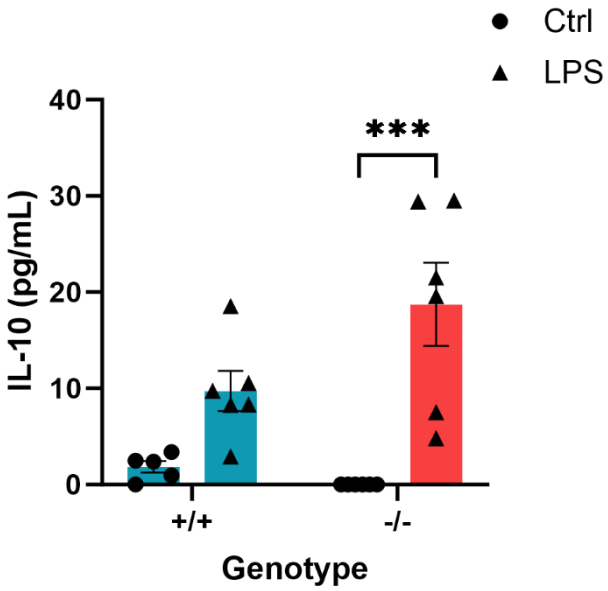

Figure 4.4.14: 24h LPS stimulation significantly increased IL-10 secretion from TSPO$^{-/-}$ MPAs but not TSPO$^{+/+}$ controls.

IL-10 secretion from TSPO$^{+/+}$ or $^{-/-}$ MPAs ± 24h lipopolysaccharide (LPS; 100ng/mL) stimulation was quantified via ELISA. There was no statistically significant effect of TSPO genotype on IL-10 secretion ($p_{genotype}$=0.1733, $F_{(1,19)}$=2.002). 24h LPS stimulation significantly modulated IL-10 secretion (p_{LPS}<0.0001, $F_{(1,19)}$=27.66), and there was a significant interaction of these two variables ($p_{interaction}$=0.0452, $F_{(1,19)}$=4.594). n=5-6 dishes from 2 independent experiments, 2-way ANOVA with Šídák's multiple comparisons test. Post-hoc analyses showed that there was no significant difference in IL-10 secretion following 24h LPS stimulation from TSPO$^{+/+}$ MPAs (p=0.2385 [TSPO$^{+/+}$ - LPS v TSPO$^{+/+}$ + LPS]), however IL-10 secretion from TSPO$^{-/-}$ MPAs was significantly increased following 24h LPS stimulation (p=0.0002 [TSPO$^{-/-}$ - LPS v TSPO$^{-/-}$ + LPS]). There was no statistically significant difference in IL-10 secretion between genotypes following 24h LPS stimulation (p=0.1056 (TSPO$^{+/+}$ + LPS v TSPO$^{-/-}$ + LPS)).

***p<0.001. Data are displayed as mean ± standard error of the mean.

Ctrl: control. LPS: lipopolysaccharide. TSPO: translocator protein 18kDa. IL-10: interleukin-10. Ctrl: vehicle-treated control (0.01% ddH_2O)

4.4.15: The metabolic phenotype of TSPO$^{-/-}$ MPAs in response to 3h LPS stimulation was consistent with TSPO$^{+/+}$ controls

Having determined that the altered TNF secretion profile from TSPO$^{-/-}$ MPAs in response to 3h LPS stimulation was not due to altered NFκB phosphorylation (**Figure 4.4.8**) or expression of proteins involved in regulating utilisation of metabolic substrates (**Figure 4.4.9**), I next wanted to ascertain if the reduced basal metabolism and increased FAO utilisation of TSPO$^{-/-}$ MPAs (**Chapter 3**) was the potential causal factor. There was a significant effect of TSPO genotype on OCR (**Figure 4.4.15 A, B**; $p_{genotype}<0.0001$, $F_{(1,66)}=18.45$), whereas 3h LPS stimulation had no significant effect on OCR (**Figure 4.4.15 A, B**; $p_{LPS}=0.5396$, $F_{(1,66)}=0.3802$) and there was no significant interaction between these variables (**Figure 4.4.15 A, B**; $p_{interaction}=0.2579$, $F_{(1,66)}=1.3002$). Post-hoc analyses showed that 3h LPS stimulation did not significantly increase the OCR of TSPO$^{+/+}$ (**Figure 4.4.15 A, B**; p=0.6612) or TSPO$^{-/-}$ MPAs (**Figure 4.4.15 A, B**; p=0.9769). OCR of LPS-stimulated TSPO$^{-/-}$ MPAs was significantly reduced compared to the OCR of LPS-stimulated TSPO$^{+/+}$ controls (**Figure 4.4.15 A, B**; p=0.0013).

There was a significant effect of TSPO genotype on ECAR (**Figure 4.4.15 C, D**; $p_{genotype}=0.0019$, $F_{(1,64)}=10.51$), however ECAR was not significantly affected by 3h LPS stimulation (**Figure 4.4.15 C, D**; $p_{LPS}=0.7230$, $F_{(1,20)}=0.1259$). There was no significant interaction between these variables (**Figure 4.4.15 C, D**; $p_{interaction}=0.6427$, $F_{(1,64)}=0.2173$). Post-hoc analyses showed that 3h LPS stimulation did not increase the ECAR of TSPO$^{-/-}$ MPAs (**Figure 4.4.15 C, D**; p=0.9146) or TSPO$^{+/+}$ controls (**Figure 4.4.15 C, D**; p=0.9999).

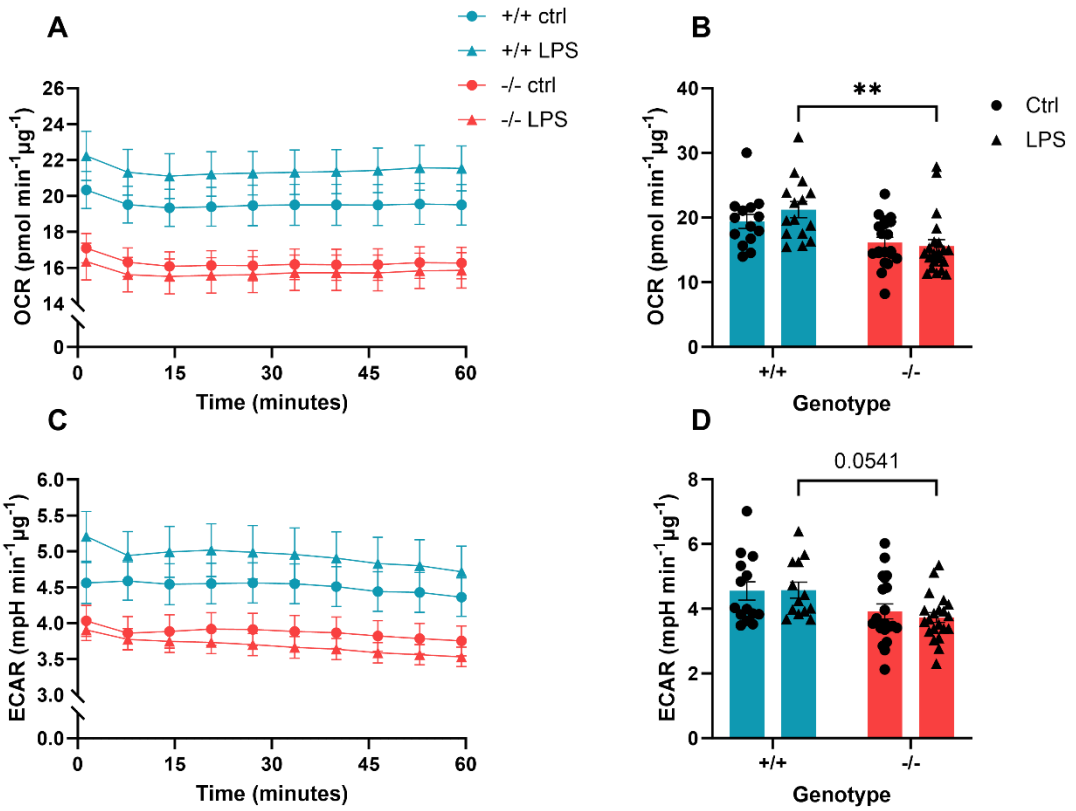

Figure 4.4.15: The metabolic phenotype of TSPO$^{-/-}$ MPAs in response to 3h LPS stimulation was consistent with TSPO$^{+/+}$ controls.

A: XY graph showing the effect of 3h lipopolysaccharide (LPS; 100ng/mL) LPS treatment on TSPO$^{-/-}$ MPA oxygen consumption rate (OCR) compared to TSPO$^{+/+}$ controls. **B:** TSPO genotype significantly affected OCR ($p_{genotype}$<0.0001, $F_{(1,66)}$=18.45), whereas 3h LPS stimulation did not (p_{LPS}=0.5396, $F_{(1,66)}$=0.3802). There was no significant interaction of these variables ($p_{interaction}$=0.2579, $F_{(1,66)}$=1.3002). n=8-10 wells per group, pooled data from 2 independent experiments. 2-way ANOVA with Tukey's multiple comparisons test. Post-hoc analyses showed that 3h LPS stimulation did not significantly increase the OCR of TSPO$^{+/+}$ MPAs (p=0.6612) or TSPO$^{-/-}$ MPAs (p=0.9769). OCR of 3h LPS-stimulated TSPO$^{-/-}$ MPAs was significantly reduced compared to the OCR of 3h LPS-stimulated TSPO$^{+/+}$ controls (p=0.0013). **C:** XY graph showing the effect of 3h LPS stimulation on TSPO$^{-/-}$ MPA extracellular acidification rate (ECAR) compared to TSPO$^{+/+}$ controls. **D:** TSPO genotype significantly affected ECAR ($p_{genotype}$=0.0019, $F_{(1,64)}$=10.51), however 3h LPS stimulation had no significant effect (p_{LPS}=0.7230, $F_{(1,20)}$=0.1259). There was no significant interaction of these variables ($p_{interaction}$=0.6427, $F_{(1,64)}$=0.2173). n=8-10 per group, pooled data from across 2 independent experiments. 2-way ANOVA with Tukey's multiple comparisons test. Post-hoc analyses showed that 3h LPS stimulation did not increase the ECAR of TSPO$^{-/-}$ MPAs (p=0.9146) or TSPO$^{+/+}$ controls (p=0.9999).

**p<0.001. Data are displayed as mean ± standard error of the mean.

Ctrl: vehicle-treated control (0.1% dH_2O).

4.4.16: The metabolic response to 24h LPS stimulation was conserved in TSPO$^{-/-}$ MPAs

As I had observed that the TSPO$^{-/-}$ MPAs were, under physiologically relevant glucose conditions, less reliant on mitochondrial metabolism and exhibited reduced ECAR while meeting more of their bioenergetic requirements via FAO (**Chapter 3**), I postulated that this may manifest as an attenuated or delayed metabolic response to inflammatory stimulation. I reasoned that, if my postulations were correct, following 24h LPS stimulation TSPO$^{-/-}$ MPAs would exhibit enhanced OCR relative to LPS-stimulated TSPO$^{+/+}$ controls and that this may explain the enhanced TNF (relative to TSPO$^{+/+}$ MPAs, **Figure 4.4.6**) and IL-10 secretion (relative to unstimulated TSPO$^{-/-}$ MPAs, **Figure 4.4.14**) I had observed. Predicting that the bioenergetic rates of TSPO$^{-/-}$ MPAs would be significantly increased compared to TSPO$^{+/+}$ controls following 24h LPS stimulation, I repeated the 24h LPS treatment paradigm.

There was no statistically significant effect of TSPO genotype on OCR (**Figure 4.4.16 A, B**; $p_{genotype}$=0.4897, $F_{(1,78)}$=0.4818). 24h LPS stimulation had a statistically significant effect on OCR (**Figure 4.4.16 A, B**; p_{LPS}<0.0001, $F_{(1,78)}$=52.35), however there was no statistically significant interaction between TSPO genotype and 24h LPS treatment (**Figure 4.4.16 A, B**; $p_{interaction}$=0.0844, $F_{(1,78)}$=3.055). Post-hoc analyses revealed that 24h LPS stimulation increased the OCR (**Figure 4.4.16 A, B**) of TSPO$^{+/+}$ and TSPO$^{-/-}$ MPAs (p=0.003 [TSPO$^{+/+}$ - LPS v TSPO$^{+/+}$ + LPS], p<0.0001 [TSPO$^{-/-}$ - LPS v TSPO$^{+/+}$ + LPS]), but, in contrast to my expectations, there was no significant difference in the OCR of TSPO$^{+/+}$ and TSPO$^{-/-}$ MPAs following 24h LPS stimulation (**Figure 4.4.16 B**; p=0.8658).

Similarly, there was no statistically significant effect of TSPO genotype on ECAR (**Figure 4.4.16 C, D**; $p_{genotype}$=0.5445, $F_{(1,78)}$=0.3704) and 24h LPS stimulation had a statistically significant effect on ECAR (**Figure 4.4.16 C, D**; p_{LPS}<0.0001, $F_{(1,78)}$=28.89). I observed no statistically significant interaction of these variables (**Figure 4.4.16 C, D**; $p_{interaction}$=0.4141, $F_{(1,78)}$=0.6742). The ECAR of TSPO$^{+/+}$ and TSPO$^{-/-}$ MPAs was similarly increased by 24h LPS stimulation (**Figure 4.4.16 C, D**; p=0.0189 [TSPO$^{+/+}$], p<0.0001 [TSPO$^{-/-}$]), and there was no significant difference between the ECAR values of 24h LPS stimulated TSPO$^{+/+}$ and TSPO$^{-/-}$ MPAs (**Figure 4.4.16 C, D**; p=0.7204).

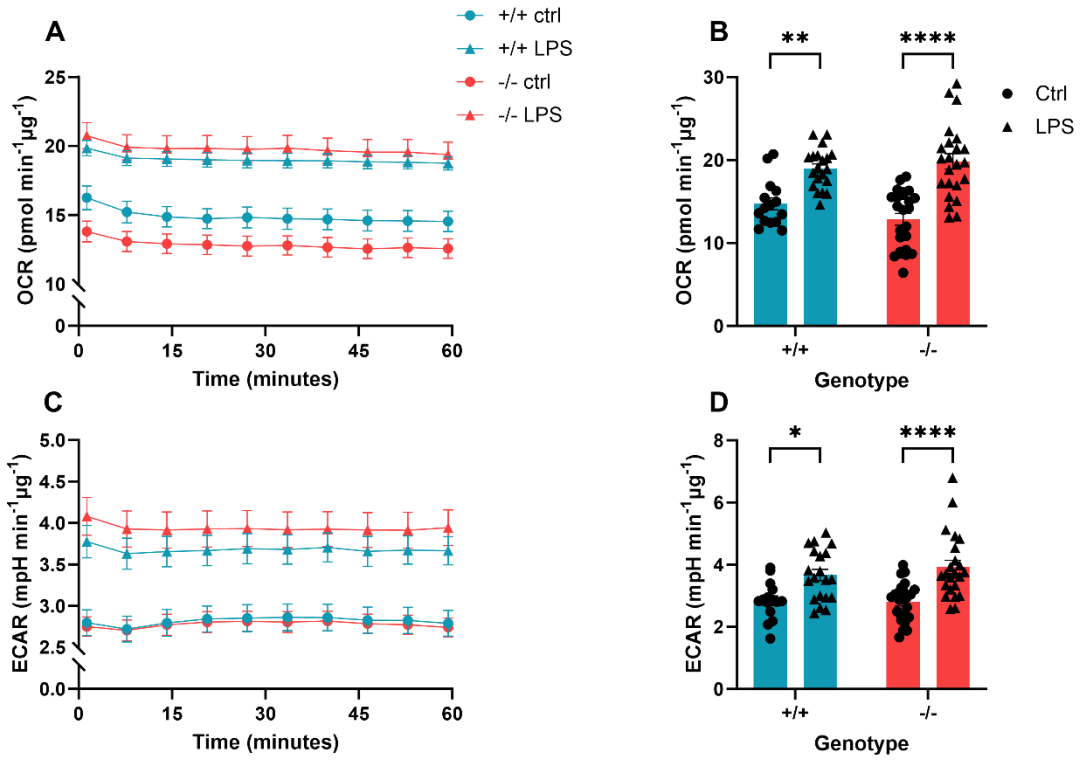

Figure 4.4.16: The metabolic response to 24h LPS stimulation was conserved in TSPO$^{-/-}$ MPAs.

A: XY graph showing the effect of 24h lipopolysaccharide (LPS; 100ng/mL) treatment on TSPO$^{-/-}$ MPA OCR compared to wildtype controls. **B:** TSPO genotype had no significant effect on oxygen consumption rate (OCR) ($p_{genotype}$=0.4897, $F_{(1,78)}$=0.4818). 24h LPS stimulation significantly affected OCR (p_{LPS}<0.0001, $F_{(1,78)}$=52.35), however there was no significant interaction between these variables ($p_{interaction}$=0.0844, $F_{(1,78)}$=3.055). n=15-24 per group, pooled data from across 2 independent experiments. 2-way ANOVA with Tukey's multiple comparisons test. Post-hoc analyses showed that LPS stimulation significantly increased the OCR of TSPO$^{+/+}$ MPAs (p=0.003) and TSPO$^{-/-}$ MPAs (p<0.0001). There was no significant difference in OCR of TSPO$^{-/-}$ MPAs compared to LPS-stimulated wildtype controls (p=0.8658). **C:** XY graph showing the effect of 24h LPS treatment on TSPO$^{-/-}$ MPA extracellular acidification rate (ECAR) compared to wildtype controls. **D:** TSPO genotype had no significant effect on ECAR ($p_{genotype}$=0.5445, $F_{(1,78)}$=0.3704). 24h LPS stimulation significantly affected ECAR (p_{LPS}<0.0001, $F_{(1,78)}$=28.89). No significant interaction was observed ($p_{interaction}$=0.4141, $F_{(1,78)}$=0.6742). n=15-24 per group, pooled data from across 2 independent experiments. 2-way ANOVA with Tukey's multiple comparisons test. Post-hoc analyses showed that 24h LPS stimulation significantly increased the ECAR of TSPO$^{-/-}$ MPAs (p<0.0001) and wildtype controls (p=0.0189). There was no significant difference between LPS-stimulated TSPO$^{-/-}$ MPAs and wildtype controls (p=0.7204).

*p<0.05, **p<0.01, ****p<0.0001. Data are expressed as mean ± standard error of the mean.

Ctrl: vehicle-treated control (0.01% ddH_2O).

4.5: Discussion

Here I have shown that loss of TSPO from astrocytes does not affect basal expression of key metabolic proteins such as GAPDH, GLUT1, HK2, and CPT1a. I reported that changes to the expression of these proteins are either unaltered by exposure to acute (3h) or chronic (24h) inflammatory stimulation (100ng/mL LPS), or in the case of GLUT1 that any alterations in response to inflammatory stimulation are unchanged by $TSPO^{+/+}$ genotype. I have further shown that in my hands chronic inflammatory stimulation does not result in reduced NFκB phosphorylation in $TSPO^{-/-}$ MPAs, despite evidence in the literature indicating that TSPO regulates NFκB expression and activity[512,513]. Despite this, $TSPO^{-/-}$ MPAs exhibited an altered cytokine release profile following LPS stimulation: TNF release was reduced following 3h LPS stimulation whereas it was enhanced at 24h, and 24h LPS-induced IL-10 release was significantly impacted by TSPO genotype. The altered cytokine release profile did not appear to be explained by the altered metabolic phenotype of $TSPO^{-/-}$ MPAs, because the metabolic response to inflammatory stimulation was conserved in these cells and was not significantly different from $TSPO^{+/+}$ controls.

4.5.1: TSPO expression during inflammation correlates with a metabolic shift in astrocytes

In this chapter, I have shown that TSPO expression is upregulated in MPAs stimulated with LPS for 24h (100ng/mL; **Figure 4.4.4, 10**) but not 3h (**Figure 4.4.2, 8**). Interestingly, this correlated with the metabolic profile of the cells in response to LPS stimulation: at 3h, LPS stimulation did not significantly modulate astrocyte metabolism (**Figure 4.4.3**), whereas at 24h LPS treatment significantly increased the OCR and ECAR of MPAs (**Figure 4.4.5**). This indicates that TSPO expression may increase to help meet the metabolic demands imposed by inflammatory responses. I did not anticipate that 24h LPS treatment would increase the ECAR of the cells, as previous evidence from our lab suggests that 24h LPS treatment reduces glycolysis (thus ECAR) in MPAs[167]. However, the methods used differed between the two studies. The evidence I have presented here indicates that following 24h LPS stimulation, MPAs are more dependent on mitochondrial respiration (OCR). While I did not measure lactate secretion from the cells, I would suggest that the enhanced ECAR observed may be due to increased lactate production (caused by enhanced aerobic glycolysis), indicating

that the cells are maximally utilising mitochondrial respiration, although I did not investigate this directly. Alternatively, the enhanced ECAR may stem from FAO, which produces protons and cannot be distinguished from glycolysis via extracellular flux analysis alone. Regardless, the correlation between a metabolic shift and enhanced TSPO expression following 24h LPS stimulation complements findings in a recent study in rat C6 glioma cells (an astrocytoma model, published in August 2023)[456]. This study suggested that TSPO overexpression may mediate LPS-induced astrocyte reactivity[456]. In their study Tournier *et al*. stimulated C6 cells overnight with a 'sublethal' dose of LPS much higher than mine (10μg/mL), and determined that this increased TSPO expression in the C6 cells via a ligand binding saturation curve and *Tspo* mRNA analysis[456]. While they do not state the precise timepoint used, an overnight treatment is likely to be temporally closer to 24h than 3h, and concurs with the data I have presented here in **Figure 4.4.2-5**. Furthermore, this supports the idea that increased TSPO expression correlates with an enhanced metabolic burden on the cells. The authors of the study also showed that increased TSPO expression augmented mitochondrial density and oxidation rate[456]. This is indicative of a potential shift in cellular metabolism and lends further support to the evidence I have presented in **Figures 4.4.2-5**. Moreover, this reinforces the previous study from our lab which demonstrated that chronic inflammatory stimulation of astrocytes promotes mitochondrial respiration[167]. Building on this, Tournier *et al.* demonstrate that overexpression of TSPO via transfection recapitulates the findings from LPS treatment (increased mitochondrial oxidation rate), supporting the notion that enhanced mitochondrial respiration is regulated by TSPO expression, as was hinted at by Tu *et al*. in 2016 using Leydig cells[366].

The work of Tournier *et al*. also examined the upstream regulation of TSPO expression in astrocytes in response to chronic inflammation, demonstrating the involvement of the STAT3 and ERK pathways, in line with other existing bodies of evidence[512,513,532]. This complements the body of work I have presented here, which attempted to unpick how TSPO regulates immunometabolic responses in astrocytes. Both STAT3 and NFκB have been touted as regulators of TSPO expression, and evidence suggests a potentially bidirectional relationship between TSPO and the NFκB signalling pathway[441,512,513,530,532]. This implies that TSPO expression regulates, and is regulated by, the inflammatory state of

astrocytes. However, I observed no difference in NFκB phosphorylation in TSPO$^{-/-}$ MPAs in response to either acute or chronic inflammatory stimulation (**Figure 4.4.8, 10**), suggesting that in my model TSPO is potentially not using this mechanism and mediates effects on NFκB through mechanisms I have not explored here[345,346,512]. However, alongside regulating cellular inflammatory responses, STAT3 and NFκB act as cellular survival signals by promoting growth and regulating cellular metabolism. Therefore, it is possible that these proteins may regulate TSPO to provide metabolic support for inflammatory responses, without TSPO directly participating in the inflammatory response.

Though I did not observe any significant difference in NFκB phosphorylation in TSPO$^{-/-}$ MPAs, I did observe an altered temporal release profile for TNF from these cells (**Figure 4.4.7**). Alongside this, compared to vehicle treated controls, 24h LPS stimulation of TSPO$^{-/-}$ MPAs significantly increased IL-10 secretion from these cells, an effect not observed in the equivalently treated TSPO$^{+/+}$ cells (**Figure 4.4.14**). This suggests that the mechanisms by which TSPO regulates the inflammatory responses of astrocytes may not involve NFκB. It is plausible that as part of the STAT3 signalling pathway, there are downstream targets regulated in part by TSPO that become impaired during TSPO deficiency which I have not accounted for here. Though my work has not examined the effect of pharmacologically inhibiting TSPO on astrocyte inflammatory responses, Tournier *et al*. provide evidence to suggest that pharmacological inhibition of TSPO via FEPPA – a TSPO inhibitor – inhibits the response of astrocytes to inflammation, in-keeping with my findings suggesting inhibited cytokine release from astrocytes in response to inflammatory stimulation (**Figure 4.4.5, 11**). Thus, my findings and the work of Tournier *et al*. support a role for TSPO as a regulator of astrocyte inflammatory responses.

4.5.2: TSPO and astrocyte immunometabolism

Studies in microglia have revealed that TSPO deficiency modulates the metabolic response to inflammation in these cells, though the precise manifestations of this remain unclear[339,340]. Building on work from Milenkovic *et al*., which demonstrated reduced respiration and mitochondrial membrane potential in TSPO$^{-/-}$ microglia[369] (supporting previous work from Tu *et al*. in Leydig cells[366]), independent studies from Yao *et al*.[339] (published in 2020) and Fairley *et al*.[340] (published in 2023) have reinforced the notion that TSPO$^{-/-}$ microglia exhibit altered cellular

immunometabolism. While both studies observed altered mitochondrial respiration in TSPO$^{-/-}$ microglia, Yao *et al*. propose that TSPO deficiency attenuates glycolysis[339], whereas Fairley *et al*. propose that TSPO deficiency promotes glycolysis in microglia[340]. Both studies, however, observed considerable modulation of facets of the microglial inflammatory response. Yao *et al*. reported that TSPO deficiency in these cells downregulates messenger RNA expression of pro-inflammatory cytokines, and reduces phagocytosis by these cells[339]. Moreover, Yao *et al*. found that TSPO deficiency significantly attenuated the glycolytic response of the microglia to LPS stimulation. This was complemented by Fairley *et al*., who found that transcription of genes associated with the inflammatory response and phagocytosis were downregulated in TSPO$^{-/-}$ microglia, which manifested as reduced phagocytic activity[340]. Together these findings support a role for TSPO regulating the immunometabolic responses of microglia. As astrocytes are participatory units of the CNS immune response, TSPO may play a similar role in these cells. However, the mechanisms through which TSPO regulates the immunometabolic responses of astrocytes are likely distinct due to functional, developmental and transcriptomic differences between microglia[206,537] and astrocytes[206,538].

The data I have presented in **Chapter 3** suggests that loss of TSPO increases astrocyte FAO and reduces glycolysis at physiologically relevant brain glucose concentrations. Therefore, I postulated that loss of TSPO may impede the astrocyte response to inflammatory stimulation, perhaps through enhanced reliance on FAO. This was supported by an altered temporal release profile of TNF from TSPO$^{-/-}$ MPAs in response to LPS stimulation (**Figure 4.4.7**), which correlated with the altered metabolic phenotype of these cells (greater reliance on FAO, **Figure 3.4.12**). However, I did not observe a concomitant temporal shift in the metabolic responses of TSPO$^{-/-}$ MPAs in response to LPS stimulation (measured by extracellular flux analyses [**Figure 4.4.15, 16**]). This suggests that TSPO deficiency does not attenuate the metabolic response of these cells to inflammatory stimulation.

In support of my extracellular flux analysis data, I investigated the possibility that expression of proteins linked to metabolism may be differentially modulated by LPS treatment in TSPO$^{-/-}$ MPAs compared to equivalently treated TSPO$^{+/+}$ controls. Existing literature from other cells suggests that TSPO deficiency alters

the expression of genes encoding proteins and enzymes associated with metabolism such as *Hk2, Glut1, Cpt1a,* and others[366,370]. These proteins play key roles in regulating cellular metabolism and/or metabolic pathways, and expression of these proteins is known to be modulated during chronic inflammation[39,167,475,476,526,533]. HK2[39,526,533] and CPT1a[475,476] expression are increased during chronic inflammation, whereas GLUT1[167] expression is reduced. Thus, I wanted to investigate any potential changes to the expression of these proteins following inflammatory stimulation in $TSPO^{-/-}$ cells.

In contrast with existing literature, I found that HK2 expression was not impacted by TSPO genotype (**Figure 4.4.11**) and 24h LPS induced changes in HK2 expression in $TSPO^{-/-}$ MPAs consistent with $TSPO^{+/+}$ controls (**Figure 4.4.11**). HK2 expression in $TSPO^{+/+}$ + 24h LPS cells was considerably closer to statistical significance than in $TSPO^{-/-}$ + 24h LPS (**Figure 4.4.11**). This may hint at a metabolic adaptation to chronic inflammatory stimuli in astrocytes that is attenuated by TSPO deficiency. Alternatively, this may reflect differences in TSPO function between cell types or limitations associated with semiquantitative analysis of immunoblots. However, additional studies and increased experimental replicates would be required to clarify this.

Similarly, GLUT1 levels were unchanged by TSPO genotype in MPAs, but were modulated in response to 24h LPS, indicating a shift away from glycolysis. Due to basal GLUT1 levels being unchanged in $TSPO^{-/-}$ MPAs compared to $TSPO^{+/+}$ cells, the observed reduction in glucose usage in $TSPO^{-/-}$ cells to meet basal bioenergetic demand (**Chapter 3**, **Figure 3.4.12**) may instead be mediated by altered GLUT1 activity or localisation, i.e., increased internalisation leading to reduce glucose uptake. However, I did not directly examine GLUT1 expression using immunocytochemistry, and therefore can only speculate as to the localisation of these transporter proteins.

While CPT1a expression was significantly impacted by TSPO genotype (**Figure 4.4.13**, $p_{genotype}=0.0165$, $F_{(1,20)}=6.848$), I only observed this during experiments involving 24h LPS stimulation. In contrast, during 3h LPS stimulation experiments (**Figure 4.4.9**, $p_{LPS}=0.6950$, $F_{(1,20)} = 0.1582$) I observed no effect of TSPO genotype on CPT1a expression, casting doubt on this finding. While increases in *Cpt1a* mRNA expression have been reported in $TSPO^{-/-}$ Leydig cells and the adrenals of Syrian hamsters (which naturally express little TSPO)[320,366], however,

changes in mRNA level do not always translate to changes in protein expression[539–543] and characterisation of CPT1a protein expression in TSPO$^{-/-}$ astrocytes was to my knowledge previously unreported. It is plausible that my findings may be an artefact of the treatment paradigm used. For example, during 3h LPS treatments, which took place under serum-free conditions, the cells were deprived of lipids from serum for an acute period, and so may not have yet modulated protein expression in response to environmental stimulation. During 24h LPS stimulation, the cells were deprived of lipids from serum for a longer period (26h in total – 2h serum-free acclimatisation and 24h treatment [0% serum]), thus expression of proteins such as CPT1a (not required in an environment with limited lipid supply) may undergo ubiquitination and subsequent proteolytic degradation, though additional studies would be needed to ascertain this. As I have previously shown that TSPO forms a complex with CPT1a (**Chapter 3**), loss of this complex may alter CPT1a activity, resulting in increased basal FAO.

Thus, my data suggest that TSPO may modulate the immunometabolic responses of astrocytes through an alternative mechanism to direct metabolic regulation, possibly via altered mitochondrial fission:fusion dynamics. A recent study in hepatocytes has demonstrated that enhanced FAO is associated with enhanced mitochondrial fusion[544], while a separate study, also in hepatocytes, demonstrated that TSPO deficiency alters mitochondrial morphology and promotes accumulation of FFAs and lipid droplets in these cells[446]. This correlation suggests that TSPO may be involved in regulating mitochondrial dynamics as has been speculated on in the existing literature[407]. While I have not directly examined the fission:fusion state of mitochondria in TSPO$^{-/-}$ MPAs this would be an interesting area for future study. Indeed, TSPO deficiency in GL261 cells has been shown to modulate expression of proteins which regulate mitochondrial fission and fusion[370]. This has led to TSPO being touted as a potential regulator of mitochondrial fission[407], presenting a mechanism by which the effects of TSPO deficiency on mitochondrial fission:fusion states reported in refs.[370,446,544] may manifest. Alongside this, TSPO has been implicated in mitochondria-ER interactions[343], so a similar role in regulating mitochondria-mitochondria interactions such as fission or fusion is not outside the realms of possibility.

Alongside metabolic regulation, TSPO has been touted as a regulator of Ca^{2+} dynamics in tanycytes[358] and microglia[545]. As outlined in **Chapter 1.3.2**, Ca^{2+} signalling is an important mechanism for signal transduction as well as intracellular and intercellular signalling in astrocytes. Mitochondria are a key hub of Ca^{2+} flux[356] in virtually all mammalian cells, alongside other organelles such as the ER[546]. Moreover, Ca^{2+} signalling is an important mediator of structural plasticity in cells, typically underlying many of the cytoskeletal rearrangements required to respond to stimuli[547]. Therefore, it is plausible that altered Ca^{2+} dynamics in $TSPO^{-/-}$ astrocytes may underlie the temporal shift in cytokine release. Though the precise mechanisms of cytokine release have not yet been fully elucidated, it is commonly accepted that this involves some degree of cytoskeletal rearrangement[548,549]. NFκB has been linked to Ca^{2+} signalling[509,550–552]. Although I did not observe any modulation of LPS-induced NFκB phosphorylation in TSPO-deficient MPAs, Ca^{2+}-dependent intracellular NFκB dynamics (such as nuclear translocation) may have been impaired and thus explain the difference in the temporal profile of cytokine release (**Figure 4.4.7**) in the absence of an altered metabolic phenotype (**Figure 4.4.15, 16**). Alternatively, TSPO deficiency may attenuate the Ca^{2+} dynamics linked to cytokine release: suppression of Ca^{2+} signalling has been shown to inhibit release of cytokines including TNF[553,554], thus may present an exciting alternative avenue through which TSPO regulates astrocyte immunometabolism. Indeed, Ca^{2+} signalling is critical for exocytosis of vesicles and their contents, as well as for facilitating morphological changes and signalling pathways critical for inflammatory responses[80,546]. This may be linked to altered mitochondrial dynamics reported in $TSPO^{-/-}$ cells in the existing literature[358,545] and may be particularly pertinent in astrocytes given the importance of Ca^{2+} signalling for astrocyte functionality[63,80,555] (**Chapter 1.3.2**). Moreover, this may represent conservation of astrocyte pan-reactivity in TSPO deficient cells, but reflect an impeded ability to take on more 'niche' intermediate reactive states[104,261]. The potential role of Ca^{2+} signalling in this could be explored via Fura-2 imaging in $TSPO^{-/-}$ MPAs ± 3 or 24h LPS stimulation. Alternatively, TSPO deficiency may have temporally delayed cytokine release from MPAs in response to LPS stimulation by modulating steroid production or responses. Steroids are renowned for their immunomodulatory qualities[556,557] and TSPO has been linked to steroid production, though this evidence base is mixed[327,328,372,558]. Moreover, astrocytes

express glucocorticoid receptors[559], and glucocorticoids have potent anti-inflammatory effects[337]. TSPO deficiency was recently shown to have no statistically significant effect on the majority of an organism-wide 'steroidome' (examining steroid production)[560]; however, this recent (2023) study relied on bulk tissue analysis and did not elucidate cell-specific effects which may have been detected by single-cell techniques. Moreover, this study focussed on steroid *production*, not release or modulation of mechanisms of action. It is conceivable, therefore, that the modulatory effects of TSPO deficiency on the production, release, or action of steroids from astrocytes specifically may contribute to the altered TNF release profile I reported in this chapter.

Thus, together, enzyme activity assays, measures of steroid production/response, characterisation of transporter protein localisation, and characterisation of mitochondrial and Ca^{2+} dynamics in $TSPO^{-/-}$ astrocytes ± LPS present exciting avenues for future studies.

4.5.3: Limitations and future directions

A key limitation of this chapter is that although much of the data presented here indicates that there is a correlation between the metabolic changes associated with TSPO deficiency in astrocytes and the inflammatory responses of these cells, further studies are needed to elucidate any causality in this relationship. While I have investigated the bioenergetic responses of $TSPO^{-/-}$ MPAs to LPS stimulation and reinforced this via immunoblotting, my work did not explore the molecular mechanisms that may regulate the bioenergetic state of $TSPO^{-/-}$ MPAs upstream of the mitochondria. In particular, adenosine monophosphate (AMP) activated protein kinase (AMPK) – a master energy sensor and regulator in mammalian cells – has been linked to regulation of TSPO expression with respect to cellular bioenergetics[358,370,532]. AMPK serves as a sensor for ATP levels: when the ratio of AMP outweighs ATP, the usually-inactive AMPK becomes activated via phosphorylation[9]. Through this, AMPK phosphorylates and inactivates acetyl-coenzyme A carboxylase (ACC)[9]. ACC is typically active in cells, promoting biogenesis of membranes and proteins, and anabolism – synthesis of fatty acids and glycogen stores[9,561]. When inactivated, catabolic processes – autophagy, mitophagy, glycolysis, FAO – are upregulated to restore energy balance in the cells[9,561]. It would be intriguing to explore AMPK and ACC activation states under basal conditions in $TSPO^{-/-}$ MPAs, as well as in response to acute and chronic

inflammatory stimulation. Indeed, I would hypothesise that TSPO$^{-/-}$ MPAs would ordinarily exhibit greater AMPK activation and ACC inactivation, as was reported in tanycytes by Kim *et al.*[358]. Furthermore, TSPO ligands have been linked to modulation of AMPK activity[358,472,477,562], which may represent a feedback mechanism through which AMPK and TSPO reciprocally regulate each other. This has the potential to serve as a fruitful avenue for further investigation in future studies.

I have shown that TSPO deficiency modulates the temporal release profile of TNF, and that TSPO$^{-/-}$ MPAs release significantly more IL-10 in response to 24h LPS stimulation whereas TSPO$^{+/+}$ do not. However, I only examined changes to the secretion profile of one cytokine (TNF) at two timepoints, and of a different cytokine (IL-10) at one timepoint. Moreover, I only examined the consequences of exposure to a single concentration of LPS. A cytokine array panel could be used to more comprehensively identify changes in cytokine secretion caused by TSPO deficiency and could be paired with a wider range of LPS concentrations, inflammatory stimuli, and timepoints to provide a more holistic picture. Additionally, despite my examination of NFκB phosphorylation in TSPO$^{-/-}$ MPAs in response to inflammatory stimulation, my work did not extend to examine changes to the STAT3/ERK axis upstream of TSPO[456,532]. My work focussed on NFκB activity due to an interest in the modulation of inflammatory outputs associated with TSPO deficiency (as TSPO has been reported to regulate NFκB activity in a potentially bidirectional relationship[512,513]) rather than the mechanisms which regulate TSPO; however, due to the fact that both LPS-stimulated TSPO$^{+/+}$ and TSPO$^{-/-}$ MPAs showed similar levels of NFκB phosphorylation, it is possible that STAT3 activity underlies the phenotypes observed. Alternatively, as inflammatory responses are evolutionary well-conserved processes, it is likely that redundant mechanisms exist that bypass TSPO, particularly as absence of TSPO expression does not preclude an inflammatory response. Indeed, it may well be that TSPO helps to determine the overall directionality (e.g., A1/A2 phenotype) of reactive astrocytes, rather than regulating astrocyte pan-reactivity. This may be linked to modulation of calcium signalling that may underlie the cytoskeletal rearrangement that forms a key part of mediating astrocyte reactivity[563]. This could be explored in future by combining TSPO deficiency with pharmacological inhibition of the ERK, STAT3 and NFκB

pathways. The effect on the reactivity of TSPO$^{-/-}$ MPAs to inflammatory potential could be explored, potentially employing proteomic and metabolomic techniques with the aim of unveiling a wealth of information regarding the role of TSPO in regulating astrocyte immunometabolism. This may be exciting when combined with a screen of astrocyte reactivity, beyond and including GFAP expression, *in vivo* – particularly if combined with phenotypic study of TSPO$^{-/-}$ mice ± LPS. For example, germline CPT1a ablation was recently linked to cognitive impairments in a murine model, suggesting that regulation of FAO is critical for neural development[89]. Exploring the effect of potentially upregulated FAO *in vivo* via targeted TSPO deletion may also be beneficial. As FAO is a tightly-regulated process, I would hypothesise that a similar phenotype to the aforementioned study[89] would arise.

4.6: Conclusion

In this chapter, I have shown that TSPO deficiency regulates the ability of astrocytes to respond to an inflammatory stimulus by temporally altering the release profile of TNF and may alter the release profile of IL-10. Importantly, this is not due to a change in the bioenergetic response of TSPO$^{-/-}$ MPAs to 3h or 24h LPS stimulation. This suggests that any immunomodulatory effects of TSPO are not hindered by the altered metabolic phenotype of TSPO$^{-/-}$ MPAs I described in **Chapter 3**. More widely, these data suggest that TSPO may alter the directionality of astrocyte inflammatory responses, potentially by affecting the structural plasticity of astrocytes by modulating Ca^{2+} signalling, though further analysis is needed to determine the mechanism by which this occurs.

Chapter 5: Pharmacological inhibition of TSPO in astrocytes

5.1: Introduction

Due to its associations with various heterogeneous functions, including regulation of cellular energy metabolism[339,340,366,367,369,370], steroidogenesis[311,316,317], haem synthesis[308,428], cholesterol metabolism[311,472] and inflammation[345,367,393,507,562,564], and correlations with a variety of neuroinflammatory[341,342,393,565,566] and psychiatric conditions[319,435,437,438,567,568], TSPO has garnered attention as an attractive therapeutic target for the treatment of a wide range of disorders. For example, therapeutic modulation of TSPO has been explored in clinical trials concerning amyotrophic lateral sclerosis (Phase 2, 3)[406] and diabetic neuropathy[412], and multiple sclerosis[411]. These trials demonstrate that TSPO holds promise as an avenue for therapeutic application beyond acting as a neuroimaging biomarker[319,347,375,391,444,498,500,569], which to date has been the main clinical use of TSPO ligands. Thus, the prospect of pharmacologically targeting TSPO in the CNS for therapeutic purposes is rapidly gaining attention.

Though a strong understanding of the pharmacokinetics of many TSPO ligands have been elucidated[376,413,414,416,445,498,570,571], a limiting feature of the majority of studies focussing on pharmacological modulation of TSPO is that most TSPO ligands have not been validated for off-target effects using a TSPO-deficient model (whether that be a germline knockout, CRISPR-Cas9-mediated knockout, or transient knockdown)[367]. This means that so-called ‘off-target effects’, i.e., results arising from ligands binding to other receptors or proteins than their expected receptor or protein, in this case TSPO, cannot or have not always been fully accounted for. This may explain the variation in findings that have been reported and likely have hindered our understanding of the function of the protein and the use of TSPO as a therapeutic target. Moreover, despite the strong understanding of the binding affinities of a variety of TSPO ligands, there is much disparity in the concentrations of TSPO ligands applied between studies focussing on the same model systems, likely due to a comparatively poorer understanding of the wider pharmacokinetic properties of these compounds. While an experiment using isolated mitochondrial preparations understandably requires a lower concentration of ligands than an intraperitoneal injection of

TSPO ligands into an animal, the concentrations of ligands applied within experimental systems (i.e., comparing experiments using mitochondrial isolations to experiments using mitochondrial isolations) are also inconsistent[367], which confounds interpretation of results and may explain heterogeneity of findings between studies.

Attempts have been made to categorise TSPO ligands by their effects, using pharmacological concepts such as agonist/antagonist nomenclature (**Chapter 1.4.6**)[373,379,436,445]. However, the current lack of consensus regarding the function of TSPO in mammalian cells that may be modulated by these ligands (**Chapter 1.4.6**) means that this terminology may not accurately apply. Recent attempts have been made to classify TSPO ligands as 'activators' or 'inhibitors', however, these are similarly hindered by the issue of TSPO not yet having had a clearly defined downstream mechanism or signalling cascade through which the effects of these ligands can be monitored.

Furthermore, as outlined in **Chapter 1.4.6.1**, attempts to therapeutically target TSPO in humans or human-derived tissues or cells have also been hindered by the presence of a common mutation in the TSPO gene known as the rs6971 polymorphism[416]. This polymorphism has been reported in human and murine models[355,416] and results in the Alanine (Ala) at amino acid 147 of the TSPO sequence being replaced by Threonine (Thr) (Ala147Thr)[416,434]. This affects the structure of a region of TSPO termed the cholesterol recognition/interaction amino acid consensus sequence (CRAC domain) (**Figure 1.4.2.1**). This region is found on the fifth TSPO transmembrane domain and has been suggested as a likely binding site for endogenous and synthetic TSPO ligands and interacting partners[305,416]. The rs6971 polymorphism exhibits a high degree of prevalence: estimates suggest that up to 30% of the general population carry this polymorphism, though this varies depending on ethnicity[416,434]. Moreover, a relationship between rs6971 'status' and incidence of neuropsychiatric conditions such as major depressive disorder[435,436], bipolar disorder[437] and schizophrenia[438,439] has been established, and the rs6971 polymorphism was recently shown to be a predictor of survivability in human males with glioblastoma[440]. Together these studies show that the rs6971 polymorphism may have clinical relevance, though the extent of this remains unclear.

Crucially, the effects of the rs6971 polymorphism on the structure of the TSPO CRAC domain have been linked to altering the binding affinity of TSPO ligands. Binding of first-generation TSPO ligands (i.e., PK-11195 and Ro5-4864) does not appear to be sensitive to the rs6971 polymorphism[305,419,420] (**Chapter 1.4.6**). However, these first-generation ligands typically exhibit several drawbacks including high non-specific binding (due to high lipophilicity) and poor binding affinity (notably Ro5-4864)[305,367,479,562]. This led to the development of second-generation TSPO ligands (such as PBR-28 and DPA-713). These ligands have greater TSPO affinity and reduced non-specific binding compared to first-generation TSPO ligands, but were found to be sensitive to the rs6971 polymorphism[305,419,420]. Recent efforts by synthetic chemists have led to the development of third-generation TSPO ligands such as *N,N*-dialkyl-2-phenylindol-3-ylglyoxylamide (PIGA) ligands[377,392,418], among other ligands such as ER-176[419] and GE-180[419] (derivatives of PK-11195). These ligands exhibit many of the benefits of second-generation TSPO ligands with less sensitivity to the rs6971 polymorphism[305,419–421]. However, the usage of these ligands is typically limited to laboratories with the facilities and knowledge to synthesise them, limiting the widespread application of these ligands at the present time. This means that, despite the limitations of first-generation TSPO ligands, the widespread commercial availability of these compounds means that they continue to be used in preclinical studies to evaluate the efficacy of TSPO as a therapeutic target. It must be emphasised that the rs6971 polymorphism is not the only TSPO polymorphism – a second mutation, rs6972, results in a similar missense mutation downstream of the CRAC motif, resulting in the mutation of arginine (Arg) 162 into histidine (His) (Arg162His). The rs6972 polymorphism affects the C-terminus of TSPO, and being downstream of the CRAC domain (composed of AAs 147-159; **Chapter 1.4.2**) is not thought to affect TSPO ligand binding. Therefore, the understanding of the potential clinical consequences of the rs6972 polymorphism remain poorly understood at present, though a study in 2001 reported that there was no correlation between either rs6971 or rs6972 genotype with bipolar disorder or major depressive disorder in a sample of Japanese participants[572]. Similarly, it is unknown whether the binding affinity of TSPO ligands is consistent across all possible TSPO variants, as several other TSPO SNPs have been reported[330,355]. As rs6971 has been reported to have clinical relevance, and is situated in the CRAC domain of TSPO (purported to be

a crucial site for TSPO ligand binding), this polymorphism has received the most attention and is the focus of this chapter.

Despite these limitations of TSPO ligands, there remains much interest in pharmacological modulation of TSPO in glial cells for the treatment of neuroinflammatory conditions. *S*tudies examining the effects of TSPO ligands in a variety of disease models *in vivo* imply that pharmacological modulation of TSPO via 'activators' or 'inhibitors' has anti-inflammatory effects that may be therapeutically beneficial[312,430,442,507,524,573]. These are supported by similarly promising results from studies in glial cells (particularly microglia) *in vitro*[371,441,506,513,574,575]. Together, these data show that regardless of the activator/inhibitor classification of the TSPO ligands used, pharmacological modulation of TSPO is a promising therapeutic target targeting microglial activation during neuroinflammation. Overall, these studies suggest that pharmacological modulation of TSPO represents a potential therapeutic target for a variety of neuroinflammatory conditions.

However, results pertaining to the effects of TSPO ligands specifically on astrocytes are more limited. In 2007, Veiga *et al*. noted that LPS-induced astrocyte reactivity was not ameliorated by PK-11195 or Ro5-4864 administration, suggesting that astrocytic TSPO may not serve as a valid therapeutic target[312]. In contrast, in 2016, Lee *et al*. demonstrated that TSPO ligands reduced proinflammatory cytokine release from astrocytes *in vitro*[576]. More recently (August 2023) Tournier *et al*. demonstrated that application of the TSPO ligand *N*-(2-(2-fluoroethoxy)benzyl)-*N*-(4-phenoxypyridin-3-yl)acetamide (FEPPA) was sufficient to ameliorate LPS-induced ROS production from C6 glioma cells *in vitro*, suggesting that pharmacological modulation of TSPO may be sufficient to reduce astrocyte reactivity[456]. However, this study observed no change to ATP production, so the effects of pharmacological modulation of TSPO on astrocyte metabolism remain unclear. Importantly, earlier evidence from the same group suggested that changes to expression of TSPO in astrocytes precedes that in microglia during Alzheimer's disease[393], raising the possibility this may also occur in other neurological disorders associated with increased TSPO expression.

While promising, the effects of many of these TSPO ligands remain unvalidated in TSPO-deficient lines, so the specificity of these effects cannot always be fully accounted for. Moreover, a key limitation of much of the existing literature is that

these studies tend to indirectly draw inferences about changes to cellular metabolism induced by pharmacological modulation of TSPO by measuring other processes, such as steroidogenesis or the pro-/anti-inflammatory proclivity of these cells. Studies directly interrogating metabolic parameters (enzyme activity, metabolite production, bioenergetics) can be found within the literature, but the effect of TSPO ligands on these parameters remains unclear.

Therefore, in this chapter, I wanted to investigate the hypothesis that pharmacological inhibition of TSPO in astrocytes would recapitulate the bioenergetic phenotype of $TSPO^{-/-}$ astrocytes. To contextualise the findings, I characterised the rs6971 genotype of my model systems: U373 astrocytoma cells and mouse primary astrocytes (MPAs). I then attempted to elucidate the effects of pharmacological inhibition of TSPO on protein complexes involving TSPO.

5.2: Hypothesis

The overarching hypothesis that I aimed to test in this chapter was that pharmacological inhibition of TSPO using PK-11195 would recapitulate the bioenergetic phenotype of $TSPO^{-/-}$ astrocytes (**Chapter 3**).

I also tested the sub-hypothesis that given the importance of the TSPO CRAC domain in both ligand binding and protein-protein interactions, 1h pre-treatment with TSPO inhibitor PK-11195 would inhibit the TSPO-CPT1a interaction I established in **Chapter 3**.

5.3: Methods

5.3.1: Design of PCR primers specific for the rs6971 locus of the *Tspo* gene in mice and humans

PCR primers for the human and mouse *Tspo* gene were designed *in silico* using a variety of software (**Table 2.1.3**). Ensembl[577] was used to choose reference sequences for the human (h) and mouse (Ms) *Tspo* genes (h: Tspo-203 [ENST00000396265, CCDS33661], Ms: Tspo-201 [ENSMUST00000047419, CCDS27705]). Reference transcripts were chosen because they contained the expected number of transcription products for the *Tspo* gene. The appropriate complementary DNA (cDNA) reference transcript was then imported to Benchling[578]. While genomic DNA reference transcripts may also have been imported, as I was interested in determining the genotype of the TSPO product,

cDNA was chosen. Furthermore, cDNA primer design is more straightforward: because the target DNA has already undergone splicing to remove introns, exon-exon boundaries can be targeted to more easily distinguish cDNA from any contaminating gDNA[579].

Once the cDNA reference sequence had been imported to Benchling, the nucleotides of interest in the transcript were identified using the NCBI reference sequence tool[434]. A surrounding region of interest (ROI), encompassing ~150bp upstream and downstream of the ROI, was selected for primer design. This ROI was imported to Primer3Plus online software[580], to automatically generate proposed primer sequences. Primers were selected based on melting and annealing temperatures (T_m, T_a) and % guanine-cytosine content. Potential primer sequences were imported to Benchling to annotate the ROI and confirm expected product size. Following this, the UCSC *in silico* PCR tool[581] was used to select final primer sequences that were specific to human or mouse *Tspo* and did not produce transcripts from other genes. Primer sequences that bound ≥100bp up/downstream from the ROI were selected. Selected primer sequences were synthesised by Integrated DNA Technologies (UK) and shipped as 25nmol stocks under standard desalting. See **Table 5.3.1.1** for primer sequence details and expected product sizes. Lyophilised primer stocks were briefly (<10 second) centrifuged using a benchtop centrifuge (Sprout Mini Centrifuge, Fisher Scientific UK) before reconstitution in 100µL ddH_2O to yield a 100µM stock solution. Prior to use, stocks were diluted to a working concentration of 10µM in ddH_2O. PCR reactions were prepared using the reagents outlined in **Chapter 2**. RNA was extracted from MPAs using an RNeasy mini kit (Qiagen) and contaminating genomic DNA removed using an RNase-free DNase kit (Qiagen), both according to the manufacturer's recommendations. RNA was extracted from U373 cells using an RNeasy Mini Plus Kit (Qiagen) according to the manufacturer's recommendations. MPA and U373 RNA was eluted in 20µL RNase-free water and quantified using a Nanodrop 2000 spectrophotometer (Fisher). RNA was converted to cDNA using a High-Capacity RNA-to-cDNA kit (Fisher). 1µL cDNA (converted from RNA at 1µg/µL) was loaded per reaction. **Table 5.3.1.2** outlines the PCR reaction settings used to produce these amplicons. Positive control primers targeting human and mouse *Gapdh* and *Gfap* genes were used to confirm successful amplifications. These primer sets (product sizes: 221 base

pairs [bp] [human *Gapdh*], 222bp [human *Gfap*], 302 [mouse *Gapdh*], 303 [mouse *Gfap*]) were designed by Asmaa Al-khalidi during her doctoral studies and were kindly donated for use as positive controls.

Table 5.3.1.1: Primers used to genotype the human and mouse *Tspo* rs6971 locus

Species	Primer Name	Sequence (5'–3')	Product size (bp)
Human	h*Tspo* forward	CCTTGGTGGATCTCCTGCT	241
Human	h*Tspo* reverse	ACAAGCGTGATGGCACCT	
Human	*Gapdh* forward	AGCTGAACGGGAAGCTCAC	221
Human	*Gapdh* reverse	GTCAAAGGTGGAGGAGTGGG	
Human	BstUI *Gapdh* forward	AGTCCATGCCATCACTGCC	201
Human	BstUI *Gapdh* reverse	TCCACCACTGACACGTTGG	
Human	*Gfap* forward	TGATGGAGCTCAATGACCGC	222
Human	*Gfap* reverse	CCTGTGCCAGATTGTCCCTC	
Mouse	Ms*Tspo* forward	GCCGATCTTCTGCTTGTCAG	275
Mouse	Ms*Tspo* reverse	GTAGACCAGCAGGCCCAATG	
Mouse	*Gapdh* forward	CCATGACAACTTTGGCATTG	302
Mouse	*Gapdh* reverse	CCTGCTTCACCACCTTCTTG	
Mouse	*Gfap* forward	TGGAGCTCAATGACCGSTTT	303
Mouse	*Gfap* reverse	CCTGTCTATACGCAGCCAGG	

Table 5.3.1.2: Settings used for human and mouse *Tspo* PCR

Temperature (°C)	Time (seconds)	No. cycles
95	180	1
95	30	35
58	30	
72	60	

72	120	1

5.3.2: Sequencing PCR products

PCR samples were 'cleaned' – i.e., remaining nucleotides and primers hydrolysed – using ExoSAP-IT (catalogue # 78200, Fisher Scientific, UK) according to the manufacturer's instructions. Briefly, 5µL of PCR product was mixed with 2µL ExoSAP-IT and incubated at 37°C for 15 minutes. Samples were then heated to 80°C for 15 minutes to inactivate enzymes. PCR products and 10nM primer stocks were sent to Genewiz for Sanger sequencing. Sequences were analysed using SnapGene Viewer (version 5.2.3).

All other methods used in this chapter are outlined in **Chapter 2**.

5.4: Results

5.4.1: U373 astrocytoma cells have the rs6971 polymorphism

To establish the *Tspo* variant expressed by U373 astrocytoma cells, following PCR, amplicons were loaded onto a 1.5% agarose gel (**Chapter 2**) for gel electrophoresis to confirm expression of *Tspo* cDNA surrounding the rs6971 locus (**Figure 5.4.1 A**). To establish the absence of DNA contaminants in reverse transcription reactions, samples from negative control reactions (PCR reactions containing no cDNA) were loaded onto gels (**Figure 5.4.1 A**, column 7-9). Transcripts for the *Gapdh* and *Gfap* genes were included as positive controls for the PCR reaction, as well as a template-free ddH_2O control as a second negative control for the PCR reaction. Following this, I purified the PCR products (**Chapter 5.3.1 A**) for sequencing, which was carried out by Genewiz. I found that at the ROI, 'ACG' (adenine-cytosine-guanine) was encoded instead of 'GCG' (guanine-cytosine-guanine) (**Figure 5.4.1 B**). This signified that the U373 astrocytoma cell *Tspo* gene encoded Thr at amino acid 147 instead of Ala and were therefore carriers of the rs6971 polymorphism. However, when examining the chromatograph data for these sequences, I observed a small uncalled peak which straddled the border of two of these nucleotides of interest (**Figure 5.4.1 C**, black arrow). My curiosity was piqued because this peak matched the colour denoting a guanine peak, which implied the existence of either a small amount of genetic divergence in the U373 astrocytoma cell sample, or contamination in the products sent for sequencing. To confirm the rs6971 genotype of the U373 astrocytoma cells, I therefore employed a restriction digest approach as a secondary method of verification. This involves inducing cleavage of the DNA amplicon at a region of interest using a bacterially-derived endonuclease. The selected endonuclease – BstUI (Fisher Scientific) – cleaves DNA sequences at guanine-cytosine borders. Hence, digestion of the PCR products with this enzyme would determine if the U373 astrocytoma cells contained a genetically divergent population at the rs6971 locus. Restriction digest of the PCR products revealed that U373 astrocytoma cells did not contain such a population of cells (no cleavage at a guanine-cytosine border occurred) and were therefore carriers of the rs6971 polymorphism (**Figure 5.4.1 D**).

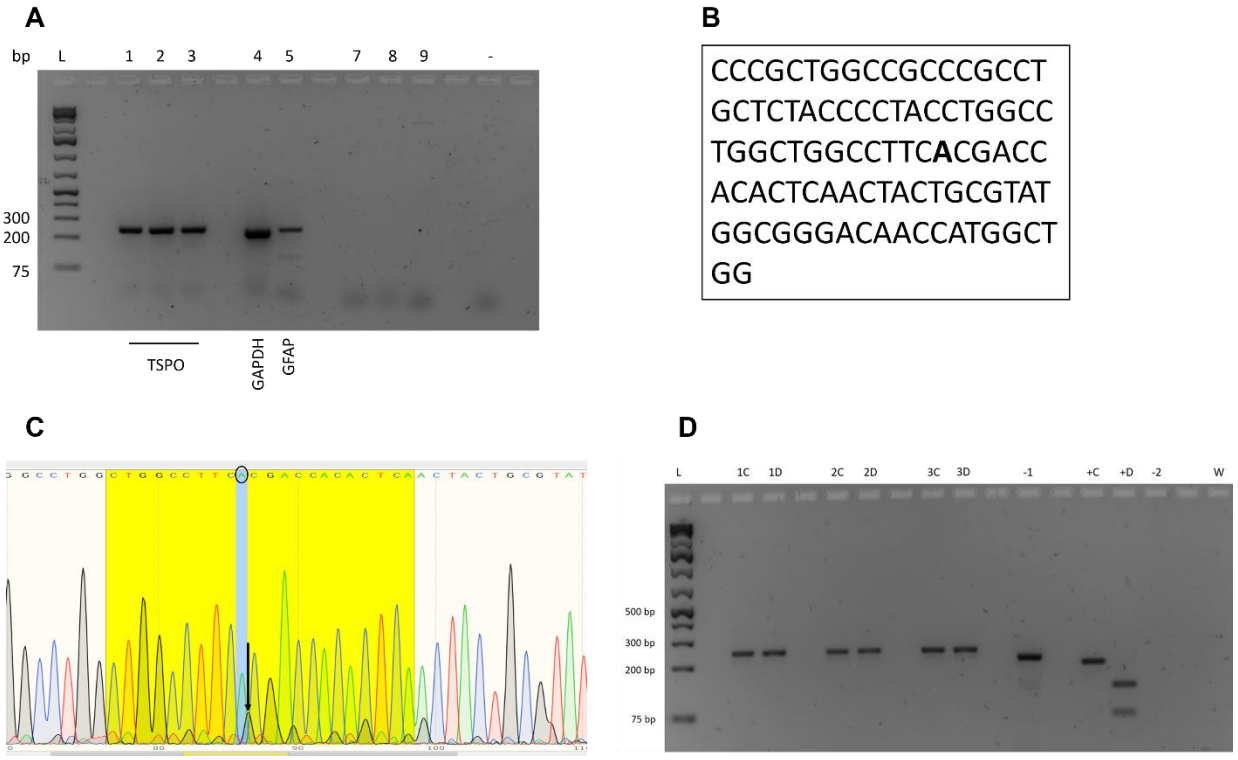

Figure 5.4.1: U373 astrocytoma cells have the rs6971 polymorphism.

A: 1.5% (w/v) agarose gel showing *Tspo* PCR amplicons for cDNA extracted from U373 astrocytoma cells. **B:** example transcript sequence for *Tspo* PCR amplicon from **A**. **C:** chromatograph data for transcript sequence from **B**. Nucleotide of interest is shown in the black circle. Arrow denotes peak of interest. **D:** 2% (w/v) agarose gel showing products of restriction digest ± BstUI restriction endonuclease. Each reaction was run ± endonuclease with a positive control amplicon (i.e., an amplicon containing a region that could be cleaved by the endonuclease) included to confirm enzymatic activity.

n=3 independent RNA extractions from separate flasks of cells.

bp: base pairs. L: ladder. TSPO: translocator protein 18kDa. GAPDH: glyceraldehyde-3-phosphate dehydrogenase. GFAP: glial fibrillary acidic protein. 1-9: PCR reaction replicate numbers. 1-3: *Tspo* amplicons. 4: *Gapdh* amplicon. 5: *Gfap* amplicon. 7-9: reverse transcription controls. -: ddH_2O contamination control. *1*C: [replicate number] control reaction (no enzyme). *1*D: [replicate number] digestion reaction (enzyme present). -1: negative control; GAPDH amplicon from **A** that did not contain a cleavage site for BstUI. +C: GAPDH amplicon that contained a cleavage site for BstUI, reaction took place without addition of BstUI enzyme. +D: GAPDH amplicon that contained a cleavage site for BstUI, rection took place in the presence of the BstUI enzyme. This served as a positive control reaction. -: template-free control. W: ddH_2O control. BstUI: restriction endonuclease. w/v: weight/volume.

Gapdh and *Gfap* primers used in **A**, and **C** (+C) were designed by Asmaa Al-khalidi during her doctoral studies.

5.4.2: C57BL/6J MPA *Tspo* encodes 147Ala

Having established that U373 cells contained the rs6971 polymorphism, I next wanted to ascertain whether the same was true in C57BL/6J mouse primary astrocytes (MPAs). I therefore employed the same methodology that I had used in **Chapter 5.4.1**, and isolated RNA from C57BL/6J MPAs before cDNA conversion and PCR analysis. Firstly, I confirmed that the C57BL/6J MPAs expressed a region of the *Tspo* gene corresponding to the rs6971 locus (**Figure 5.4.2 A**). As before, these PCR products were 'cleaned', and sent for sequencing. I found that the C57BL/6J MPAs expressed 'guanine-cytosine-cytosine' (GCC) at the syntenic locus for rs6971, thus encoded Ala at amino acid 147 (**Figure 5.4.2 B**). Absence of ambiguous peaks in the chromatograph files confirmed the specificity of this result (**Figure 5.4.2 C**).

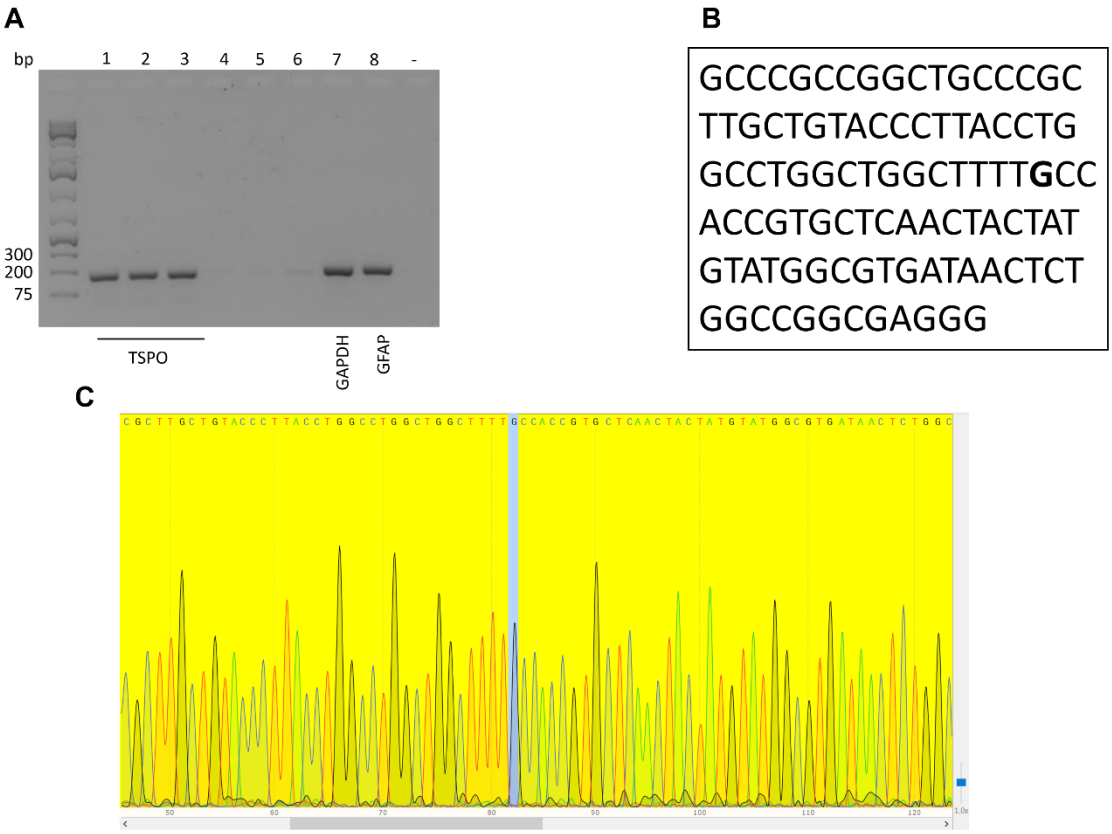

Figure 5.4.2: C57BL/6J MPA *Tspo* encodes 147Ala.

A: 1.5% (w/v) agarose gel showing *Tspo* PCR amplicons for cDNA extracted from C57BL/6J MPAs. **B:** example transcript sequence for PCR amplicon from **A**. **C:** chromatograph data for transcript sequence from **B**. Nucleotide of interest is highlighted in blue.

n=3 independent RNA extractions from separate flasks of cells, over 3 independent collections of MPAs.

bp: base pairs. 1-8: PCR amplicons. 1-3: *Tspo* PCR amplicon. 4-6: negative controls for reverse transcription. 7: *Gapdh* positive control. 8: *Gfap* positive control. -: ddH_2O contamination control. TSPO: translocator protein 18kDa. GAPDH: glyceraldehyde-3-phosphate dehydrogenase. GFAP: glial fibrillary acidic protein. MPA: mouse primary astrocyte. cDNA: complementary deoxyribonucleic acid. PCR: polymerase chain reaction.

Gapdh and *Gfap* primers used in **A** were designed by Asmaa Al-khalidi during her doctoral studies.

5.4.3: TSPO$^{+/+}$ MPA *Tspo* encodes 147Ala

Next, I wanted to confirm the rs6971 genotype of TSPO$^{+/+}$ MPAs. This was because these mice were initially established on a C57BL/6N background, a strain which has a slightly different genetic background from the C57BL/6J mice that these mice were later backcrossed onto.

As before, I confirmed that TSPO$^{+/+}$ MPAs expressed a region of TSPO syntenic to the rs6971 locus via PCR (**Figure 5.4.3 A**). I then sent the PCR amplicons for sequencing and found that the sequence encoded at the region of interest was the same as for C57BL/6J MPAs, being guanine-cytosine-cytosine and thus encoding Ala at the *Tspo*147 locus (**Figure 5.4.3 B**). Examination of the chromatograph data showed clear peaks, with no ambiguous peaks, confirming the validity of this result (**Figure 5.4.3 C**).

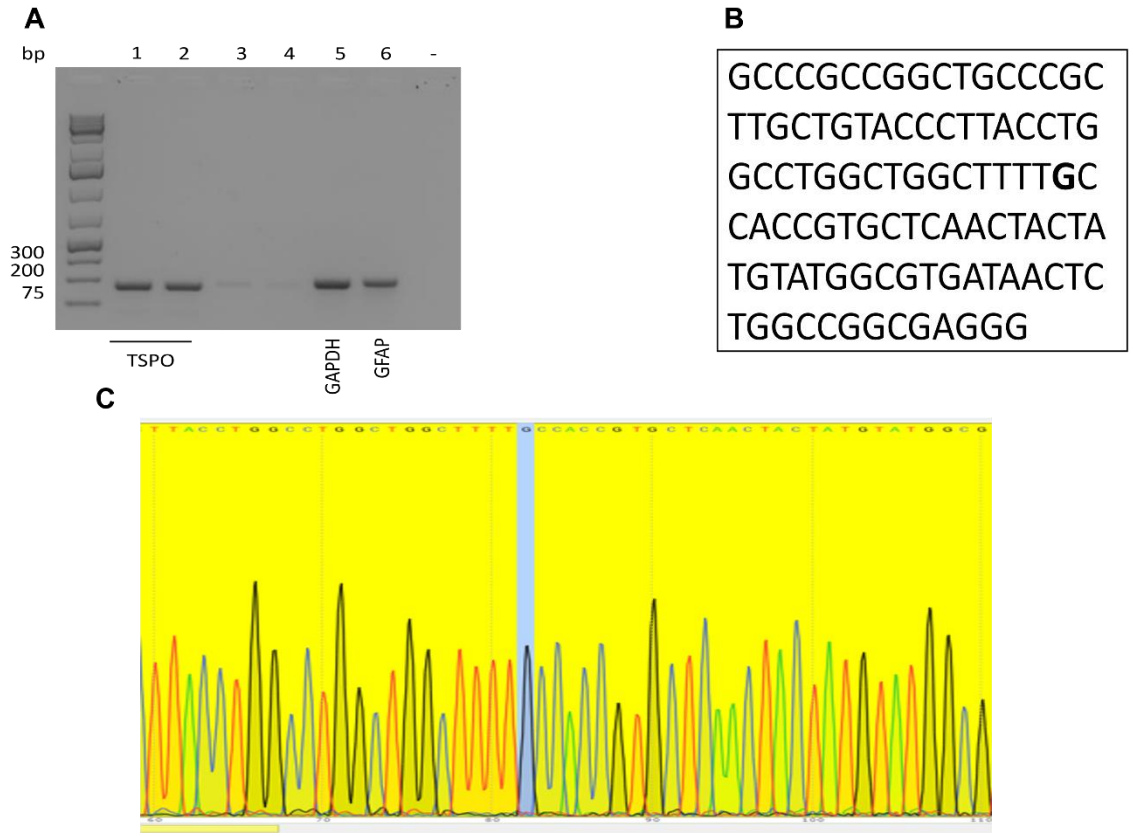

Figure 5.4.3: TSPO$^{+/+}$ MPA *Tspo* encodes 147Ala.

A: 1.5% (w/v) agarose gel showing PCR amplicons for cDNA extracted from C57BL/6N TSPO$^{+/+}$ MPAs. **B:** example transcript sequence for PCR amplicon from **A**. **C:** chromatograph data for transcript sequence from **B**. Nucleotide of interest is highlighted in blue.

bp: base pairs. 1-6: PCR amplicons. 1,2: *Tspo* amplicons. 3,4: negative controls for reverse transcription. 5: *Gapdh* positive control. 6: *Gfap* positive control. -: ddH_2O contamination control. TSPO: translocator protein 18kDa. GAPDH: glyceraldehyde-3-phosphate dehydrogenase. GFAP: glial fibrillary acidic protein. MPA: mouse primary astrocyte. cDNA: complementary deoxyribonucleic acid. PCR: polymerase chain reaction. w/v: weight/volume.

n=2 independent RNA extractions from separate flasks of cells, over 2 independent collections of MPAs.

Gapdh and *Gfap* primers used in **A** were designed by Asmaa Al-khalidi during her doctoral studies.

5.4.4: PK-11195 pre-treatment did not inhibit TSPO$^{+/+}$ MPA bioenergetics

A previous doctoral student in the Ellacott laboratory generated preliminary data indicating that pharmacological inhibition of TSPO in C57BL/6J MPAs by applying 25nM PK-11195 (0.1% DMSO vehicle, 1h pre-treatment) significantly increased the basal ECAR and OCR of these cells without altering uptake of tetramethylrhodamine ester, a dye which indicates the mitochondrial membrane potential of the cells, or affecting glucose uptake[452]. The student also found that, in TSPO$^{+/+}$ U373 astrocytoma cells, the same concentration of PK-11195 applied for 1h significantly increased ECAR. Crucially, no effect was observed in TSPO$^{-/-}$ U373s[452].

I first sought to investigate whether I could recapitulate these data, and extend this to assess the metabolic effects of pharmacological TSPO inhibition in MPAs. I repeated their experimental paradigm with TSPO$^{+/+}$ and TSPO$^{-/-}$ MPAs using the same concentration range of PK-11195: 0, 5, 10, 25nM PK-11195, 0.1% DMSO vehicle, applied for 1h. The effect of genotype on OCR previously observed (**Chapter 3.4.1**) was conserved (**Figure 5.4.4 A**; $p_{genotype}<0.0001$, $F_{(1,198)}=31.5$). In contrast to my expectations, I observed no overall effect of PK-11195 on the OCR of MPAs of either TSPO genotype (**Figure 5.4.4 A**; ($p_{drug}=0.3878$, $F_{(5,198)}=1.053$) nor evidence of an interaction between genotype and PK-11195 concentration (**Figure 5.4.4 A**; $p_{interaction}=0.3069$, $F_{(5,198)}=1.208$). However, post-hoc analyses revealed that the OCR of TSPO$^{-/-}$ MPAs treated with 5 and 10nM PK-11195 were significantly increased compared to equivalently treated TSPO$^{+/+}$ controls.

Similarly, the previously observed (**Chapter 3.4.1**) effect of genotype on ECAR was conserved ($p_{genotype}=0.0006$, $F_{(1,207)}=12.11$), and PK-11195 concentration had a significant effect on ECAR ($p_{drug}=0.0397$, $F_{(5,207)}=2.382$). I found no evidence of an interaction between genotype and PK-11195 concentration ($p_{interaction}=0.1265$, $F_{(5,207)}=1.742$). Post-hoc analyses did not reveal any additional statistically significant effects.

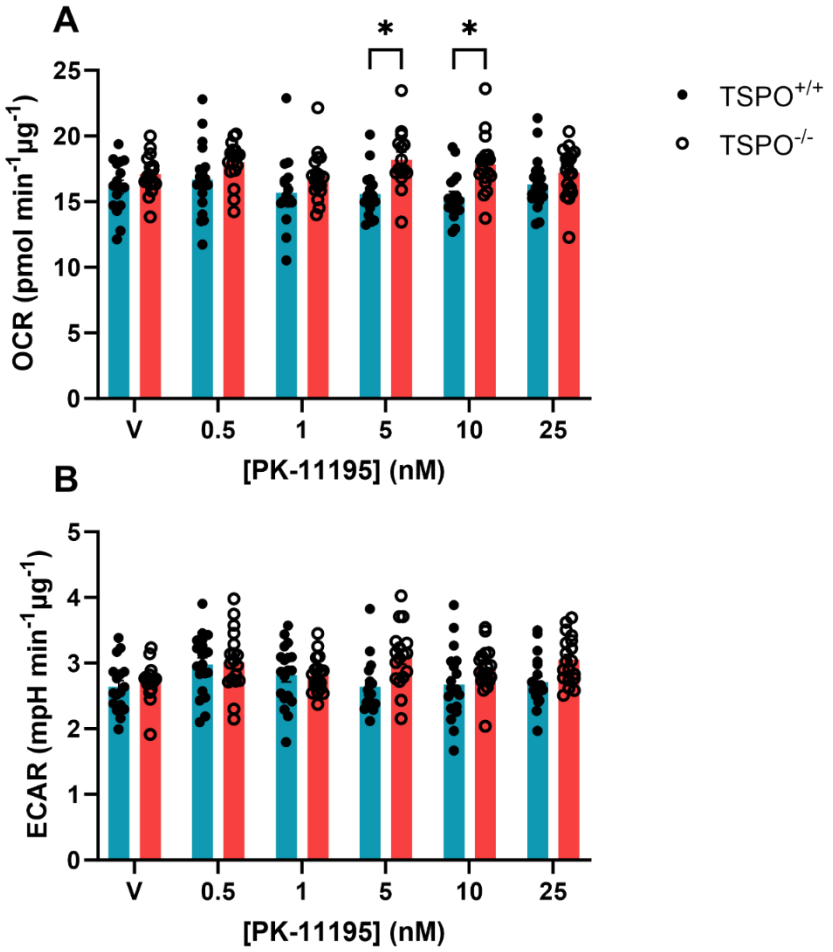

Figure 5.4.4: PK-11195 pre-treatment did not inhibit TSPO$^{+/+}$ MPA bioenergetics.

A: OCR of TSPO$^{-/-}$ MPAs and wildtype controls following 1h pre-treatment with PK-11195 (0.1% DMSO vehicle) at a range of concentrations from 0.5-25nM. There was an effect of genotype on OCR ($p_{genotype}$<0.0001, $F_{(1,198)}$=31.5, though no effect of PK-11195 on this output (p_{drug}=0.3878, $F_{(5,198)}$=1.053), nor evidence of an interaction between genotype and PK-11195 concentration ($p_{interaction}$=0.3069, $F_{(5,198)}$=1.208). n=16-18 wells per concentration, data were pooled from across 3 independent experiments. 2-way ANOVA with Šídák's multiple comparisons test. Post-hoc analyses showed that PK-11195 did not significantly affect TSPO$^{+/+}$ or TSPO$^{-/-}$ MPA bioenergetics (p>0.05), except following 5 and 10nM treatments (p<0.05). **B:** ECAR of TSPO$^{-/-}$ MPAs and wildtype controls following 1h pre-treatment with PK-11195 at a range of concentrations from 0.5-25nM. There was an effect of genotype on ECAR ($p_{genotype}$=0.0006, $F_{(1,207)}$=12.11), and PK-11195 treatment also had a significant effect on ECAR (p_{drug}=0.0397, $F_{(5,207)}$=2.382). There was no evidence of an interaction between genotype and PK-11195 concentration ($p_{interaction}$=0.1265, $F_{(5,207)}$=1.742). n=16-18 wells per concentration, data are pooled from across 3 independent experiments. 2-way ANOVA with Šídák's multiple comparisons test. Post-hoc analyses showed that ECAR of TSPO$^{-/-}$ was not significantly different to wildtype controls regardless of concentration (p>0.05).

*p<0.05. Data are displayed as mean ± standard error of the mean.

OCR: oxygen consumption rate. ECAR: extracellular acidification rate.

V = vehicle (0.1% dimethyl sulfoxide [DMSO]). TSPO: translocator protein 18kDa. MPA: mouse primary astrocytes.

5.4.5: PK-11195 pre-treatment did not inhibit TSPO$^{+/+}$ U373 bioenergetics

Finding that PK-11195 pre-treatment did not significantly reduce the metabolic rates of TSPO$^{+/+}$ MPAs, I next repeated this experiment in using TSPO$^{-/-}$ U373 astrocytoma cells and empty vector-transfected TSPO$^{+/+}$ controls using a wider range of PK-11195 concentrations.

Unexpectedly, the previously observed effect of genotype on OCR (**Figure 3.4.10**) was not conserved ($p_{genotype}$=0.4776, $F_{(1,176)}$=0.5065), however PK-11195 concentration significantly affected OCR (p_{drug}=0.0064, $F_{(6,176)}$=3.109). No interaction was observed between these variables ($p_{interaction}$=0.1216, $F_{(6,176)}$=1.708). Post-hoc testing indicated that there was no significant difference in OCR at any of the concentrations of PK-11195 used (**Figure 5.4.5 A**, p>0.05), though 1pM PK-11195 trended towards a significant increase in TSPO$^{+/+}$ U373 OCR (p=0.0629).

Similarly, there was no effect of genotype on ECAR (**Figure 5.4.5 B**, $p_{genotype}$=0.9379, $F_{(1,174)}$=0.006088). In contrast to OCR, PK-11195 concentration did not affect ECAR (p_{drug}=0.0522, $F_{(6,174)}$=2.130), though this was just above the threshold for significance. No interaction was observed ($p_{interaction}$=0.1560, $F_{(6,174)}$=1.578).

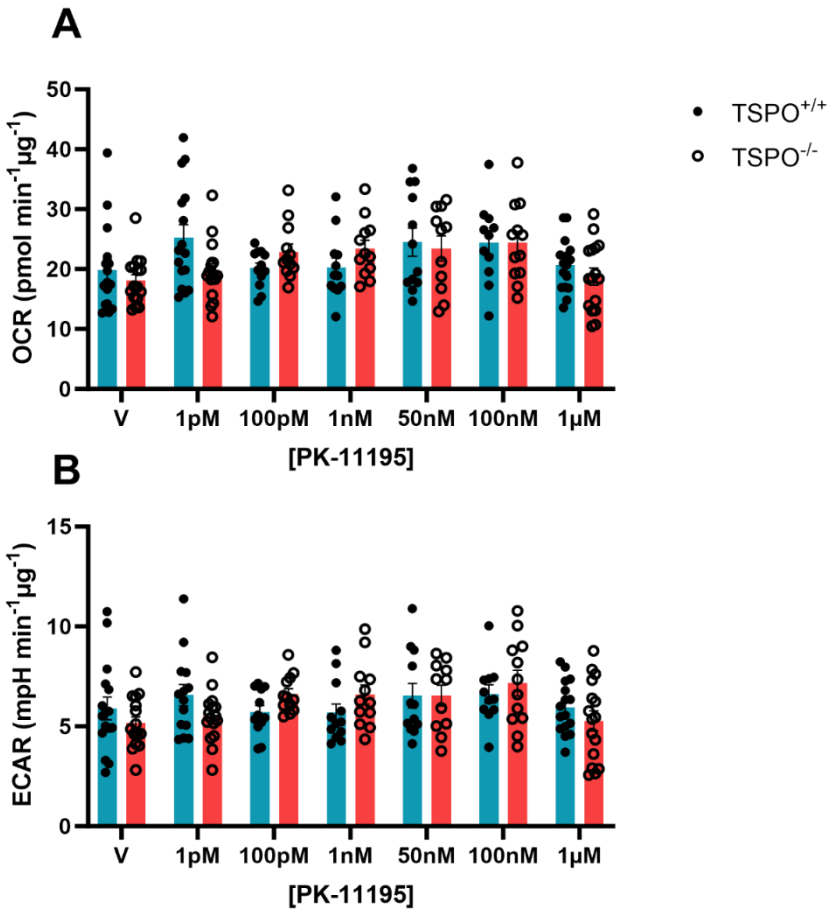

Figure 5.4.5: PK-11195 pre-treatment did not inhibit TSPO$^{+/+}$ U373 bioenergetics.

A: OCR of TSPO$^{-/-}$ U373 astrocytoma cells and wildtype controls following 1h pre-treatment with PK-11195 (0.1% DMSO vehicle). 2-way ANOVA with Šídák's multiple comparisons test. There was no effect of genotype on OCR ($p_{genotype}$=0.4776, $F_{(1,176)}$=0.5065), however PK-11195 concentration significantly affected OCR (p_{drug}=0.0064, $F_{(6,176)}$=3.109). No interaction was observed between these variables ($p_{interaction}$=0.1216, $F_{(6,176)}$=1.708). n=14-16 wells per concentration. Data are pooled from across 3 independent experiments. Post-hoc analysis revealed that there was no significant difference in OCR at any of the concentrations used compared to vehicle-treated controls (p>0.05). **B:** ECAR of TSPO$^{-/-}$ U373 astrocytoma cells and wildtype controls following 1h pre-treatment with PK-11195. 2-way ANOVA with Šídák's multiple comparisons test. There was no effect of genotype on ECAR ($p_{genotype}$=0.9379, $F_{(1,174)}$=0.006088). PK-11195 concentration did not significantly affect ECAR (p_{drug}=0.0522, $F_{(6,174)}$=2.130). No interaction was observed ($p_{interaction}$=0.1560, $F_{(6,174)}$=1.578). n=14-16 wells per concentration. Data were pooled from across 3 independent experiments. Post-hoc analysis revealed that there was no significant difference in ECAR at any of the concentrations used compared to vehicle-treated controls (p>0.05).

Data are displayed as mean ± standard error of the mean.

OCR: oxygen consumption rate. ECAR: extracellular acidification rate.

V = vehicle (0.1% dimethyl sulfoxide [DMSO]).

5.4.6: Transfection of U373 astrocytoma cells with a tagged TSPO construct did not modulate expression of key proteins and enzymes

Having established that, in my hands, PK-11195 treatment had no significant effect on astrocyte bioenergetics, I wanted to investigate the effect of treatment with this drug on the TSPO-CPT1a complex I reported in **Chapter 3**. Modulation of other cellular functions, such as steroidogenesis, have been reported following treatment of whole cells with 100nM PK-11195. Therefore, despite observing no effect on the basal bioenergetics of U373 astrocytoma cells treated with this PK-11195 concentration (**Figure 5.4.5**), I treated U373 astrocytoma cells with this concentration. As I had not observed an effect of PK-11195 concentration on astrocyte bioenergetics, I included 2-deoxyglucose (2DG) treatments as a positive control for metabolic manipulation.

I used the TSPO-Myc transfection paradigm I employed in **Chapter 3** to examine the TSPO-CPT1a interaction. Cells were treated for 1h either with vehicle, 10mM 2DG, or 100nM PK-11195. To ensure that any effect I may have observed on the TSPO-CPT1a interaction was due to a change in the interaction and not due to altered protein expression. I first determined whether the plasmid type (TSPO-Myc or EV) was affecting GAPDH function via a 2-way ANOVA. There was no effect of plasmid ($p_{plasmid}$=0.8969, $F_{(1,28)}$=0.01909) or drug treatment (p_{drug}=0.6915, $F_{(2,28)}$=0.3737) on GAPDH expression nor was there an interaction between these variables ($p_{interaction}$=0.9368, $F_{(2,28)}$=0.06225). Using pairwise comparisons, I determined that 2DG and PK-11195 treatment did not significantly reduce GAPDH expression in TSPO-Myc or EV-transfected cells (**Figure 5.4.6 B**, p>0.05) relative to vehicle-treated controls. This finding supported the use of GAPDH expression as a loading control for the immunoblots.

I next determined the effect of 2DG and PK-11195 treatment on endogenous TSPO expression. There was no effect of plasmid type ($p_{plasmid}$=0.5558, $F_{(2,27)}$=0.7177) or drug treatment (p_{drug}=0.7054, $F_{(2,27)}$=0.3536) nor was there an interaction between these variables ($p_{interaction}$=0.5558, $F_{(2,27)}$=0.6004). Post-hoc analysis revealed that compared to vehicle-treated cells, endogenous TSPO-expression was unaffected by either treatment (**Figure 5.4.6 C**, p>0.05). Similarly, CPT1a expression was unchanged by plasmid type ($p_{plasmid}$=0.5492, $F_{(1,29)}$=0.3673) or drug treatment (p_{drug}=0.9295, $F_{(2,27)}$=0.07329), and there was

no interaction between these variables ($p_{interaction}$=0.9191, $F_{(2,29)}$=0.08466). Post-hoc analysis revealed that compared to vehicle-treated controls, CPT1a expression was unaffected by either 2DG or PK-11195 treatment (**Figure 5.4.6 D**, p>0.05). Myc [TSPO-Myc] expression was unaffected by 2DG (**Figure 5.4.6 E**, p=0.9946) or PK-11195 treatment (p=0.9335).

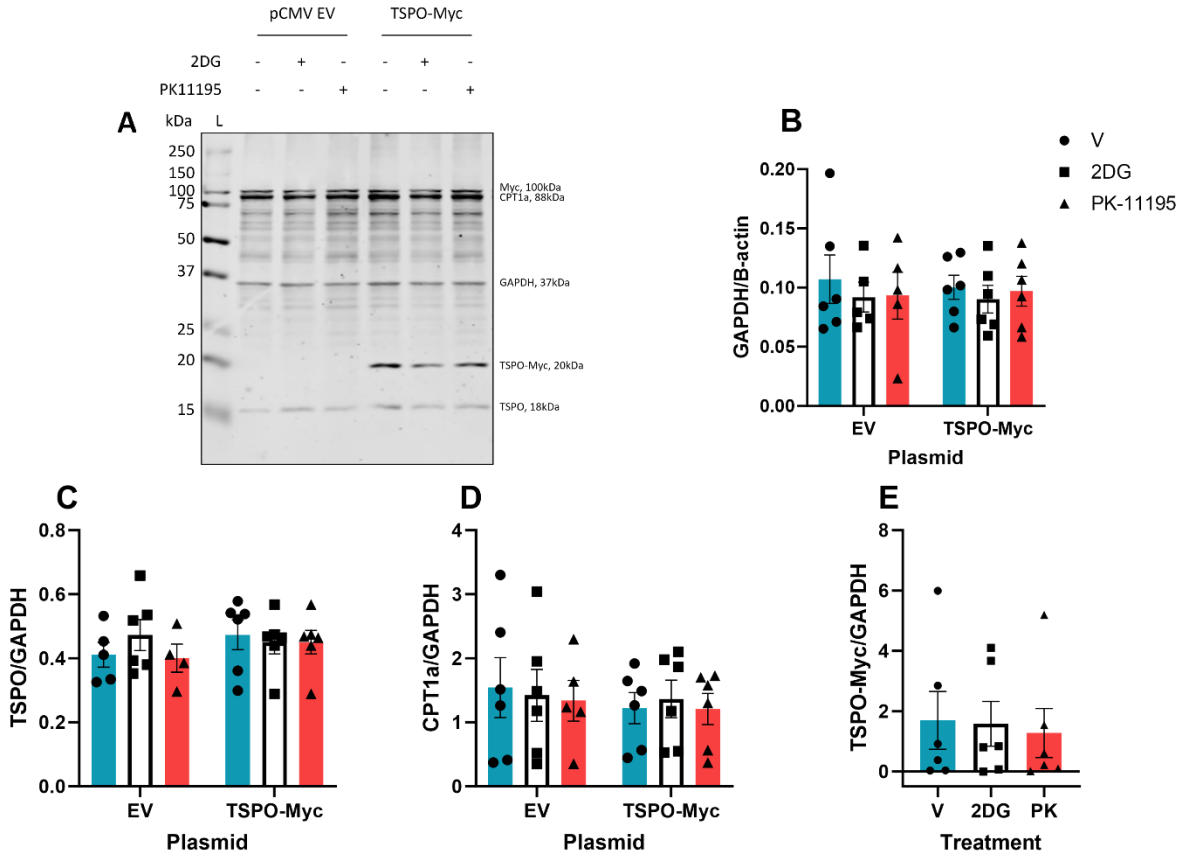

Figure 5.4.6: Transfection of U373 astrocytoma cells with a Myc-tagged TSPO construct did not modulate expression of key proteins and enzymes.

A: Representative immunoblot showing expression of Myc, CPT1a, GAPDH, TSPO, and Myc [TSPO-Myc] ± 1h 2-deoxyglucose (2DG; 10mM, 2% ddH_2O)) or PK-11195 (100nM, 0.1% DMSO) treatment. **B:** quantification of **A** showing no change in GAPDH expression ($p>0.05$). n=6 replicates from 3 independent experiments, 2-way ANOVA with Šídák's multiple comparisons test. There was no effect of plasmid ($p_{plasmid}=0.8969$, $F_{(1,28)}=0.01909$) or treatment ($p_{drug}=0.6915$, $F_{(2,28)}=0.3737$) on GAPDH expression nor was there an interaction between these variables ($p_{interaction}=0.9368$, $F_{(2,28)}=0.06225$). **C:** quantification of **A** showing no change in endogenous TSPO expression ($p>0.05$). n=6 replicates from 3 independent experiments, 2-way ANOVA with Šídák's multiple comparisons test. TSPO expression was unchanged by plasmid type ($p_{plasmid}=0.5558$, $F_{(2,27)}=0.7177$) or treatment ($p_{drug}=0.7054$, $F_{(2,27)}=0.3536$) nor was there an interaction between these variables ($p_{interaction}=0.5558$, $F_{(2,27)}=0.6004$). **D:** quantification of **A** showing no change in CPT1a expression. n=6 replicates from 3 independent experiments, 2-way ANOVA with Šídák's multiple comparisons test. CPT1a expression was unchanged by plasmid type ($p_{plasmid}=0.5492$, $F_{(1,29)}=0.3673$) or drug treatment ($p_{drug}=0.9295$, $F_{(2,27)}=0.07329$), and there was no interaction between these variables ($p_{interaction}=0.9191$, $F_{(2,29)}=0.08466$). **E:** quantification of **A** showing no change in TSPO-Myc expression ($p=0.9946$ (2DG), $p=0.9335$ (PK-11195). n=6 replicates from 3 independent experiments, one-way ANOVA.

L: ladder: kDa: kildodaltons. TSPO: translocator protein 18kDa. CPT1a: carnitine palmitoyltransferase 1a. GAPDH: glyceraldehyde-3-phosphate dehydrogenase. TSPO-Myc: Myc-tagged TSPO construct. EV: empty vector. V = vehicle (0.1% dimethyl sulfoxide [DMSO], 2% ddH_2O).

5.4.7: Pharmacological inhibition of cellular metabolism and TSPO activity in U373 astrocytoma cells may alter TSPO protein complex stoichiometry

Having established that neither 1h 2DG nor PK-11195 treatment significantly modulated expression of TSPO-Myc or CPT1a, this gave me confidence that any change I may see in subsequent co-immunoprecipitations (co-IPs) would be due to changes in the formation of the TSPO-CPT1a complex, so I proceeded to repeat the co-IP paradigm I established in **Chapter 3**. Firstly, I confirmed that I could again demonstrate the TSPO-CPT1a interaction (**Figure 5.4.7**). I found that 2DG treatment modulated the amount of TSPO-Myc pulled down, with no apparent difference being made to the level of CPT1a in the complex. Treatment with PK-11195, reduced the amount of TSPO and CPT1a that co-immunoprecipitated. It must be noted however that unfortunately formal semi-quantification of this result was not possible, so this remains preliminary and subjective.

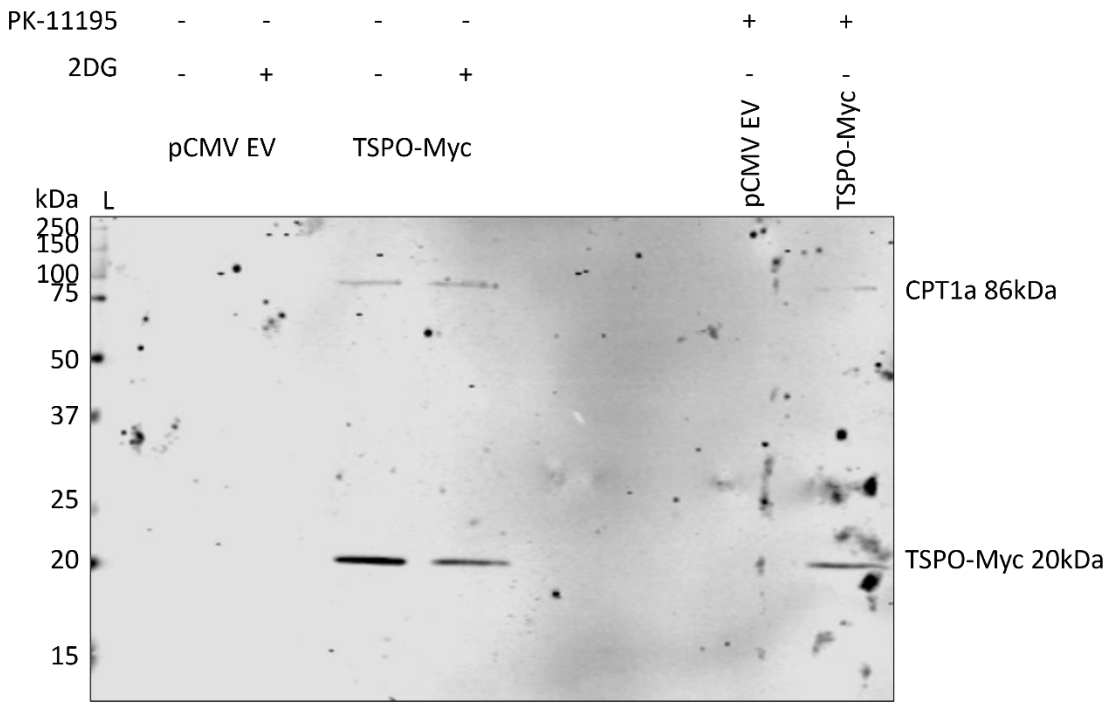

Figure 5.4.7: Pharmacological inhibition of cellular metabolism and TSPO activity in U373 astrocytoma cells may alter TSPO protein complex stoichiometry.

Immunoblot of co-immunoprecipitation (co-IP) products, showing co-IP of TSPO-Myc and CPT1a. While this interaction was conserved throughout treatment protocols, I observed a reduction in the intensity of the TSPO-Myc band following 2-deoxyglucose (2DG; 10mM [ddH_2O]) treatment (fifth column from the left), and a reduction in the intensity of both the CPT1a and TSPO-Myc bands following PK-11195 treatment (0.1% DMSO) (rightmost column). Co-IP specificity was confirmed using an empty vector plasmid.

Representative immunoblot of treatments. n=3 independent immunoprecipitations.

L: ladder: kDa: kildodaltons. CPT1a: carnitine palmitoyltransferase 1a. TSPO-Myc: Myc-tagged TSPO construct. EV: empty vector. V: vehicle (0.1% dimethyl sulfoxide [DMSO], 2% ddH_2O).

5.5: Discussion

In this chapter, I have characterised the rs6971 genotype of U373 astrocytoma cells which were found to carry the SNP (Thr147). In contrast, I found that C57BL/6J MPAs and TSPO$^{+/+}$ MPAs encoded Ala147 at the syntenic locus, thus do not carry the polymorphism. I found that 1h PK-11195 pre-treatment did not significantly reduce TSPO$^{+/+}$ astrocyte bioenergetics in MPAs or U373s. However, in MPAs, there was a significant difference in the OCR of TSPO$^{-/-}$ and TSPO$^{+/+}$ cells following 5 and 10nM PK-11195 pre-treatment, though this was not significantly different from vehicle-treated controls, so should be interpreted with caution. Transfecting GM-naïve U373 cells with a tagged TSPO plasmid did not affect expression of GAPDH or CPT1a, nor did 1h PK-11195 (100nM) pre-treatment affect expression of these proteins or TSPO (Myc-tagged or endogenous). I found that 1h pre-treatment with 2DG (10mM) or PK-11195 (100nM) modulated the results of the TSPO-CPT1a co-immunoprecipitation I reported in **Chapter 3**.

5.5.1: Pharmacological modulation of TSPO and astrocyte bioenergetics

Various studies in the existing literature[339,340,358,366–368,428,472], and work I have presented in **Chapters 3 and 4**, demonstrate that TSPO plays a role in regulating cellular metabolism and bioenergetics. However, these bodies of work have relied upon genetic modulation of TSPO expression[339,340,366,369] to determine the resulting effects on cellular metabolism. Many studies, including my own work, have relied upon organisms with germline TSPO deficiency[324,339,340,366], which may result in adaptions/compensation within cells. Other studies have employed transient knockdown of TSPO, facilitated by small interfering RNAs[358,530]. Pharmacological modulation (activation or inhibition) of TSPO, which better addresses therapeutic potential of targeting this protein, may lead to fundamentally different outcomes compared to the genetic models, though the magnitude of these differences remains unclear. Crucially, to date many studies using TSPO ligands have failed to account for off-target effects by comparing their results to a TSPO-deficient model to ensure that the compounds at the concentrations used do not affect the measured output in the TSPO-deficient models[367].

Using TSPO$^{-/-}$ MPAs and TSPO$^{+/+}$ controls, I showed that 1h PK-11195 pre-treatment did not significantly affect the basal OCR (**Figure 5.4.4 A**) or ECAR (**Figure 5.4.4 B**) (proxies of respiration and glycolysis respectively) compared to vehicle-treated controls. Though pairwise comparisons revealed no significant difference between the bioenergetic rates of vehicle-treated TSPO$^{-/-}$ and TSPO$^{+/+}$ MPAs, the previous effect of genotype on these parameters I observed in **Chapter 3** was conserved, supporting the validity of these findings. This is in contrast to evidence generated by a previous student in the Ellacott group, who found that 1h 25nM PK-11195 pre-treatment was sufficient to increase the OCR and ECAR of C57BL/6J MPAs[452]. I observed no significant effect of PK-11195 pre-treatment on TSPO$^{+/+}$ MPA bioenergetics compared to vehicle-treated cells at any concentration (**Figure 5.4.4 A, B**). Similarly, I observed no effect of PK-11195 pre-treatment on the basal bioenergetics of TSPO$^{-/-}$ cells, which served as a negative control in this assay. These results contrast with existing literature: in 2020, Fu *et al*. showed that PK-11195 pre-treatment reduced the basal mitochondrial respiration of GL261 glioma cells (measured using the mitochondrial stress test) and increased glycolysis (measured via the glycolysis stress test)[370]. However, this study did not control for off-target effects of PK-11195 using TSPO$^{-/-}$ controls nor state the concentration of PK-11195 used during this study, so additional controls are needed to increase certainty that these results are directly caused by pharmacological modulation of TSPO.

In support of my data generated in MPAs, I repeated the PK-11195 treatment paradigm in U373 astrocytoma cells and used a wider range of PK-11195 concentrations from 1pM to 1μM (**Figure 5.4.5**). This was an attempt to generate a sigmoidal concentration-response curve, from which I could then derive pharmacokinetic values (such as the inhibitory constant, IC_{50}) for whole-cell metabolic experiments. However, congruent with my work in MPAs, I observed no significant effect of PK-11195 on U373 astrocytoma cell bioenergetics compared to DMSO vehicle control (**Figure 5.4.5 A, B**). As such, unfortunately pharmacokinetic parameters could not be derived from these data. I found it curious that I observed no effect of TSPO genotype on the basal bioenergetics of U373 astrocytoma cells, which I would hesitantly attribute to the DMSO vehicle. As with the TSPO$^{-/-}$ MPAs, I did not include a vehicle-free control group and thus do not have any experimental evidence for any effect of DMSO on cellular

bioenergetics. As the difference in bioenergetics in the TSPO$^{+/+}$ and $^{-/-}$ MPAs was conserved even in the presence of the DMSO control, this is unlikely but still possible. Together, my bioenergetics data suggest that PK-11195 pre-treatment at the concentrations tested has no effect on astrocyte bioenergetics, but the loss of the genotype effect in the U373 cells does potentially call into question the reliability of these data.

PK-11195 has been shown to reduce cell migration, an energy-intensive process. In a study using Jurkat cells, which naturally express little-to-no TSPO, Liu *et al*. demonstrated using a chemotaxis assay that PK-11195 (100nM) reduced motility of cells transfected with a TSPO-containing plasmid[368]. These effects were significantly diminished in cells transfected with a control plasmid, as well as wildtype cells, suggesting that PK-11195 exerts TSPO-specific effects on cellular functions[368]. This may be linked to altered bioenergetics in PK-11195-treated cells, as explored by Fu *et al*. in 2020[370]. This study showed that PK-11195 pre-treatment promoted glycolysis and reduced mitochondrial respiration in glioma cells. As glycolysis is a less energy-efficient form of metabolism than mitochondrial respiration (**Chapter 1.1.1, 1.1.2**), this may explain the reduced motility effects observed by Liu *et al*. In contrast to Fu *et al.* my bioenergetics assays (**Figure 5.4.4, 5.4.5**) only examined the metabolic rates of PK-11195-treated TSPO$^{+/+}$ and TSPO$^{-/-}$ MPAs and U373 astrocytoma cells under basal conditions. It may have been beneficial to include additional assays to further evaluate energetics, such as the mitochondrial stress test or glycolysis stress test. Alternatively, I could have examined changes to metabolite production, such as lactate. This may well have revealed changes to cellular bioenergetics in PK-11195-treated astrocytes that I am unable to account for with the data presented here.

An alternative class of TSPO ligand that could have been employed for this study are the third generation *N,N*-dialkyl-2-phenylindol-3-ylglyoxylamide (PIGA) compounds (**Chapter 1.4.6**). These ligands have been shown to increase pregnenolone synthesis in rat C6 and human U87MG glioma cells[392]. Although the subject of some debate, steroidogenesis is a purported TSPO function, but is also a metabolically expensive process. Da Pozzo *et al*. demonstrated that the oxidative state of astrocytes (a measure of astrocyte functionality) correlates with steroidogenesis[392], though they did not compare these findings directly and did

not confirm the absence of off-target effects using a TSPO-deficient model. A future study could investigate the effect of PIGA ligands on astrocyte bioenergetics using metabolic flux assays combined with a TSPO-deficient model to account for off-target effects.

5.5.2: TSPO protein complex stoichiometry in response to metabolic state

In **Chapter 3**, I demonstrated that TSPO deficiency increased fatty acid oxidation (FAO) in astrocytes and confirmed that TSPO forms a protein complex containing carnitine palmitoyltransferase 1a (CPT1a). Among other endogenous and synthetic TSPO ligands, PK-11195 is thought to bind to the CRAC domain of TSPO. The CRAC domain is thought to be intimately involved with TSPO ligand binding[329,332,429], and has been implicated in regulating the formation of protein complexes involving TSPO[304,308,347,466], thus the modulation of these complexes may manifest as changes in cellular metabolism. Although PK-11195 pre-treatment did not alter astrocyte basal bioenergetics in my hands, 100nM PK-11195 has previously been reported to have effects on parameters related to cellular metabolism[367,368,379]. Using co-immunoprecipitations (co-IPs), I attempted to characterise the mechanism by which pharmacological TSPO inhibition might modulate cellular metabolism. Perturbation of astrocyte metabolism with 10mM 2DG treatment and inhibition of TSPO with 100nM PK-11195 both modestly reduced the intensity of TSPO-Myc I was able to immunoprecipitate, and PK-11195 modestly reduced the intensity of the CPT1a band in the co-IP. This is suggestive of a shift in TSPO protein complex stoichiometry. However, these experiments were limited – lacking a suitable loading control - so I could not employ semi-quantitative densitometry to reinforce my results. Thus, my interpretation of these data is preliminary and highly subjective. Future studies could employ techniques with greater sensitivity (such as immunoprecipitation-mass spectrometry or displacement assays) to quantify fluctuations to this interaction.

As outlined in **Chapter 1.4.2,** TSPO has a rich and varied interactome, with reported interacting partners including the voltage-dependent anion channel (VDAC)[347,472], adenine nucleotide transporter (ANT)[426], hexokinase-2 (HK2)[340,347], steroidogenic acute regulatory protein (StAR)[447], 14-3-3 theta[347], and translocase of the outer mitochondrial membrane complex subunit 20

(TOMM20)[347], among others. The function of TSPO in the context of these interactions remains unclear. Interestingly, alongside these heterogeneous complexes, TSPO has been reported to undergo homo-oligomerisation in a variety of model organisms from bacteria[354] to murine[332,353] and human cells[304,355] (**Chapter 1.4.2**). TSPO oligomerisation has been touted as a mechanism which regulates TSPO function[355]. A study investigating TSPO dynamics reported that monomeric TSPO readily dimerises and the authors suggest that this might represent a mechanism controlling TSPO functionality[351]. Further evidence suggests that TSPO oligomerisation may determine interactions between the different transmembrane domains of TSPO and availability of ligand binding sites[351,353,355]. By interacting with the different transmembrane domains of TSPO, and thus impacting stoichiometry, TSPO ligands may influence the binding or formation of homo- and hetero-oligomers involving TSPO[351,355]. Altered TSPO stoichiometry may be a determinant of the interactions and functionality of TSPO. The reduction in TSPO-Myc immunoprecipitate I observed following 1h 2DG or PK-11195 treatment in **Figure 5.4.7** might thus indicate a splitting of TSPO oligomers into monomers, which would explain the reduced intensity of this band. Given that there was no obvious reduction in CPT1a immunoprecipitate following 2DG treatment, this may represent TSPO monomers being recruited into other complexes that I was unable to detect. As 2DG treatment competitively inhibits glycolysis, this may, therefore, represent a mechanism by which CPT1a activity increases in response to a metabolic perturbation and supports the hypothesis that TSPO ordinarily inhibits CPT1a function.

Similarly, PK-11195 treatment reduced the immunoprecipitation of TSPO-Myc and CPT1a compared to vehicle-treated cells. PK-11195 binding has been reported to alter the structure of TSPO[351]. These findings, therefore, might indicate disruption of TSPO oligomers and TSPO-CPT1a complexes. In this way, CPT1a would no longer be bound to TSPO, and therefore no longer inhibited by it; if TSPO indeed acts as an inhibitor of CPT1a function. However, this all remains highly speculative, hindered by the fact that the co-IP studies I have presented here are not quantifiable because I lacked a suitable loading control for densitometric analysis. Thus, further studies could incorporate more sensitive techniques such as immunoprecipitation-mass spectrometry to more sensitively detect and characterise TSPO complexes in astrocytes under basal conditions

and following TSPO inhibition. Metabolomics assays could be combined with this to provide a measure of any corresponding shift in the metabolic phenotype of these astrocytes to provide inferences regarding the implications of pharmacologically modulating TSPO activity on cellular metabolism.

5.5.3: The effect of rs6971 genotype on choice of TSPO ligand for these studies

The rs6971 polymorphism is known to modulate the binding affinity of ligands for TSPO[305,416,479,504,582,583]. Therefore, the importance of determining the presence of the rs6971 polymorphism of human-derived biomaterials (cell lines, or primary blood and tissue samples) is becoming increasingly recognised and commonplace in studies focussing on pharmacological modulation of TSPO[309,416,437]. The modulatory effects of the rs6971 polymorphism on TSPO ligand pharmacokinetics were first noted with the advent of second-generation TSPO ligands[305,419–421], which were primarily used as neuroimaging markers to monitor neuroinflammation in a variety of disorders in clinical and preclinical settings[305,419,420]. Beyond this, the clinical importance of the rs6971 polymorphism was not recognised until the recent associations between presence of this polymorphism and susceptibility to neuropsychiatric conditions[314,330,347] including bipolar disorder[437,567] and schizophrenia[319,438,568]; suggesting that this polymorphism is clinically relevant beyond determining the choice of ligand for neuroimaging purposes.

Relevant to the work I have presented here, the rs6971 polymorphism is a major determinant of ligand selection in studies concerning the pharmacological modulation of TSPO using human-derived models[305,416,419–421]. Because the U373 astrocytoma cells were homozygous carriers of rs6971 (**Figure 5.4.1**), thus rendering second-generation ligands unsuitable, the choice of ligands I could employ for these studies was limited to either widely commercially-available first-generation TSPO ligands (insensitive to the polymorphism but with issues concerning stability and non-specific binding[305,419–421]), or the more recent innovations of third-generation TSPO ligands (insensitive to the polymorphism, more stable than first-generation ligands, and greater specificity and sensitivity[305,419–421]) with more limited commercial availability. Because I had found that both the C57BL/6J and TSPO$^{+/+}$ MPAs encoded Ala at TSPO AA 147, while the U373 astrocytoma cells encoded Thr at this locus, I elected to first utilise

the ‘classic’ first-generation TSPO ligand PK-11195, which would be unaffected by the presence of the rs6971 polymorphism, to carry out the initial characterisation of any effects of pharmacologically inhibiting TSPO on astrocyte metabolism.

Though, ultimately, I was only able to carry out studies investigating pharmacological modulation of TSPO utilising PK-11195 and not later-generation TSPO ligands, these findings have value: future work studying TSPO functionality in U373 cells may benefit from the results of my genotyping analysis. Importantly, the effects of the rs6971 polymorphism span beyond determining ligand choice: a recent study from Asih *et al*. using co-immunoprecipitations demonstrated that the complexes formed by TSPO are modulated by this polymorphism[347] (published in May 2022, after I had begun my work in September 2020). While work has demonstrated that this modulates treatment choices and susceptibility to psychiatric conditions[319,435–438,445,567,568], the bearing of these changes on neuroinflammatory conditions remain unclear.

5.6: Conclusion

To conclude, here I have presented evidence regarding the rs6971 genotype of a human astrocytoma cell line and C57BL/6J mice, which may have implications for future studies regarding pharmacological manipulation of TSPO in astrocytes. I could not replicate previous studies showing that PK-11195 application modulated parameters of cellular metabolism in primary astrocytes or an astrocytoma model, but I have supported these findings using a TSPO-deficient model to control for off-target effects. Moreover, I confirmed that acute (1h) PK-11195 treatment does not affect the expression of key metabolic enzymes or proteins such as GAPDH, CPT1a, and TSPO. I have provided evidence that pharmacological inhibition of TSPO and metabolic perturbations in astrocytes achieve similar but distinct effects on the TSPO-CPT1a protein complex, which may hold implications for the wider functioning of TSPO and the potential function of TSPO as a regulator of cellular metabolism.

Chapter 6: General discussion

6.1: Statement of key findings and contribution to knowledge

The first aim of this thesis was to examine the role of TSPO in regulating astrocyte metabolism. In **Chapter 3** I explored this concept and found that TSPO deficiency reduced astrocyte bioenergetic rates while promoting FAO in these cells (**Chapter 3**), without influencing the expression of key proteins associated with metabolism (**Chapter 4**). I also found that TSPO forms a protein complex with CPT1a in U373 cells (**Chapter 3**), potentially providing a mechanistic basis for these findings. The second aim of this thesis was to evaluate the effect of TSPO deficiency on the metabolic responses of astrocytes to inflammatory stimulation. In **Chapter 4**, I showed that TSPO deficiency in MPAs modulated neither the metabolic response to LPS stimulation nor NFκB phosphorylation in response to this stimulus, yet temporally modulated TNF secretion following LPS stimulation. The third and final aim of this thesis was to determine whether a TSPO ligand can recapitulate the metabolic phenotype of TSPO deficiency in astrocytes. While I was unable to determine any significant shift in astrocyte bioenergetics, in **Chapter 5** I report that TSPO ligands may modulate the stoichiometry of TSPO and thus influence the protein complexes it forms. This chapter will examine these findings in the wider context of the CNS under physiological and pathophysiological conditions. The limitations of the methods employed throughout this thesis will be discussed, and questions that remain to be answered during future research will be highlighted.

6.1.1: TSPO as a regulator of astrocyte metabolism

Collectively, the data in this thesis provide evidence that TSPO is important for regulating metabolic flexibility in astrocytes. In **Chapter 3**, I demonstrated that TSPO deficiency in MPAs reduces the contribution of aerobic glycolysis to mitochondrial respiration (**Figure 3.4.2, 7, 11**) and increases the contribution of fatty acid oxidation (FAO) to meeting ATP demand in these cells (**Figure 3.4.12**). In support of these data, I later showed that the expression profiles of the key metabolic proteins hexokinase 2 (HK2), glucose transporter 1 (GLUT1), and carnitine palmitoyltransferase 1a (CPT1a) were unchanged in TSPO-deficient astrocytes (**Figure 4.4.9, 11-13**), except in the case of CPT1a following 24h serum starvation (**Figure 4.4.13**). Considered together, these data are in contrast with existing published evidence suggesting that TSPO deficiency regulates the

mRNA levels of genes encoding these proteins[320,339,366,370]. In addition to transcriptional regulation, the activity of these proteins is also modulated by localisation[340,584] and/or substrate availability[206,224,561], which I did not examine and thus cannot account for. Despite this, the notion that TSPO acts as a metabolic regulator in astrocytes complements existing bodies of evidence. For example, links between TSPO and cellular metabolism have previously been drawn from studies in peripheral cells and tissues (Leydig cells[366], hepatocytes[446], adrenal cortices[320]) as well as microglia[339,340,369], tanycytes[358] and glioma cell lines[370,376,377,456]. Importantly, the evidence reported in some neural cells[340,446,456] were published after I had begun my doctoral studies in 2020 (2021[446], 2023[340,456]) and thus could not have informed the initial hypotheses. Tournier *et al*.[456] recently provided further evidence in support of the data presented in this thesis when they implied that TSPO expression may correlate with a metabolic shift during astrocyte reactivity using C6 astrocytoma cells.

Collectively, these data support a wider role for TSPO in regulating the dynamics and/or activity of proteins associated with metabolism and include the TSPO-CPT1a interaction I report in **Chapter 3**. Thus, based on my findings and these published bodies of evidence, I propose that TSPO may affect the metabolic flexibility of astrocytes as part of a regulatory protein complex influencing the activity of different metabolic pathways, particularly glycolysis and fatty acid oxidation. This is supported by the recently-reported TSPO-HK2[340] interaction in microglia (published in February 2023 by Fairley *et al*.[340]). As TSPO exhibits extensive genetic conservation I would speculate that a TSPO-HK2 relationship is also present in astrocytes and may partially underlie the metabolic plasticity of these cells. Moreover, the results I generated using TSPO$^{-/-}$ MPAs using the glycolysis stress test paradigm (**Figure 3.4.3**) are supportive of this possibility. However, the results from Fairley *et al*. [340] showing enhanced glycolysis in TSPO$^{-/-}$ microglia are in contrast with the results from Yao *et al*.[339], who in 2020 demonstrated that TSPO deficiency impairs glycolysis in microglia under basal conditions; thus, the role TSPO plays in regulating glycolysis remains to be fully clarified. Importantly, these separate bodies of work do not clearly state the glucose concentrations under which the experiments were performed, which may influence their observations. However, the data I have presented in this thesis correlates with the findings of both studies when considered within distinct

contexts: reintroduction of physiologically relevant and supraphysiological glucose concentrations. I would argue that this reinforces the importance of fully reporting compositions of cell culture media, which once accounted for may provide a clearer picture of the potentially state-dependent function TSPO plays in regulating glycolysis.

A role for TSPO in regulating cellular metabolism may explain the previously-established existence of TSPO-VDAC[347,348] and TSPO-ANT[56,350] interactions. Existing studies in the literature have suggested that a TSPO-VDAC-ANT complex may facilitate the mitochondrial permeability transition pore (MPTP). The MPTP is formed during cellular or mitochondrial stress; thus, potentially explaining the association between TSPO and stress responses in a variety of models[361–363]. However, this may better be supported by a role for TSPO in regulating ATP import/export to/from the mitochondria in response to the energetic needs of the cell. Moreover, because ATP is critical for a myriad of cellular processes, it is plausible that compensatory mechanisms exist to facilitate ATP transport in the absence of TSPO. This may explain a report suggesting that TSPO deficiency does not modulate cellular ATP levels[366].

Independently, HK2 and VDAC[585] and CPT1a and VDAC[464,465,586] have been reported to interact. Coupled with the data I presented in **Chapter 3** this implies that TSPO may form part of a TSPO-VDAC-ANT-HK2-CPT1a metabolic regulatory 'supercomplex' that facilitates state-dependent control of cellular metabolism (**Figure 6.1.1**). During an 'energy replete' state, TSPO may help promote glycolysis over FAO in astrocytes, whereas during a prolonged 'energy deficit' or period of heightened energetic requirements, TSPO may help promote FAO over glycolysis to facilitate greater ATP production (**Chapter 1.1.3.1**). This may explain why $TSPO^{-/-}$ astrocytes derive more of their energy from FAO (**Figure 3.4.12**). A theoretical model for how the role of TSPO in this complex may be modulated via cellular energy-sensing mechanisms is described in more detail in **Chapter 6.3.1** below. This 'supercomplex' may explain how TSPO deficiency modulates cellular metabolism but does not ablate it, which suggests that TSPO is a dispensable member of the complex that may help refine cellular energy use. Importantly, it remains unclear whether these protein-protein interactions occur directly or indirectly, thus the order of interactions presented in **Figure 6.1.1** are hypothetical. Another key question that remains is the order of these interactions

in the metabolic regulatory 'supercomplex'. Future studies could employ techniques such as co-immunoprecipitation-mass spectrometry[587], weak affinity chromatography[587], fluorescence resonance energy transfer[587], two- or three-dimensional SDS-PAGE[587], density gradients[587], site-directed mutagenesis[588], or proteomic analyses[587,589,590] to discern the order of interactions and whether they are direct or indirect. In addition, the potential effects of post-translational modifications in regulating the constitution of this 'supercomplex' may prove to be a fruitful avenue for investigation[590].

This proposition provides a possible explanation for the reduced ECAR and OCR I report in the basal metabolism studies (**Figure 3.4.1**), suggesting that TSPO deficiency attenuates import of the products of aerobic glycolysis to the mitochondria of MPAs. This may imply that loss of TSPO impacts activity of mitochondrial pyruvate carrier (MPC), potentially via its known interaction with VDAC (**Figure 1.1.2**). Crucially, the precise mechanisms regulating the activity of the MPC remain unclear[591,592] providing an interesting avenue for further exploration. I must emphasise that this is pure speculation, as I have presented no evidence to support the existence of a TSPO-MPC protein complex in astrocytes in this thesis. Similarly, because of the role of the MPC in amino acid metabolism[593,594], this may hint at a role for TSPO in this process, a notion that is potentially supported by the data I have presented. In **Chapter 3**, I did not observe any significant differences in the metabolic response of $TSPO^{-/-}$ MPAs to the reintroduction of L-glutamine apart from a greater reduction in ECAR following injection of 1000μM L-glutamine. This suggests that TSPO may regulate the import of amino acids to the mitochondria for downstream metabolism, or potentially the metabolism of amino acids, though I must reinforce that this is a single finding from a single tested concentration of a single amino acid and so must be regarded with caution. Thus, it would be beneficial to explore this further with a wider variety of amino acids and at a wider range of concentrations, as well as exploring possible protein-protein complexes between TSPO and proteins associated with amino acid metabolism.

Future studies could advance our understanding of the effects of TSPO ligands on these protein-protein complexes. Considering the attraction of TSPO as a therapeutic target, this would be beneficial knowledge. I attempted to examine

this via co-immunoprecipitations in **Chapter 5**, however my attempts were hindered by technical issues when immunoblotting the samples generated.

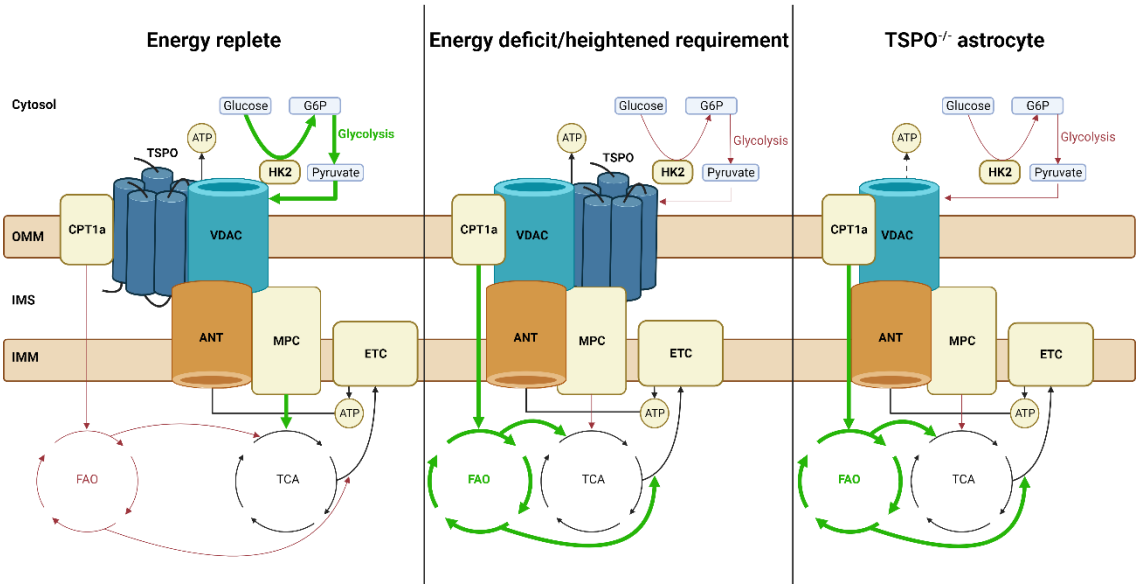

Figure 6.1.1: A proposed model for TSPO as a state-dependent regulator of astrocyte metabolism.

Hypothetical figure proposing how TSPO may regulate metabolic flexibility in astrocytes by inhibiting key proteins of various metabolic pathways in different energetic states. During an 'energy replete' state, astrocytes derive much of their energy from glycolysis. TSPO may work to supress CPT1a function (**Figure 3.4.12, 14**) and facilitate mitochondrial localisation of $HK2^{340}$. During an energy deficit or period of heightened energy requirements, TSPO may suppress glycolysis by modulating mitochondrial localisation of $HK2^{340}$ and promoting FAO to increase ATP generation. In $TSPO^{-/-}$ MPAs, CPT1a can freely associate with the complex, reducing HK2 activity and increasing the contribution of FAO to cellular metabolism (**Figure 3.4.12, 14**).

Created with BioRender.com.

OMM: Outer mitochondrial membrane. IMS: intermembrane space. IMM: inner mitochondrial membrane. TSPO: translocator protein 18kDa. CPT1a: carnitine palmitoyltransferase 1a. HK2: hexokinase 2. MPC: mitochondrial pyruvate carrier. FAO: fatty acid oxidation. TCA: tricarboxylic acid cycle. ETC: electron transport chain. ATP: adenosine triphosphate. VDAC: voltage dependent anion channel. ANT: adenine nucleotide transporter. G6P: glucose-6-phosphate.

6.1.2: Altered temporal profile of LPS-induced cytokine release in TSPO$^{-/-}$ MPAs

TSPO has been posited as a regulator of inflammatory responses[339,340,573,595,343,344,372,378,397,444,505,508] and *Nfkb* gene expression[512,513] which together indicate that TSPO might regulate inflammatory responses via NFκB. My data do not support this notion: in **Chapter 4** I observed no statistically significant impact of TSPO genotype on NFκB protein expression. Moreover, I did not observe any statistically significant differences in NFκB phosphorylation at the Ser536 residue in response to LPS stimulation (**Figure 4.4.8, 10**), suggesting that TSPO does not mediate the cellular inflammatory responses of astrocytes via this mechanism. Collectively, existing evidence posits that TSPO regulates cellular inflammatory responses by modulating cellular metabolism[306,339,574,595,340,347,358,368,369,428,524,573]. In contrast to this line of thought, I did not observe any statistically significant effects of TSPO deficiency on the metabolic response of MPAs to 3h or 24h LPS stimulation (**Figure 4.4.15, 16**), suggesting that this is not the case. Although I had previously determined that TSPO$^{-/-}$ MPAs have altered metabolic substrate preferences, the data that I have presented lead me to conclude that in astrocytes this change to basal cellular metabolism does not impede the metabolic plasticity required to fuel an inflammatory response, at least following 3 or 24h LPS stimulation. This may be explained by the finding that TSPO$^{-/-}$ MPAs met a greater proportion of their bioenergetic requirements through FAO (**Figure 3.4.12**) – for example, it is possible that rates of FAO increased to meet the metabolic demand placed on these cells incurred by LPS stimulation.

Despite seeing no change in NFκB phosphorylation or cellular bioenergetics, I observed that TSPO deficiency modulated the temporal release profile of TNF in response to LPS stimulation (**Figure 4.4.7**). This suggests that alongside modulating cellular metabolism, TSPO may somehow regulate cytokine release. One mechanism by which this may occur could be through regulation of the Ca^{2+} signalling required for cytokine release[596,597]. Links between TSPO and regulation of cellular Ca^{2+} flux have been drawn in other cell types[357,358]. Release of TNF is indirectly mediated by Ca^{2+} flux (**Figure 6.1.2**). Briefly, under basal conditions TNF is stored as a larger structure termed pro-TNF[598–600]. Following inflammatory stimulation, pro-TNF is rapidly cleaved by a disintegrin and metalloprotease 17

(ADAM17), producing TNF[598–600] which is replenished by JAK/STAT and NFκB-mediated translation of the *Tnf* gene[518,601,602]. Importantly, ADAM17 is activated via the mitogen activated protein kinase (MAPK) pathway[603,604], which has previously been linked to regulation of TSPO expression[304,456,472,532] and is itself regulated by Ca^{2+} signalling[605–607]. Thus, altered Ca^{2+} dynamics in $TSPO^{-/-}$ astrocytes might explain temporal modulations in TNF release (**Figure 6.1.2**). Moreover, TSPO has been linked to NLRP3 inflammasome formation in microglia[342,343,345,346]. Inflammasomes form a part of astrocyte inflammatory responses[608–610], are strongly linked to Ca^{2+} signalling[548,611–614] and indirectly influence TNF secretion[615]; therefore, modulation of Ca^{2+} signalling via TSPO deficiency may impair inflammasome activation in these cells and thus explain the modulated temporal release profile of TNF in $TSPO^{-/-}$ MPAs (**Figure 6.1.2**).

Importantly, although I did not investigate any potential effects of PK-11195 treatment on the calcium dynamics of MPAs, existing evidence in the literature suggests that pharmacological modulation of TSPO has downstream effects on these cellular inflammatory responses, reinforcing the concept of TSPO as an inflammatory mediator[312,391,397,430,441,506,508,513]. Moreover, TSPO ligands[379] including PK-11195[616] have been reported to modulate Ca^{2+} signalling, suggesting that TSPO is involved in this process. Therefore, modulation of Ca^{2+} dynamics by TSPO may underlie the effects of TSPO ligands on inflammatory responses. Future studies could focus on ascertaining whether pharmacological inhibition of TSPO recapitulates the published effects of TSPO deficiency on the Ca^{2+} dynamics of these cells ± LPS stimulation, though PK-11195 has been reported to induce Ca^{2+}-associated apoptosis[616]. This would offer insight into the downstream processes manipulated by PK-11195 and potentially contribute to a wider consensus on TSPO functionality, thus providing an intriguing avenue for further study.

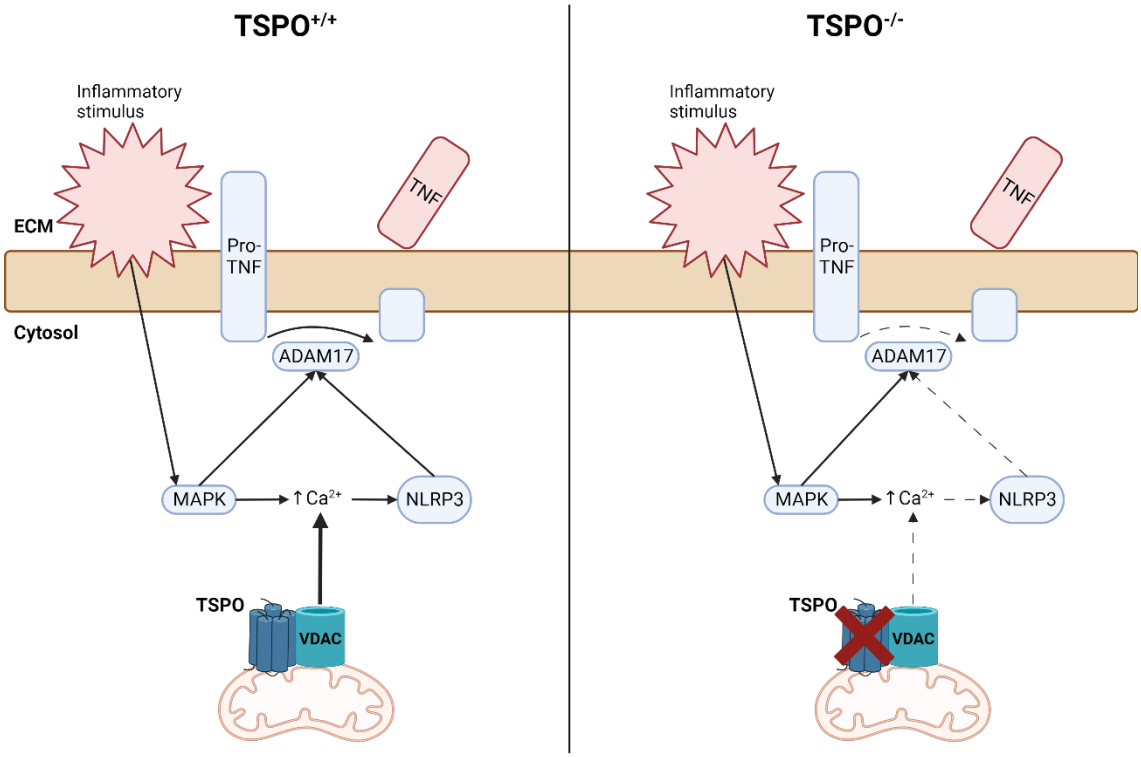

Figure 6.1.2: TSPO may regulate inflammatory responses by influencing Ca^{2+} flux.

Schematic outlining how TSPO might affect TNF secretion from astrocytes. In $TSPO^{+/+}$ astrocytes, MAPK is rapidly activated in response to an inflammatory stimulus. This leads to concomitant activation of ADAM17[603,604] and increased cytosolic Ca^{2+} levels[605–607], which contribute to NLRP3 inflammasome formation[548,611–614]. ADAM17 cleaves pro-TNF, producing TNF. Activation of the NLRP3 inflammasome indirectly increases ADAM17 activity and TNF production[615]. In $TSPO^{-/-}$ astrocytes or following pharmacological inhibition of TSPO, VDAC-dependent[349] mitochondrial Ca^{2+} release may be impinged, impeding NLRP3 inflammasome formation and/or ADAM17 activation, thus temporally modulating but not ablating TNF secretion (**Figure 4.4.7**).

Created with BioRender.com.

TSPO: translocator protein 18kDa. $^{+/+}$: expressing. $^{-/-}$: deficient. TNF: tumour necrosis factor. MAPK: mitogen-activated protein kinase. ADAM17: a disintegrin and metalloprotease 17. NLRP3: Nod-like receptor family pyrin domain containing 3. ECM: extracellular matrix. OXPHOS: oxidative phosphorylation. FAO: fatty acid oxidation. VDAC: voltage dependent anion channel.

6.2: General limitations

While the limitations pertinent to each chapter have been highlighted in the relevant discussion section, there are overarching limitations that apply to this body of work, which will be discussed below.

6.2.1: The models of TSPO deficiency used

The TSPO$^{-/-}$ MPAs used in this body of work were isolated from animals that were germline deficient, i.e., TSPO had never been present in any of these organisms. While germline genetic ablation is a useful method of studying gene/protein function, the deficits induced by germline deficiencies are often mitigated by compensatory mechanisms[617,618]. It is therefore likely that the TSPO$^{-/-}$ MPAs exhibited adaptations that may have influenced the results. If it had been available to us, an alternative model, such as an inducible TSPO knockout, may have been a better tool to study the functionality of this protein. This would have simplified the workflow and allowed MPAs to be isolated in bulk, and TSPO deficiency induced post-isolation by incubation with the appropriate trigger (e.g., tamoxifen[619,620]). However, inducible knockouts come with the caveat that complete ablation of the gene is not guaranteed[621,622]. As an alternative, a transient knockdown could have been employed. However, the drawback of this technique is that it would need to be repeated between every experiment, and therefore there may be day-to-day variation in efficiency that is difficult to account for.

The TSPO$^{-/-}$ U373 cells were generated by Daisy Stewart using CRISPR-Cas9 technology during her Professional Training Year, which took place in our research group. While the CRISPR-Cas9 system is widely used, it is not without its limitations. Notably, off-target effects are a major concern, despite attempts to minimise these[622–625]. Though the TSPO$^{-/-}$ U373s were validated using immunocytochemistry, PCR, and immunoblotting to confirm TSPO deficiency, it is possible that off-target cleavage of other genes occurred which was not accounted for by these methods of validation. Moreover, the single colony selection and expansion following CRISPR-Cas9 utilisation hugely increases the passage number of the cells. This poses the inherent risk of phenotypic drift within the population[626–628]. TSPO$^{+/+}$ control cells transfected with an empty vector plasmid were equivalently maintained to account for this, but it nonetheless

remains possible that the phenotype of these cells does not accurately reflect those of the (slightly) more physiologically relevant cells that have not been cultured on plasticware for an extended period. This technical limitation may have been overcome using a transient TSPO knockdown, perhaps mediated by siRNAs, however this would need to be repeated as part of every experimental protocol that made use of these cells. Species differences, mouse vs human, may also potentially account for differences in the metabolic profile of $TSPO^{-/-}$ MPAs and U373s. Finally, U373 cells are an astrocytoma (brain cancer) cell line and therefore, these cells do not accurately represent the non-pathological physiological state of astrocytes[381]. However, increased TSPO expression is clinically associated with gliomas, thus the findings from these cells may be of relevance when considering this pathological state[375,629].

6.2.2: Reliance on metabolic flux analyses

While this thesis has provided insight into the role of TSPO in regulating astrocyte bioenergetics, the main means by which this was assessed was through extracellular flux analysis (EFA). EFA is a well-recognised and widely-employed means of gauging cellular bioenergetics and therefore the metabolic state of cells[630–632]. However, EFA is inherently reliant on proxies of cellular metabolism, such as oxygen consumption rate (OCR) as a proxy for mitochondrial respiration[633,634] and acidification of the culture media (extracellular acidification rate; ECAR) for glycolysis[631,635,636]. Although these processes are widely recognised as major contributors to these outputs, they nonetheless remain simplified proxies for an extremely complex interplay of various cellular pathways. Importantly, EFA alone struggles to distinguish between the contributions made by various metabolic pathways to OCR and ECAR, though this may be somewhat elucidated through careful employment of selective inhibitory agents to discern the contribution of a particular pathway within a given context (for example, the fatty acid oxidation stress test). While I have reinforced the results of EFA where possible by measuring concentrations of metabolic products (i.e., lactate secretion), alternative measurements such as glucose uptake or pyruvate production assays could have been employed to provide a more holistic insight into the metabolic changes underlying any change in EFA results. As an alternative secondary measure of cellular metabolism, enzyme activity assays could have been employed in place of characterising total expression of these

proteins via immunoblotting. Similarly, interrogation of changes to pathways involved in energy homeostasis, such as phosphorylation of the key energy sensor AMPK or its target ACC, could have been employed to provide more direct interrogations of the metabolic consequences that may arise from TSPO deficiency or pharmacological inhibition of TSPO. Future studies could employ these more varied techniques to further support the findings from EFA, which provides a valuable and accessible insight into cellular bioenergetics.

6.2.3: Limitations of *in vitro* methodology

All the work presented in this thesis is derived from study of *ex vivo* MPAs or astrocytoma cells, which were maintained *in vitro* using a two-dimensional plasticware-based culture system. While MPAs have greater physiological relevance than astrocytoma cells, a key and widely-recognised limitation of the two-dimensional cell culture methodology employed within this thesis is that the astrocytes are unable to assume a physiologically relevant morphology, instead becoming more morphologically fibrotic and reminiscent of gliotic or reactive astrocytes[637]. The fibrotic and arguably gliotic phenotype of these cells is exacerbated by the inclusion of sera in the culture media to support cell growth[637]. Sera is known to increase expression of GFAP in astrocytes, a marker of astrocyte reactivity *in vivo*. Removal of sera from two-dimensional astrocyte cultures has been demonstrated to reduce GFAP expression and the fibrotic morphology of astrocytes[637]. Moreover, the morphology of astrocytes in two-dimensional culture is not reflective of their state in the intact animal. *In vivo*, astrocytes exhibit a complex stellate morphology characterised by the extension of various processes to facilitate intercellular interactions[80,637]. Thus, a three-dimensional culture system could have been employed to facilitate this more physiologically relevant morphology, perhaps through the use of a hydrogel or organoid system[637,638]. While this does not eliminate the limiting factor of a cellular monoculture, this would at the very least encourage the astrocytes to adopt a more physiologically relevant morphology. Future studies of astrocyte functionality *in vitro* could certainly explore using these techniques, which are becoming increasingly popular in existing literature. If a three-dimensional culture system is not feasible, a neuronal co-culture model could be employed to determine any change to the ability of astrocytes to provide homeostatic or metabolic support to neurons. Alternatively, an acute brain slice culture system

could be used to examine the functionality of these astrocytes more holistically in a native environment.

6.3: Outstanding questions

This thesis has presented evidence supporting a role for TSPO in regulating the cellular bioenergetics of astrocytes, in addition to a potential role in influencing cytokine release from these cells. Alongside these key findings, intriguing questions have been raised, presenting exciting avenues for further study which are outlined below.

6.3.1: How is TSPO regulated?

Despite decades of widespread interest, our knowledge of how TSPO function/activity is regulated remains extremely limited. Existing evidence in the literature suggests that TSPO may be regulated via a phosphorylation event[315,433,532,639,640], however the precise residue this occurs at remains to be determined. TSPO phosphorylation was reported in mice in 1994[315,640] and 2010[315,532]. In 2014, TSPO was shown to undergo phosphorylation by protein kinase A (PKA) in rat hypothalamic astrocytes following stimulation with oestradiol[433], which was later independently recapitulated using brain homogenate[639]. PKA is activated in response to increased cyclic AMP (cAMP) concentrations[641,642], with a variety of associated downstream effects including steroidogenesis[433,643], FAO[644,645], and gluconeogenesis[641,646,647]; alongside other signalling mechanisms such as Ca^{2+} flux[648–650]. Similarly, in tanycytes and microglia, TSPO deficiency has been linked to modulation of Ca^{2+} signalling[357,358], and alongside the evidence presented in this thesis, a role for TSPO in regulating cellular metabolism is emerging in the published literature[304,315,320,357,358,366,368,370,446]. Thus, these functions may be regulated by PKA signalling. Importantly, the effects of PKA signalling on cellular metabolism are similar to the observations I reported in $TSPO^{-/-}$ MPAs (**Chapter 3**), implying that PKA signalling may indeed regulate TSPO activity in astrocytes in response to cellular energy levels (**Figure 6.3.1**).

Notably, the downstream effects of the PKA pathway on cellular energy use are not dissimilar to those of AMPK, a master energy regulator which is phosphorylated in response to low ATP levels[9,72]. This suggests that either AMPK or PKA may regulate TSPO activity to maintain cellular ATP levels. Moreover,

AMPK indirectly regulates FAO, and thus might inhibit TSPO to facilitate greater CPT1a activity. Importantly, the mechanisms regulating CPT1a activity are poorly understood, but are currently accepted as being related to malonyl-CoA production. When AMPK is active, it rapidly phosphorylates (inactivates) acetyl-CoA carboxylase[9,561]. This prevents conversion of acetyl-CoA to malonyl-CoA. Malonyl-CoA inhibits CPT1a function, thus inhibition of acetyl-CoA carboxylase allows acyl-CoAs to undergo FAO following mitochondrial import, which is mediated via CPT1a[58,206,224,561,651] (**Figure 1.1.3.1**). Similarly to PKA, AMPK activation promotes other processes associated with ATP generation and energy expenditure, such as glycolysis[8,9,72]. In addition to activation in response to low ATP, AMPK can also undergo phosphorylation from calcium/calmodulin-dependent protein kinase kinase 2[8] (CaMKKβ), which has also linked to energy homeostasis and Ca^{2+} signalling[8,652,653]. TSPO has been posited as a regulator of AMPK subunit gene expression[370], and PK-11195 has been linked to AMPK activation[477], which substantiates a link between these proteins. Thus, alongside PKA, AMPK may also regulate TSPO activity via phosphorylation in response to fluctuations in cellular energy levels.

Importantly, aside from limiting substrate availability (and thus turnover rate), regulation of the activity of proteins such as CPT1a and MPC are poorly understood. In this thesis I have presented evidence to suggest that TSPO may control FAO via a complex with CPT1a. As TSPO-deficient astrocytes have increased FAO capacity, this implies that TSPO may somehow inhibit CPT1a function. Therefore, regulation of TSPO activity via phosphorylation represents a tangible mechanism by which TSPO may regulate cellular energy use. This is in line with some extremely recent observations of TSPO function: in early 2023, TSPO was shown to regulate mitochondrial localisation of HK2[340], thus governing the activity of this enzyme. This body of evidence supports the argument that TSPO may regulate the activity of mitochondrial proteins to effect changes on cellular metabolism, which I propose may be mediated by via these protein-protein complexes (**Figure 6.1.1**). Furthermore, I suggest that activity of TSPO may in turn be regulated by a phosphorylation event potentially mediated by PKA and/or AMPK in response to cellular energy deficits (**Figure 6.3.1**), providing a mechanistic basis for dynamic control of cellular metabolism via TSPO.

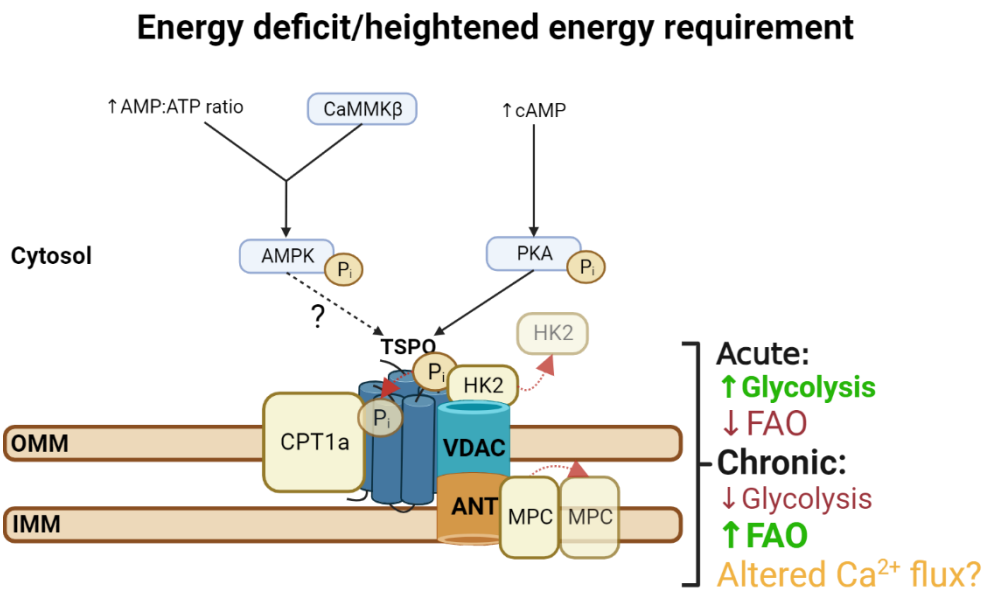

Figure 6.3.1: Theoretical mechanisms regulating TSPO activity and their potential effects on TSPO-containing complexes.

Schematic outlining how TSPO activity may be regulated by the metabolism-associated kinases AMPK and PKA. Following activation of AMPK[8,9,72,652,653] or PKA[641,642] during an energy deficit or period of heightened energetic requirements, TSPO may be the subject of an AMPK-mediated (speculative) or PKA-mediated (previously confirmed[433]) phosphorylation event. Here, TSPO is phosphorylated at one residue in response to an AMPK/PKA activation, promoting mitochondrial localisation of HK2 and the MPC to facilitate aerobic glycolysis. Persistent TSPO phosphorylation leads to gradual conformational changes/phosphorylation of an alternative residue, promoting CPT1a recruitment to the complex in place of HK2 and MPC. Thus, a gradual increase in FAO-based ATP production in the longer term may be observed. Modulation of VDAC- and ANT-containing complexes may affect mitochondrial Ca^{2+} efflux.

Black dotted arrows indicate speculative processes. Red dotted arrows and more transparent icons indicate potential conformational changes, or movement of proteins in and out of a complex. This may also be seen as representing a three-dimensional shift in the complex to promote one process (FAO) over another (glycolysis). Created with BioRender.com.

AMP: adenosine monophosphate. ATP: adenosine triphosphate. AMPK: AMP-activate protein kinase. CaMKKβ: calcium/calmodulin-dependent protein kinase kinase β. PKA: protein kinase A. cAMP: cyclic AMP. TSPO: translocator protein 18kDa. Pi: inorganic phosphate. CPT1a: carnitine palmitoyltransferase 1a. HK2: hexokinase 2. MPC: mitochondrial pyruvate carrier. VDAC: voltage-dependent anion channel. ANT: adenine nucleotide transporter. OMM/IMM: outer/inner mitochondrial matrix. FAO: fatty acid oxidation.

6.3.2: Does TSPO regulate calcium signalling in astrocytes?

Another outstanding question is the mechanism by which TSPO deficiency temporally modulates TNF secretion (**Figure 4.4.7**). As discussed in **Chapter 6.3**, this may suggest a wider role for TSPO as an influencer of astrocyte $[Ca^{2+}]_i$, a key regulatory mechanism underlying the secretion of various molecules from astrocytes and other cells. In microglia and tanycytes, TSPO has been linked to Ca^{2+} signalling[357,358]; however, whether this mechanism is conserved in astrocytes remains unclear. Modulation of this key mechanism may provide insight into the function of TSPO protein complexes reported in the existing literature, such as with VDAC1, which remains consistently reported but functionally poorly understood[357,428,438,654]. This may also represent a means by which TSPO may affect mitochondrial parameters such as fission:fusion status, which were not examined in this thesis. Existing work in the literature has linked TSPO to regulating these processes through mechanisms which remain unclear[448,655]. Elucidating this is pertinent when one considers the increasing recognition of distinct subclasses of astrocytes, which fulfil myriad functions within the CNS parenchyma[80,656–658]. Published literature has proposed that the function of TSPO likely varies depending on the physiological context[357,358]: the particular type of cell and/or stimulus being interrogated. Therefore, in a population of cells functionally and phenotypically diverse as astrocytes, it is crucial to ascertain any sub-type and/or state-dependent differences in TSPO functionality if TSPO is to be therapeutically manipulated; particularly bearing in mind the recent revelation that in at least one pathophysiological context[393] astrocytes are among the first classes of cells to upregulate TSPO expression.

For future studies, genetically encoded calcium indicators may provide an accessible route to studying this *in vivo*, particularly if coupled with a TSPO-deficient model and a chemogenetic switch to provide dynamic control over the activity of calcium channels. However, this is likely to pose logistical challenges, which may be better accounted for in an *ex vivo* model such as acute slice culture or a three-dimensional cell co-culture. This could then be coupled with genetically encoded Ca^{2+} sensors or more traditional fluorometric methods to interrogate Ca^{2+} signalling. Regardless of the outcomes of these studies, an improved knowledge of the role of TSPO in regulating cellular metabolism and its relation to the inflammatory state of the astrocyte, and an enhanced understanding of the

role TSPO plays in regulating cellular Ca^{2+} dynamics, may thus help unify two apparently distinct functions of TSPO.

6.3.3: What comes first *in situ*: the metabolic shift, or the inflammatory stimulus?

The body of work presented here has examined the role of TSPO in regulating astrocyte metabolism and in regulating the expression of proteins associated with cellular metabolism in the context of an inflammatory stimulus. However, the precise order of events, and thus the function of TSPO in astrocytes, remains somewhat unclear. As existing evidence and this thesis attempt to highlight, inflammatory responses and metabolic shifts are not distinct cellular processes[255,289,290,384,389,493,533,659] and are closely interlinked, likely bidirectional, parameters[40,167,289,290,659]. *In vivo*, TSPO expression increases during chronic neuroinflammation[317,444,501,574,660]. Whether this is in response to the increased metabolic demand placed on the CNS parenchyma or because TSPO is a key regulator of the inflammatory response remains unclear. However, evidence published in 2020 suggested that TSPO expression increases in astrocytes prior to microglia during Alzheimer's disease[393], and in 2023 the same group demonstrated that TSPO is regulated by the STAT3/ERK pathway in response to inflammatory signalling, and may regulate cellular metabolism in astrocytes[456]. While this valuable study further substantiates a link between TSPO and immunometabolism, this body of evidence was published well into my doctoral studies (August 2023) and therefore could not have informed any of my experimental procedures. Moreover, the findings of this published study were derived from the C6 astrocytoma cell lines, which like U373 cells, do not accurately represent primary astrocytes (**Chapter 6.2.1**). Nonetheless, this indicates TSPO may primarily regulate cellular metabolism, and subsequently affects energetically expensive immune responses associated with mitochondria (reactive oxygen species production, inflammasome activation, Ca^{2+} homeostasis), thus supporting the findings I have presented in this thesis. Crucially, astrocytes play key roles in providing trophic support to neurons and the wider brain parenchyma, which may help drive the inflammatory responses aimed to resolve the origin of CNS trauma. This could be investigated using murine models that allow dynamic control of TSPO expression. This could be achieved via astrocyte-specific reporters (for example, GFAP-, ALDH1L1-, or S100β-linked genetic manipulation), or targeted TSPO ablation at various points

throughout disease pathology in various models. By linking TSPO expression to reporter genes, one may be able to discern between different astrocyte subtypes (for example, cortical compared to brainstem or hypothalamic) and the function of TSPO within these distinct populations of cells.

6.3.4: Are these outputs truly modulated by TSPO ligands?

Much effort has been made to decode the therapeutic potential of TSPO ligands, with the end goal typically being to employ these ligands as an adjunct to the treatment of various conditions associated with a neuroinflammatory element. However, as discussed in **Chapter 5**, the ligand specificity and lack of consensus regarding downstream functions regulated by TSPO has hindered this. Whilst more recent studies have endeavoured to account for potential off-target effects of TSPO ligands using $TSPO^{-/-}$ models[379], a more holistic understanding of TSPO-associated functions reinforced by findings from a variety of studies encompassing stable and transient TSPO deficiency may first be beneficial and could be addressed via a meta-analysis. Considering that the potential for therapeutic employment of TSPO ligands is being explored in clinical trials for neurodegenerative conditions[406,411,412], and given the promising neuroprotective effects of TSPO ligands in multiple preclinical models[397,399,430,442,444,595], this may prove to be a fruitful and highly impactful endeavour. Reports of the rs6971 TSPO variant being adversely associated with bipolar disorder (tentatively linked to aberrant modulation of hypothalamic-pituitary-adrenal axis and increased cortisol secretion[437]) and major depressive disorder[435,436] (through an as-yet-unknown mechanism) further suggest that despite historical limitations, TSPO still holds promise as a therapeutic target. In this thesis I have presented evidence for TSPO as a modulator of cellular metabolism in astrocytes, which is congruent with findings from microglia[339,340] and cells of the periphery[366,446]. Moreover, cellular metabolism is gaining appeal as a therapeutic target for various conditions[77,661–663]. The evidence I have presented herein concerning the role of TSPO as a metabolic regulator is an interesting parallel with the modulated steroidogenesis observed in studies of bipolar disorder, as steroidogenesis is a metabolically expensive process and potentially suggests that the rs6971 polymorphism may alter cellular metabolism. To the best of my knowledge this interesting hypothesis has yet to be investigated and could be tackled through the use of patient-derived stem cells to accurately determine the effect of TSPO

variants on cellular metabolism in a variety of clinically relevant *in vitro* settings (with the aforementioned caveats of 2-dimensional cell culture, **Chapter 6.2.3**), which could then inform clinical trials in neuropsychiatric and neurodegenerative conditions to more accurately inform the validity of TSPO as a therapeutic target. Inclusion of appropriate age-matched controls would be vital for maximum research output from these studies, in addition to consistent sampling between studies to build an accurate picture of the therapeutic potential of pharmacological TSPO manipulation. Following this, the dedicated development of TSPO ligands designed to modulate specific functions beyond serving as bioimaging markers is likely required to therapeutically target TSPO. Accounting for any off-target effects of these ligands in both *in vivo* and *in vitro* studies will certainly yield greater insight into the true therapeutic potential and functionality of TSPO in a variety of cells. Studying apparently widely conserved functions of TSPO, such as regulating cellular metabolism, in this manner may thus be of benefit for a variety of conditions. Holistic and high-throughput techniques, such as cytokine array panels, metabolomics, single-cell/nucleus RNA sequencing, and proteomics could yield a wealth of data regarding the functionality of TSPO in a variety of cells, including astrocytes. Correlates could then be drawn with patient samples to investigate the potential role of TSPO variants in modulating developmental risk or therapeutic outcomes in a variety of conditions. In sum, this approach may help to elucidate the true therapeutic potential of, and any inherent risks associated with, pharmacologically modulating TSPO.

6.4: Conclusions and future directions

In this thesis, I have used models of TSPO deficiency (MPAs and U373 cells) to characterise the potential role of TSPO in regulating cellular metabolism. Crucially, I have demonstrated that absence of TSPO reduces the bioenergetic rates of astrocytes; a finding which is explained by an increased contribution of FAO to maintaining the metabolism of these cells. Furthermore, I have independently recapitulated evidence demonstrating that TSPO forms a protein complex with CPT1a, the rate-limiting enzyme of FAO, in astrocytoma cells. Contrary to my expectations, TSPO deficiency did not appear to affect the metabolic response of MPAs to LPS stimulation. Whilst I did not observe any regulatory effect of TSPO deficiency on proteins associated with metabolism, I found that ablation of TSPO temporally modulated the release of TNF following LPS stimulation. This implies that TSPO may serve multiple roles in MPAs. Finally, I presented evidence suggesting that pharmacological inhibition of TSPO does not appear to modulate astrocyte bioenergetics but may modulate the stoichiometry of TSPO protein complexes. Potential directions for future studies include: characterisation of Ca^{2+} dynamics in $TSPO^{-/-}$ astrocytes of a variety of subtypes (e.g., cortical vs hypothalamic astrocytes); interrogation of enzymatic function in $TSPO^{-/-}$ astrocytes, such as HK2 or enzymes associated with FAO, or metabolomics arrays, to support the bioenergetics data presented here; immunocytochemistry examining the mitochondrial dynamics and/or lipid droplet distributions in $TSPO^{-/-}$ MPAs; and, validation of a wider array of TSPO ligands in conjunction with a $TSPO^{-/-}$ model to account for off-target effects, with the intention of providing a consensus on readily measurable downstream functions potentially impacted by TSPO that may serve as viable therapeutic targets. These studies could include a wide variety of inflammatory stimuli and timepoints to provide a more holistic overview of TSPO function in a physiological and pathophysiological context.

Appendix

Appendix 1: Regulation of astrocyte metabolism by mitochondrial translocator protein.

Firth W, Robb JL, Stewart D, Pye KR, Bamford R, Oguro-Ando A, Beall C, Ellacott KLJ. **BioRxiv preprint (2023).**

doi: 10.1101/2023.09.29.560159.

Abstract: The mitochondrial translocator protein 18kDa (TSPO) has been linked to a variety of functions from steroidogenesis to regulation of cellular metabolism and is an attractive therapeutic target for chronic CNS inflammation. Studies in the periphery using Leydig cells and hepatocytes, as well as work in microglia, indicate that the function of TSPO may vary between cells depending on their specialised roles. Astrocytes are critical for providing trophic and metabolic support in the brain as part of their role in maintaining brain homeostasis. Recent work has highlighted that TSPO expression increases in astrocytes under inflamed conditions and may drive astrocyte reactivity. However, relatively little is known about the role TSPO plays in regulating astrocyte metabolism and whether this protein is involved in immunometabolic processes in these cells. Using TSPO-deficient ($TSPO^{-/-}$) mouse primary astrocytes in vitro (MPAs) and a human astrocytoma cell line (U373 cells), we performed metabolic flux analyses. We found that loss of TSPO reduced basal astrocyte respiration and increased the bioenergetic response to glucose reintroduction following glucopenia, while increasing fatty acid oxidation (FAO). Lactate production was significantly reduced in $TSPO^{-/-}$ astrocytes. Co-immunoprecipitation studies in U373 cells revealed that TSPO forms a complex with carnitine palmitoyltransferase 1a, which presents a mechanism wherein TSPO may regulate FAO in astrocytes. Compared to $TSPO^{+/+}$ cells, inflammation induced by 3h lipopolysaccharide (LPS) stimulation of $TSPO^{-/-}$ MPAs revealed attenuated tumour necrosis factor release, which was enhanced in $TSPO^{-/-}$ MPAs at 24h LPS stimulation. Together these data suggest that while TSPO acts as a regulator of metabolic flexibility in astrocytes, loss of TSPO does not appear to modulate the metabolic response of astrocytes to inflammation, at least in response to the stimulus/time course used in this study.

References

1. Yang J, Ueharu H, Mishina Y. Energy metabolism: A newly emerging target of BMP signaling in bone homeostasis. Bone [Internet]. 2020;138(March):115467. Available from: https://doi.org/10.1016/j.bone.2020.115467

2. Fox CJ, Hammerman PS, Thompson CB. Fuel feeds function: Energy metabolism and the T-cell response. Nat Rev Immunol. 2005;5(11):844–52.

3. Lunt SY, Vander Heiden MG. Aerobic glycolysis: Meeting the metabolic requirements of cell proliferation. Annu Rev Cell Dev Biol. 2011;27:441–64.

4. Strasser B. Physical activity in obesity and metabolic syndrome. Ann N Y Acad Sci. 2013;1281(1):141–59.

5. NamKoong C, Song WJ, Kim CY, Chun DH, Shin S, Sohn JW, et al. Chemogenetic manipulation of parasympathetic neurons (DMV) regulates feeding behavior and energy metabolism. Neurosci Lett [Internet]. 2019;712(March):134356. Available from: https://doi.org/10.1016/j.neulet.2019.134356

6. Tremblay A, Bellisle F. Nutrients, satiety, and control of energy intake. Appl Physiol Nutr Metab. 2015;40(10):971–9.

7. Garcia D, Shaw RJ. AMPK: Mechanisms of Cellular Energy Sensing and Restoration of Metabolic Balance. Mol Cell [Internet]. 2017;66(6):789–800. Available from: http://dx.doi.org/10.1016/j.molcel.2017.05.032

8. Mihaylova MM, Shaw RJ. The AMPK signalling pathway coordinates cell growth, autophagy and metabolism. Nat Cell Biol. 2011;13(9):1016–23.

9. Herzig S, Shaw RJ. AMPK: Guardian of metabolism and mitochondrial homeostasis. Nat Rev Mol Cell Biol [Internet]. 2018;19(2):121–35. Available from: http://dx.doi.org/10.1038/nrm.2017.95

10. Baker SA, Rutter J. Metabolites as signalling molecules. Nat Rev Mol Cell Biol. 2023;24(5):355–74.

11. Wise DR, Ward PS, Shay JES, Cross JR, Gruber JJ, Sachdeva UM, et al.

Hypoxia promotes isocitrate dehydrogenasedependent carboxylation of α-ketoglutarate to citrate to support cell growth and viability. Proc Natl Acad Sci U S A. 2011;108(49):19611–6.

12. Chinopoulos C. Which way does the citric acid cycle turn during hypoxia? The critical role of α-ketoglutarate dehydrogenase complex. J Neurosci Res. 2013;91(8):1030–43.

13. Órdenes P, Villar PS, Tarifeño-Saldivia E, Salgado M, Elizondo-Vega R, Araneda RC, et al. Lactate activates hypothalamic POMC neurons by intercellular signaling. Sci Rep [Internet]. 2021;11(1):1–12. Available from: https://doi.org/10.1038/s41598-021-00947-7

14. Douglass JD, Dorfman MD, Thaler JP. Glia: silent partners in energy homeostasis and obesity pathogenesis. Diabetologia [Internet]. 2017;60(2):226–36. Available from: http://dx.doi.org/10.1007/s00125-016-4181-3

15. García-Cáceres C, Balland E, Prevot V, Luquet S, Woods SC, Koch M, et al. Role of astrocytes, microglia, and tanycytes in brain control of systemic metabolism. Nat Neurosci [Internet]. 2019;22(1):7–14. Available from: http://dx.doi.org/10.1038/s41593-018-0286-y

16. Barros LF. Metabolic signaling by lactate in the brain. Trends Neurosci [Internet]. 2013;36(7):396–404. Available from: http://dx.doi.org/10.1016/j.tins.2013.04.002

17. Tanaka K, Choi J, Cao Y, Stacey G. Extracellular ATP acts as a damage-associated molecular pattern (DAMP) signal in plants. Front Plant Sci. 2014;5(SEP):1–9.

18. Gazzerro E, Baratto S, Assereto S, Baldassari S, Panicucci C, Raffaghello L, et al. The Danger Signal Extracellular ATP Is Involved in the Immunomediated Damage of α-Sarcoglycan–Deficient Muscular Dystrophy. Am J Pathol [Internet]. 2019;189(2):354–69. Available from: http://dx.doi.org/10.1016/j.ajpath.2018.10.008

19. Virgilio F Di, Sarti AC, Coutinho-Silva R. Purinergic signaling, DAMPs, and inflammation. Am J Physiol - Cell Physiol. 2020;318(5):C832–5.

20. Burda JE, Bernstein AM, Sofroniew M V. Astrocyte roles in traumatic brain injury. Exp Neurol [Internet]. 2016;275:305–15. Available from: http://dx.doi.org/10.1016/j.expneurol.2015.03.020

21. Karve IP, Taylor JM, Crack PJ. The contribution of astrocytes and microglia to traumatic brain injury. Br J Pharmacol. 2016;173(4):692–702.

22. Mills EL, Ryan DG, Prag HA, Dikovskaya D, Menon D, Zaslona Z, et al. Itaconate is an anti-inflammatory metabolite that activates Nrf2 via alkylation of KEAP1. Nature. 2018;556(7699):113–7.

23. Corda D, Zizza P, Varone A, Filippi BM, Mariggiò S. The glycerophosphoinositols: Cellular metabolism and biological functions. Cell Mol Life Sci. 2009;66(21):3449–67.

24. Falasca M, Marino M, Carvelli A, Iurisci C, Leoni S, Corda D. Changes in the levels of glycerophosphoinositols during differentiation of hepatic and neuronal cells. Eur J Biochem. 1996;241(2):386–92.

25. Vessichelli M, Mariggiò S, Varone A, Zizza P, Di Santo A, Amore C, et al. The natural phosphoinositide derivative glycerophosphoinositol inhibits the lipopolysaccharide-induced inflammatory and thrombotic responses. J Biol Chem. 2017;292(31):12828–41.

26. Patrussi L, Mariggiò S, Corda D, Baldari CT. The glycerophosphoinositols: From lipid metabolites to modulators of T-cell signaling. Front Immunol. 2013;4(JUL):1–6.

27. Coronel-Hernández J, Pérez-Yépez EA, Delgado-Waldo I, Contreras-Romero C, Jacobo-Herrera N, Cantú-De León D, et al. Aberrant Metabolism as Inductor of Epigenetic Changes in Breast Cancer: Therapeutic Opportunities. Front Oncol. 2021;11(October):1–8.

28. Whitehall JC, Greaves LC. Aberrant mitochondrial function in ageing and cancer. Biogerontology [Internet]. 2020;21(4):445–59. Available from: https://doi.org/10.1007/s10522-019-09853-y

29. Wolters-Eisfeld G, Hackert T, Güngör C. Unmasking metabolic dependencies in pancreatic cancer: aberrant polyamine synthesis as a promising new therapeutic target. Signal Transduct Target Ther.

2023;8(1):1–2.

30. Li X, Yang Y, Zhang B, Lin X, Fu X, An Y, et al. Lactate metabolism in human health and disease. Signal Transduct Target Ther. 2022;7(1).

31. Yu L, Jin J, Xu Y, Zhu X. Aberrant energy metabolism in Alzheimer's disease. J Transl Intern Med. 2022;10(3):197–206.

32. Tribble JR, Otmani A, Sun S, Ellis SA, Cimaglia G, Vohra R, et al. Nicotinamide provides neuroprotection in glaucoma by protecting against mitochondrial and metabolic dysfunction. Redox Biol. 2021;43(April).

33. Wu SF, Lin CY, Tsai RK, Wen YT, Lin FH, Chang CY, et al. Mitochondrial Transplantation Moderately Ameliorates Retinal Degeneration in Royal College of Surgeons Rats. Biomedicines. 2022;10(11).

34. Chang JC, Chao YC, Chang HS, Wu YL, Chang HJ, Lin YS, et al. Intranasal delivery of mitochondria for treatment of Parkinson's Disease model rats lesioned with 6-hydroxydopamine. Sci Rep [Internet]. 2021;11(1):1–14. Available from: https://doi.org/10.1038/s41598-021-90094-w

35. Thorens B, Mueckler M. Glucose transporters in the 21st Century. Am J Physiol - Endocrinol Metab. 2010;298(2):1–16.

36. Murray B, Rosenbloom C. Fundamentals of glycogen metabolism for coaches and athletes. Nutr Rev. 2018;76(4):243–59.

37. Brown AM, Ransom B. Astrocyte Glycogen and Brain Energy Metabolism. Glia. 2007;55:1263–71.

38. Li XB, Gu JD, Zhou QH. Review of aerobic glycolysis and its key enzymes - new targets for lung cancer therapy. Thorac Cancer. 2015;6(1):17–24.

39. Roberts DJ, Miyamoto S. Hexokinase II integrates energy metabolism and cellular protection: Akting on mitochondria and TORCing to autophagy. Cell Death Differ. 2015;22(2):248–57.

40. Pålsson-McDermott EM, O'Neill LAJ. Targeting immunometabolism as an anti-inflammatory strategy. Cell Res [Internet]. 2020;30(4):300–14. Available from: http://dx.doi.org/10.1038/s41422-020-0291-z

41. Soto-Heredero G, Gómez de las Heras MM, Gabandé-Rodríguez E, Oller

J, Mittelbrunn M. Glycolysis – a key player in the inflammatory response. FEBS J. 2020;287(16):3350–69.

42. Caslin HL, Abebayehu D, Pinette JA, Ryan JJ. Lactate Is a Metabolic Mediator That Shapes Immune Cell Fate and Function. Front Physiol. 2021;12(October).

43. Dichtl S, Lindenthal L, Zeitler L, Behnke K, Schlösser D, Strobl B, et al. Lactate and IL6 define separable paths of inflammatory metabolic adaptation. Sci Adv. 2021;7(26):1–11.

44. Manosalva C, Quiroga J, Hidalgo AI, Alarcón P, Anseoleaga N, Hidalgo MA, et al. Role of Lactate in Inflammatory Processes: Friend or Foe. Front Immunol. 2022;12(January):1–14.

45. Pucino V, Certo M, Bulusu V, Cucchi D, Goldmann K, Pontarini E, et al. Lactate Buildup at the Site of Chronic Inflammation Promotes Disease by Inducing CD4+ T Cell Metabolic Rewiring. Cell Metab [Internet]. 2019;30(6):1055-1074.e8. Available from: https://doi.org/10.1016/j.cmet.2019.10.004

46. Proia P, di Liegro CM, Schiera G, Fricano A, Di Liegro I. Lactate as a metabolite and a regulator in the central nervous system. Int J Mol Sci. 2016;17(9).

47. Karagiannis A, Gallopin T, Lacroix A, Plaisier F, Piquet J, Geoffroy H, et al. Lactate is an energy substrate for rodent cortical neurons and enhances their firing activity. Elife. 2021;10:1–40.

48. Bozzo L, Puyal J, Chatton JY. Lactate Modulates the Activity of Primary Cortical Neurons through a Receptor-Mediated Pathway. PLoS One. 2013;8(8):1–9.

49. Sfera A, Klein C, Anton JJ, Kozlakidis Z, Andronescu C V. The Role of Lactylation in Mental Illness: Emphasis on Microglia. Neuroglia. 2023;4(2):119–40.

50. Chen X, Zhang Y, Wang H, Liu L, Li W, Xie P. The regulatory effects of lactic acid on neuropsychiatric disorders. Discov Ment Heal [Internet]. 2022;2(1). Available from: https://doi.org/10.1007/s44192-022-00011-4

51. Wang J, Lu T, Gui Y, Zhang X, Cao X, Li Y, et al. HSPA12A controls cerebral lactate homeostasis to maintain hippocampal neurogenesis and mood stabilization. Transl Psychiatry. 2023;13(1):1–11.

52. Lemasters JJ, Holmuhamedov E. Voltage-dependent anion channel (VDAC) as mitochondrial governator - Thinking outside the box. Biochim Biophys Acta - Mol Basis Dis. 2006;1762(2):181–90.

53. Nolfi-Donegan D, Braganza A, Shiva S. Mitochondrial electron transport chain: Oxidative phosphorylation, oxidant production, and methods of measurement. Redox Biol [Internet]. 2020;37:101674. Available from: https://doi.org/10.1016/j.redox.2020.101674

54. Neupane P, Bhuju S, Thapa N, Bhattarai HK. ATP Synthase: Structure, Function and Inhibition. Biomol Concepts. 2019;10(1):1–10.

55. Rich PR. The molecular machinery of Keilin's respiratory chain. Biochem Soc Trans. 2003;31(6):1095–105.

56. Hagen T, Lagace CJ, Modica-Napolitano JS, Aprille JR. Permeability transition in rat liver mitochondria is modulated by the ATP-Mg/Pi carrier. Am J Physiol - Gastrointest Liver Physiol. 2003;285(2 48-2).

57. Houten SM, Violante S, Ventura F V., Wanders RJA. The Biochemistry and Physiology of Mitochondrial Fatty Acid β-Oxidation and Its Genetic Disorders. Annu Rev Physiol. 2016;78:23–44.

58. Schlaepfer IR, Joshi M. CPT1A-mediated Fat Oxidation, Mechanisms, and Therapeutic Potential [Internet]. Vol. 161, Endocrinology (United States). Endocrine Society; 2020 [cited 2021 Jun 3]. Available from: https://pubmed.ncbi.nlm.nih.gov/31900483/

59. Console L, Scalise M, Giangregorio N, Tonazzi A, Barile M, Indiveri C. The Link Between the Mitochondrial Fatty Acid Oxidation Derangement and Kidney Injury. Front Physiol. 2020;11(July):1–7.

60. Yao CH, Liu GY, Wang R, Moon SH, Gross RW, Patti GJ. Identifying off-target effects of etomoxir reveals that carnitine palmitoyltransferase i is essential for cancer cell proliferation independent of β-oxidation. PLoS Biol. 2018;16(3):1–26.

61. Chandel NS. Amino acid metabolism. Cold Spring Harb Perspect Biol. 2021;13(4):1–18.

62. Beard E, Lengacher S, Dias S, Magistretti PJ, Finsterwald C. Astrocytes as Key Regulators of Brain Energy Metabolism: New Therapeutic Perspectives. Front Physiol. 2022;12(January).

63. Barres BA. The Mystery and Magic of Glia: A Perspective on Their Roles in Health and Disease. Neuron [Internet]. 2008;60(3):430–40. Available from: http://dx.doi.org/10.1016/j.neuron.2008.10.013

64. Kennedy MB. Synaptic signaling in learning and memory. Cold Spring Harb Perspect Biol. 2016;8(2):1–16.

65. Ikeda K, Kawakami K, Onimaru H, Okada Y, Yokota S, Koshiya N, et al. The respiratory control mechanisms in the brainstem and spinal cord: integrative views of the neuroanatomy and neurophysiology. J Physiol Sci. 2017;67(1):45–62.

66. Sternson SM, Eiselt AK. Three Pillars for the Neural Control of Appetite. Annu Rev Physiol. 2017;79:401–23.

67. Baik JH. Dopaminergic control of the feeding circuit. Endocrinol Metab. 2021;36(2):229–39.

68. Ehrlich A. Neural control of feeding behavior. Psychol Bull. 1964;61(2):100–14.

69. Strope TA, Birky CJ, Wilkins HM. The Role of Bioenergetics in Neurodegeneration. Int J Mol Sci. 2022;23(16):1–15.

70. Gallo G. The bioenergetics of neuronal morphogenesis and regeneration: Frontiers beyond the mitochondrion. Dev Neurobiol. 2020;80(7–8):263–76.

71. Herrero-Mendez A, Almeida A, Fernández E, Maestre C, Moncada S, Bolaños JP. The bioenergetic and antioxidant status of neurons is controlled by continuous degradation of a key glycolytic enzyme by APC/C-Cdh1. Nat Cell Biol. 2009;11(6):747–52.

72. Bolaños JP. Bioenergetics and redox adaptations of astrocytes to neuronal activity. J Neurochem. 2016;139:115–25.

73. Yellen G. Fueling thought: Management of glycolysis and oxidative phosphorylation in neuronal metabolism. J Cell Biol. 2018;217(7):2235–46.

74. Zheng X, Boyer L, Jin M, Mertens J, Kim Y, Ma L, et al. Metabolic reprogramming during neuronal differentiation from aerobic glycolysis to neuronal oxidative phosphorylation. Elife. 2016;5(JUN2016):1–25.

75. Rasband MN. Glial contributions to neural function and disease. Mol Cell Proteomics [Internet]. 2016;15(2):355–61. Available from: http://dx.doi.org/10.1074/mcp.R115.053744

76. Weightman Potter PG, Vlachaki Walker JM, Robb JL, Chilton JK, Williamson R, Randall AD, et al. Basal fatty acid oxidation increases after recurrent low glucose in human primary astrocytes. Diabetologia. 2019;62(1):187–98.

77. Afridi R, Kim JH, Rahman MH, Suk K. Metabolic Regulation of Glial Phenotypes: Implications in Neuron–Glia Interactions and Neurological Disorders. Front Cell Neurosci. 2020;14(February):1–17.

78. MacVicar BA, Choi HB. Astrocytes Provide Metabolic Support for Neuronal Synaptic Function in Response to Extracellular K+. Neurochem Res. 2017;42(9):2588–94.

79. Bonvento G, Bolaños JP. Astrocyte-neuron metabolic cooperation shapes brain activity. Cell Metab. 2021;33(8):1546–64.

80. Verkhratsky A, Nedergaard M. Physiology of astroglia. Physiol Rev. 2018;98(1):239–389.

81. Verkhratsky A, Parpura V. Recent advances in (patho)physiology of astroglia. Acta Pharmacol Sin. 2010;31(9):1044–54.

82. Verkhratsky A. Glial calcium signaling in physiology and pathophysiology. Acta Pharmacol Sin. 2006;27(7):773–80.

83. Fields RD, Stevens-graham B. New Insights into Neuron-Glia Communication. 2002;298(October):556–63.

84. Nägler K, Mauch DH, Pfrieger FW. Glia-derived signals induce synapse formation in neurones of the rat central nervous system. J Physiol.

2001;533(3):665–79.

85. Pfrieger FW. Roles of glial cells in synapse development. Cell Mol Life Sci. 2009;66(13):2037–47.

86. Um JW. Roles of glial cells in sculpting inhibitory synapses and neural circuits. Front Mol Neurosci. 2017;10(November):1–8.

87. Lee E, Chung WS. Glial control of synapse number in healthy and diseased brain. Front Cell Neurosci. 2019;13(February):1–8.

88. Kim SK, Nabekura J, Koizumi S. Astrocyte-mediated synapse remodeling in the pathological brain. Glia. 2017;65(11):1719–27.

89. Morant-Ferrando B, Jimenez-Blasco D, Alonso-Batan P, Agulla J, Lapresa R, Garcia-Rodriguez D, et al. Fatty acid oxidation organizes mitochondrial supercomplexes to sustain astrocytic ROS and cognition. Nat Metab. 2023;5(August).

90. Hirrlinger J, Nimmerjahn A. A perspective on astrocyte regulation of neural circuit function and animal behavior. Glia. 2022;70(8):1554–80.

91. Chen N, Sugihara H, Kim J, Fu Z, Barak B, Sur M, et al. Direct modulation of GFAP-expressing glia in the arcuate nucleus bi-directionally regulates feeding. Elife. 2016;5(OCTOBER2016):1–21.

92. Piirainen S, Chithanathan K, Bisht K, Piirsalu M, Savage JC, Tremblay ME, et al. Microglia contribute to social behavioral adaptation to chronic stress. Glia. 2021;69(10):2459–73.

93. Damulewicz M, Doktór B, Baster Z, Pyza E. The Role of Glia Clocks in the Regulation of Sleep in Drosophila melanogaster. J Neurosci. 2022;42(36):6848–60.

94. Mastorakos P, McGavern D. The anatomy and immunology of vasculature in the central nervous system. Sci Immunol. 2019;4(37):1–15.

95. Bell AH, Miller SL, Castillo-Melendez M, Malhotra A. The Neurovascular Unit: Effects of Brain Insults During the Perinatal Period. Front Neurosci. 2020;13(January):1–19.

96. Muldoon LL, Alvarez JI, Begley DJ, Boado RJ, Del Zoppo GJ, Doolittle ND,

et al. Immunologic privilege in the central nervous system and the blood-brain barrier. J Cereb Blood Flow Metab. 2013;33(1):13–21.

97. Mishra A, Reynolds JP, Chen Y, Gourine A V., Rusakov DA, Attwell D. Astrocytes mediate neurovascular signaling to capillary pericytes but not to arterioles. Nat Neurosci. 2016;19(12):1619–27.

98. Li Z, McConnell HL, Stackhouse TL, Pike MM, Zhang W, Mishra A. Increased 20-HETE Signaling Suppresses Capillary Neurovascular Coupling After Ischemic Stroke in Regions Beyond the Infarct. Front Cell Neurosci. 2021;15(November):1–15.

99. Hall CN, Reynell C, Gesslein B, Hamilton NB, Mishra A, Sutherland BA, et al. Capillary pericytes regulate cerebral blood flow in health and disease. Nature [Internet]. 2014;508(1):55–60. Available from: http://dx.doi.org/10.1038/nature13165

100. Aloisi F. Immune function of microglia. Glia. 2001;36(2):165–79.

101. Colonna M, Butovsky O. Microglia function in the central nervous system during health and neurodegeneration. Annu Rev Immunol. 2017;35:441–68.

102. Giovannoni F, Quintana FJ. The Role of Astrocytes in CNS Inflammation. Trends Immunol. 2020;41(9):805–19.

103. Yang Q qiao, Zhou J wei. Neuroinflammation in the central nervous system: Symphony of glial cells. Glia. 2019;67(6):1017–35.

104. Liddelow SA, Guttenplan KA, Clarke LE, Bennett FC, Bohlen CJ, Schirmer L, et al. Neurotoxic reactive astrocytes are induced by activated microglia. Nat Publ Gr [Internet]. 2017;541(7638):481–7. Available from: http://dx.doi.org/10.1038/nature21029

105. Liddelow SA, Marsh SE, Stevens B. Microglia and Astrocytes in Disease: Dynamic Duo or Partners in Crime? Trends Immunol [Internet]. 2020;41(9):820–35. Available from: https://doi.org/10.1016/j.it.2020.07.006

106. Paolicelli RC, Bolasco G, Pagani F, Maggi L, Scianni M, Panzanelli P, et al. Synaptic pruning by microglia is necessary for normal brain development. Science (80-). 2011;333(6048):1456–8.

107. Rasband MN, Peles E. The nodes of Ranvier: Molecular assembly and maintenance. Cold Spring Harb Perspect Biol. 2016;8(3):1–16.

108. Almeida RG, Pan S, Cole KLH, Williamson JM, Early JJ, Czopka T, et al. Myelination of Neuronal Cell Bodies when Myelin Supply Exceeds Axonal Demand. Curr Biol [Internet]. 2018;28(8):1296-1305.e5. Available from: https://doi.org/10.1016/j.cub.2018.02.068

109. Hughes AN, Appel B. Oligodendrocytes express synaptic proteins that modulate myelin sheath formation. Nat Commun [Internet]. 2019;10(1):1–15. Available from: http://dx.doi.org/10.1038/s41467-019-12059-y

110. Gerhards R, Pfeffer LK, Lorenz J, Starost L, Nowack L, Thaler FS, et al. Oligodendrocyte myelin glycoprotein as a novel target for pathogenic autoimmunity in the CNS. Acta Neuropathol Commun [Internet]. 2020;8(1):1–17. Available from: https://doi.org/10.1186/s40478-020-01086-2

111. Nickel M, Gu C. Regulation of central nervous system myelination in higher brain functions. Neural Plast. 2018;2018.

112. Langlet F. Tanycytes: A Gateway to the Metabolic Hypothalamus. J Neuroendocrinol. 2014;26(11):753–60.

113. Bolborea M, Dale N. Hypothalamic tanycytes: Potential roles in the control of feeding and energy balance. Trends Neurosci [Internet]. 2013;36(2):91–100. Available from: http://dx.doi.org/10.1016/j.tins.2012.12.008

114. Porniece Kumar M, Cremer AL, Klemm P, Steuernagel L, Sundaram S, Jais A, et al. Insulin signalling in tanycytes gates hypothalamic insulin uptake and regulation of AgRP neuron activity. Nat Metab. 2021;3(12):1662–79.

115. Imbernon M, Saponaro C, Helms HCC, Duquenne M, Fernandois D, Deligia E, et al. Tanycytes control hypothalamic liraglutide uptake and its anti-obesity actions. Cell Metab. 2022;34(7):1054-1063.e7.

116. Elizondo-Vega RJ, Recabal A, Oyarce K. Nutrient sensing by hypothalamic tanycytes. Front Endocrinol (Lausanne). 2019;10(MAR).

117. Jurga AM, Paleczna M, Kadluczka J, Kuter KZ. Beyond the GFAP-

astrocyte protein markers in the brain. Biomolecules. 2021;11(9).

118. Du J, Yi M, Zhou F, He W, Yang A, Qiu M, et al. S100B is selectively expressed by gray matter protoplasmic astrocytes and myelinating oligodendrocytes in the developing CNS. Mol Brain [Internet]. 2021;14(1):1–11. Available from: https://doi.org/10.1186/s13041-021-00865-9

119. Liddelow SA, Barres BA. Reactive Astrocytes: Production, Function, and Therapeutic Potential. Immunity [Internet]. 2017;46(6):957–67. Available from: http://dx.doi.org/10.1016/j.immuni.2017.06.006

120. Beyer F, Lüdje W, Karpf J, Saher G, Beckervordersandforth R. Distribution of Aldh1L1-CreERT2 Recombination in Astrocytes Versus Neural Stem Cells in the Neurogenic Niches of the Adult Mouse Brain. Front Neurosci. 2021;15(September):1–10.

121. Zhang Z, Ma Z, Zou W, Guo H, Liu M, Ma Y, et al. The Appropriate Marker for Astrocytes: Comparing the Distribution and Expression of Three Astrocytic Markers in Different Mouse Cerebral Regions. Biomed Res Int. 2019;2019.

122. O'Leary LA, Davoli MA, Belliveau C, Tanti A, Ma JC, Farmer WT, et al. Characterization of Vimentin-Immunoreactive Astrocytes in the Human Brain. Front Neuroanat. 2020;14(July).

123. Schildge S, Bohrer C, Beck K, Schachtrup C. Isolation and culture of mouse cortical astrocytes. J Vis Exp. 2013;(71):1–7.

124. Weightman Potter PG, Ellacott KLJ, Randall AD, Beall C. Glutamate Prevents Altered Mitochondrial Function Following Recurrent Low Glucose in Hypothalamic but Not Cortical Primary Rat Astrocytes. Cells. 2022;11(21).

125. Peterson AR, Binder DK. Astrocyte Glutamate Uptake and Signaling as Novel Targets for Antiepileptogenic Therapy. Front Neurol. 2020;11(September):1–7.

126. Kellner V, Kersbergen CJ, Li S, Babola TA, Saher G, Bergles DE. Dual metabotropic glutamate receptor signaling enables coordination of

astrocyte and neuron activity in developing sensory domains. Neuron [Internet]. 2021;109(16):2545-2555.e7. Available from: https://doi.org/10.1016/j.neuron.2021.06.010

127. Martinez D, Rogers RC, Hermann GE, Hasser EM, Kline DD. Astrocytic glutamate transporters reduce the neuronal and physiological influence of metabotropic glutamate receptors in nucleus tractus solitarii. Am J Physiol Regul Integr Comp Physiol. 2020;318(3):R545–64.

128. Mölders A, Koch A, Menke R, Klöcker N. Heterogeneity of the astrocytic AMPA-receptor transcriptome. Glia. 2018;66(12):2604–16.

129. Jimenez-Blasco D, Santofimia-Castanõ P, Gonzalez A, Almeida A, Bolanõs JP. Astrocyte NMDA receptors' activity sustains neuronal survival through a Cdk5-Nrf2 pathway. Cell Death Differ. 2015;22(11):1877–89.

130. Boddum K, Jensen TP, Magloire V, Kristiansen U, Rusakov DA, Pavlov I, et al. Astrocytic GABA transporter activity modulates excitatory neurotransmission. Nat Commun [Internet]. 2016;7:1–10. Available from: http://dx.doi.org/10.1038/ncomms13572

131. Sun XL, Zeng XN, Zhou F, Dai CP, Ding JH, Hu G. KATP channel openers facilitate glutamate uptake by GluTs in rat primary cultured astrocytes. Neuropsychopharmacology. 2008;33(6):1336–42.

132. Wang J, Li Z, Feng M, Ren K, Shen G, Zhao C, et al. Opening of Astrocytic Mitochondrial ATP-Sensitive Potassium Channels Upregulates Electrical Coupling between Hippocampal Astrocytes in Rat Brain Slices. PLoS One. 2013;8(2).

133. Hariharan A, Robertson CD, Garcia DCG, Longden TA. Brain capillary pericytes are metabolic sentinels that control blood flow through a KATP channel-dependent energy switch. Cell Rep [Internet]. 2022;41(13):111872. Available from: https://doi.org/10.1016/j.celrep.2022.111872

134. de Ceglia R, Ledonne A, Litvin DG, Lind BL, Carriero G, Latagliata EC, et al. Specialized astrocytes mediate glutamatergic gliotransmission in the CNS. Nature. 2023;622(October).

135. Cuellar-Santoyo AO, Ruiz-Rodríguez VM, Mares-Barbosa TB, Patrón-Soberano A, Howe AG, Portales-Pérez DP, et al. Revealing the contribution of astrocytes to glutamatergic neuronal transmission. Front Cell Neurosci. 2023;16(January):1–15.

136. Liu JH, Li ZL, Liu YS, Chu H De, Hu NY, Wu DY, et al. Astrocytic GABAB Receptors in Mouse Hippocampus Control Responses to Behavioral Challenges through Astrocytic BDNF. Neurosci Bull [Internet]. 2020;36(7):705–18. Available from: https://doi.org/10.1007/s12264-020-00474-x

137. Liu J, Feng X, Wang Y, Xia X, Zheng JC. Astrocytes: GABAceptive and GABAergic Cells in the Brain. Front Cell Neurosci. 2022;16(June):1–12.

138. Ou Z, Ma Y, Sun Y, Zheng G, Wang S, Xing R, et al. A GPR17-cAMP-Lactate Signaling Axis in Oligodendrocytes Regulates Whole-Body Metabolism. Cell Rep [Internet]. 2019;26(11):2984-2997.e4. Available from: https://doi.org/10.1016/j.celrep.2019.02.060

139. Rabinowitz JD, Enerbäck S. Lactate: the ugly duckling of energy metabolism. Nat Metab [Internet]. 2020;2(7):566–71. Available from: http://dx.doi.org/10.1038/s42255-020-0243-4

140. Jones W, Bianchi K. Aerobic glycolysis: Beyond proliferation. Front Immunol. 2015;6(MAY):1–5.

141. Takahashi S. Neuroprotective function of high glycolytic activity in astrocytes: Common roles in stroke and neurodegenerative diseases. Int J Mol Sci. 2021;22(12).

142. Horvat A, Zorec R, Vardjan N. Lactate as an Astroglial Signal Augmenting Aerobic Glycolysis and Lipid Metabolism. Front Physiol. 2021;12(September).

143. Vardjan N, Chowdhury HH, Horvat A, Velebit J, Malnar M, Muhič M, et al. Enhancement of astroglial aerobic glycolysis by extracellular lactate-mediated increase in cAMP. Front Mol Neurosci. 2018;11(May):1–15.

144. Rumpf S, Sanal N, Marzano M. Energy metabolic pathways in neuronal development and function. Oxford Open Neurosci. 2023;2(March):1–7.

145. Hall CN, Klein-Flügge MC, Howarth C, Attwell D. Oxidative phosphorylation, not glycolysis, powers presynaptic and postsynaptic mechanisms underlying brain information processing. J Neurosci. 2012;32(26):8940–51.

146. Song S, Yu L, Hasan MN, Paruchuri SS, Mullett SJ, Sullivan MLG, et al. Elevated microglial oxidative phosphorylation and phagocytosis stimulate post-stroke brain remodeling and cognitive function recovery in mice. Commun Biol. 2022;5(1):1–15.

147. Matsui T, Omuro H, Liu YF, Soya M, Shima T, Mcewen BS, et al. Astrocytic glycogen-derived lactate fuels the brain during exhaustive exercise to maintain endurance capacity. Proc Natl Acad Sci U S A. 2017;114(24):6358–63.

148. Bak LK, Walls AB. Astrocytic glycogen metabolism in the healthy and diseased brain. J Biol Chem [Internet]. 2018;293(19):7108–16. Available from: http://dx.doi.org/10.1074/jbc.R117.803239

149. Newman LA, Korol DL, Gold PE. Lactate produced by glycogenolysis in astrocytes regulates memory processing. PLoS One. 2011;6(12).

150. Descalzi G, Gao V, Steinman MQ, Suzuki A, Alberini CM. Lactate from astrocytes fuels learning-induced mRNA translation in excitatory and inhibitory neurons. Commun Biol [Internet]. 2019;2(1). Available from: http://dx.doi.org/10.1038/s42003-019-0495-2

151. Iqbal Z, Liu S, Lei Z, Ramkrishnan AS, Akter M, Li Y. Astrocyte L-Lactate Signaling in the ACC Regulates Visceral Pain Aversive Memory in Rats. Cells. 2023;12(1).

152. Lezmy J. How astrocytic ATP shapes neuronal activity and brain circuits. Curr Opin Neurobiol [Internet]. 2023;79:102685. Available from: https://doi.org/10.1016/j.conb.2023.102685

153. Zhang JM, Wang HK, Ye CQ, Ge W, Chen Y, Jiang ZL, et al. ATP Released by Astrocytes Mediates Glutamatergic Activity-Dependent Heterosynaptic Suppression. Neuron. 2003;40(5):971–82.

154. Verderio C, Matteoli M. ATP Mediates Calcium Signaling Between

Astrocytes and Microglial Cells: Modulation by IFN-γ. J Immunol. 2001;166(10):6383–91.

155. Xiong Y, Sun S, Teng S, Jin M, Zhou Z. Ca2+-Dependent and Ca2+-Independent ATP Release in Astrocytes. Front Mol Neurosci. 2018;11(July):1–5.

156. Peng W, Liu X, Ma G, Wu Z, Wang Z, Fei X, et al. Adenosine-independent regulation of the sleep–wake cycle by astrocyte activity. Cell Discov. 2023;9(1).

157. Yang L, Qi Y, Yang Y. Astrocytes Control Food Intake by Inhibiting AGRP Neuron Activity via Adenosine A1 Receptors. Cell Rep [Internet]. 2015;11(5):798–807. Available from: http://dx.doi.org/10.1016/j.celrep.2015.04.002

158. Di Virgilio F, Vultaggio-Poma V, Falzoni S, Giuliani AL. Extracellular ATP: A powerful inflammatory mediator in the central nervous system. Neuropharmacology [Internet]. 2023;224(October 2022):109333. Available from: https://doi.org/10.1016/j.neuropharm.2022.109333

159. Cotrina ML, Nedergaard M. ATP as a messenger in astrocyte-neuronal communication. Neuroscientist. 2000;6(2):120–6.

160. Guthrie PB, Knappenberger J, Segal M, Bennett MVL, Charles AC, Kater SB. ATP released from astrocytes mediates glial calcium waves. J Neurosci. 1999;19(2):520–8.

161. Koizumi S, Fujishita K, Inoue K. Regulation of cell-to-cell communication mediated by astrocytic ATP in the CNS. Purinergic Signal. 2005;1(3):211–7.

162. Abbott NJ, Rönnbäck L, Hansson E. Astrocyte-endothelial interactions at the blood-brain barrier. Nat Rev Neurosci. 2006;7(1):41–53.

163. Cabezas R, Ávila M, Gonzalez J, El-Bachá RS, Báez E, García-Segura LM, et al. Astrocytic modulation of blood brain barrier: Perspectives on Parkinson's disease. Front Cell Neurosci. 2014;8(AUG):1–11.

164. Didier N, Romero IA, Créminon C, Wijkhuisen A, Grassi J, Mabondzo A. Secretion of interleukin-1β by astrocytes mediates endothelin-1 and tumour

necrosis factor-α effects on human brain microvascular endothelial cell permeability. J Neurochem. 2003;86(1):246–54.

165. Díaz-Castro B, Robel S, Mishra A. Astrocyte Endfeet in Brain Function and Pathology: Open Questions. Annu Rev Neurosci. 2023;46:101–21.

166. Stokum JA, Shim B, Huang W, Kane M, Smith JA, Gerzanich V, et al. A large portion of the astrocyte proteome is dedicated to perivascular endfeet, including critical components of the electron transport chain. J Cereb Blood Flow Metab. 2021;41(10):2546–60.

167. Robb JL, Hammad NA, Weightman Potter PG, Chilton JK, Beall C, Ellacott KLJ. The metabolic response to inflammation in astrocytes is regulated by nuclear factor-kappa B signaling. Glia. 2020;68(11):2246–63.

168. Ioghen O, Chițoiu L, Gherghiceanu M, Ceafalan LC, Hinescu ME. CD36 – A novel molecular target in the neurovascular unit. Eur J Neurosci. 2021;53(8):2500–10.

169. Ebrahimi M, Yamamoto Y, Sharifi K, Kida H, Kagawa Y, Yasumoto Y, et al. Astrocyte-expressed FABP7 regulates dendritic morphology and excitatory synaptic function of cortical neurons. Glia. 2016;64(1):48–62.

170. Konings SC, Torres-Garcia L, Martinsson I, Gouras GK. Astrocytic and Neuronal Apolipoprotein E Isoforms Differentially Affect Neuronal Excitability. Front Neurosci. 2021;15(September):1–16.

171. Jackson RJ, Meltzer JC, Nguyen H, Commins C, Bennett RE, Hudry E, et al. APOE4 derived from astrocytes leads to blood-brain barrier impairment. Brain. 2022;145(10):3582–93.

172. Lanfranco MF, Sepulveda J, Kopetsky G, Rebeck GW. Expression and secretion of apoE isoforms in astrocytes and microglia during inflammation. Glia. 2021;69(6):1478–93.

173. Lenart B, Kintner DB, Shull GE, Sun D. Na-K-Cl cotransporter-mediated intracellular Na+ accumulation affects Ca2+ signaling in astrocytes in an In vitro ischemic model. J Neurosci. 2004;24(43):9585–97.

174. Jayakumar AR, Norenberg MD. The Na-K-Cl Co-transporter in astrocyte swelling. Metab Brain Dis. 2010;25(1):31–8.

175. Christie IN, Theparambil SM, Braga A, Doronin M, Hosford PS, Brazhe A, et al. Astrocytes produce nitric oxide via nitrite reduction in mitochondria to regulate cerebral blood flow during brain hypoxia. Cell Rep [Internet]. 2023;42(12):113514. Available from: https://doi.org/10.1016/j.celrep.2023.113514

176. Lu L, Hogan-Cann AD, Globa AK, Lu P, Nagy JI, Bamji SX, et al. Astrocytes drive cortical vasodilatory signaling by activating endothelial NMDA receptors. J Cereb Blood Flow Metab. 2019;39(3):481–96.

177. Linnerbauer M, Wheeler MA, Quintana FJ. Astrocyte Crosstalk in CNS Inflammation. Neuron [Internet]. 2020;108(4):608–22. Available from: https://doi.org/10.1016/j.neuron.2020.08.012

178. Choi SS, Lee HJ, Lim I, Satoh JI, Kim SU. Human astrocytes: Secretome profiles of cytokines and chemokines. PLoS One. 2014;9(4).

179. Shinozaki Y, Shibata K, Yoshida K, Shigetomi E, Gachet C, Ikenaka K, et al. Transformation of Astrocytes to a Neuroprotective Phenotype by Microglia via P2Y1 Receptor Downregulation. Cell Rep [Internet]. 2017;19(6):1151–64. Available from: http://dx.doi.org/10.1016/j.celrep.2017.04.047

180. Yilmaz C, Karali K, Fodelianaki G, Gravanis A, Chavakis T, Charalampopoulos I, et al. Neurosteroids as regulators of neuroinflammation. Front Neuroendocrinol. 2019;55(June).

181. Chen Y, Qin C, Huang J, Tang X, Liu C, Huang K, et al. The role of astrocytes in oxidative stress of central nervous system: A mixed blessing. Cell Prolif. 2020;53(3):1–13.

182. Sheng WS, Hu S, Feng A, Rock RB. Reactive oxygen species from human astrocytes induced functional impairment and oxidative damage. Neurochem Res. 2013;38(10):2148–59.

183. Bellesi M, Vivo L De, Chini M, Gilli F, Tononi G, Cirelli C. Sleep loss promotes astrocytic phagocytosis and microglial activation in mouse cerebral cortex. J Neurosci. 2017;37(21):5263–73.

184. Konishi H, Koizumi S, Kiyama H. Phagocytic astrocytes: Emerging from the

shadows of microglia. Glia. 2022;70(6):1009–26.

185. Morizawa YM, Hirayama Y, Ohno N, Shibata S, Shigetomi E, Sui Y, et al. Reactive astrocytes function as phagocytes after brain ischemia via ABCA1-mediated pathway. Nat Commun [Internet]. 2017;8(1):1–14. Available from: http://dx.doi.org/10.1038/s41467-017-00037-1

186. Hart CG, Karimi-Abdolrezaee S. Recent insights on astrocyte mechanisms in CNS homeostasis, pathology, and repair. J Neurosci Res. 2021;99(10):2427–62.

187. Magistretti PJ, Pellerin L. Astrocytes couple synaptic activity to glucose utilization in the brain. News Physiol Sci. 1999;14(5):177–82.

188. Pellerin L, Magistretti PJ. Sweet sixteen for ANLS. J Cereb Blood Flow Metab. 2012;32(7):1152–66.

189. Lundgaard I, Li B, Xie L, Kang H, Sanggaard S, Haswell JDR, et al. Direct neuronal glucose uptake heralds activity-dependent increases in cerebral metabolism. Nat Commun. 2015;6.

190. Perez-Catalan NA, Doe CQ, Ackerman SD. The role of astrocyte-mediated plasticity in neural circuit development and function. Neural Dev. 2021;16(1):1–14.

191. Erlichman JS, Hewitt A, Damon TL, Hart M, Kurascz J, Li A, et al. Inhibition of monocarboxylate transporter 2 in the retrotrapezoid nucleus in rats: A test of the astrocyte-neuron lactate-shuttle hypothesis. J Neurosci. 2008;28(19):4888–96.

192. Mason S. Lactate shuttles in neuroenergetics-homeostasis, allostasis and beyond. Front Neurosci. 2017;11(FEB):1–15.

193. Bhatti MS, Frostig RD. Astrocyte-neuron lactate shuttle plays a pivotal role in sensory-based neuroprotection in a rat model of permanent middle cerebral artery occlusion. Sci Rep [Internet]. 2023;13(1):1–15. Available from: https://doi.org/10.1038/s41598-023-39574-9

194. Muraleedharan R, Gawali M V., Tiwari D, Sukumaran A, Oatman N, Anderson J, et al. AMPK-Regulated Astrocytic Lactate Shuttle Plays a Non-Cell-Autonomous Role in Neuronal Survival. Cell Rep. 2020;32(9).

195. Rossi MJ, Pekkurnaz G. Powerhouse of the mind: mitochondrial plasticity at the synapse. Curr Opin Neurobiol [Internet]. 2019;57:149–55. Available from: https://doi.org/10.1016/j.conb.2019.02.001

196. Bernardinelli Y, Randall J, Janett E, Nikonenko I, König S, Jones EV, et al. Activity-dependent structural plasticity of perisynaptic astrocytic domains promotes excitatory synapse stability. Curr Biol. 2014;24(15):1679–88.

197. Derouiche A, Haselau J, Korf H. Fine Astrocyte Processes Contain Very Small Mitochondria: Glial Oxidative Capability May Fuel Transmitter Metabolism. 2015;2402–13. Available from: https://link.springer.com/article/10.1007/s11064-015-1563-8

198. Wilson JE. Isozymes of mammalian hexokinase: Structure, subcellular localization and metabolic function. J Exp Biol. 2003;206(12):2049–57.

199. Almeida A, Moncada S, Bolaños JP. Nitric oxide switches on glycolysis through the AMP protein kinase and 6-phosphofructo-2-kinase pathway. Nat Cell Biol. 2004;6(1):45–51.

200. Sterpka A, Yang J, Strobel M, Zhou Y, Pauplis C, Chen X. Diverged morphology changes of astrocytic and neuronal primary cilia under reactive insults. Mol Brain. 2020;13(1):1–16.

201. Zhou B, Zuo YX, Jiang RT. Astrocyte morphology: Diversity, plasticity, and role in neurological diseases. CNS Neurosci Ther. 2019;25(6):665–73.

202. Schiweck J, Eickholt BJ, Murk K. Important shapeshifter: Mechanisms allowing astrocytes to respond to the changing nervous system during development, injury and disease. Front Cell Neurosci. 2018;12(August):1–17.

203. Baldwin KT, Murai KK, Khakh BS. Astrocyte morphology. Trends Cell Biol [Internet]. 2023;xx(xx):1–19. Available from: https://doi.org/10.1016/j.tcb.2023.09.006

204. Gorina Y V., Salmina AB, Erofeev AI, Can Z, Bolshakova A V., Balaban PM, et al. Metabolic Plasticity of Astrocytes. J Evol Biochem Physiol. 2021;57(6):1207–24.

205. Morita M, Ikeshima-Kataoka H, Kreft M, Vardjan N, Zorec R, Noda M.

Metabolic plasticity of astrocytes and aging of the brain. Int J Mol Sci. 2019;20(4).

206. Jernberg JN, Bowman CE, Wolfgang MJ, Scafidi S. Developmental regulation and localization of carnitine palmitoyltransferases (CPTs) in rat brain. J Neurochem. 2017;142(3):407–19.

207. Bernier LP, York EM, Kamyabi A, Choi HB, Weilinger NL, MacVicar BA. Microglial metabolic flexibility supports immune surveillance of the brain parenchyma. Nat Commun [Internet]. 2020;11(1). Available from: http://dx.doi.org/10.1038/s41467-020-15267-z

208. Panov A, Orynbayeva Z, Vavilin V, Lyakhovich V. Fatty acids in energy metabolism of the central nervous system. Biomed Res Int. 2014;2014.

209. Rose J, Brian C, Pappa A, Panayiotidis MI, Franco R. Mitochondrial Metabolism in Astrocytes Regulates Brain Bioenergetics, Neurotransmission and Redox Balance. Front Neurosci. 2020;14(November):1–20.

210. Ioannou MS, Jackson J, Sheu SH, Chang CL, Weigel A V., Liu H, et al. Neuron-Astrocyte Metabolic Coupling Protects against Activity-Induced Fatty Acid Toxicity. Cell [Internet]. 2019;177(6):1522-1535.e14. Available from: https://doi.org/10.1016/j.cell.2019.04.001

211. Andersen J V., Christensen SK, Westi EW, Diaz-delCastillo M, Tanila H, Schousboe A, et al. Deficient astrocyte metabolism impairs glutamine synthesis and neurotransmitter homeostasis in a mouse model of Alzheimer's disease. Neurobiol Dis [Internet]. 2021;148(November 2020):105198. Available from: https://doi.org/10.1016/j.nbd.2020.105198

212. Newsholme P, Diniz VLS, Dodd GT, Cruzat V. Glutamine metabolism and optimal immune and CNS function. Proc Nutr Soc. 2022;22–31.

213. Andersen J V., Markussen KH, Jakobsen E, Schousboe A, Waagepetersen HS, Rosenberg PA, et al. Glutamate metabolism and recycling at the excitatory synapse in health and neurodegeneration. Neuropharmacology [Internet]. 2021;196(July):108719. Available from: https://doi.org/10.1016/j.neuropharm.2021.108719

214. Massucci FA, DiNuzzo M, Giove F, Maraviglia B, Castillo IP, Marinari E, et al. Energy metabolism and glutamate-glutamine cycle in the brain: A stoichiometric modeling perspective. BMC Syst Biol. 2013;7.

215. Ma G, Zhang Z, Li P, Zhang Z, Zeng M, Liang Z, et al. Reprogramming of glutamine metabolism and its impact on immune response in the tumor microenvironment. Cell Commun Signal [Internet]. 2022;20(1):1–15. Available from: https://doi.org/10.1186/s12964-022-00909-0

216. Allen SP, Hall B, Woof R, Francis L, Gatto N, Shaw AC, et al. C9orf72 expansion within astrocytes reduces metabolic flexibility in amyotrophic lateral sclerosis. Brain. 2019;142(12):3771–90.

217. Mitra S, Banik A, Saurabh S, Maulik M, Khatri SN. Neuroimmunometabolism: A New Pathological Nexus Underlying Neurodegenerative Disorders. J Neurosci. 2022;42(10):1888–907.

218. Verkhratsky A, Marutle A, Rodríguez-Arellano JJ, Nordberg A. Glial Asthenia and Functional Paralysis: A New Perspective on Neurodegeneration and Alzheimers Disease. Neuroscientist. 2015;21(5):552–68.

219. Qi G, Mi Y, Shi X, Gu H, Brinton RD, Yin F. ApoE4 Impairs Neuron-Astrocyte Coupling of Fatty Acid Metabolism. Cell Rep [Internet]. 2021;34(1):108572. Available from: https://doi.org/10.1016/j.celrep.2020.108572

220. Schönfeld P, Reiser G. How the brain fights fatty acids' toxicity. Neurochem Int. 2021;148(April).

221. Mahan TE, Wang C, Bao X, Choudhury A, Ulrich JD, Holtzman DM. Selective reduction of astrocyte apoE3 and apoE4 strongly reduces Aβ accumulation and plaque-related pathology in a mouse model of amyloidosis. Mol Neurodegener [Internet]. 2022;17(1):1–20. Available from: https://doi.org/10.1186/s13024-022-00516-0

222. Yu TS, Tensaouti Y, Stephanz EP, Chintamen S, Rafikian EE, Yang M, et al. Astrocytic ApoE underlies maturation of hippocampal neurons and cognitive recovery after traumatic brain injury in mice. Commun Biol. 2021;4(1):1–12.

223. Hara T, Umaru BA, Sharifi K, Yoshikawa T, Owada Y, Kagawa Y. Fatty acid binding protein 7 is involved in the proliferation of reactive astrocytes, but not in cell migration and polarity. Acta Histochem Cytochem. 2020;53(4):73–81.

224. Ohlrogge JB, Jaworski JG. Regulation of fatty acid synthesis. Annu Rev Plant Biol. 1997;48:109–36.

225. Dennis EA, Norris PC. Eicosanoid storm in infection and inflammation. Nat Rev Immunol. 2015;15(8):511–23.

226. Chen B, Sun Y, Niu J, Jarugumilli GK, Wu X. Protein Lipidation in Cell Signaling and Diseases: Function, Regulation, and Therapeutic Opportunities. Cell Chem Biol. 2018;25(7):817–31.

227. Hidalgo MA, Carretta MD, Burgos RA. Long Chain Fatty Acids as Modulators of Immune Cells Function: Contribution of FFA1 and FFA4 Receptors. Front Physiol. 2021;12(July):1–18.

228. Thombare K, Ntika S, Wang X, Krizhanovskii C. Long chain saturated and unsaturated fatty acids exert opposing effects on viability and function of GLP-1-producing cells: Mechanisms of lipotoxicity. PLoS One. 2017;12(5):1–14.

229. Thomas P, Leslie KA, Welters HJ, Morgan NG. Long-chain saturated fatty acid species are not toxic to human pancreatic β-cells and may offer protection against pro-inflammatory cytokine induced β-cell death. Nutr Metab [Internet]. 2021;18(1):1–7. Available from: https://doi.org/10.1186/s12986-021-00541-8

230. Thomas P, Arden C, Corcoran J, Hacker C, Welters HJ, Morgan NG. Differential routing and disposition of the long-chain saturated fatty acid palmitate in rodent vs human beta-cells. Nutr Diabetes. 2022;12(1):1–8.

231. Cornell-Bell AH, Finkbeiner SM, Cooper MS, Smith SJ. Glutamate Induces Calcium Waves in Cultured Astrocytes: Long-Range Glial Signaling. Science (80-). 1990;247(24):2–5.

232. Khakh BS, McCarthy KD. Astrocyte calcium signaling: From observations to functions and the challenges therein. Cold Spring Harb Perspect Biol.

2015;7(4):1–18.

233. Shah D, Gsell W, Wahis J, Luckett ES, Jamoulle T, Vermaercke B, et al. Astrocyte calcium dysfunction causes early network hyperactivity in Alzheimer's disease. Cell Rep. 2022;40(8).

234. Serrat R, Covelo A, Kouskoff V, Delcasso S, Ruiz-Calvo A, Chenouard N, et al. Astroglial ER-mitochondria calcium transfer mediates endocannabinoid-dependent synaptic integration. Cell Rep. 2021;37(12).

235. Babich A, Burkhardt JK. Coordinate control of cytoskeletal remodeling and calcium mobilization during T-cell activation. Immunol Rev. 2013;256(1):80–94.

236. Gasperini RJ, Pavez M, Thompson AC, Mitchell CB, Hardy H, Young KM, et al. How does calcium interact with the cytoskeleton to regulate growth cone motility during axon pathfinding? Mol Cell Neurosci [Internet]. 2017;84(July):29–35. Available from: http://dx.doi.org/10.1016/j.mcn.2017.07.006

237. Ding Z Bin, Song LJ, Wang Q, Kumar G, Yan YQ, Ma CG. Astrocytes: A double-edged sword in neurodegenerative diseases. Neural Regen Res. 2021;16(9):1702–10.

238. Douglass JD, Dorfman MD, Fasnacht R, Shaffer LD, Thaler JP. Astrocyte IKKβ/NF-κB signaling is required for diet-induced obesity and hypothalamic inflammation. Mol Metab [Internet]. 2017;6(4):366–73. Available from: http://dx.doi.org/10.1016/j.molmet.2017.01.010

239. González-García I, García-Cáceres C. Hypothalamic astrocytes as a specialized and responsive cell population in obesity. Int J Mol Sci. 2021;22(12).

240. Lau BK, Murphy-Royal C, Kaur M, Qiao M, Bains JS, Gordon GR, et al. Obesity-induced astrocyte dysfunction impairs heterosynaptic plasticity in the orbitofrontal cortex. Cell Rep [Internet]. 2021;36(7):109563. Available from: https://doi.org/10.1016/j.celrep.2021.109563

241. Buckman LB, Thompson MM, Moreno HN, Ellacott KLJ. Regional astrogliosis in the mouse hypothalamus in response to obesity. J Comp

Neurol. 2013;521(6):1322–33.

242. Sun Y, Koyama Y, Shimada S. Inflammation From Peripheral Organs to the Brain: How Does Systemic Inflammation Cause Neuroinflammation? Front Aging Neurosci. 2022;14(June):1–10.

243. Reid JK, Kuipers HF. She Doesn't Even Go Here: The Role of Inflammatory Astrocytes in CNS Disorders. Front Cell Neurosci. 2021;15(September):1–12.

244. Clark IC, Gutiérrez-Vázquez C, Wheeler MA, Li Z, Rothhammer V, Linnerbauer M, et al. Barcoded viral tracing of single-cell interactions in central nervous system inflammation. Science (80-). 2021;372(6540).

245. Gorina R, Font-Nieves M, Márquez-Kisinousky L, Santalucia T, Planas AM. Astrocyte TLR4 activation induces a proinflammatory environment through the interplay between MyD88-dependent NFκB signaling, MAPK, and Jak1/Stat1 pathways. Glia. 2011;59(2):242–55.

246. Bsibsi M, Ravid R, Gveric D, Van Noort JM. Broad expression of Toll-like receptors in the human central nervous system. J Neuropathol Exp Neurol. 2002;61(11):1013–21.

247. Liu X, Nemeth DP, McKim DB, Zhu L, DiSabato DJ, Berdysz O, et al. Cell-Type-Specific Interleukin 1 Receptor 1 Signaling in the Brain Regulates Distinct Neuroimmune Activities. Immunity [Internet]. 2019;50(2):317-333.e6. Available from: https://doi.org/10.1016/j.immuni.2018.12.012

248. Quintana A, Erta M, Ferrer B, Comes G, Giralt M, Hidalgo J. Astrocyte-specific deficiency of interleukin-6 and its receptor reveal specific roles in survival, body weight and behavior. Brain Behav Immun [Internet]. 2013;27(1):162–73. Available from: http://dx.doi.org/10.1016/j.bbi.2012.10.011

249. Gajtkó A, Bakk E, Hegedűs K, Ducza L, Holló K. IL-1β Induced Cytokine Expression by Spinal Astrocytes Can Play a Role in the Maintenance of Chronic Inflammatory Pain. Front Physiol. 2020;11(November):1–17.

250. Abd-El-Basset EM, Rao MS, Alshawaf SM, Ashkanani HK, Kabli AH. Tumor necrosis factor (TNF) induces astrogliosis, microgliosis and

promotes survival of cortical neurons. AIMS Neurosci. 2021;8(4):558–84.

251. Hyvärinen T, Hagman S, Ristola M, Sukki L, Veijula K, Kreutzer J, et al. Co-stimulation with IL-1β and TNF-α induces an inflammatory reactive astrocyte phenotype with neurosupportive characteristics in a human pluripotent stem cell model system. Sci Rep. 2019;9(1):1–15.

252. Dorf ME, Berman MA, Tanabe S, Heesen M, Luo Y. Astrocytes express functional chemokine receptors. J Neuroimmunol. 2000;111(1–2):109–21.

253. Luo X, Tai WL, Sun L, Pan Z, Xia Z, Chung SK, et al. Crosstalk between astrocytic CXCL12 and microglial CXCR4 contributes to the development of neuropathic pain. Mol Pain. 2016;12:1–15.

254. Yang XL, Wang X, Shao L, Jiang GT, Min JW, Mei XY, et al. TRPV1 mediates astrocyte activation and interleukin-1β release induced by hypoxic ischemia (HI). J Neuroinflammation. 2019;16(1):1–16.

255. Chao CC, Gutiérrez-Vázquez C, Rothhammer V, Mayo L, Wheeler MA, Tjon EC, et al. Metabolic Control of Astrocyte Pathogenic Activity via cPLA2-MAVS. Cell. 2019;179(7):1483-1498.e22.

256. Hartmann K, Sepulveda-Falla D, Rose IVL, Madore C, Muth C, Matschke J, et al. Complement 3+-astrocytes are highly abundant in prion diseases, but their abolishment led to an accelerated disease course and early dysregulation of microglia. Acta Neuropathol Commun. 2019;7(1):83.

257. Pekna M, Pekny M. The complement system: A powerful modulator and effector of astrocyte function in the healthy and diseased central nervous system. Cells. 2021;10(7).

258. Kwon HS, Koh SH. Neuroinflammation in neurodegenerative disorders: the roles of microglia and astrocytes. Transl Neurodegener. 2020;9(1):1–12.

259. Zhu G, Wang X, Chen L, Lenahan C, Fu Z, Fang Y, et al. Crosstalk Between the Oxidative Stress and Glia Cells After Stroke: From Mechanism to Therapies. Front Immunol. 2022;13(February):1–16.

260. Johnstone M, Gearing AJH, Miller KM. A central role for astrocytes in the inflammatory response to β- amyloid; chemokines, cytokines and reactive oxygen species are produced. J Neuroimmunol. 1999;93(1–2):182–93.

261. Escartin C, Galea E, Lakatos A, O'Callaghan JP, Petzold GC, Serrano-Pozo A, et al. Reactive astrocyte nomenclature, definitions, and future directions [Internet]. Vol. 24, Nature Neuroscience. Nature Research; 2021 [cited 2021 Jun 3]. p. 312–25. Available from: https://doi.org/10.1038/s41593-020-00783-4

262. Sofroniew M V. Astrocyte Reactivity: Subtypes, States, and Functions in CNS Innate Immunity. Trends Immunol [Internet]. 2020;41(9):758–70. Available from: https://doi.org/10.1016/j.it.2020.07.004

263. Chen ZP, Wang S, Zhao X, Fang W, Wang Z, Ye H, et al. Lipid-accumulated reactive astrocytes promote disease progression in epilepsy. Vol. 26, Nature Neuroscience. Springer US; 2023. 542–554 p.

264. Xiong XY, Tang Y, Yang QW. Metabolic changes favor the activity and heterogeneity of reactive astrocytes. Trends Endocrinol Metab [Internet]. 2022;33(6):390–400. Available from: https://doi.org/10.1016/j.tem.2022.03.001

265. Kang W, Balordi F, Su N, Chen L, Fishell G, Hébert JM. Astrocyte activation is suppressed in both normal and injured brain by FGF signaling. Proc Natl Acad Sci U S A. 2014;111(29).

266. Lu H, Ai L, Zhang B. TNF-α induces AQP4 overexpression in astrocytes through the NF-κB pathway causing cellular edema and apoptosis. Biosci Rep. 2022;42(3):1–13.

267. Arighi A, Arcaro M, Fumagalli GG, Carandini T, Pietroboni AM, Sacchi L, et al. Aquaporin-4 cerebrospinal fluid levels are higher in neurodegenerative dementia: looking at glymphatic system dysregulation. Alzheimer's Res Ther [Internet]. 2022;14(1):1–10. Available from: https://doi.org/10.1186/s13195-022-01077-6

268. Zhang R, Liu Y, Chen Y, Li Q, Marshall C, Wu T, et al. Aquaporin 4 deletion exacerbates brain impairments in a mouse model of chronic sleep disruption. CNS Neurosci Ther. 2020;26(2):228–39.

269. Chen Z, Yuan Z, Yang S, Zhu Y, Xue M, Zhang J, et al. Brain Energy Metabolism: Astrocytes in Neurodegenerative Diseases. CNS Neurosci Ther. 2023;29(1):24–36.

270. Kumar A, Fontana IC, Nordberg A. Reactive astrogliosis: A friend or foe in the pathogenesis of Alzheimer's disease. J Neurochem. 2023;164(3):309–24.

271. Moulson AJ, Squair JW, Franklin RJM, Tetzlaff W, Assinck P. Diversity of Reactive Astrogliosis in CNS Pathology: Heterogeneity or Plasticity? Front Cell Neurosci. 2021;15(July).

272. Gao Z, Zhu Q, Zhang Y, Zhao Y, Cai L, Shields CB, et al. Reciprocal modulation between microglia and astrocyte in reactive gliosis following the CNS injury. Mol Neurobiol. 2013;48(3):690–701.

273. Buffo A, Rite I, Tripathi P, Lepier A, Colak D, Horn AP, et al. Origin and progeny of reactive gliosis: A source of multipotent cells in the injured brain. Proc Natl Acad Sci U S A. 2008;105(9):3581–6.

274. Babcock KJ, Abdolmohammadi B, Kiernan PT, Mahar I, Cherry JD, Alvarez VE, et al. Interface astrogliosis in contact sport head impacts and military blast exposure. Acta Neuropathol Commun [Internet]. 2022;10(1):1–14. Available from: https://doi.org/10.1186/s40478-022-01358-z

275. Verkhratsky A, Rodrigues JJ, Pivoriunas A, Zorec R, Semyanov A. Astroglial atrophy in Alzheimer's disease. Pflugers Arch Eur J Physiol. 2019;471(10):1247–61.

276. Vargas MR, Johnson JA. Astrogliosis in Amyotrophic Lateral Sclerosis: Role and Therapeutic Potential of Astrocytes. Neurotherapeutics. 2010;7(4):471–81.

277. Tripathi P, Rodriguez-Muela N, Klim JR, de Boer AS, Agrawal S, Sandoe J, et al. Reactive Astrocytes Promote ALS-like Degeneration and Intracellular Protein Aggregation in Human Motor Neurons by Disrupting Autophagy through TGF-β1. Stem Cell Reports [Internet]. 2017;9(2):667–80. Available from: http://dx.doi.org/10.1016/j.stemcr.2017.06.008

278. Zhang R, Wu Y, Xie F, Zhong Y, Wang Y, Xu M, et al. RGMa mediates reactive astrogliosis and glial scar formation through TGFβ1/Smad2/3 signaling after stroke. Cell Death Differ [Internet]. 2018;25(8):1503–16. Available from: http://dx.doi.org/10.1038/s41418-018-0058-y

279. Sims NR, Yew WP. Reactive astrogliosis in stroke: Contributions of astrocytes to recovery of neurological function. Neurochem Int [Internet]. 2017;107:88–103. Available from: http://dx.doi.org/10.1016/j.neuint.2016.12.016

280. Scimemi A. Astrocytes and the Warning Signs of Intracerebral Hemorrhagic Stroke. Neural Plast. 2018;2018.

281. Wurm J, Behringer SP, Ravi VM, Joseph K, Neidert N, Maier JP, et al. Astrogliosis releases pro-oncogenic chitinase 3-like 1 causing mapk signaling in glioblastoma. Cancers (Basel). 2019;11(10):1–13.

282. Sofroniew M V. Astrogliosis. 2023;

283. Chancellor KB, Chancellor SE, Duke-Cohan JE, Huber BR, Stein TD, Alvarez VE, et al. Altered oligodendroglia and astroglia in chronic traumatic encephalopathy. Acta Neuropathol [Internet]. 2021;142(2):295–321. Available from: https://doi.org/10.1007/s00401-021-02322-2

284. Viola A, Munari F, Sánchez-Rodríguez R, Scolaro T, Castegna A. The metabolic signature of macrophage responses. Front Immunol. 2019;10(JULY):1–16.

285. Liu Y, Xu R, Gu H, Zhang E, Qu J, Cao W, et al. Metabolic reprogramming in macrophage responses. Biomark Res. 2021;9(1):1–17.

286. Dang B, Gao Q, Zhang L, Zhang J, Cai H, Zhu Y, et al. The glycolysis/HIF-1α axis defines the inflammatory role of IL-4-primed macrophages. Cell Rep [Internet]. 2023;42(5):112471. Available from: https://doi.org/10.1016/j.celrep.2023.112471

287. Bernier LP, York EM, MacVicar BA. Immunometabolism in the Brain: How Metabolism Shapes Microglial Function. Trends Neurosci [Internet]. 2020;43(11):854–69. Available from: https://doi.org/10.1016/j.tins.2020.08.008

288. Fairley LH, Wong JH, Barron AM. Mitochondrial Regulation of Microglial Immunometabolism in Alzheimer's Disease. Front Immunol. 2021;12(February):1–10.

289. O'Neill LAJ, Kishton RJ, Rathmell J. A guide to immunometabolism for

immunologists. Nat Rev Immunol. 2016;16(9):553–65.

290. Robb JL, Morrissey NA, Weightman Potter PG, Smithers HE, Beall C, Ellacott KLJ. Immunometabolic Changes in Glia – A Potential Role in the Pathophysiology of Obesity and Diabetes. Neuroscience [Internet]. 2020;447(2019):167–81. Available from: https://doi.org/10.1016/j.neuroscience.2019.10.021

291. Pinto-Benito D, Paradela-Leal C, Ganchala D, de Castro-Molina P, Arevalo MA. IGF-1 regulates astrocytic phagocytosis and inflammation through the p110α isoform of PI3K in a sex-specific manner. Glia. 2022;70(6):1153–69.

292. Sawada M, Suzumura A, Marunouchi T. TNFα induces IL-6 production by astrocytes but not by microglia. Brain Res. 1992;583(1–2):296–9.

293. Lu M, Sun XL, Qiao C, Liu Y, Ding JH, Hu G. Uncoupling protein 2 deficiency aggravates astrocytic endoplasmic reticulum stress and nod-like receptor protein 3 inflammasome activation. Neurobiol Aging [Internet]. 2014;35(2):421–30. Available from: http://dx.doi.org/10.1016/j.neurobiolaging.2013.08.015

294. Dai DL, Li M, Lee EB. Human Alzheimer's disease reactive astrocytes exhibit a loss of homeostastic gene expression. Acta Neuropathol Commun [Internet]. 2023;11(1):1–19. Available from: https://doi.org/10.1186/s40478-023-01624-8

295. Steele ML, Robinson SR. Reactive astrocytes give neurons less support: Implications for Alzheimer's disease. Neurobiol Aging [Internet]. 2012;33(2):423.e1-423.e13. Available from: http://dx.doi.org/10.1016/j.neurobiolaging.2010.09.018

296. Bertani B, Ruiz N. Function and Biogenesis of Lipopolysaccharides. EcoSal Plus. 2018;8(1).

297. Gauthier AE, Rotjan RD, Kagan JC. Lipopolysaccharide detection by the innate immune system may be an uncommon defence strategy used in nature. Open Biol. 2022;12(10).

298. Astakhova A, Chistyakov D, Thomas D, Geisslinger G, Brüne B, Sergeeva M, et al. Inhibitors of Oxidative Phosphorylation Modulate Astrocyte

Inflammatory Responses through AMPK-Dependent Ptgs2 mRNA Stabilization. Cells. 2019;8(10):1185.

299. Gijsel-Bonnello M v, Baranger K, Benech P, Rivera S, Khrestchatisky M, de Reggi M, et al. Metabolic changes and inflammation in cultured astrocytes from the 5xFAD mouse model of Alzheimer ' s disease: Alleviation by pantethine. PLoS One. 2017;1–22.

300. Wilson RS, Wang T, Yu L, Bennett DA, Boyle PA. Normative Cognitive Decline in Old Age. Ann Neurol. 2020;87(6):816–29.

301. Sanada F, Taniyama Y, Muratsu J, Otsu R, Shimizu H, Rakugi H, et al. Source of Chronic Inflammation in Aging. Front Cardiovasc Med. 2018;5(February):1–5.

302. Jiang T, Cadenas E. Astrocytic metabolic and inflammatory changes as a function of age. Aging Cell. 2014;13(6):1059–67.

303. Guyenet SJ, Nguyen HT, Hwang BH, Schwartz MW, Baskin DG, Thaler JP. High-fat diet feeding causes rapid, non-apoptotic cleavage of caspase-3 in astrocytes. Brain Res [Internet]. 2013;1512:97–105. Available from: http://dx.doi.org/10.1016/j.brainres.2013.03.033

304. Gatliff J, Campanella M. TSPO: Kaleidoscopic 18-kDa amid biochemical pharmacology, control and targeting of mitochondria. Biochem J. 2016;473(2):107–21.

305. Viviano M, Barresi E, Siméon FS, Costa B, Taliani S, Da Settimo F, et al. Essential Principles and Recent Progress in the Development of TSPO PET Ligands for Neuroinflammation Imaging. Curr Med Chem. 2022;29(28):4862–90.

306. Gut P. Targeting mitochondrial energy metabolism with TSPO ligands. Biochem Soc Trans. 2015;43:537–42.

307. Braestrup C, Squires RF. Specific benzodiazepine receptors in rat brain characterized by high-affinity [3H]diazepam binding (affinity binding/diazepam/anxiolytic activity/brain membranes/regional distribution). Vol. 74, Biochemistry. 1977.

308. Papadopoulos V, Fan J, Zirkin B. Translocator protein (18 kDa): an update

on its function in steroidogenesis. J Neuroendocrinol. 2018;30(2):1–9.

309. Owen DR, Fan J, Campioli E, Venugopal S, Midzak A, Daly E, et al. TSPO mutations in rats and a human polymorphism impair the rate of steroid synthesis. Biochem J. 2017;474(23):3985–99.

310. Šileikyte J, Blachly-Dyson E, Sewell R, Carpi A, Menabò R, Di Lisa F, et al. Regulation of the mitochondrial permeability transition pore by the outer membrane does not involve the peripheral benzodiazepine receptor (translocator protein of 18 kDa (TSPO)). J Biol Chem. 2014;289(20):13769–81.

311. Fan J, Lindemann P, Papadopoulos V. Structural and Functional Evolution of the Translocator Protein (18 kDa). Curr Mol Med. 2012;12:369–86.

312. Veiga S, Carrero P, Pernia O, Azcoitia I, Garcia-Segura LM. Translocator Protein (18 kDa) is Involved in the Regulation of Reactive Gliosis. Glia [Internet]. 2007;55:1426–36. Available from: http://www.unscn.org/en/home/

313. Wang M, Wang X, Zhao L, Ma W, Rodriguez IR, Fariss RN, et al. Macroglia-microglia interactions via TSPO signaling regulates microglial activation in the mouse retina. J Neurosci. 2014;34(10):3793–806.

314. Kreisl WC, Lyoo CH, McGwier M, Snow J, Jenko KJ, Kimura N, et al. In vivo radioligand binding to translocator protein correlates with severity of Alzheimer's disease. Brain [Internet]. 2013 Jul 1 [cited 2021 Jun 3];136(7):2228–38. Available from: http://pdsp.med.

315. Hiser C, Montgomery BL, Ferguson-Miller S. TSPO protein binding partners in bacteria, animals, and plants. J Bioenerg Biomembr [Internet]. 2021;53(4):463–87. Available from: https://doi.org/10.1007/s10863-021-09905-4

316. Lee Y, Park Y, Nam H, Lee JW, Yu SW. Translocator protein (TSPO): the new story of the old protein in neuroinflammation. BMB Rep. 2020;53(1):20–7.

317. Bonsack F, Sukumari-Ramesh S. TSPO: An evolutionarily conserved protein with elusive functions. Int J Mol Sci. 2018;19(6).

318. Notter T, Schalbetter SM, Clifton NE, Mattei D, Richetto J, Thomas K, et al. Neuronal activity increases translocator protein (TSPO) levels. Mol Psychiatry [Internet]. 2021;26(6):2025–37. Available from: http://dx.doi.org/10.1038/s41380-020-0745-1

319. Downer OM, Marcus REG, Zürcher NR, Hooker JM. Tracing the History of the Human Translocator Protein to Recent Neurodegenerative and Psychiatric Imaging. ACS Chem Neurosci. 2020;11(15):2192–200.

320. Koganti PP, Selvaraj V. Lack of adrenal TSPO/PBR expression in hamsters reinforces correlation to triglyceride metabolism. J Endocrinol. 2020;247(1):1–10.

321. Yeliseev AA, Krueger KE, Kaplan S. A mammalian mitochondrial drug receptor functions as a bacterial “oxygen” sensor. Proc Natl Acad Sci U S A. 1997;94(10):5101–6.

322. Papadopoulos V, Amri H, Li H, Boujrad N, Vidic B, Garnier M. Targeted disruption of the peripheral-type benzodiazepine receptor gene inhibits steroidogenesis in the R2C leydig tumor cell line. J Biol Chem [Internet]. 1997;272(51):32129–35. Available from: http://dx.doi.org/10.1074/jbc.272.51.32129

323. Stocco DM. The role of PBR/TSPO in steroid biosynthesis challenged. Endocrinology. 2014;155(1):6–9.

324. Banati RB, Middleton RJ, Chan R, Hatty CR, Wai-Ying Kam W, Quin C, et al. Positron emission tomography and functional characterization of a complete PBR/TSPO knockout. Nat Commun [Internet]. 2014;5:1–12. Available from: http://dx.doi.org/10.1038/ncomms6452

325. Tu LN, Morohaku K, Manna PR, Pelton SH, Butler WR, Stocco DM, et al. Peripheral benzodiazepine receptor/translocator protein global knock-out mice are viable with no effects on steroid hormone biosynthesis. J Biol Chem. 2014;289(40):27444–54.

326. Morrissey NA, Beall C, Ellacott KLJ. Absence of the mitochondrial translocator protein 18 kDa in mice does not affect body weight or food intake responses to altered energy availability. J Neuroendocrinol. 2021;33(9):1–14.

327. Fan J, Campioli E, Papadopoulos V. Nr5a1-Cre-mediated Tspo conditional knockout mice with low growth rate and prediabetes symptoms – A mouse model of stress diabetes. Biochim Biophys Acta - Mol Basis Dis. 2019 Jan 1;1865(1):56–62.

328. Morohaku K, Pelton SH, Daugherty DJ, Butler WR, Deng W, Selvaraj V. Translocator protein/peripheral benzodiazepine receptor is not required for steroid hormone biosynthesis. Endocrinology. 2014;155(1):89–97.

329. Jaremko L, Jaremko M, Giller K, Becker S, Zweckstetter M. Structure of the Mitochondrial Translocator Protein in Complex with a Diagnostic Ligand. Science (80-). 2014;343(6177):1363–7.

330. Milenkovic VM, Bader S, Sudria-Lopez D, Siebert R, Brandl C, Nothdurfter C, et al. Effects of genetic variants in the TSPO gene on protein structure and stability. PLoS One. 2018;13(4):1–20.

331. Guilarte TR, Rodichkin AN, McGlothan JL, Acanda De La Rocha AM, Azzam DJ. Imaging neuroinflammation with TSPO: A new perspective on the cellular sources and subcellular localization. Pharmacol Ther. 2022;234.

332. Jaipuria G, Leonov A, Giller K, Vasa SK, Jaremko Á, Jaremko M, et al. Cholesterol-mediated allosteric regulation of the mitochondrial translocator protein structure. Nat Commun. 2017;8:1–8.

333. Rone MB, Fan J, Papadopoulos V. Cholesterol transport in steroid biosynthesis: Role of protein-protein interactions and implications in disease states. Biochim Biophys Acta - Mol Cell Biol Lipids [Internet]. 2009;1791(7):646–58. Available from: http://dx.doi.org/10.1016/j.bbalip.2009.03.001

334. Miller WL, Auchus RJ. The molecular biology, biochemistry, and physiology of human steroidogenesis and its disorders. Endocr Rev. 2011 Feb;32(1):81–151.

335. Bassi G, Sidhu SK, Mishra S. The expanding role of mitochondria, autophagy and lipophagy in steroidogenesis. Cells. 2021;10(8):1–22.

336. Bellavance MA, Rivest S. The HPA - immune axis and the

immunomodulatory actions of glucocorticoids in the brain. Front Immunol. 2014;5(MAR):1–13.

337. Petrillo MG razi., Fettucciari K, Montuschi P, Ronchetti S, Cari L, Migliorati G, et al. Transcriptional regulation of kinases downstream of the T cell receptor: another immunomodulatory mechanism of glucocorticoids. BMC Pharmacol Toxicol. 2014;15:35.

338. Franco L, Gadkari M, Howe K, Sun J, Kardava L, Kumar P, et al. Immune regulation by glucocorticoids can be linked to cell type-dependent transcriptional responses. J Exp Med. 2019;206(2):384–406.

339. Yao R, Pan R, Shang C, Li X, Cheng J, Xu J, et al. Translocator Protein 18 kDa (TSPO) Deficiency Inhibits Microglial Activation and Impairs Mitochondrial Function. Front Pharmacol. 2020;11(June):1–10.

340. Fairley LH, Lai KO, Wong JH, Chong WJ, Vincent AS, D'Agostino G, et al. Mitochondrial control of microglial phagocytosis by the translocator protein and hexokinase 2 in Alzheimer's disease. Proc Natl Acad Sci [Internet]. 2023;120:12. Available from: https://doi.org/10.1073/pnas.2209177120

341. Zhang H, Wang H, Gao F, Yang J, Xu Y, Fu Y, et al. TSPO deficiency accelerates amyloid pathology and neuroinflammation by impairing microglial phagocytosis. Neurobiol Aging. 2021;106:292–303.

342. Guilarte TR, Loth MK, Guariglia SR. TSPO Finds NOX2 in Microglia for Redox Homeostasis. Trends Pharmacol Sci [Internet]. 2016;37(5):334–43. Available from: http://dx.doi.org/10.1016/j.tips.2016.02.008

343. Loth MK, Guariglia SR, Re DB, Perez J, de Paiva VN, Dziedzic JL, et al. A Novel Interaction of Translocator Protein 18 kDa (TSPO) with NADPH Oxidase in Microglia. Mol Neurobiol. 2020;57(11):4467–87.

344. Wolf A, Herb M, Schramm M, Langmann T. The TSPO-NOX1 axis controls phagocyte-triggered pathological angiogenesis in the eye. Nat Commun [Internet]. 2020;11(1):1–17. Available from: http://dx.doi.org/10.1038/s41467-020-16400-8

345. Rashid K, Verhoyen M, Taiwo M, Langmann T. Translocator protein (18 kDa) (TSPO) ligands activate Nrf2 signaling and attenuate inflammatory

responses and oxidative stress in human retinal pigment epithelial cells. Biochem Biophys Res Commun. 2020 Jul 23;528(2):261–8.

346. Feng H, Liu Y, Zhang R, Liang Y, Sun L, Lan N, et al. TSPO Ligands PK11195 and Midazolam Reduce NLRP3 Inflammasome Activation and Proinflammatory Cytokine Release in BV-2 Cells. Front Cell Neurosci [Internet]. 2020 Dec 10 [cited 2021 Jun 3];14:427. Available from: www.frontiersin.org

347. Asih PR, Poljak A, Kassiou M, Ke YD, Ittner LM. Differential mitochondrial protein interaction profile between human translocator protein and its A147T polymorphism variant. PLoS One [Internet]. 2022; Available from: https://doi.org/10.1101/2021.07.23.453531

348. Gatliff J, East D, Crosby J, Abeti R, Harvey R, Craigen W, et al. TSPO interacts with VDAC1 and triggers a ROS-mediated inhibition of mitochondrial quality control. Autophagy [Internet]. 2014 [cited 2021 Jun 10];10(12):2279–96. Available from: http://dx.doi.org/10.4161/15548627.2014.991665

349. Bernardi P, Gerle C, Halestrap AP, Jonas EA, Karch J, Mnatsakanyan N, et al. Identity, structure, and function of the mitochondrial permeability transition pore: controversies, consensus, recent advances, and future directions. Cell Death Differ. 2023;30(8):1869–85.

350. Rone MB, Liu J, Blonder J, Ye X, Veenstra TD, Young JC, et al. Targeting and insertion of the cholesterol-binding translocator protein into the outer mitochondrial membrane. Biochemistry. 2009;48(29):6909–20.

351. Rao R, Diharce J, Dugué B, Ostuni MA, Cadet F, Etchebest C. Versatile Dimerisation Process of Translocator Protein (TSPO) Revealed by an Extensive Sampling Based on a Coarse-Grained Dynamics Study. J Chem Inf Model. 2020;60(8):3944–57.

352. Li F, Xia Y, Meiler J, Ferguson-Miller S. Characterization and modeling of the oligomeric state and ligand binding behavior of purified translocator protein 18 kDa from Rhodobacter sphaeroides. Biochemistry. 2013;52(34):5884–99.

353. Delavoie F, Li H, Hardwick M, Robert JC, Giatzakis C, Péranzi G, et al. In

vivo and in vitro peripheral-type benzodiazepine receptor polymerization: Functional significance in drug ligand and cholesterol binding. Biochemistry. 2003;42(15):4506–19.

354. Zeng J, Guareschi R, Damre M, Cao R, Kless A, Neumaier B, et al. Structural prediction of the dimeric form of the mammalian translocator membrane protein TSPO: A key target for brain diagnostics. Int J Mol Sci. 2018;19(9).

355. Lacapere JJ, Duma L, Finet S, Kassiou M, Papadopoulos V. Insight into the Structural Features of TSPO: Implications for Drug Development. Trends Pharmacol Sci [Internet]. 2020 Feb 1 [cited 2020 Dec 15];41(2):110–22. Available from: https://doi.org/10.1016/j.tips.2019.11.005

356. Marchi S, Patergnani S, Missiroli S, Morciano G, Rimessi A, Wieckowski MR, et al. Mitochondrial and endoplasmic reticulum calcium homeostasis and cell death. Cell Calcium [Internet]. 2018;69:62–72. Available from: https://doi.org/10.1016/j.ceca.2017.05.003

357. Gatliff J, East DA, Singh A, Alvarez MS, Frison M, Matic I, et al. A role for TSPO in mitochondrial Ca2+ homeostasis and redox stress signaling. Cell Death Dis [Internet]. 2017;8(6):1–15. Available from: http://dx.doi.org/10.1038/cddis.2017.186

358. Kim S, Kim N, Park S, Jeon Y, Lee J, Yoo SJ, et al. Tanycytic TSPO inhibition induces lipophagy to regulate lipid metabolism and improve energy balance. Autophagy. 2020 Jul 2;16(7):1200–20.

359. Davey ME, De Bruijn FJ. A homologue of the tryptophan-rich sensory protein TspO and fixL regulate a novel nutrient deprivation-induced Sinorhizobium meliloti locus. Appl Environ Microbiol. 2000;66(12):5353–9.

360. Busch AWU, Montgomery BL. The tryptophan-rich sensory protein (TSPO) is involved in stress-related and light-dependent processes in the Cyanobacterium Fremyella diplosiphon. Front Microbiol. 2015;6(DEC):1–15.

361. Leneveu-Jenvrin C, Bouffartigues E, Maillot O, Cornelis P, Feuilloley MGJ, Connil N, et al. Expression of the translocator protein (TSPO) from

Pseudomonas fluorescens Pf0-1 requires the stress regulatory sigma factors AlgU and RpoH. Front Microbiol. 2015;6(SEP):1–13.

362. Balsemão-Pires E, Jaillais Y, Olson BJSC, Andrade LR, Umen JG, Chory J, et al. The Arabidopsis translocator protein (AtTSPO) is regulated at multiple levels in response to salt stress and perturbations in tetrapyrrole metabolism. BMC Plant Biol. 2011;11.

363. Guillaumot D, Guillon S, Déplanque T, Vanhee C, Gumy C, Masquelier D, et al. The Arabidopsis TSPO-related protein is a stress and abscisic acid-regulated, endoplasmic reticulum-Golgi-localized membrane protein. Plant J. 2009;60(2):242–56.

364. Bressendorff S, Azevedo R, Kenchappa CS, de León IP, Olsen J V., Rasmussen MW, et al. An innate immunity pathway in the moss Physcomitrella patens. Plant Cell. 2016;28(6):1328–42.

365. Lehtonen MT, Akita M, Frank W, Reski R, Valkonen JPT. Involvement of a class III peroxidase and the mitochondrial protein TSPO in oxidative burst upon treatment of moss plants with a fungal elicitor. Mol Plant-Microbe Interact. 2012;25(3):363–71.

366. Tu LN, Zhao AH, Hussein M, Stocco DM, Selvaraj V. Translocator protein (TSPO) affects mitochondrial fatty acid oxidation in steroidogenic cells. Endocrinology. 2016;157(3):1110–21.

367. Selvaraj V, Tu LN. Current status and future perspectives: TSPO in steroid neuroendocrinology. J Endocrinol. 2016;231(1):1–30.

368. Liu GJ, Middleton RJ, Kam WWY, Chin DY, Hatty CR, Chan RHY, et al. Functional gains in energy and cell metabolism after TSPO gene insertion. Cell Cycle [Internet]. 2017;16(5):436–47. Available from: http://dx.doi.org/10.1080/15384101.2017.1281477

369. Milenkovic VM, Slim D, Bader S, Koch V, Heinl ES, Alvarez-Carbonell D, et al. CRISPR-cas9 mediated TSPO gene knockout alters respiration and cellular metabolism in human primary microglia cells. Int J Mol Sci. 2019;20(13).

370. Fu Y, Wang D, Wang H, Cai M, Li C, Zhang X, et al. TSPO deficiency

induces mitochondrial dysfunction, leading to hypoxia, angiogenesis, and a growth-promoting metabolic shift toward glycolysis in glioblastoma. Neuro Oncol. 2020;22(2):240–52.

371. Karlstetter M, Nothdurfter C, Aslanidis A, Moeller K, Horn F, Scholz R, et al. Translocator protein (18 kDa) (TSPO) is expressed in reactive retinal microglia and modulates microglial inflammation and phagocytosis. J Neuroinflammation. 2014;11.

372. Daugherty DJ, Selvaraj V, Chechneva O V., Liu XB, Pleasure DE, Deng W. A TSPO ligand is protective in a mouse model of multiple sclerosis. EMBO Mol Med. 2013;5(6):891–903.

373. Hernstadt H, Wang S, Lim G, Mao J. Spinal translocator protein (TSPO) modulates pain behavior in rats with CFA-induced monoarthritis. Brain Res [Internet]. 2009;1286:42–52. Available from: http://dx.doi.org/10.1016/j.brainres.2009.06.043

374. Betlazar C, Harrison-Brown M, Middleton RJ, Banati R, Liu GJ. Cellular sources and regional variations in the expression of the neuroinflammatory marker translocator protein (TSPO) in the normal brain. Int J Mol Sci. 2018;19(9).

375. Roncaroli F, Su Z, Herholz K, Gerhard A, Turkheimer FE. TSPO expression in brain tumours: is TSPO a target for brain tumour imaging? [Internet]. Vol. 4, Clinical and Translational Imaging. Springer-Verlag Italia s.r.l.; 2016 [cited 2021 Jun 3]. p. 145–56. Available from: /pmc/articles/PMC4820497/

376. M. Scarf A, Luus C, Da Pozzo E, Selleri S, Guarino C, Martini C, et al. Evidence for Complex Binding Profiles and Species Differences at the Translocator Protein (TSPO) (18 kDa). Curr Mol Med. 2012;12(4):488–93.

377. Santoro A, Mattace Raso G, Taliani S, Da Pozzo E, Simorini F, Costa B, et al. TSPO-ligands prevent oxidative damage and inflammatory response in C6 glioma cells by neurosteroid synthesis. Eur J Pharm Sci. 2016 Jun 10;88:124–31.

378. Monga S, Denora N, Laquintana V, Franco M, Marek I, Singh S, et al. The protective effect of the TSPO ligands 2,4-Di-Cl-MGV-1, CB86, and CB204 against LPS-induced M1 pro-inflammatory activation of microglia. Brain,

Behav Immun - Heal. 2020 May 1;5(March):1–10.

379. Bader S, Wolf L, Milenkovic VM, Gruber M, Nothdurfter C, Rupprecht R, et al. Differential effects of TSPO ligands on mitochondrial function in mouse microglia cells. Psychoneuroendocrinology. 2019;106(September 2018):65–76.

380. Hart MN, Petito CK, Earle KM. Mixed gliomas. Cancer. 1974;33(1):134–40.

381. Kaur G, Dufour JM. Cell lines. Spermatogenesis. 2012;2(1):1–5.

382. Divakaruni AS, Hsieh WY, Minarrieta L, Duong TN, Kim KKO, Desousa BR, et al. Etomoxir Inhibits Macrophage Polarization by Disrupting CoA Homeostasis. Cell Metab. 2018;28(3):490-503.e7.

383. Arroyo V, Angeli P, Moreau R, Jalan R, Clària J, Trebicka J, et al. The systemic inflammation hypothesis: Towards a new paradigm of acute decompensation and multiorgan failure in cirrhosis. J Hepatol [Internet]. 2021;74(3):670–85. Available from: https://doi.org/10.1016/j.jhep.2020.11.048

384. Russell DG, Huang L, VanderVen BC. Immunometabolism at the interface between macrophages and pathogens. Nat Rev Immunol [Internet]. 2019;19(5):291–304. Available from: http://dx.doi.org/10.1038/s41577-019-0124-9

385. Zago G, Saavedra PHV, Keshari KR, Perry JSA. Immunometabolism of Tissue-Resident Macrophages – An Appraisal of the Current Knowledge and Cutting-Edge Methods and Technologies. Front Immunol. 2021;12(May):1–20.

386. Ménégaut L, Jalil A, Thomas C, Masson D. Macrophage fatty acid metabolism and atherosclerosis: The rise of PUFAs. Atherosclerosis [Internet]. 2019;291(October):52–61. Available from: https://doi.org/10.1016/j.atherosclerosis.2019.10.002

387. Chandra P, He L, Zimmerman M, Yang G, Köster S, Ouimet M, et al. Inhibition of fatty acid oxidation promotes macrophage control of mycobacterium tuberculosis. MBio. 2020;11(4):1–15.

388. Remmerie A, Scott CL. Macrophages and lipid metabolism. Cell Immunol

[Internet]. 2018;330(January):27–42. Available from: https://doi.org/10.1016/j.cellimm.2018.01.020

389. Batista-Gonzalez A, Vidal R, Criollo A, Carreño LJ. New Insights on the Role of Lipid Metabolism in the Metabolic Reprogramming of Macrophages. Front Immunol. 2020;10(January):1–7.

390. Hradilkova K, Maschmeyer P, Westendorf K, Schliemann H, Husak O, von Stuckrad ASL, et al. Regulation of Fatty Acid Oxidation by Twist 1 in the Metabolic Adaptation of T Helper Lymphocytes to Chronic Inflammation. Arthritis Rheumatol. 2019;71(10):1756–65.

391. Lavisse S, Guillermier M, Hérard AS, Petit F, Delahaye M, Van Camp N V., et al. Reactive astrocytes overexpress TSPO and are detected by TSPO positron emission tomography imaging. J Neurosci. 2012;32(32):10809–18.

392. Da Pozzo E, Giacomelli C, Costa B, Cavallini C, Taliani S, Barresi E, et al. TSPO PIGA Ligands Promote Neurosteroidogenesis and Human Astrocyte Well-Being. Int J Mol Sci. 2016;17(7).

393. Tournier BB, Tsartsalis S, Ceyz K. Astrocytic TSPO Upregulation Appears Before Microglial TSPO in Alzheimer ' s Disease. J Alzheimer's Dis. 2020;77:1043–56.

394. Xu L, Liu R, Qin Y, Wang T. Brain metabolism in Alzheimer's disease: biological mechanisms of exercise. Transl Neurodegener [Internet]. 2023;12(1):1–21. Available from: https://doi.org/10.1186/s40035-023-00364-y

395. Li HD, Li M, Shi E, Jin WN, Wood K, Gonzales R, et al. A translocator protein 18 kDa agonist protects against cerebral ischemia/reperfusion injury. J Neuroinflammation. 2017;14(1):1–9.

396. Bonsack F, Alleyne CH, Sukumari-Ramesh S. Augmented expression of TSPO after intracerebral hemorrhage: A role in inflammation? J Neuroinflammation [Internet]. 2016;13(1):1–14. Available from: http://dx.doi.org/10.1186/s12974-016-0619-2

397. Li M, Ren H, Sheth KN, Shi FD, Liu Q. A TSPO ligand attenuates brain

injury after intracerebral hemorrhage. FASEB J. 2017;31(8):3278–87.

398. Varlow C, Knight AC, Mcquade P, Vasdev N. Characterization of neuroinflammatory positron emission tomography biomarkers in chronic traumatic encephalopathy. Brain Commun. 2022;4(1):1–12.

399. Shehadeh M, Palzur E, Apel L, Soustiel JF. Reduction of traumatic brain damage by Tspo ligand etifoxine. Int J Mol Sci. 2019;20(11).

400. Delage C, Vignal N, Guerin C, Taib T, Barboteau C, Mamma C, et al. From positron emission tomography to cell analysis of the 18-kDa Translocator Protein in mild traumatic brain injury. Sci Rep [Internet]. 2021;11(1):1–11. Available from: https://doi.org/10.1038/s41598-021-03416-3

401. Garland EF, Dennett O, Lau LC, Chatelet DS, Bottlaender M, Nicoll JAR, et al. The mitochondrial protein TSPO in Alzheimer's disease: relation to the severity of AD pathology and the neuroinflammatory environment. J Neuroinflammation [Internet]. 2023;20(1):1–15. Available from: https://doi.org/10.1186/s12974-023-02869-9

402. Frison M, Faccenda D, Abeti R, Rigon M, Strobbe D, England-Rendon BS, et al. The translocator protein (TSPO) is prodromal to mitophagy loss in neurotoxicity. Mol Psychiatry [Internet]. 2021;26(7):2721–39. Available from: http://dx.doi.org/10.1038/s41380-021-01050-z

403. Lemprière S. Neuroinflammation predicts cognitive decline in FTD. Nat Rev Neurol. 2023;19(5):258.

404. Giannaccini G, Betti L, Palego L, Pirone A, Schmid L, Lanza M, et al. Serotonin transporter (SERT) and translocator protein (TSPO) expression in the obese ob/ob mouse. BMC Neurosci. 2011;12:1–8.

405. Gao N, Ma B, Jia H, Hao C, Jin T, Liu X. Translocator protein alleviates allodynia and improves Schwann cell function against diabetic peripheral neuropathy via activation of the Nrf2-dependent antioxidant system and promoting autophagy. Diabet Med. 2023;40(6):1–13.

406. Bethesda (MD): National Library of Medicine (US) NC for BI. Identifier: NCT00868166, Safety and Efficacy of TRO19622 as add-on Therapy to Riluzole Versus Placebo in Treatment of Patients Suffering From ALS

(MITOTARGET) [Internet]. Available from: https://clinicaltrials.gov/study/NCT00868166?tab=history

407. Nutma E, Ceyzériat K, Amor S, Tsartsalis S, Millet P, Owen DR, et al. Cellular sources of TSPO expression in healthy and diseased brain. Eur J Nucl Med Mol Imaging. 2021;49(1):146–63.

408. O'Brien ER, Kersemans V, Tredwell M, Checa B, Serres S, Soto MS, et al. Glial activation in the early stages of brain metastasis: TSPO as a diagnostic biomarker. J Nucl Med. 2014;55(2):275–80.

409. Owen DRJ, Gunn RN, Rabiner EA, Bennacef I, Fujita M, Kreisl WC, et al. Mixed-affinity binding in humans with 18-kDa translocator protein ligands. J Nucl Med. 2011;52(1):24–32.

410. Song YS. Perspectives in TSPO PET Imaging for Neurologic Diseases. Nucl Med Mol Imaging (2010). 2019;53(6):382–5.

411. Medicine B (MD): NL of, (US). Identifier: NCT03850301, Validation of the 18 kiloDalton Translocator Protein (TSPO) as a Novel Neuroimmunodulatory Target (TSPO) [Internet]. [cited 2023 Sep 19]. Available from: https://clinicaltrials.gov/study/NCT03850301

412. Bethesda (MD): National Library of Medicine (US) NC for BI. Identifier: NCT00502515, Dose-effect of SSR180575 in Diabetic Neuropathy [Internet]. Available from: https://clinicaltrials.gov/study/NCT00502515?tab=table

413. Cappelli A, Anzini M, Vomero S, De Benedetti PG, Menziani MC, Giorgi G, et al. Mapping the peripheral benzodiazepine receptor binding site by conformationally restrained derivatives of 1-(2-chlorophenyl)-N-methyl-N-(1- methylpropyl)-3-isoquinolinecarboxamide (PK11195). J Med Chem. 1997;40(18):2910–21.

414. Awad M, Gavish M. Binding of [3H]Ro 5–4864 and [3H]PK 11195 to Cerebral Cortex and Peripheral Tissues of Various Species: Species Differences and Heterogeneity in Peripheral Benzodiazepine Binding Sites. J Neurochem. 1987;49(5):1407–14.

415. Fujita M, Kobayashi M, Ikawa M, Gunn RN, Rabiner EA, Owen DR, et al.

Comparison of four 11C-labeled PET ligands to quantify translocator protein 18 kDa (TSPO) in human brain: (R)-PK11195, PBR28, DPA-713, and ER176—based on recent publications that measured specific-to-non-displaceable ratios. EJNMMI Res. 2017;7.

416. Owen DR, Yeo AJ, Gunn RN, Song K, Wadsworth G, Lewis A, et al. An 18-kDa Translocator Protein (TSPO) polymorphism explains differences in binding affinity of the PET radioligand PBR28. J Cereb Blood Flow Metab. 2012;32(1):1–5.

417. Mizrahi R, Rusjan PM, Kennedy J, Pollock B, Mulsant B, Suridjan I, et al. Translocator protein (18 kDa) polymorphism (rs6971) explains in-vivo brain binding affinity of the PET radioligand [18F]-FEPPA. J Cereb Blood Flow Metab [Internet]. 2012 Jun [cited 2021 Jun 3];32(6):968–72. Available from: /pmc/articles/PMC3367231/

418. Costa B, Da Pozzo E, Giacomelli C, Barresi E, Taliani S, Da Settimo F, et al. TSPO ligand residence time: A new parameter to predict compound neurosteroidogenic efficacy. Sci Rep. 2016 Jan 11;6.

419. Werry EL, Bright FM, Kassiou M. TSPO PET Imaging as a Biomarker of Neuroinflammation in Neurodegenerative Disorders. Neuromethods. 2022;173:407–27.

420. Zhang L, Hu K, Shao T, Hou L, Zhang S, Ye W, et al. Recent developments on PET radiotracers for TSPO and their applications in neuroimaging. Acta Pharm Sin B [Internet]. 2021;11(2):373–93. Available from: https://doi.org/10.1016/j.apsb.2020.08.006

421. Lee SH, Denora N, Laquintana V, Mangiatordi GF, Lopedota A, Lopalco A, et al. Radiosynthesis and characterization of [18F]BS224: a next-generation TSPO PET ligand insensitive to the rs6971 polymorphism. Eur J Nucl Med Mol Imaging [Internet]. 2021;49(1):110–24. Available from: https://doi.org/10.1007/s00259-021-05617-4

422. Tonon MC, Vaudry H, Chuquet J, Guillebaud F, Fan J, Masmoudi-Kouki O, et al. Endozepines and their receptors: Structure, functions and pathophysiological significance. Pharmacol Ther [Internet]. 2020;208:107386. Available from:

https://doi.org/10.1016/j.pharmthera.2019.06.008

423. Alquier T, Christian-Hinman CA, Alfonso J, Færgeman NJ. From benzodiazepines to fatty acids and beyond: revisiting the role of ACBP/DBI. Trends Endocrinol Metab. 2021;32(11):890–903.

424. Joseph A, Moriceau S, Sica V, Anagnostopoulos G, Pol J, Martins I, et al. Metabolic and psychiatric effects of acyl coenzyme A binding protein (ACBP)/diazepam binding inhibitor (DBI). Cell Death Dis [Internet]. 2020;11(7). Available from: http://dx.doi.org/10.1038/s41419-020-2716-5

425. Veenman L, Vainshtein A, Yasin N, Azrad M, Gavish M. Tetrapyrroles as endogenous TSPO ligands in eukaryotes and prokaryotes: Comparisons with synthetic ligands. Int J Mol Sci. 2016;17(6):1–26.

426. Mcenery MW, Snowman AM, Trifiletti RR, Snyder SH. Isolation of the mitochondrial benzodiazepine receptor: Association with the voltage-dependent anion channel and the adenine nucleotide carrier. Proc Natl Acad Sci U S A. 1992;89(8):3170–4.

427. Verma A, Nye JS, Snyder SH. Porphyrins are endogenous ligands for the mitochondrial (peripheral-type) benzodiazepine receptor. Proc Natl Acad Sci U S A. 1987;84(8):2256–60.

428. Shoshan-Barmatz V, Pittala S, Mizrachi D. Molecular Sciences VDAC1 and the TSPO: Expression, Interactions, and Associated Functions in Health and Disease States. J Mol Sci [Internet]. 2019 [cited 2021 Jun 10];20:3348. Available from: www.mdpi.com/journal/ijms

429. Costa B, Pini S, Gabelloni P, Da Pozzo E, Abelli M, Lari L, et al. The spontaneous Ala147Thr amino acid substitution within the translocator protein influences pregnenolone production in lymphomonocytes of healthy individuals. Endocrinology. 2009;150(12):5438–45.

430. Mages K, Grassmann F, Jägle H, Rupprecht R, Weber BHF, Hauck SM, et al. The agonistic TSPO ligand XBD173 attenuates the glial response thereby protecting inner retinal neurons in a murine model of retinal ischemia. J Neuroinflammation. 2019;16(1):1–16.

431. Gong J, Szego ÉM, Leonov A, Benito E, Becker S, Fischer A, et al.

Translocator protein ligand protects against neurodegeneration in the MPTP mouse model of parkinsonism. J Neurosci. 2019;39(19):3752–69.

432. Mokrov G V., Deeva OA, Gudasheva TA, Yarkov SA, Yarkova MA, Seredenin SB. Design, synthesis and anxiolytic-like activity of 1-arylpyrrolo[1,2-a]pyrazine-3-carboxamides. Bioorganic Med Chem [Internet]. 2015;23(13):3368–78. Available from: http://dx.doi.org/10.1016/j.bmc.2015.04.049

433. Chen C, Kuo J, Wong A, Micevych P. Estradiol modulates translocator protein (tspo) and steroid acute regulatory protein (StAR) via Protein Kinase A (PKA) signaling in hypothalamic astrocytes. Endocrinology. 2014;155(8):2976–85.

434. Bethesda (MD): National Library of Medicine (US) NC for BI. dbSNP [Internet]. 1998 [cited 2023 Sep 19]. Available from: https://www.ncbi.nlm.nih.gov/snp/

435. Setiawan E, Wilson AA, Mizrahi R, Rusjan PM, Miler L, Rajkowska G, et al. Role of translocator protein density, a marker of neuroinflammation, in the brain during major depressive episodes. JAMA Psychiatry. 2015;72(3):268–75.

436. Qiu ZK, He JL, Liu X, Zhang GH, Zeng J, Nie H, et al. The antidepressant-like activity of AC-5216, a ligand for 18KDa translocator protein (TSPO), in an animal model of diabetes mellitus. Sci Rep [Internet]. 2016 Nov 25 [cited 2021 Jun 3];6(1):1–13. Available from: www.nature.com/scientificreports

437. Colasanti A, Owen DR, Grozeva D, Rabiner EA, Matthews PM, Craddock N, et al. Bipolar disorder is associated with the rs6971 polymorphism in the gene encoding 18kDa translocator protein (TSPO). Psychoneuroendocrinology [Internet]. 2013 Nov [cited 2021 Jun 3];38(11):2826–9. Available from: /pmc/articles/PMC3820042/

438. Pouget JG, Gonçalves VF, Nurmi EL, P Laughlin C, Mallya KS, McCracken JT, et al. Investigation of TSPO variants in schizophrenia and antipsychotic treatment outcomes. Pharmacogenomics. 2015;16(1):5–22.

439. Gerritsen C, Iyengar Y, DaSilva T, Koppel A, Rusjan P, Bagby RM, et al. Personality traits in psychosis and psychosis risk linked to TSPO

expression: a neuroimmune marker. Personal Neurosci. 2020;3(2018).

440. Troike KM, de la Rocha AMA, Alban TJ, Grabowski MM, Otvos B, Cioffi G, et al. The translocator protein (TSPO) genetic polymorphism A147T is associated with worse survival in male glioblastoma patients. Cancers (Basel). 2021;13(18).

441. Zhao YY, Yu JZ, Li QY, Ma CG, Lu CZ, Xiao BG. TSPO-specific ligand Vinpocetine exerts a neuroprotective effect by suppressing microglial inflammation. Neuron Glia Biol. 2011;7(2–4):187–97.

442. Barron AM, Garcia-Segura LM, Caruso D, Jayaraman A, Lee JW, Melcangi RC, et al. Ligand for translocator protein reverses pathology in a mouse model of Alzheimer's disease. J Neurosci. 2013;33(20):8891–7.

443. Papadopoulos V, Lecanu L. Translocator protein (18 kDa) TSPO: An emerging therapeutic target in neurotrauma. Exp Neurol [Internet]. 2009;219(1):53–7. Available from: http://dx.doi.org/10.1016/j.expneurol.2009.04.016

444. Fairley LH, Sahara N, Aoki I, Ji B, Suhara T, Higuchi M, et al. Neuroprotective effect of mitochondrial translocator protein ligand in a mouse model of tauopathy. J Neuroinflammation [Internet]. 2021 Dec 1 [cited 2021 Jun 3];18(1):1–13. Available from: https://doi.org/10.1186/s12974-021-02122-1

445. Zhang LM, Zhao N, Guo WZ, Jin ZL, Qiu ZK, Chen HX, et al. Antidepressant-like and anxiolytic-like effects of YL-IPA08, a potent ligand for the translocator protein (18 kDa). Neuropharmacology [Internet]. 2014;81:116–25. Available from: http://dx.doi.org/10.1016/j.neuropharm.2013.09.016

446. Li Y, Chen L, Li L, Sottas C, Petrillo SK, Lazaris A, et al. Cholesterol-binding translocator protein TSPO regulates steatosis and bile acid synthesis in nonalcoholic fatty liver disease. iScience. 2021;24(5).

447. Liu J, Rone MB, Papadopoulos V. Protein-protein interactions mediate mitochondrial cholesterol transport and steroid biosynthesis. J Biol Chem. 2006;281(50):38879–93.

448. Garza S, Chen L, Galano M, Cheung G, Sottas C, Li L, et al. Mitochondrial dynamics, Leydig cell function, and age-related testosterone deficiency. FASEB J. 2022;36(12):1–17.

449. Firth W, Robb JL, Stewart D, Pye KR, Bamford R, Oguro-Ando A, et al. Regulation of astrocyte metabolism by mitochondrial translocator protein 18kDa. 2023;

450. Schindelin J, Arganda-Carreras I, Frise E, Kaynig V, Longair M, Pietzsch T, et al. Fiji: An open-source platform for biological-image analysis. Nat Methods. 2012;9(7):676–82.

451. U-373 MG (Uppsala) (ECACC 08061901) [Internet]. Available from: https://www.culturecollections.org.uk/products/celllines/generalcell/detail.jsp?refId=08061901&collection=ecacc_gc

452. Robb JL. Characterisation of immunometabolic responses in astrocytes [PhD thesis]. Univ Exet [Internet]. 2020; Available from: https://ore.exeter.ac.uk/repository/handle/10871/121246

453. Ltd. M. “Four Parameter Logistic Curve” online data analysis tool [Internet]. [cited 2023 Nov 6]. Available from: https://www.myassays.com/four-parameter-logistic-curve.assay

454. Crowley LC, Scott AP, Marfell BJ, Boughaba JA, Chojnowski G, Waterhouse NJ. Measuring cell death by propidium iodide uptake and flow cytometry. Cold Spring Harb Protoc. 2016;2016(7):647–51.

455. Kogel V, Trinh S, Gasterich N, Beyer C, Seitz J. Long-Term Glucose Starvation Induces Inflammatory Responses and Phenotype Switch in Primary Cortical Rat Astrocytes. J Mol Neurosci [Internet]. 2021;71(11):2368–82. Available from: https://doi.org/10.1007/s12031-021-01800-2

456. Tournier BB, Bouteldja F, Amoss Q, Nicolaides A, Azevedo MD, Tenenbaum L, et al. 18 kDa Translocator Protein TSPO Is a Mediator of Astrocyte Reactivity. 2023;

457. Marlene Wade F, Wakade C, Mahesh VB, Brann DW. Differential expression of the peripheral benzodiazepine receptor and gremlin during

adipogenesis. Obes Res. 2005;13(5):818–22.

458. Thompson MM, Manning HC, Ellacott KLJ. Translocator protein 18 kDa (TSPO) is regulated in white and brown adipose tissue by obesity. PLoS One. 2013;8(11):1–10.

459. Houmard JA. Intramuscular lipid oxidation and obesity. Am J Physiol - Regul Integr Comp Physiol. 2008;294(4):1111–6.

460. Malandrino MI, Fucho R, Weber M, Calderon-Dominguez M, Mir JF, Valcarcel L, et al. Enhanced fatty acid oxidation in adipocytes and macrophages reduces lipid-induced triglyceride accumulation and inflammation. Am J Physiol - Endocrinol Metab. 2015;308(9):E756–69.

461. Silver IA, Erecinska M. Extracellular glucose concentration in mammalian brain: Continuous monitoring of changes during increased neuronal activity and upon limitation in oxygen supply in normo-, hypo-, and hyperglycemic animals. J Neurosci. 1994;14(8):5068–76.

462. Güemes A, Georgiou P. Review of the role of the nervous system in glucose homoeostasis and future perspectives towards the management of diabetes. Bioelectron Med. 2018;4(1):1–18.

463. Isobe M, Suzuki Y, Sugiura H, Shibata M, Ohsaki Y, Kametaka S. Novel cell-based system to assay cell-cell fusion during myotube formation. Biomed Res. 2022;43(4):107–14.

464. Liang K. Mitochondrial CPT1A: Insights into structure, function, and basis for drug development. Front Pharmacol. 2023;14(March):1–14.

465. Lee K, Kerner J, Hoppel CL. Mitochondrial carnitine palmitoyltransferase 1a (CPT1a) is part of an outer membrane fatty acid transfer complex. J Biol Chem [Internet]. 2011;286(29):25655–62. Available from: http://dx.doi.org/10.1074/jbc.M111.228692

466. Papadopoulos V, Aghazadeh Y, Fan J, Campioli E, Zirkin B, Midzak A. Translocator protein-mediated pharmacology of cholesterol transport and steroidogenesis. Mol Cell Endocrinol [Internet]. 2015;408:90–8. Available from: http://dx.doi.org/10.1016/j.mce.2015.03.014

467. Muthuramu I, Singh N, Amin R, De Geest B. Role of lipids and lipoproteins

in myocardial biology and in the development of heart failure. Clin Lipidol. 2015;10(4):329–42.

468. Zhou Z, Okamoto K, Onodera J, Hiragi T, Andoh M, Ikawa M, et al. Astrocytic cAMP modulates memory via synaptic plasticity. Proc Natl Acad Sci U S A. 2021;118(3):1–10.

469. DiNuzzo M. Astrocyte-neuron interactions during learning may occur by lactate signaling rather than metabolism. Front Integr Neurosci. 2016;10(JAN):1–5.

470. Ginhoux F, Lim S, Hoeffel G, Low D, Huber T. Origin and differentiation of microglia. Front Cell Neurosci. 2013;7(MAR):1–14.

471. Loving BA, Bruce KD. Lipid and Lipoprotein Metabolism in Microglia. Front Physiol. 2020;11(April):1–20.

472. Betlazar C, Middleton RJ, Banati R, Liu GJ. The Translocator Protein (TSPO) in Mitochondrial Bioenergetics and Immune Processes. Cells. 2020;9(2):1–18.

473. Asano S, Hayashi Y, Iwata K, Okada-Ogawa A, Hitomi S, Shibuta I, et al. Microglia–astrocyte communication via c1q contributes to orofacial neuropathic pain associated with infraorbital nerve injury. Int J Mol Sci. 2020;21(18):1–15.

474. Lian H, Litvinchuk A, Chiang ACA, Aithmitti N, Jankowsky JL, Zheng H. Astrocyte-microglia cross talk through complement activation modulates amyloid pathology in mouse models of alzheimer's disease. J Neurosci. 2016;36(2):577–89.

475. Fondevila MF, Fernandez U, Heras V, Parracho T, Gonzalez-Rellan MJ, Novoa E, et al. Inhibition of carnitine palmitoyltransferase 1A in hepatic stellate cells protects against fibrosis. J Hepatol [Internet]. 2022;77(1):15–28. Available from: https://doi.org/10.1016/j.jhep.2022.02.003

476. Calle P, Muñoz A, Sola A, Hotter G. CPT1a gene expression reverses the inflammatory and anti-phagocytic effect of 7-ketocholesterol in RAW264.7 macrophages. Lipids Health Dis. 2019;18(1):1–10.

477. Wu L pan, Gong Z fan, Wang H, Zhou Z shu, Zhang M ming, Liu C, et al.

TSPO ligands prevent the proliferation of vascular smooth muscle cells and attenuate neointima formation through AMPK activation. Acta Pharmacol Sin [Internet]. 2020;41(1):34–46. Available from: http://dx.doi.org/10.1038/s41401-019-0293-x

478. Papadopoulos V, Amri H, Boujrad N, Cascio C, Culty M, Garnier M, et al. Peripheral benzodiazepine receptor in cholesterol transport and steroidogenesis. Steroids. 1997;62(1):21–8.

479. Berroterán-Infante N, Tadić M, Hacker M, Wadsak W, Mitterhauser M. Binding affinity of some endogenous and synthetic TSPO ligands regarding the rs6971 polymorphism. Int J Mol Sci. 2019;20(3).

480. Bravo-San Pedro JM, Sica V, Madeo F, Kroemer G. Acyl-CoA-binding protein (ACBP): The elusive “hunger factor” linking autophagy to food intake. Cell Stress. 2019;3(10):312–8.

481. He J, Liu K, Zheng S, Wu Y, Zhao C, Yan S, et al. The acyl-CoA-binding protein Acb1 regulates mitochondria, lipid droplets, and cell proliferation. FEBS Lett. 2022;596(14):1795–808.

482. Heiden MGV, Cantley LC, Thompson CB. Understanding the warburg effect: The metabolic requirements of cell proliferation. Science (80-). 2009;324(5930):1029–33.

483. Sotgia F, Martinez-Outschoorn UE, Pavlides S, Howell A, Pestell RG, Lisanti MP. Understanding the Warburg effect and the prognostic value of stromal caveolin-1 as a marker of a lethal tumor microenvironment. Breast Cancer Res. 2011;13(4):1–13.

484. Liberti M V., Locasale JW. The Warburg Effect: How Does it Benefit Cancer Cells? Trends Biochem Sci [Internet]. 2016;41(3):211–8. Available from: http://dx.doi.org/10.1016/j.tibs.2015.12.001

485. Bucher M, Kadam L, Ahuna K, Myatt L. Differences in glycolysis and mitochondrial respiration between cytotrophoblast and syncytiotrophoblast in-vitro: Evidence for sexual dimorphism. Int J Mol Sci. 2021;22(19).

486. Sofroniew M V. Astrocyte barriers to neurotoxic inflammation. Nat Rev Neurosci. 2015;16(May):249–63.

487. Yin F, Sancheti H, Patil I, Cadenas E. Energy metabolism and inflammation in brain aging and Alzheimer's disease. Free Radic Biol Med [Internet]. 2016;100:108–22. Available from: http://dx.doi.org/10.1016/j.freeradbiomed.2016.04.200

488. Lee S, Devanney NA, Golden LR, Smith CT, Schwartz JL, Walsh AE, et al. APOE modulates microglial immunometabolism in response to age, amyloid pathology, and inflammatory challenge. Cell Rep [Internet]. 2023;42(3):112196. Available from: https://doi.org/10.1016/j.celrep.2023.112196

489. Strogulski NR, Portela L V., Polster BM, Loane DJ. Fundamental Neurochemistry Review: Microglial immunometabolism in traumatic brain injury. J Neurochem. 2023;(July):1–25.

490. Yang F, Zhao D, Cheng M, Liu Y, Chen Z, Chang J, et al. mTOR-Mediated Immunometabolic Reprogramming Nanomodulators Enable Sensitive Switching of Energy Deprivation-Induced Microglial Polarization for Alzheimer's Disease Management. ACS Nano. 2023;

491. Kučić N, Rački V, Šverko R, Vidović T, Grahovac I, Mršić-pelčić J. Immunometabolic modulatory role of naltrexone in bv-2 microglia cells. Int J Mol Sci. 2021;22(16):1–16.

492. Dumitru C, Kabat AM, Maloy KJ. Metabolic adaptations of CD4+ T cells in inflammatory disease. Front Immunol. 2018;9(MAR):1–17.

493. Lee YS, Olefsky J. Chronic tissue inflammation and metabolic disease. Genes Dev. 2021;35(5–6):307–28.

494. Smith RL, Soeters MR, Wüst RCI, Houtkooper RH. Metabolic flexibility as an adaptation to energy resources and requirements in health and disease. Endocr Rev. 2018;39(4):489–517.

495. Caputa G, Castoldi A, Pearce EJ. Metabolic adaptations of tissue-resident immune cells. Nat Immunol [Internet]. 2019;20(7):793–801. Available from: http://dx.doi.org/10.1038/s41590-019-0407-0

496. van den Brink W, van Bilsen J, Salic K, Hoevenaars FPM, Verschuren L, Kleemann R, et al. Current and Future Nutritional Strategies to Modulate

Inflammatory Dynamics in Metabolic Disorders. Front Nutr. 2019;6(August):1–14.

497. Li H, Meng Y, He S, Tan X, Zhang Y, Zhang X, et al. Macrophages, Chronic Inflammation, and Insulin Resistance. Cells. 2022;11(19):1–24.

498. Winkeler A, Boisgard R, Awde AR, Dubois A, Thézé B, Zheng J, et al. The translocator protein ligand [18F]DPA-714 images glioma and activated microglia in vivo. Eur J Nucl Med Mol Imaging. 2012;39(5):811–23.

499. Alam M, Lee J, Lee S. Recent Progress in the Development of TSPO PET Ligands for Neuroinflammation Imaging in Neurological Diseases. Nucl Med Mol Imaging. 2017;51:283–96.

500. Airas L, Rissanen E, Rinne JO. Imaging neuroinflammation in multiple sclerosis using TSPO-PET. Clin Transl Imaging. 2015;3(6):461–73.

501. Van Camp N, Lavisse S, Roost P, Gubinelli F, Hillmer A, Boutin H. TSPO imaging in animal models of brain diseases. Vol. 49, European Journal of Nuclear Medicine and Molecular Imaging. European Journal of Nuclear Medicine and Molecular Imaging; 2021. 77–109 p.

502. Victorio CBL, Msallam R, Novera W, Ong J, Yang TJ, Ganasarajah A, et al. TSPO expression in a Zika virus murine infection model as an imaging target for acute infection-induced neuroinflammation. Eur J Nucl Med Mol Imaging [Internet]. 2023;50(3):742–55. Available from: https://doi.org/10.1007/s00259-022-06019-w

503. Cash A, Theus MH. Mechanisms of blood–brain barrier dysfunction in traumatic brain injury. Int J Mol Sci. 2020;21(9).

504. Vettermann FJ, Harris S, Schmitt J, Unterrainer M, Lindner S, Rauchmann B-S, et al. Impact of TSPO Receptor Polymorphism on [18F]GE-180 Binding in Healthy Brain and Pseudo-Reference Regions of Neurooncological and Neurodegenerative Disorders. Life [Internet]. 2021 May 26 [cited 2021 Jun 3];11(6):484. Available from: https://www.mdpi.com/2075-1729/11/6/484

505. Monga S, Nagler R, Amara R, Weizman A, Gavish M. Inhibitory Effects of the Two Novel TSPO Ligands 2-Cl-MGV-1 and MGV-1 on LPS-induced

Microglial Activation. Cells. 2019;8.

506. Azrad M, Zeineh N, Weizman A, Veenman L, Gavish M. The TSPO ligands 2-CL-MGV-1, MGV-1, and PK11195 differentially suppress the inflammatory response of BV-2 microglial cell to LPS. Int J Mol Sci. 2019;20(3):1–14.

507. Zhou D, Ji L, Chen Y. TSPO Modulates IL-4-Induced Microglia/Macrophage M2 Polarization via PPAR-γ Pathway. J Mol Neurosci. 2020;70(4):542–9.

508. Zhou J, Zhang X, Peng J, Xie Y, Du F, Guo K, et al. TSPO ligand Ro5-4864 modulates microglia/macrophages polarization after subarachnoid hemorrhage in mice. Neurosci Lett [Internet]. 2020;729(April):134977. Available from: https://doi.org/10.1016/j.neulet.2020.134977

509. Capece D, Verzella D, Flati I, Arboretto P, Cornice J, Franzoso G. NF-κB: blending metabolism, immunity, and inflammation. Trends Immunol [Internet]. 2022;43(9):757–75. Available from: https://doi.org/10.1016/j.it.2022.07.004

510. Kracht M, Müller-Ladner U, Schmitz ML. Mutual regulation of metabolic processes and proinflammatory NF-κB signaling. J Allergy Clin Immunol. 2020;146(4):694–705.

511. Mauro C, Leow SC, Anso E, Rocha S, Thotakura AK, Tornatore L, et al. NF-κB controls energy homeostasis and metabolic adaptation by upregulating mitochondrial respiration. Nat Cell Biol [Internet]. 2011;13(10):1272–9. Available from: http://dx.doi.org/10.1038/ncb2324

512. Fan J, Papadopoulos V. Mitochondrial tspo deficiency triggers retrograde signaling in ma-10 mouse tumor leydig cells. Int J Mol Sci. 2021;22(1):1–16.

513. Da Pozzo E, Tremolanti C, Costa B, Giacomelli C, Milenkovic VM, Bader S, et al. Microglial pro-inflammatory and anti-inflammatory phenotypes are modulated by translocator protein activation. Int J Mol Sci. 2019;20(18):1–21.

514. Liu X, Yin S, Chen Y, Wu Y, Zheng W, Dong H, et al. LPS-induced

proinflammatory cytokine expression in human airway epithelial cells and macrophages via NF-κB, STAT3 or AP-1 activation. Mol Med Rep. 2018;17(4):5484–91.

515. Ngkelo A, Meja K, Yeadon M, Adcock I, Kirkham PA. LPS induced inflammatory responses in human peripheral blood mononuclear cells is mediated through NOX4 and G iα dependent PI-3kinase signalling. J Inflamm. 2012;9:2–8.

516. Yücel G, Zhao Z, El-Battrawy I, Lan H, Lang S, Li X, et al. Lipopolysaccharides induced inflammatory responses and electrophysiological dysfunctions in human-induced pluripotent stem cell derived cardiomyocytes. Sci Rep. 2017;7(1):1–13.

517. Klaska IP, Muckersie E, Martin-Granados C, Christofi M, Forrester J V. Lipopolysaccharide-primed heterotolerant dendritic cells suppress experimental autoimmune uveoretinitis by multiple mechanisms. Immunology. 2017;150(3):364–77.

518. Liu Y, Fang S, Li X, Feng J, Du J, Guo L, et al. Aspirin inhibits LPS-induced macrophage activation via the NF-κB pathway. Sci Rep [Internet]. 2017;7(1):1–11. Available from: http://dx.doi.org/10.1038/s41598-017-10720-4

519. Tucureanu MM, Rebleanu D, Constantinescu CA, Deleanu M, Voicu G, Butoi E, et al. Lipopolysaccharide-induced inflammation in monocytes/macrophages is blocked by liposomal delivery of Gi-protein inhibitor. Int J Nanomedicine. 2018;13:63–76.

520. Fanying. M, Lowell CA. Lipopolysaccharide (LPS)-induced Macrophage Activation and Signal Transduction in the Absence of Src-Family Kinases Hck, Fgr, and Lyn. J Exp Med. 1997;185(9).

521. Wang X, Lin Y. Tumor necrosis factor and cancer, buddies or foes? Acta Pharmacol Sin. 2008;29(11):1275–88.

522. Kane MT. Variability in different lots of commercial bovine serum albumin affects cell multiplication and hatching of rabbit blastocysts in culture. 1983;25–8.

523. Hulse WL, Gray J, Forbes RT. Evaluating the inter and intra batch variability of protein aggregation behaviour using Taylor dispersion analysis and dynamic light scattering. Int J Pharm [Internet]. 2013;453(2):351–7. Available from: http://dx.doi.org/10.1016/j.ijpharm.2013.05.062

524. Ma L, Zhang H, Liu N, Wang P qi, Guo W zhi, Fu Q, et al. TSPO ligand PK11195 alleviates neuroinflammation and beta-amyloid generation induced by systemic LPS administration. Brain Res Bull. 2016;121:192–200.

525. Pajak B, Siwiak E, Sołtyka M, Priebe A, Zieliński R, Fokt I, et al. 2-Deoxy-D-Glucose and its analogs: From diagnostic to therapeutic agents. Int J Mol Sci. 2020;21(1).

526. Su W, Li J, Jiang L, Lei L, Li H. Hexokinase 2-mediated glycolysis supports inflammatory responses to Porphyromonas gingivalis in gingival fibroblasts. BMC Oral Health [Internet]. 2023;23(1):1–12. Available from: https://doi.org/10.1186/s12903-023-02807-4

527. Schmidt CA, Fisher-Wellman KH, Darrell Neufer P. From OCR and ECAR to energy: Perspectives on the design and interpretation of bioenergetics studies. J Biol Chem [Internet]. 2021;297(4):101140. Available from: https://doi.org/10.1016/j.jbc.2021.101140

528. Jiwaji Z, Tiwari SS, Avilés-Reyes RX, Hooley M, Hampton D, Torvell M, et al. Reactive astrocytes acquire neuroprotective as well as deleterious signatures in response to Tau and Aß pathology. Nat Commun. 2022;13(1).

529. Slota JA, Sajesh B V., Frost KF, Medina SJ, Booth SA. Dysregulation of neuroprotective astrocytes, a spectrum of microglial activation states, and altered hippocampal neurogenesis are revealed by single-cell RNA sequencing in prion disease. Acta Neuropathol Commun [Internet]. 2022;10(1):1–23. Available from: https://doi.org/10.1186/s40478-022-01450-4

530. Horiguchi Y, Ohta N, Yamamoto S, Koide M, Fujino Y. Midazolam suppresses the lipopolysaccharide-stimulated immune responses of human macrophages via translocator protein signaling. Int Immunopharmacol [Internet]. 2019;66(March 2018):373–82. Available

from: https://doi.org/10.1016/j.intimp.2018.11.050

531. Dodington DW, Desai HR, Woo M. JAK/STAT – Emerging Players in Metabolism. Trends Endocrinol Metab [Internet]. 2018;29(1):55–65. Available from: http://dx.doi.org/10.1016/j.tem.2017.11.001

532. Batarseh A, Li J, Papadopoulos V. Protein kinase Cε regulation of translocator protein (18 kDa) Tspo gene expression is mediated through a MAPK pathway targeting STAT3 and c-Jun transcription factors. Biochemistry. 2010;49(23):4766–78.

533. Hinrichsen F, Hamm J, Westermann M, Schröder L, Shima K, Mishra N, et al. Microbial regulation of hexokinase 2 links mitochondrial metabolism and cell death in colitis. Cell Metab. 2021;33(12):2355-2366.e8.

534. Burmeister AR, Marriott I. The interleukin-10 family of cytokines and their role in the CNS. Front Cell Neurosci. 2018;12(November):1–13.

535. Lobo-Silva D, Carriche GM, Castro AG, Roque S, Saraiva M. Balancing the immune response in the brain: IL-10 and its regulation. J Neuroinflammation [Internet]. 2016;13(1):1–10. Available from: http://dx.doi.org/10.1186/s12974-016-0763-8

536. Iyer SS, Cheng G. Role of interleukin 10 transcriptional regulation in inflammation and autoimmune disease. Crit Rev Immunol. 2012;32(1):23–63.

537. Wurm J, Konttinen H, Andressen C, Malm T, Spittau B. Microglia development and maturation and its implications for induction of microglia-like cells from human ipscs. Int J Mol Sci. 2021;22(6):1–13.

538. Kriegstein A, Alvarez-Buylla A. The glial nature of embryonic and adult neural stem cells. Annu Rev Neurosci. 2009;32:149–84.

539. Koussounadis A, Langdon SP, Um IH, Harrison DJ, Smith VA. Relationship between differentially expressed mRNA and mRNA-protein correlations in a xenograft model system. Sci Rep. 2015;5(September 2014):1–9.

540. Jiang D, Cope AL, Zhang J, Pennell M. On the Decoupling of Evolutionary Changes in mRNA and Protein Levels. Mol Biol Evol [Internet]. 2023;40(8):1–14. Available from: https://doi.org/10.1093/molbev/msad169

541. Shebl FM, Pinto LA, García-Piñeres A, Lempicki R, Williams M, Harro C, et al. Comparison of mRNA and protein measures of cytokines following vaccination with human papillomavirus-16 L1 virus-like particles. Cancer Epidemiol Biomarkers Prev. 2010;19(4):978–81.

542. Gedeon T, Bokes P. Delayed protein synthesis reduces the correlation between mRNA and protein fluctuations. Biophys J. 2012;103(3):377–85.

543. Csárdi G, Franks A, Choi DS, Airoldi EM, Drummond DA. Accounting for Experimental Noise Reveals That mRNA Levels, Amplified by Post-Transcriptional Processes, Largely Determine Steady-State Protein Levels in Yeast. PLoS Genet. 2015;11(5):1–32.

544. Ngo J, Choi DW, Stanley IA, Stiles L, Molina AJA, Chen P, et al. Mitochondrial morphology controls fatty acid utilization by changing CPT1 sensitivity to malonyl-CoA . EMBO J. 2023;42(11).

545. Cells CM, Bader S, Würfel T, Jahner T, Nothdurfter C, Rupprecht R, et al. Mitochondrial Function and the Inflammatory State of Human. 2023;

546. Bootman MD, Bultynck G. Fundamentals of cellular calcium signaling: A primer. Cold Spring Harb Perspect Biol. 2020;12(1).

547. Hepler PK. The cytoskeleton and its regulation by calcium and protons. Plant Physiol. 2016;170(1):3–22.

548. Murakami T, Ockinger J, Yu J, Byles V, McColl A, Hofer AM, et al. Critical role for calcium mobilization in activation of the NLRP3 inflammasome. Proc Natl Acad Sci U S A. 2012;109(28):11282–7.

549. Vig M, Kinet JP. Calcium signaling in immune cells. Nat Immunol. 2009;10(1):21–7.

550. Berry CT, May MJ, Freedman BD. Analysis of Calcium Control of Canonical NF-κB Signaling in B Lymphocytes. Methods Mol Biol. 2021;2366.

551. Berry CT, May MJ, Freedman BD. STIM- and Orai-mediated calcium entry controls NF-κB activity and function in lymphocytes. Cell Calcium [Internet]. 2018;74(July):131–43. Available from: https://doi.org/10.1016/j.ceca.2018.07.003

552. Lilienbaum A, Israël A. From Calcium to NF-κB Signaling Pathways in Neurons. Mol Cell Biol. 2003;23(8):2680–98.

553. Liu X, Yao M, Li N, Wang C, Zheng Y, Cao X. CaMKII promotes TLR-triggered proinflammatory cytokine and type I interferon production by directly binding and activating TAK1 and IRF3 in macrophages. Blood. 2008;112(13):4961–70.

554. Nakata Y, Hide I. Calcium signaling and protein kinase C for TNF-α secretion in a rat mast cell line. Life Sci. 1998;62(17–18):1653–7.

555. Jackson FR, You S, Crowe LB. Regulation of rhythmic behaviors by astrocytes. Wiley Interdiscip Rev Dev Biol. 2020;9(4):1–8.

556. Newton R. Molecular mechanisms of glucocorticoid action: what is important? Thorax. 2000;(55):603–13.

557. Barnes P, Adcock I. Anti-inflammatory actions of steroids: molecular mechanisms. TiPS Rev. 1993;

558. Germelli L, Pozzo E Da, Giacomelli C, Tremolanti C, Marchetti L, Wetzel CH, et al. De novo neurosteroidogenesis in human microglia: Involvement of the 18 kda translocator protein. Int J Mol Sci. 2021;22(6):1–24.

559. Maatouk L, Yi C, Carrillo-de Sauvage MA, Compagnion AC, Hunot S, Ezan P, et al. Glucocorticoid receptor in astrocytes regulates midbrain dopamine neurodegeneration through connexin hemichannel activity. Cell Death Differ [Internet]. 2019;26(3):580–96. Available from: http://dx.doi.org/10.1038/s41418-018-0150-3

560. Liere P, Liu GJ, Pianos A, Middleton RJ, Banati RB, Akwa Y. The Comprehensive Steroidome in Complete TSPO/PBR Knockout Mice under Basal Conditions. Int J Mol Sci. 2023;24(3).

561. Wang Y, Yu W, Li S, Guo D, He J, Wang Y. Acetyl-CoA Carboxylases and Diseases. Front Oncol. 2022;12(March):1–10.

562. Dimitrova-Shumkovska J, Krstanoski L, Veenman L. Diagnostic and Therapeutic Potential of TSPO Studies Regarding Neurodegenerative Diseases, Psychiatric Disorders, Alcohol Use Disorders, Traumatic Brain Injury, and Stroke: An Update. Cells. 2020;9(4):870.

563. Wakida NM, Gomez-Godinez V, Li H, Nguyen J, Kim EK, Dynes JL, et al. Calcium Dynamics in Astrocytes During Cell Injury. Front Bioeng Biotechnol. 2020;8(August):1–19.

564. Pannell M, Economopoulos V, Wilson TC, Kersemans V, Isenegger PG, Larkin JR, et al. Imaging of translocator protein upregulation is selective for pro-inflammatory polarized astrocytes and microglia. Glia. 2020;(February 2019):280–97.

565. Camara AKS, Zhou YF, Wen PC, Tajkhorshid E, Kwok WM. Mitochondrial VDAC1: A key gatekeeper as potential therapeutic target [Internet]. Vol. 8, Frontiers in Physiology. Frontiers Media S.A.; 2017 [cited 2021 Jun 3]. p. 460. Available from: www.frontiersin.org

566. Heindl S, Gesierich B, Benakis C, Llovera G. Automated Morphological Analysis of Microglia After Stroke. 2018;12(April):1–11.

567. Prossin AR, Chandler M, Ryan KA, Saunders EF, Kamali M, Papadopoulos V, et al. Functional TSPO polymorphism predicts variance in the diurnal cortisol rhythm in bipolar disorder. Psychoneuroendocrinology [Internet]. 2018 Mar 1 [cited 2020 Dec 15];89:194–202. Available from: /pmc/articles/PMC6048960/?report=abstract

568. Da Pozzo E, Costa B, Martini C. Translocator Protein (TSPO) and Neurosteroids: Implications in Psychiatric Disorders. Curr Mol Med [Internet]. 2012 Nov 13 [cited 2021 Jun 3];12(4):426–42. Available from: https://pubmed.ncbi.nlm.nih.gov/22348611/

569. Sokias R, Werry EL, Chua SW, Reekie TA, Munoz L, Wong ECN, et al. Determination and reduction of translocator protein (TSPO) ligand rs6971 discrimination. Medchemcomm [Internet]. 2017 Jan 26 [cited 2021 Jun 3];8(1):202–10. Available from: www.rsc.org/medchemcomm

570. Wang Y, Yue X, Kiesewetter DO, Niu G, Teng G, Chen X. PET imaging of neuroinflammation in a rat traumatic brain injury model with radiolabeled TSPO ligand DPA-714. Eur J Nucl Med Mol Imaging. 2014;41(7):1440–9.

571. Cleary J, Johnson KM, Opipari AW, Glick GD. Inhibition of the mitochondrial F1F0-ATPase by ligands of the peripheral benzodiazepine receptor. Bioorganic Med Chem Lett. 2007;17(6):1667–70.

572. Kurumaji A, Nomoto H, Yamada K, Yoshikawa T, Toru M. No association of two missense variations of the benzodiazepine receptor (peripheral) gene and mood disorders in a Japanese sample. Am J Med Genet - Neuropsychiatr Genet. 2001;105(2):172–5.

573. Xue X, Duan R, Zheng G, Chen H, Zhang W, Shi L. Translocator protein (18 kDa) regulates the microglial phenotype in Parkinson's disease through P47. Bioengineered [Internet]. 2022;13(4):11061–71. Available from: https://doi.org/10.1080/21655979.2022.2068754

574. Choi J, Ifuku M, Noda M, Guilarte TR. Translocator protein (18 kDa)/peripheral benzodiazepine receptor specific ligands induce microglia functions consistent with an activated state. Glia. 2011;59(2):219–30.

575. Bae KR, Shim HJ, Balu D, Kim SR, Yu SW. Translocator protein 18 kDa negatively regulates inflammation in microglia. J Neuroimmune Pharmacol. 2014;9(3):424–37.

576. Lee JW, Nam H, Yu SW. Systematic analysis of translocator protein 18 kDa (TSPO) ligands on toll-like receptors-mediated pro-inflammatory responses in microglia and astrocytes. Exp Neurobiol [Internet]. 2016 Oct 1 [cited 2021 Jun 3];25(5):262–8. Available from: /pmc/articles/PMC5081472/

577. Martin FJ, Amode MR, Aneja A, Austine-Orimoloye O, Azov AG, Barnes I, et al. Ensembl 2023. Nucleic Acids Res. 2023;51(1 D):D933–41.

578. Benchling [Biology Software] [Internet]. Available from: www.benchling.com

579. Daron Smith R, Ogden CW, Penny MA. Exclusive Amplification of cDNA Template (EXACT) RT-PCR to Avoid Amplifying Contaminating Genomic Pseudogenes. Biotechniques. 2001;31:776–82.

580. Untergasser A, Cutcutache I, Koressaar T, Ye J, Faircloth BC, Remm M, et al. Primer3-new capabilities and interfaces. Nucleic Acids Res. 2012;40(15):1–12.

581. UCSC in-silico PCR tool [Internet]. Available from: https://genome.ucsc.edu/cgi-bin/hgPcr

582. Felsky D, De Jager PL, Schneider JA, Arfanakis K, Fleischman DA,

Arvanitakis Z, et al. Cerebrovascular and microglial states are not altered by functional neuroinflammatory gene variant. J Cereb Blood Flow Metab [Internet]. 2015 [cited 2021 Jun 3];36(4):819–30. Available from: /pmc/articles/PMC4821029/

583. Benedet AL, Pascoal TA, Chamoun M, Savard M, Schoemaker D, Mathotaarachchi S, et al. IC-P-064: THE IMPACT OF TSPO RS6971 POLYMORPHISM IN A CANADIAN NEUROIMAGING STUDY OF NEUROINFLAMMATION. Alzheimer's Dement [Internet]. 2018 Jul 1 [cited 2021 Jun 3];14(7S_Part_1):P58–9. Available from: https://alz-journals.onlinelibrary.wiley.com/doi/full/10.1016/j.jalz.2018.06.2129

584. Yan Q, Lu Y, Zhou L, Chen J, Xu H, Cai M, et al. Mechanistic insights into GLUT1 activation and clustering revealed by super-resolution imaging. Proc Natl Acad Sci U S A. 2018;115(27):7033–8.

585. Pastorino JG, Hoek JB. Regulation of hexokinase binding to VDAC. J Bioenerg Biomembr. 2008;40(3):171–82.

586. Hu A, Wang H, Xu Q, Pan Y, Jiang Z, Li S, et al. A novel CPT1A covalent inhibitor modulates fatty acid oxidation and CPT1A-VDAC1 axis with therapeutic potential for colorectal cancer. Redox Biol. 2023;68(September):102959.

587. Miernyk JA, Thelen JJ. Biochemical approaches for discovering protein-protein interactions. Plant J. 2008;53(4):597–609.

588. Kube E, Becker T, Weber K, Gerke V. Protein-protein interaction studied by site-directed mutagenesis. Characterization of the annexin II-binding site on p11, a member of the S100 protein family. J Biol Chem [Internet]. 1992;267(20):14175–82. Available from: http://dx.doi.org/10.1016/S0021-9258(19)49694-4

589. Richards AL, Eckhardt M, Krogan NJ. Mass spectrometry-based protein–protein interaction networks for the study of human diseases. Mol Syst Biol. 2021;17(1):1–18.

590. Elhabashy H, Merino F, Alva V, Kohlbacher O, Lupas AN. Exploring protein-protein interactions at the proteome level. Structure [Internet]. 2022;30(4):462–75. Available from:

https://doi.org/10.1016/j.str.2022.02.004

591. Feng J, Ma Y, Chen Z, Hu J, Yang Q, Ding G. Mitochondrial pyruvate carrier 2 mediates mitochondrial dysfunction and apoptosis in high glucose-treated podocytes. Life Sci [Internet]. 2019;237(October):116941. Available from: https://doi.org/10.1016/j.lfs.2019.116941

592. Zangari J, Petrelli F, Maillot B, Martinou JC. The multifaceted pyruvate metabolism: Role of the mitochondrial pyruvate carrier. Biomolecules. 2020;10(7):1–18.

593. Tavoulari S, Sichrovsky M, Kunji ERS. Fifty years of the mitochondrial pyruvate carrier: New insights into its structure, function, and inhibition. Acta Physiol. 2023;238(4):1–21.

594. Ferguson D, Eichler SJ, Yiew NKH, Colca JR, Cho K, Patti GJ, et al. Mitochondrial pyruvate carrier inhibition initiates metabolic crosstalk to stimulate branched chain amino acid catabolism. Mol Metab [Internet]. 2023;70(February):101694. Available from: https://doi.org/10.1016/j.molmet.2023.101694

595. Giatti S, Pesaresi M, Cavaletti G, Bianchi R, Carozzi V, Lombardi R, et al. Neuroprotective effects of a ligand of translocator protein-18kDa (Ro5-4864) in experimental diabetic neuropathy. Neuroscience. 2009 Dec 1;164(2):520–9.

596. Yang R, Lirussi D, Thornton TM, Jelley-Gibbs DM, Diehl SA, Case LK, et al. Mitochondrial Ca2+ and membrane potential, an alternative pathway for Interleukin 6 to regulate CD4 cell effector function. Elife. 2015;4(MAY):1–22.

597. Trebak M, Kinet JP. Calcium signalling in T cells. Nat Rev Immunol [Internet]. 2019;19(3):154–69. Available from: http://dx.doi.org/10.1038/s41577-018-0110-7

598. Moatti A, Cohen JL. The TNF-α/TNFR2 Pathway: Targeting a Brake to Release the Anti-tumor Immune Response. Front Cell Dev Biol. 2021;9(October):1–18.

599. Raffaele S, Lombardi M, Verderio C, Fumagalli M. TNF Production and

Release from Microglia via Extracellular Vesicles: Impact on Brain Functions. Cells. 2020;9(10):1–22.

600. Lu S, Wang Y, Liu J. Tumor necrosis factor-α signaling in nonalcoholic steatohepatitis and targeted therapies. J Genet Genomics [Internet]. 2022;49(4):269–78. Available from: https://doi.org/10.1016/j.jgg.2021.09.009

601. de Jong PR, Schadenberg AWL, van den Broek T, Beekman JM, van Wijk F, Coffer PJ, et al. STAT3 regulates monocyte TNF-alpha production in systemic inflammation caused by cardiac surgery with cardiopulmonary bypass. PLoS One. 2012;7(4):1–9.

602. Liu T, Zhang L, Joo D, Sun SC. NF-κB signaling in inflammation. Signal Transduct Target Ther. 2017;2(March).

603. Grötzinger J, Lorenzen I, Düsterhöft S. Molecular insights into the multilayered regulation of ADAM17: The role of the extracellular region. Biochim Biophys Acta - Mol Cell Res [Internet]. 2017;1864(11):2088–95. Available from: http://dx.doi.org/10.1016/j.bbamcr.2017.05.024

604. Chen Q, Li Y, Bie B, Zhao B, Zhang Y, Fang S, et al. P38 MAPK activated ADAM17 mediates ACE2 shedding and promotes cardiac remodeling and heart failure after myocardial infarction. Cell Commun Signal [Internet]. 2023;21(1):1–19. Available from: https://doi.org/10.1186/s12964-023-01087-3

605. Chao TSO, Byron KL, Lee KM, Villereal M, Rosner MR. Activation of MAP kinases by calcium-dependent and calcium-independent pathways. Stimulation by thapsigargin and epidermal growth factor. J Biol Chem [Internet]. 1992;267(28):19876–83. Available from: http://dx.doi.org/10.1016/S0021-9258(19)88637-4

606. Scimeca JC, Servant MJ, Dyer JO, Meloche S. Essential role of calcium in the regulation of MAP kinase phosphatase-1 expression. Oncogene. 1997;15(6):717–25.

607. Rosen LB, Ginty DD, Weber MJ, Greenberg ME. Membrane depolarization and calcium influx stimulate MEK and MAP kinase via activation of Ras. Neuron. 1994;12(6):1207–21.

608. Li S, Sun Y, Song M, Song Y, Fang Y, Zhang Q, et al. NLRP3/caspase-1/GSDMD-mediated pyroptosis exerts a crucial role in astrocyte pathological injury in mouse model of depression. JCI Insight. 2021;6(23).

609. Liu L, Chen M, Lin K, Xiang X, Zheng Y, Zhu S. Inhibiting caspase-12 mediated inflammasome activation protects against oxygen-glucose deprivation injury in primary astrocytes. Int J Med Sci. 2020;17(13):1936–45.

610. She N, Shi Y, Feng Y, Ma L, Yuan Y, Zhang Y, et al. NLRP3 inflammasome regulates astrocyte transformation in brain injury induced by chronic intermittent hypoxia. BMC Neurosci [Internet]. 2022;23(1):1–14. Available from: https://doi.org/10.1186/s12868-022-00756-2

611. Jäger E, Murthy S, Schmidt C, Hahn M, Strobel S, Peters A, et al. Calcium-sensing receptor-mediated NLRP3 inflammasome response to calciprotein particles drives inflammation in rheumatoid arthritis. Nat Commun [Internet]. 2020;11(1). Available from: http://dx.doi.org/10.1038/s41467-020-17749-6

612. Rada B, Park JJ, Sil P, Geiszt M, Leto TL. NLRP3 inflammasome activation and interleukin-1β release in macrophages require calcium but are independent of calcium-activated NADPH oxidases. Inflamm Res. 2014;63(10):821–30.

613. Horng T. Calcium signaling and mitochondrial destabilization in the triggering of the NLRP3 inflammasome. Trends Immunol [Internet]. 2014;35(6):253–61. Available from: http://dx.doi.org/10.1016/j.it.2014.02.007

614. Bai R, Lang Y, Shao J, Deng Y, Refuhati R, Cui L. The Role of NLRP3 Inflammasome in Cerebrovascular Diseases Pathology and Possible Therapeutic Targets. Vol. 13, ASN Neuro. 2021.

615. Zheng D, Liwinski T, Elinav E. Inflammasome activation and regulation: toward a better understanding of complex mechanisms. Cell Discov [Internet]. 2020;6(1). Available from: http://dx.doi.org/10.1038/s41421-020-0167-x

616. Campanella M, Szabadkai G, Rizzuto R. Modulation of intracellular Ca2+

signalling in HeLa cells by the apoptotic cell death enhancer PK11195. Biochem Pharmacol. 2008;76(11):1628–36.

617. Dooley CM, Wali N, Sealy IM, White RJ, Stemple DL, Collins JE, et al. The gene regulatory basis of genetic compensation during neural crest induction. Vol. 15, PLoS Genetics. 2019. 1–32 p.

618. El-Brolosy MA, Stainier DYR. Genetic compensation: A phenomenon in search of mechanisms. PLoS Genet. 2017;13(7):1–17.

619. Jones ME, Kondo M, Zhuang Y. A tamoxifen inducible knock-in allele for investigation of E2A function. BMC Dev Biol. 2009;9(1):1–13.

620. Sohal DS, Nghiem M, Crackower MA, Witt SA, Kimball TR, Tymitz KM, et al. Temporally regulated and tissue-specific gene manipulations in the adult and embryonic heart using a tamoxifen-inducible Cre protein. Circ Res. 2001;89(1):20–5.

621. Eisener-Dorman AF, Lawrence DA, Bolivar VJ. Cautionary insights on knockout mouse studies: The gene or not the gene? Brain Behav Immun [Internet]. 2009;23(3):318–24. Available from: http://dx.doi.org/10.1016/j.bbi.2008.09.001

622. Xiao D, Zhang W, Wang Q, Li X, Zhang Y, Rasouli J, et al. CRISPR-mediated rapid generation of neural cell-specific knockout mice facilitates research in neurophysiology and pathology. Mol Ther - Methods Clin Dev [Internet]. 2021;20(March):755–64. Available from: https://doi.org/10.1016/j.omtm.2021.02.012

623. Ran FA, Hsu PD, Wright J, Agarwala V, Scott DA, Zhang F. Genome engineering using the CRISPR-Cas9 system. Nat Protoc. 2013;8(11):2281–308.

624. Zhang XH, Tee LY, Wang XG, Huang QS, Yang SH. Off-target effects in CRISPR/Cas9-mediated genome engineering. Mol Ther - Nucleic Acids. 2015;4(11):e264.

625. Höijer I, Emmanouilidou A, Östlund R, van Schendel R, Bozorgpana S, Tijsterman M, et al. CRISPR-Cas9 induces large structural variants at on-target and off-target sites in vivo that segregate across generations. Nat

Commun. 2022;13(1):1–10.

626. Torsvik A, Stieber D, Enger PO, Golebiewska A, Molven A, Svendsen A, et al. U-251 revisited: Genetic drift and phenotypic consequences of long-term cultures of glioblastoma cells. Cancer Med. 2014;3(4):812–24.

627. Franzen J, Georgomanolis T, Selich A, Kuo CC, Stöger R, Brant L, et al. DNA methylation changes during long-term in vitro cell culture are caused by epigenetic drift. Commun Biol. 2021;4(1):1–12.

628. Kaur R, Jain R, Budholiya N, Rathore AS. Long term culturing of CHO cells: phenotypic drift and quality attributes of the expressed monoclonal antibody. Biotechnol Lett [Internet]. 2023;45(3):357–70. Available from: https://doi.org/10.1007/s10529-023-03346-2

629. Ammer LM, Vollmann-Zwerenz A, Ruf V, Wetzel CH, Riemenschneider MJ, Albert NL, et al. The role of translocator protein TSPO in hallmarks of glioblastoma. Cancers (Basel). 2020;12(10):1–26.

630. Pike Winer LS, Wu M. Rapid analysis of glycolytic and oxidative substrate flux of cancer cells in a microplate. PLoS One. 2014;9(10).

631. Janssen JJE, Lagerwaard B, Bunschoten A, Savelkoul HFJ, van Neerven RJJ, Keijer J, et al. Novel standardized method for extracellular flux analysis of oxidative and glycolytic metabolism in peripheral blood mononuclear cells. Sci Rep [Internet]. 2021;11(1):1–15. Available from: https://doi.org/10.1038/s41598-021-81217-4

632. Vijayakumar S, Conway M, Lio P, Angione C. Seeing the wood for the trees: A forest of methods for optimization and omic-network integration in metabolic modelling. Brief Bioinform. 2017;19(6):1218–35.

633. Salin K, Auer SK, Rey B, Selman C, Metcalfe NB. Variation in the link between oxygen consumption and ATP production, and its relevance for animal performance. Proc R Soc B Biol Sci. 2015;282(1812).

634. Takahashi E, Yamaoka Y. Simple and inexpensive technique for measuring oxygen consumption rate in adherent cultured cells. J Physiol Sci. 2017;67(6):731–7.

635. Mookerjee SA, Goncalves RLS, Gerencser AA, Nicholls DG, Brand MD.

The contributions of respiration and glycolysis to extracellular acid production. Biochim Biophys Acta - Bioenerg [Internet]. 2015;1847(2):171–81. Available from: http://dx.doi.org/10.1016/j.bbabio.2014.10.005

636. Mookerjee SA, Brand MD. Measurement and analysis of extracellular acid production to determine glycolytic rate. J Vis Exp. 2015;2015(106):1–9.

637. Liddelow S. Purification and Culture Methods for Astrocytes. Soc Neurosci. 2017;20–6.

638. Civita P, Leite DM, Pilkington GJ. Pre-clinical drug testing in 2d and 3d human in vitro models of glioblastoma incorporating non-neoplastic astrocytes: Tunneling nano tubules and mitochondrial transfer modulates cell behavior and therapeutic respons. Int J Mol Sci. 2019;20(23).

639. Wang J, Li HY, Shen SY, Zhang JR, Liang LF, Huang HJ, et al. The antidepressant and anxiolytic effect of GPER on translocator protein (TSPO) via protein kinase a (PKA) signaling in menopausal female rats. J Steroid Biochem Mol Biol [Internet]. 2021;207(November 2020):105807. Available from: https://doi.org/10.1016/j.jsbmb.2020.105807

640. Whalin ME, Boujrad N, Papadopoulos V, Krueger KE. Studies on the phosphorylation of the 18 kda mitochondrial benzodiazepine receptor protein. J Recept Signal Transduct. 1994;14(3–4):217–28.

641. Sassone-Corsi P. The Cyclic AMP pathway. Cold Spring Harb Perspect Biol. 2012;4(12):1–4.

642. Robinson-White A, Stratakis CA. Protein kinase a signaling: “Cross-talk” with other pathways in endocrine cells. Ann N Y Acad Sci. 2002;968:256–70.

643. Stocco DM, Wang XJ, Jo Y, Manna PR. Multiple signaling pathways regulating steroidogenesis and steroidogenic acute regulatory protein expression: More complicated than we thought. Mol Endocrinol. 2005;19(11):2647–59.

644. Gerhart-Hines Z, Dominy JE, Blättler SM, Jedrychowski MP, Banks AS, Lim JH, et al. The cAMP/PKA Pathway Rapidly Activates SIRT1 to Promote Fatty Acid Oxidation Independently of Changes in NAD +. Mol Cell.

2011;44(6):851–63.

645. Lim JH, Gerhart-Hines Z, Dominy JE, Lee Y, Kim S, Tabata M, et al. Oleic acid stimulates complete oxidation of fatty acids through protein kinase A-dependent activation of SIRT1-PGC1α complex. J Biol Chem [Internet]. 2013;288(10):7117–26. Available from: http://dx.doi.org/10.1074/jbc.M112.415729

646. Cao W, Collins QF, Becker TC, Robidoux J, Lupo EG, Xiong Y, et al. P38 Mitogen-Activated Protein Kinase Plays a Stimulatory Role in Hepatic Gluconeogenesis. J Biol Chem [Internet]. 2005;280(52):42731–7. Available from: http://dx.doi.org/10.1074/jbc.M506223200

647. Yang H, Yang L. Targeting cAMP/PKA pathway for glycemic control and type 2 diabetes therapy. J Mol Endocrinol. 2016;57(2):R93–108.

648. Howe AK. Cross-talk between calcium and protein kinase A in the regulation of cell migration. Curr Opin Cell Biol [Internet]. 2011;23(5):554–61. Available from: http://dx.doi.org/10.1016/j.ceb.2011.05.006

649. Sang L, Dick IE, Yue DT. Protein kinase A modulation of CaV1.4 calcium channels. Nat Commun. 2016;11(8):1508–30.

650. Halls ML, Cooper DMF. Regulation by Ca2+-signaling pathways of adenylyl cyclases. Cold Spring Harb Perspect Biol. 2011;3(1):1–22.

651. Saddik M, Gamble J, Witters LA, Lopaschuk GD. Acetyl-CoA carboxylase regulation of fatty acid oxidation in the heart. J Biol Chem. 1993;268(34):25836–45.

652. Williams JN, Sankar U. CaMKK2 Signaling in Metabolism and Skeletal Disease: a New Axis with Therapeutic Potential. Curr Osteoporos Rep. 2019;17(4):169–77.

653. Sabbir MG, Taylor CG, Zahradka P. CAMKK2 regulates mitochondrial function by controlling succinate dehydrogenase expression, post-translational modification, megacomplex assembly, and activity in a cell-type-specific manner. Cell Commun Signal [Internet]. 2021;19(1):1–29. Available from: https://doi.org/10.1186/s12964-021-00778-z

654. Gatliff J, East D, Crosby J, Abeti R, Harvey R, Craigen W, et al. TSPO

interacts with VDAC1 and triggers a ROS-mediated inhibition of mitochondrial quality control. Autophagy [Internet]. 2014 [cited 2021 Jun 10];10(12):2279–96. Available from: http://dx.doi.org/10.4161/15548627.2014.991665

655. Issop L, Ostuni MA, Lee S, Laforge M, Péranzi G, Rustin P, et al. Translocator Protein-mediated stabilization of mitochondrial architecture during inflammation stress in colonic cells. PLoS One. 2016;11(4):1–23.

656. Holt MG. Astrocyte heterogeneity and interactions with local neural circuits. Essays Biochem. 2023;67(1):93–106.

657. Tabata H. Diverse subtypes of astrocytes and their development during corticogenesis. Front Neurosci. 2015;9(APR):1–7.

658. Matias I, Morgado J, Gomes FCA. Astrocyte Heterogeneity: Impact to Brain Aging and Disease. Front Aging Neurosci. 2019;11(March):1–18.

659. Tandon P, Abrams ND, Carrick DM, Chander P, Dwyer J, Fuldner R, et al. Metabolic Regulation of Inflammation and Its Resolution: Current Status, Clinical Needs, Challenges, and Opportunities. J Immunol. 2021;207(11):2625–30.

660. Owen DR, Narayan N, Wells L, Healy L, Smyth E, Rabiner EA, et al. Pro-inflammatory activation of primary microglia and macrophages increases 18 kDa translocator protein expression in rodents but not humans. J Cereb Blood Flow Metab. 2017;37(8):2679–90.

661. Vernier M, Giguère V. Aging, senescence and mitochondria: The pgc-1/err axis. J Mol Endocrinol. 2021;66(1):R1–14.

662. Killen MJ, Giorgi-Coll S, Helmy A, Hutchinson PJA, Carpenter KLH. Metabolism and inflammation: implications for traumatic brain injury therapeutics. Expert Rev Neurother [Internet]. 2019;19(3):227–42. Available from: https://doi.org/10.1080/14737175.2019.1582332

663. O'Sullivan D, Pearce EL. Targeting T cell metabolism for therapy. Trends Immunol [Internet]. 2015;36(2):71–80. Available from: http://dx.doi.org/10.1016/j.it.2014.12.004